Evaluation of old store-and-release covers on discard dumps and backfilled pits to improve and predict their performance for rehabilitated mines at Mpumalanga Highveld, South Africa

by

Roeline van Schalkwyk

Dissertation presented for the degree of
Doctor of Philosophy in Agricultural Science

at
Stellenbosch University
Department of Soil Science, Faculty of AgriScience

Supervisor: Dr. J.E. Hoffman

Co-supervisor: Dr. J. van Zyl

December 2021

Declaration

By submitting this dissertation electronically, I declare that the entirety of the work contained therein is my own, original work, that I am the sole author thereof (save to the extent explicitly otherwise stated) that reproduction and publication thereof by Stellenbosch University will not infringe any third party rights and that I have not previously in its entirety or in part submitted it for obtaining any qualification.

Date: December 2021

Summary

Store-and-release covers (SRCs) are an important mitigation method to protect the environment at rehabilitated mines in the Mpumalanga Highveld, South Africa. The long-term performance of SRCs can be influenced by soil cover-, soil hydraulic-, and vegetation properties. Currently, a Technical Guideline for Soil Covers Development is not in place in South Africa. In addition, data sets of well- and poorly constructed covers, and the availability of data on appropriate input parameters for predicting long-term performance of such covers are limited. This need includes data for saturated hydraulic conductivity (K_{sat}), soil water retention curves (SWRCs), and photosynthetic active leaf-area index (LAI). Moreover, the measurement of K_{sat} and SWRCs is time-consuming, labour intensive and costly. Consequently, a multidisciplinary study to investigate the impact of soil cover-, soil hydraulic- and vegetation properties on long-term performance of SRCs was initiated. Most importantly, pedotransfer functions (PTFs) to predict K_{sat} and SWRCs were developed from particle-size distribution, soil organic matter (SOM) and bulk density. Leaf area index values for good and poor vegetation covers were determined for rehabilitated mines in Mpumalanga Highveld.

Soil cover properties *viz.* cover configurations, soil texture, Atterberg limits, bulk density and soil nutrient availability were determined. Saturated hydraulic conductivity were measured using two types of double-ring infiltrometer, a single-ring infiltrometer, and a constant-head permeameter. Soil water retention curves were established using the pressure plate apparatus. The SRCs data-set was split into training and testing sets to validate the SWRC model. After the SRCs data-set was split into moderately- and very dense SRCs data sets, and an additional site was used to validate the moderately dense K_{sat} model. The data-set of very dense SRCs was also split into training and testing sets to validate the very dense K_{sat} model. Monthly LAI from September 2018 to August 2019 was destructively measured using a LI-3100C Area Meter.

The dual-layered SRCs were constructed with sandier growth medium (top layer) underlaid by a loamy to clayey water retention layer (sub-layer). Monolithic SRCs were constructed of sandy loam or sandy clay loam soil covers. After the SRCs were split into moderately- and very dense soil cover conditions, the moderately dense SRCs performed significantly better and had acceptable bulk densities, good vegetation covers with good root distribution in the growth medium, steep slope in the desaturation function of the growth medium and high water-holding capacity (WHC) in the water retention layers. The K_{sat} and WHC of the moderate SRCs over 20 years had values similar to that of the soils, but the values of sandier soil cover layers were lower than critical threshold values due to low resistance to compaction.

The statistical analysis of best-fit moderately- and very dense K_{sat}. models yielded an adjusted R^2 of 0.749 and 0.999, respectively from sand-, silt- and clay content, SOM and bulk density. The statistical analysis of the best-fit SWRC model of 14 matric potentials had an adjusted R^2 = 0.827 from three fractions of sand-, two fractions of silt-, clay content, SOM, and bulk density. The

photosynthetic active LAI for good and poor vegetation cover of rehabilitated mines at Mpumalanga Highveld was ~1.2 and 0.8 $m^2.m^{-2}$, respectively.

Poorly constructed soil covers result in high bulk density, low to very low K_{sat} and WHC values and poor vegetation properties and should be avoided at any cost. The critical threshold values for bulk density, K_{sat} and WHC of soils can be used to evaluate long-term soil cover performance. The developed PTFs can be used to predict soil covers' hydraulic properties having soil physical properties similar to the old SRCs. These results can be considered as a possible amendment to the Technical Guidelines on Soil Cover Development in South Africa.

Opsomming

Berg-en-vrystel bedekkings (BVBs) by gerehabiliteerde myne in Mpumalanga Hoëveld, Suid-Afrika is ‘n belangrike metode om die omgewing te beskerm. Die langtermyn prestasievermoë van BVBs kan deur die bedekkings-, hidrouliese- en vegetasie eienskappe beïnvloed word. Tans is die Tegniese Riglyn vir Ontwikkeling van Grondbedekking nie in orde in Suid-Afrika nie. Bygesê, datastelle vir goeie en swak gekonstrueerde grondbedekking en die beskikbaarheid van data met aanvaarde insette om die langtermyn prestasievermoë van grondbedekkings te bepaal is beperk. Hierdie beperkte datastelle sluit versadigde hidrouliese geleivermoë (K_w), grondwaterkenkromme (GWKK) en blaar-area indeks (BAI) in. Die meting van K_w en GWKK is langdradig, verg intensiewe arbeid en is ‘n duur proses. Gevolglik, is ‘n multidissiplinêre projek uitgevoer waar die impak van bedekkings-, hidrouliese- en vegetasie eienskappe op die langtermyn prestasievermoë van grondbedekkings geëvalueer is. Die belangrikste was die pedo-oordrag funksies (POFs) vir die bepaling van K_w en GWKK vanaf deeltjiegrootteverspreiding, organiese materiaal in grond (OM) en bulkdigtheid. Die fotosintetiese aktiewe BAI vir goeie en swak plantbedekking vir gerehabiliteerde myne in Mpumalanga Hoëveld is ook bepaal.

Grondbedekkingseienskappe wat bepaal is sluit in konfigurasie van die grondbedekkings, grondtekstuur, bulkdigtheid en toeganklike voedingstowwe. Versadigde hidrouliese geleivermoë is gemeet met twee soorte dubbelring-infiltrometers, ’n enkelring-infiltrometer en ’n konstante-vloei permeameter. Grondwaterkenkromme is m.b.v. drukpotte bepaal. Die BVBs datastel is verdeel in opleiding- en toetsing stelle om die GWKK model te kon valideer. Nadat die BVBs datastel in matig- en hoog verdigte BVBs datastelle verdeel is, is ’n addisionele veld se data gebruik om die matig verdigte K_w model te valideer. Die hoog verdigte BVBs datastel was verdeel in ’n opleiding- en ’n toetsing stel om die hoog verdigte K_w model te kon valideer. Maandelikse BAI is m.b.v. ’n LI-3100C Area Meter gemeet vanaf September 2018 tot Augustus 2019.

Die dubbellaag BVBs se groeimedium (boonste grondlaag) het ’n sanderige tekstuur gehad terwyl die waterretensielaag (ondergrondlaag) se tekstuur leem tot kleierig was. Die enkellaag BVBs was sanderige leem of sanderige kleileem gronde. Nadat die BVBs in matig- en hoog verdigte grondbedekking kondisie verdeel is, was die matig verdigte BVBs se langtermyn prestasievermoë die beste, weens aanvaarbare bulkdigthede, beter plantbedekkings met goeie wortelverspreiding in die groeimedium, ’n styl helling in die desaturasie funksie van GWKK in die groeimedium en hoë waterhouvermoë in die waterretensielaag. Die matig verdigte BVBs (> 20 jaar oue grondbedekkings) se K_w en waterhouvermoë was dieselfde as dié van gronde, alhoewel die sanderige grondbedekkingslae was laer as die kritiese drempelwaardes a.g.v. lae weerstand teen kompaksie.

Die statistiese ontleding van die mees geskikte matig- en hoog verdigte K_w modelle het ’n aangepaste R^2 van 0.749 en 0.999 onderskeidelik met sand-, slik-, en klei-inhoud, OM en bulkdigtheid as insette gehad. Die statistiese ontleding vir die mees geskikte GWKK model met 14 matrikspotensiale het ’n aangepaste R^2 van 0.827 met drie fraksies van sand-, twee fraksies van

slik-, en klei-inhoud, OM en bulkdigtheid as insette gehad. Die fotosintetiese aktiewe BAI was ~1.2 en 0.8 $m^2.m^{-2}$ vir goeie en swak plantbedekkings onderskeidelik by gerehabiliteerde myne in Mpumalanga Hoëveld.

Swak gekonstrueerde grondbedekkings kan hoë bulkdigthede, lae tot baie lae K_w en waterhouvermoë waardes, swak plantbedekkings tot gevolg hê en hierdie soort grondbedekkings moet vermy word teen alle koste. Kritiese drempelwaardes vir bulkdigthede, K_w en waterhouvermoë van gronde kan gebruik word om die langtermyn prestasievermoë van BVB te evalueer. Die ontwikkelde POFs kan gebruik word om die grondhidrouliese eienskappe te bepaal vir grondbedekkings met grondfisiese eienskappe soortgelyk aan die ou bestaande BVBs. Hierdie resultate kan moontlike wysigings wees vir Tegniese Riglyn vir Ontwikkeling van Grondbedekking in Suid-Afrika.

This dissertation is dedicated to Albert van Zyl

Biographical sketch

Roeline van Schalkwyk was born on 20 June 1993 in Kuils River. She started her school career at Mikro Primary School in Kuils River, and matriculated from De Kuilen High School, Kuils River in 2011. In 2012, she enrolled at Stellenbosch University and obtained a Bachelor of Science in Agriculture (BScAgric) degree in 2016, majoring in Soil Science and Chemistry. In 2018, she obtained her Master of Science in Agriculture (MScAgric) in Soil Science from Stellenbosch University. In 2018 to 2020, she started working at Terrasim cc in Pretoria as a Junior Researcher.

Acknowledgements

“Sonder grond is ons niks”

Roeline van Schalkwyk

First and foremost, I want to thank my Lord for giving me strength and walk with me through this adventure of studying for my PhD. I also thank Him for His helping or otherwise I would not have been able to finish it on my own.

I would like to express my gratitude to my parents, my family and my friends for their consistent support during this dissertation:

- I humbly thanks to my parents, Iain and Irma van Schalkwyk, for believing in me, their encouragement and love when I was down and at rock bottom;
- my boyfriend, Jaco Greyling, for supporting me at the last stages of this dissertation;
- my brother, Helgard van Schalkwyk, and sister-in-law, Dominique van Schalkwyk, for supporting and helping me during the adventure;
- aunt René van Schalkwyk for cheering me up, keeping me calm and believing in me;
- Uncle André and aunt Eunice van Schalkwyk for their support and guidance; and
- my best friend, Marelize Brand, for listening to me, thanks for your positive words and that you helped me to fulfil my dreams.

I sincerely thank Dr. Eduard Hoffman and Dr. Johan van Zyl for all your effort, giving advice and guidance during this dissertation.

During 2018–2021 several people were involved in the study. Therefore, I would like to thank:

- Albert van Zyl for as a Research Manager of the project and organising the fieldworks;
- Piet Steenekamp for characterised the cover configurations of the store-and-release covers;
- Eugene Lategan for helping me with the soil water retention curve and some of the other soil physical experiments;
- Teneille Nel, another best friend of mine, for helping some soil physical properties;
- For all the students who helped during the laboratory experiments, thank you;
- For all the workers who helped me during the fieldwork, thanks for the research assistances;
- All members at the Department of Soil Science, thanks for all the positive words. I spent a great time with everybody; and
- Water Research Commission of South Africa and Coaltech Research Association.

Table of Contents

List of Abbreviations

Adjusted R^2	Adjusted coefficient of determination
AMD	Acid mine drainage
AWC	Plant-available water capacity
CEC	Cation exchange capacitive
CV	Coefficient of variation
E	Evaporation
EC	Electrical conductivity
EC_e	Electrical conductivity of saturated paste
Fe	Iron
FC	Field capacity
GWC	Gravimetric water content
K	Potassium
KCl	Potassium chloride
K_{sat}	Saturated hydraulic conductivity
LAI	Leaf area index
mhasl	mean height above sea level
Mg	Magnesium
Mn	Manganese
MLR	Multiple linear regression
N	Nitrogen
P	Phosphorus
Predicted R^2:	Predicted coefficient of determination
PTF	Pedotransfer function
PWP	Permanent wilting point
R	Pearson correlation coefficient
R^2	Coefficient of determination

RMSE	Root mean square error
SD	Standard deviation
SRC	Store-and-release covers
SOM	Soil organic matter
SWC	Soil water content
SWD	Soil water dynamics
SWRC	Soil water retention curve
SWS	Soil water storage
VWC	Volumetric water content
WHC	Water holding capacity
Zn	Zinc

List of Tables

List of Figures

Chapter 1: Long-term soil cover performances of store-and-release covers

1.1 Background

Mining is a global industry and it is one of the largest industry sectors, and of significant economic importance. Coal mining is currently the most important energy source to generate electricity in the world. Coal is also one of the cheapest and most abundant energy carrier. In South Africa, an average of 224 million tonnes (Eskom, 2018) of marketable coal are produced per year. According to Mathu & Chinomona (2013), 6% of the coal production is exported internationally and this makes South Africa the sixth largest coal exporting country.

1.1.1 Geological description of coal mines

The majority of coal mines are located in the north eastern parts of South Africa, where coal mining takes place mainly in the Mpumalanga Province (Figure 1.1). The major coal-bearing strata in South Africa are associated with the Permian-aged rocks of the Karoo Supergroup (Cairncross, 2001). According to The Mine Manager of Landau Colliery (2001), the Ecca Subgroup, a division of the Karoo Supergroup, consisting of sandstones and mudstones, together with coal seams, were laid down by large river deltas that entered the ancient Karoo Sea. The rocks of Ecca Subgroup are widespread in South Africa and the coal deposits are limited to the main Karoo Supergroup, also known as Karoo Basin, extending from Welkom in Free State Province to Nongoma in KwaZulu-Natal. These Permian coals were deposited on Gondwana during a period of warming. Vegetation change reflected the changing climate with tundra vegetation giving way to swamps and deciduous Glossopteris (Banks *et al.*, 2011). According to Hobday (1987), the coal quality and geometry were influenced by variable subsidence and sedimentation rates in the foredeep, rift and epicratonic basin settings; local palaeotopography, and eustatically induced changes in base level, where palaeotopography and depositional environment were most important. These coals have a high inertinite and variable semifusinite content and are low in sulphur (Cadle *et al.*, 1993). The northern margin of the Emalahleni (Witbank) coalfields in Mpumalanga Province represented Vryheid Formation sediments of the Ecca Subgroup (Hobbs *et al.*, 2008). Mpumalanga produced 83% of the coal mines in South Africa with the residual produced in Limpopo, KwaZulu-Natal, and the Free State (Chamber of Mines of South Africa, 2018).

1.1.2 Environmental impacts of coal mining

Mining operations often result in mine residue stockpiles and residue deposits which may have a seepage impact (Lloyd, 2002; Van Zyl, 2002). Basson *et al.,* (1997) reported that extensive coal mining resulted in poor quality acidic water in the Mpumalanga Highveld coalfields. Vermaak *et al.* (2004) reported that the coal mining industry is responsible for the major part of mine residues which have an environmental impact, contributing to 318 million tonnes, or 75% of the mine residues per annum of the total mine residue stockpiles.

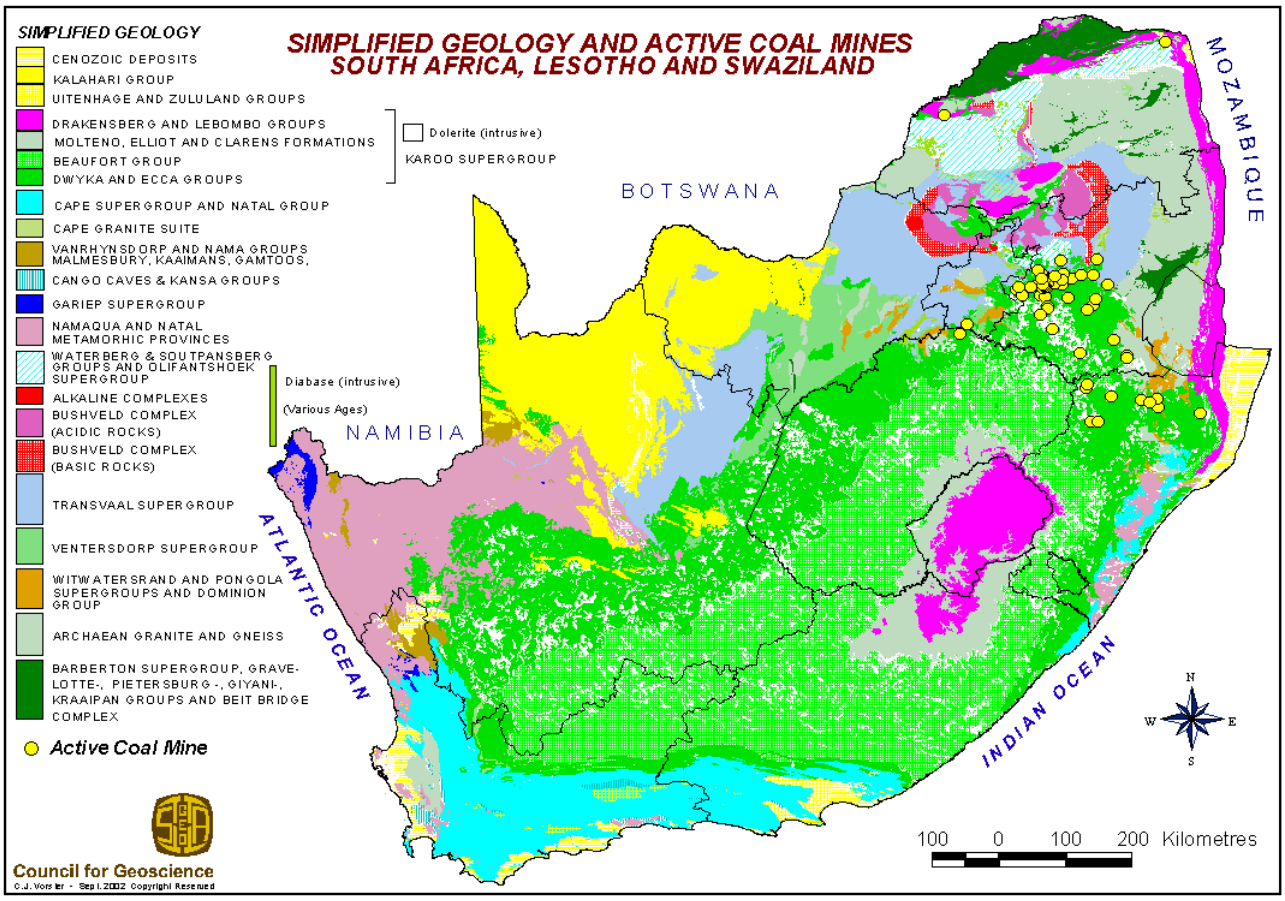

Figure 1.1: Simplified geological map and active coal mines of South Africa (Basson *et al.*, 1997).

According to Schneider *et al*., (2010), the main residue deposits of coal mining are acid mine drainage (AMD) and the release of chemical contaminants into the water resources.

1.1.3 Acid mine drainage

During mining operations and decommissioning of the life-cycle of mines (Department of Water Affairs and Forestry, 2007), the coal discard or spoil, dominated by pyrite, is exposed to oxygen and soil water. Due to exposure to oxygen and soil water content, a natural phenomenon occurs, namely AMD. The rate of AMD produced greatly increases when the coal discard or spoil is fractured and crushed (McCarthy, 2011). The AMD production is mainly a function of the geochemistry of the mine geology, the activity of microorganisms, and the amount of oxygen- and water ingress into pyrite-containing coal (McCarthy, 2011). According to Durkin & Herrmann (1994), AMD do not only occur as a result of the oxidation of sulphide minerals, but also pyrrhotite, marcasite, galena, sphalerite and chalcopyrite. The reaction is assisted by the presence of catalysing bacteria namely *Thiobacillus ferrooxidans* (Vermaak *et al.*, 2004). Verburg *et al*., (2009) reported that the pyrite undergoes oxidation in a two-stage process, the first producing sulphuric acid and ferrous sulphate and the second orange-red ferric hydroxide and more sulphuric acid. The AMD generation may be expressed as follows (Akcil & Koldas, 2006):

$$4FeS_2 + 15O_2 + 8H_2O \xrightarrow{\text{bacteria}} 2Fe_2O_3 + 8SO_4^{2-} + 16H^+$$

The chemical and biological reactions result in low pH which has the potential to mobilise heavy metals contained in the coal discard or spoil. Elevated metals and sulphate from the AMD generation process are then transported to the receiving environment. Characterised by low pH and high concentrations of heavy metals, Adler & Rascher (2007) reported three environmental consequences of AMD:

- It reaches to the streams which result in lower pH, thereby harming the river ecology;
- May leach metals from the coal into the groundwater and surface water resources, thereby contaminating water supplies; and
- Degradation of soil quality, increase salinity as well as decline in soil microbial activity.

Every coal mine is unique in terms of its AMD potential; therefore, the nature and size of the associated risk and feasibility of mitigation options will vary from site to site. The government rules and regulations rely on the containment philosophy for pollution prevention. The purpose of the containment is to prevent water movement into coal discard or spoil and control seepage impact. Almost all containment systems employ a cover to (1) minimise the oxygen- and water ingress through the coal discard or spoil; and (2) isolate the coal discard or spoil from the water resources. These two goals are common to all cover designs and their implementation may include conventional or alternative covers based on regulatory requirements. Cover systems are intended to remain in place and protect the environment for an extended period; therefore, they should be durable and self-renewing (Hauser, 2009). If cover systems meet the infiltration requirement, it usually satisfies the second requirement. Therefore, it is recommended that any cover system must meet the site requirement, or objective of the groundwater pollution prevention based on regulations.

1.1.4 Soil covers as a mitigation method

Soil covers are a widely-used, but relatively new method for contaminant containment (Peng & Jiang, 2009). Usually, rehabilitated mine residue facilities use geosynthetic clay liner, a typical compliant covers, however, there is an increasing trend in using soil cover as an alternative because of its cost-effectiveness. As a motivation for the soil cover option according to Hodgson & Krantz (1998), the proper design and construction of covers play a major role in limiting oxygen- and water ingress into coal discard or spoil. In turn, soil covers inhibit AMD production and ultimately reduce the volume and quality of seepage into the groundwater. Well-designed and constructed covers are one of the most important passive mine water mitigation prevention measures (Australian Alternative Cover Assessment Program, 2011).

1.1.5 Store-and-release covers

Engineered soil covers for AMD control became popular in the 1990's with the development of the science of unsaturated media that enabled prediction of evapotranspiration from soil cover systems. There are several types of soil covers, whereas only one type soil cover was evaluated in this research project, namely store-and-release covers (SRCs). The SRCs have "the capacity to store infiltration during wetting periods, and through evapotranspiration to remove the stored water during

drier periods" (Apiwantragoon *et al.*, 2014). The first/top soil layer for cover systems is called the growth medium and the second/sublayer is called the water retention layer. The SRCs are used to minimise the oxygen- and water ingress to meet the objective of the seepage impact. Another advantage of SRCs is that it requires little long-term maintenance and has a low potential for long-term degradation (Wels *et al.*, 2002). Store-and-release covers can also be used in the dry climate of Mpumalanga Highveld, which is a semi-arid region. The functions and properties of the SRCs are explained in Table 1.1.

1.1.6 Guidelines on soil cover design, construction and maintenance: Rehabilitation

In South Africa, rehabilitation isn't a luxury, but it is necessary to protect the ecosystems. Tomlinson (1984) defines rehabilitation as follows: "The restoration of a disturbed area to a land form and productivity which is in unison with the land form and productivity of the locality before the disturbance took place". The list of the South African guidelines and international guidelines are shown in Table 1.2. The Department of Water Affairs and Forestry have a series of Best Practise Guidelines for Water Resource Protection in the South African Mining Industry, where only a few is relevant to soil cover development. The international guidelines exclusively explain how to develop a soil cover system for a site-specific region in four phases: (1) planning, (2) design, (3) construction and (4) post-closure care and maintenance which include monitoring of the physical aspects of rehabilitation success which is termed as long-term soil cover performance. International guidelines on soil cover development include four phases that are listed in Table 1.3. In the case of SRCs, rehabilitation has other common aims which include re-establishing above-ground and below-ground biodiversity and ultimately reaching a self-sustaining ecosystem (Banning *et al.*, 2011).

Rehabilitation respects the history of a site and has been linked to natural ecological succession with sustainability in developing soil covers. (Bell, 2001). The selection of an appropriate final soil cover system requires careful consideration of the varied metrics for soil cover performance, site-specific details, regulatory requirements and cost.

Table 1.1: The function and properties of store-and-release covers.

Soil layer	Function and properties of the soil layer
Top layer	A layer of soil that stores water during wet season and depletes the soil water *via* evapotranspiration in dry season (Zhan *et al.*, 2014). This soil layer must also function as a growth medium to allow rapid and profilic root growth in all parts of the soil cover (O'Kane & Ayres, 2012).
Sublayer	Store-and-release covers have a second layer which function as a water retention layer. This layer relies on the mechanism of water holding capacity of soil to limit percolation of deep infiltrated water into the coal discard or spoil (Hauser, 2009).

Table 1.2: List of South African and international guidelines for cover development.

South African guidelines	International guidelines
Best Practise Guidelines (Department of Water Affairs and Forestry, 2008)	Global Acid Rock Drainage Guide (INAP, 2014)
Decision Support System on mine residue facilities (Rademeyer *et al.*, 2008)	The Global Cover System Guidance Document (INAP, 2017)
Guidelines for the rehabilitation of mined land (Chamber of Mines of South Africa / Coaltech, 2007)	Waste Management Association of Australian guideline on phytocaps (Australian Alternative Cover Assessment Program, 2011)
	Guidelines on Water Balance Cover for Waste: Principles and Practice (Albright *et al.*, 2009)

The criteria to evaluate soil cover performance are based on land capability, erosion potential, soil cover-, hydraulic- and vegetation properties (Morgenthal, 2003). Additional factors specific to each discard dump or opencast backfilled pit may also affect the selection of the final soil cover system, such as depth of groundwater, proximity to existing or planned use of groundwater resources and longevity requirements.

1.1.7 Importance to consider long-term cover performance

Identification of successful long-term soil cover performance can be a challenging exercise. The success criteria must be scientifically rigorous, satisfy the stakeholders and be informative to decision-makers (Bell, 1996). Since soil cover performance design is based on the soil hydraulic properties, INAP (2017) stated significant changes occur with the aging of covers for arid and semi-arid climates. Long-term soil cover performance should be considered when designing covers and for assessing the post-closure impacts that represent the soil cover- and vegetation properties impacted by cover aging (Albright *et al*., 2010). Normally, computer simulations with the three properties as input parameters are being used to predict the long-term soil cover performance.

According to Benson *et al.* (2001), the computer models are used to compare the different soil cover types, and the difference in performance between a well-designed and constructed soil cover and poorly-designed and constructed soil cover together with a sustainable ecosystem. Informed by prediction, the design of soil cover is refined in an iterative process to meet the objective of the seepage impact prevention as well as other constraints.

1.2 Problem statements and project objectives

1.2.1 Problem statements

The long-term changes in soil cover performance of well-constructed and poorly constructed SRCs have not been systematically assessed for coal mines of South Africa. Consequently, information to predict long-term soil cover performance to limit seepage impacts is limited. The biggest limitation is the availability of data on appropriate input parameters for soil covers that have been exposed to prevailing climatic conditions and environmental processes for a considerable period of time.

Table 1.3: Phases of soil cover development.

Phase	Global Cover System Guidance Document	Australian guidelines[a]
Planning	Establish design objective	Cover goals and regulatory requirements
		Stakeholder requirements
Design	Characterise available materials	
	Develop design alternative covers	Design
		Risk assessment, mitigation and management
	Cover system field trials	
Construction	Full-scale cover system construction	Construction
Post-closure care and maintenance	Long-term performance monitoring	Post-closure care

[a]Waste Management Association of Australian guideline on phytocaps (Australian Alternative Cover Assessment Program, 2011).

This includes changes in saturated hydraulic conductivity (K_{sat}) and soil water retention curves (SWRCs) with cover aging. The soil cover performance prediction is dependent upon the accuracy of K_{sat} and SWRCs measurements (Malaya & Sreedeep, 2011). Unfortunately, soil hydraulic properties vary spatially and temporally (Karahan & Erşahin, 2016). In addition, the direct measurement of K_{sat} and SWRCs are labour-intensive and expensive (Elhakeem *et al.*, 2018). For example, to determine the K_{sat} of a clayey soil can take longer than one day and a complete SWRC takes six months or longer. Furthermore, pedotransfer functions (PTFs) as an indirect method to predict soil hydraulic properties are not readily available for soil covers in South Africa.

Root development and leaf area index (LAI) are important vegetation properties as input parameters for designing and soil cover performance modelling (Rao & Revanasiddappa, 2000). Photosynthetic active LAI of rehabilitated mines in Mpumalanga Highveld is not readily available. Although, Vermaak *et al.* (2004) used the LAI of 3.0 and 1.0 $m^2.m^{-2}$ for good and poor vegetation cover, respectively of rehabilitated mines in KwaZulu-Natal, but these values are not necessarily suitable for grassland in Highveld due to differences in climate.

1.2.2 Project objectives

The specific objectives of the project were:

- To determine the effect of soil cover-, soil hydraulic- and vegetation properties on the long-term soil cover performance, whilst considering bulk density as the determining factor;
- To develop PTFs for K_{sat} and SWRC for old SRCs using multiple linear regression which is easy to perform and not time-consuming; and
- To establish photosynthetic active LAI values for good and poor vegetation covers, and establish a relationship between photosynthetic active LAI and active vegetation biomass.

Concerning this dissertation, the data sets of K_{sat} and SWRCs will be presented.

1.3 Literature review

In the investigation of SRCs, it is necessary to analyse or predict the long-term soil cover performance and the failure of the soil cover. Unfortunately, South African guidelines for Soil Cover Development lack to mention the importance of long-term SRCs performance. According to Yanful *et al.* (2003), the soil cover performance to store and dispose received rainfall is dependent on several soil cover-, hydraulic- and vegetation properties. Soil cover properties include soil cover thickness, soil material, soil structure, and soil physical properties. These soil physical properties include soil texture (Mccartney & Zornberg, 2002) with soil organic matter (SOM), compacted condition (bulk density), and characteristics of preferential flow paths if present (Benson *et al.*, 2001). Soil hydraulic properties include K_{sat} and SWRCs (Gorakhki & Bareither, 2017). Vegetation properties include root penetration depth and root distribution (Bossé *et al.*, 2013), as well as leaf area index together with above-ground biomass (Limpitlaw *et al.*, 1997). According to the Australian Alternative Cover Assessment Program (2011), soil texture, SOM, bulk density, K_{sat}, SWRCs and LAI are the typical required soil cover-, hydraulic- and vegetation properties as input parameters for modelling software. Depending on the modelling software, other soil cover properties such as soil chemical properties *viz*., pH, cation exchange capacity (CEC) and electrical conductivity (EC) may also be required as input parameters.

1.3.1 Gaps in the South African guidelines for store-and-release cover development

Currently, the regulator specifies compliant covers such as a geosynthetic clay liner to protect the groundwater. It is up to the applicant to demonstrate the following when alternative cover options such as SRCs are motivated:

- Demonstrate through dedicated soil cover design that the designed soil cover will protect the groundwater;
- Demonstrate that the constructed soil cover meets the soil cover design criteria; and
- Demonstrate that the latent risk on groundwater is mitigated through long-term soil cover performance.

The following components of international soil cover guidelines are in place for South Africa and no further development will be required:

- Processes in engaging with the regulator regarding soil covers to protect groundwater;
- Processes and procedures on stakeholder engagement, which should be used to determine and communicate required soil cover functionality and design objectives;
- Procedures and tools/models on engineering design, mine water and salt balance modelling, hydrological-, geohydrological-, and geochemical characterisation and modelling; and
- Guidelines on rehabilitation of mined land.

These processes, procedures and tools/modelling are supported by international soil cover guidelines that are standard practice in South Africa.

The lessons learned from international soil cover guidelines (Table 1.4) and field trials on why the functionality of a soil cover fails to meet performance expectations can mainly be ascribed to the following:

(1) *Planning:* No clearly defined and communicated cover system objectives and design criteria, gap communication between soil scientists, engineers and operators;
(2) *Design*: No dedicated soil cover design to optimise the SRC specific to protect groundwater. Lack of incorporating site-specific climate conditions and site-specific cover material properties into the design of SRC;
(3) *Construction*: Although "Guidelines for Rehabilitation of Mined Land" (Chamber of Mines of South Africa / Coaltech, 2007) includes soil cover construction and revegetation, is does not mention characterisation of borrow materials, nor construction quality assurance and fails to establish vegetation; and
(4) *Post-closure care and maintenance*: Fails to understand the long-term soil cover performance expectations, as measured against site-specific human health and safety, risk, cost and end land use.

Currently, Technical Guideline for Soil Cover Development in South Africa is not in place compared to the recent international guidelines on soil covers. It should also be noted that for compliant covers there are detailed procedures on the planning, design, construction quality assurance and performance monitoring for South Africa. Therefore, it is of key importance that similar procedures are developed and implemented for soil covers as alternative option to protect groundwater.

1.3.2 Soil cover properties

Soil properties affect the availability and movement of water as well as root development. Selecting soil is the most crucial step to design a SRC. Soil with high water-holding capacity (WHC) is considered an important factor for the success of SRCs (Hauser, 2009). Construction of soil covers may modify the soil physical properties, explaining why the hydraulic properties of soil covers are lower than the soils. In conclusion, the "ideal" soil for SCRs is a soil with slightly acidic to slightly alkaline pH, no salinity, low swelling potential, low to moderate K_{sat} and high WHC (Australian Alternative Cover Assessment Program, 2011).

1.3.2.1 *Soil texture*

Soil texture is one of the most fundamental soil physical properties and can be defined as the range of particle sizes in a soil and consists of coarse fragments, sand, silt and clay (Fernandez-illescas *et al.*, 2001). The typical soils for SRC design are sandy loam, silt loam, sandy clay loam, clay loam, silty clay loam and clay (Australian Alternative Cover Assessment Program, 2011). There are numerous studies about the SRC design and the different soil textures of monolithic SRCs that can be used (Table 1.5).

Table 1.4: Gap-analysis of the four phases for alternative soil cover development between the international and South African guidelines.

Phase	Elements	International guidelines				South African guidelines		
		Global Acid Rock Drainage Guide	Global Cover System Guidance Document	Australia[a]	Guidelines on Water Balance Cover for Waste: Principles and Practice	Best Practice Guidelines	Decision Support System on Mine Residue Facilities	Guidelines for Rehabilitation of Mined land
Planning	Regulator and stakeholder requirements	✓[b]	✓	✓	✓	✓	✓	×
	Objectives for soil cover design	✓	✓	✓	✓	×	×	×
Design	Soil cover performance criteria	×	✓	✓	✓	×	×	×
	Screening level risk assessment	✓	×	✓	✓	✓	×	×
	Site-specific climate and characterisation of site cover materials	✓	✓	✓	✓	×	×	×
	Conceptual cover design based on soil cover modelling	×	✓	✓	✓	×	×	×
	Field trials	×	✓	✓	✓	×	×	×
	Final designing based on calibrated soil cover modelling	×	✓	✓	✓	×	×	×
Construction	Cover construction criteria	×	×	✓	×	×	×	×
	Soil cover materials specifications	×	×	✓	✓	×	×	×
	Construction methods, soil cover material stripping, handling and placement	×	×	✓	✓	×	×	✓
	Vegetation establishment and weed control	×	×	✓	✓	×	×	✓
	Construction quality assurance and quality control	×	×	✓	✓	×	×	×
	Record keeping	×	×	✓	×	×	×	✓
	Soil cover construction certification	×	×	✓	×	×	×	×
Post-closure care and maintenance	Final post-closure planning	✓	✓	✓	✓	✓	×	✓
	Monitoring requirements	✓	✓	✓	✓	×	×	✓
	Long-term cover performance monitoring and evaluation	×	✓	✓	✓	×	×	×

[a]Waste Management Association of Australian guideline on phytocaps (Australian Alternative Cover Assessment Program, 2011).
[b]The correct and wrong mark indicate whether the guideline does include the element or not.

Table 1.5: List of studies of monolithic soil cover with different soil textures under semi-arid climatic conditions in the United States.

Author(s)	Site location	Average annual precipitation (mm)	Thickness (mm)	Soil texture
Albright *et al.* (2009) and Benson *et al.* (2002)	Sacramento, Calif.	434	1080 2450	Silt loam Silt loam
Benson *et al.* (2002)	Boardman, Ore.	220	1800 1500	Silt loam
McGuire & England (2000)	Central Colorado	-	1220	Clay loam
Zornberg *et al.* (2003)	California	379	1500	Sandy clay loam / clay loam

A dual-layered SRCs have normally a sandy growth medium underlaid by a water retention layer, where Yuen *et al.* (2011) conducted a five-year national research program of several SRCs in Southern Waste Depot McLaren Vale, Australia and a duel-layered SRC was designed as a sandy loam growth medium with a sandy clay loam water retention layer. A trail by Venkatraman *et al.* (2007) was carried out to evaluate two type of SRCs at Lakes Creek landfill, Rockhampton, Australia, where the growth medium was sandy loam with a sandy clay loam water retention layer.

The borrow materials to construct the SRC should have low or medium swelling potentials. Swelling clay soils can create desiccation cracks and preferential flow (Greco, 2002). The preferential flow can increase oxygen- and water ingress into the coal discard or spoil. The arrangement of particle sizes can influence the porosity of the soil. The porosity of sandy soils is less than clayey soils, since sandy soils have larger particle sizes than clayey soils (Hacke *et al.*, 2000). Therefore, soil texture influences the water movement. Hultine *et al.* (2005) found that water infiltrates faster in sandy soils than clayey soils. After the infiltration of water into the soil, the soil water moves further downward which is redistribution. The change of water content over time in sandy soils is faster due to larger and fewer pores, and only a small amount of the water is retained in the pores (Dodd & Lauenroth, 1997). To conclude, soil texture influences soil nutrient availability (Franzluebbers & Hons, 1996), infiltration rate (Mamedov *et al.*, 2001), and WHC (Chestworth, 2008) as summarised in Table 1.6.

1.3.2.2 *Bulk density*

The weight of vehicles and adoption of minimum traffic of rehabilitated coal mines highlights the importance of the impact by wheels changing the structure and volume of soil (Cannell *et al.*, 1979). The changes in volume are controlled by the mechanical stability of the soil (McNabb *et al.*, 2001) or internal forces, *e.g.* swelling and drying cycles (Bartoli *et al.*, 2007; Peng & Horn, 2005). The wide impact of bulk density on numerous soil processes have been studied by several authors and is another important soil cover property.

Table 1.6: Effect of particle size fractions on soil cover performance.

Textural fraction	Bulk density	Soil nutrient availability	Infiltration rate	Water-holding capacity
Gravel/rock	High	Decrease considerably	Increase exponential for >30–50% gravel[a]	Decrease considerably
Sand	High	Decrease	Increase	Decrease
Silt	Moderate	Increase	Decrease	Increase
Clay	Low	Increase	Decrease	Increase

[a]Gravel content greatly influences the infiltration rate (Brakensiek & Rawls, 1994).

1.3.2.2.1 *Effect of soil texture on bulk density*

Sandy soils have a higher bulk density than clayey soils (USDA, 1998). Chaudhari *et al.* (2013) found that sandy soils had a bulk density range between 1.25 and 1.80 g.cm^{-3}, whereas the bulk density of typical clayey soils reported by Neves *et al*. (2003) ranged between 1.04 and 1.62 g.cm^{-3}. However, the bulk densities of soil covers may be higher (see Section 1.3.2.2). Table 1.7 summarises the study of Chinkulkijniwat *et al.* (2010), where four different gravel contents were mixed with three soil textural classes to test the influence of gravel content on bulk density. The effect of the amount of gravel content in soil can increase the bulk density according to Babalola & Lal (1977). Rücknagel *et al.* (2013) found that high gravel content (average 6 mm) levels of more than 15–20% significantly increased the bulk density if compaction was applied. However, if the bulk density is adjusted (bulk density without gravel content), the bulk density may decrease (Stewart *et al.*, 1970), although, Flint & Childs (1984) found a moderate positive correlation between bulk density and adjusted bulk density. Moreover, in some cases, if the gravel content increases, the soil porosity increases and the bulk density decreases (Flint & Childs, 1984). These correlations were confirmed by Torri *et al.* (1994). Garga & Madureira (1985) investigated the effect of gravel on compaction characteristics and also found that the interference of ~20–25% gravel content began affecting the compaction of soil with <2 mm textural fractions. Similar results are reported by Chinkulkijniwat *et al.* (2010), while Winter *et al.* (1998) concluded the behaviour of soil matrix is determined by ~45–50% gravel content (>2 mm).

1.3.2.2.2 *Bulk density as soil compaction indicator*

Bulk density can be used as an indicator for soil compaction as well as for soil porosity (Logsdon & Karlen, 2004; Panayiotopoulos *et al.*, 1994). When soil is compacted, the bulk density increases with decreasing soil porosity as larger pores are compressed and finer pores created (Richard *et al.*, 2001). A decrease in soil porosity of compacted soils is widely reported. Blackwell *et al.* (1986) found that an uncompacted soil had ~52–59% total porosity and compacted soil had ~45–54% in the 300 mm soil layer. An experiment on loamy and acidic soils in Belgium by Herbauts *et al.* (1996) showed that increased bulk density caused decreased soil porosity in the 0–300 mm soil layer of two different sites.

Table 1.7: Summary of the effect of gravel content on soil bulk density (after Chinkulkijniwat *et al.*, 2010)

Soil texture	Gravel content (%)	ρ_b of soil mixed with fine gravel[a] ($g.cm^{-3}$)	Adjusted ρ_b of soil mixed with fine gravel[a] ($g.cm^{-3}$)	ρ_b of soil mixed with medium gravel[a] ($g.cm^{-3}$)	Adjusted ρ_b of soil mixed with medium gravel[a] ($g.cm^{-3}$)
Silty sand 1	0	1.965	1.965	1.965	1.965
	10	2.012	1.961	2.015	1.965
	20	2.060	1.956	2.061	1.957
	30.3	2.100	1.933	2.110	1.946
	40.3	2.130	1.904	2.145	1.911
Silty clay 2	0	1.770	1.770	1.770	1.770
	10	1.830	1.771	1.830	1.770
	20	1.890	1.767	1.890	1.771
	30.5	1.925	1.724	1.940	1.767
	40.6	1.955	1.666	1.980	1.742
Red clay	0	1.530	1.530	1.530	1.530
	10	1.600	1.534	1.600	1.530
	20	1.660	1.521	1.665	1.534
	32	1.720	1.481	1.740	1.526
	42.2	1.770	1.419	1.800	1.503

Note: ρ_b = soil bulk density, adjusted ρ_b = adjusted soil bulk density without gravel content.
[a]The fraction size of fine gravel is 4.75–9.75 mm and medium gravel is 9.47–18.9 mm.

Da Silva *et al.* (2008) further concluded that soil compaction increased bulk density and soil microporosity, and reduced total porosity and macroporosity.

Factors that affect soil compaction are natural phenomenon caused by freezing and drying (Fabiola *et al.*, 2003) or mechanically applied forces and soil textural classes (Bennie & Krynauw, 1985). The biggest change in these soil cover designs is that bulk density increases of the sublayer if the soil covers were not properly constructed (King, 1988). Studies by Davies *et al.* (1992) also confirmed that the high bulk density in the sublayer is a major problem. Since deep ripping of the replaced top layer is required for the rehabilitated mine land in Highveld Mpumalanga (Limpitlaw *et al.*, 1997), compaction can also occur in the top layer if the cultivation or wheeled traffic is not carefully controlled (Needham *et al.*, 2004; Soane *et al.*, 1980). Limpitlaw *et al.* (1997) reported that during soil cover construction, soil compaction can be caused by improper soil emplacement using earth scrapers, mechanical shovels, bulldozers and dump trucks (Ramsay, 1986). Blackwell & Soane (1981) reported that wheeled traffic will result in higher bulk density when running on wet soil (at optimum water content). The observations of Trouse (1966) showed that the bulk density was higher after heavy machines had run over cultivated soil than before cultivation (Table 1.8). In some cases, natural dense top layers can develop and may produce the same effects as man-made compaction.

Table 1.8: The effect of compaction on soil bulk density from different vehicles (after Trouse, 1966).

Vehicle	Average contact pressure (kPa)	ρ_b	
		Before tillage ($kg.m^{-3}$)	After tillage ($kg.m^{-3}$)
Before traffic	-	1.020	1.050
D8 crawler	62	1.080	1.190

Note: ρ_b = soil bulk density in $g.cm^{-3}$.

Soil compaction may occur in soil with different textures, but some soil texture types are more susceptible to compaction. Very high compacted soils (> 2 $g.cm^{-3}$) can be obtained if the soil has a decent amount of coarse sand (Bodman & Constantin, 1965). An experiment by Van der Watt (1972) showed that the coarse sand-silty clay mixture was more compacted compared to fine sand-silty clay mixtures if the same compaction pressure was applied. Moolman (1981) further established that high compactibility is associated with well-sorted fine sandy loams and loamy fine sands with high sand fraction. In contrast, de Lima *et al.* (2017) observed that clayey soils have a higher degree of compaction due to diminishing friction effect.

Assouline *et al.* (1997) mentioned that soil compaction is not only affected by soil texture, but can have a complex interaction with pH, SOM, CEC and clay particle thickness. They also found that one of the two soils similar in the textural analysis was more sensitive to soil compaction because of higher pH and CEC, lower SOM and coarser clay particles. El-Swaify & Emerson (1975) showed that slightly acidic soil decreased soil compaction sensitivity. In addition, studies on two soil types in a long-term field experiment, O'Sullivan (1992) found that soils with higher SOM reduce the sensitivity to soil compaction. Soane (1990) also showed that there is a negative correlation between SOM and soil compaction. Furthermore, thinner clay particles have larger surface area contact in between soil constituents, therefore higher aggregate stability reduces compaction sensitivity (Diamond & Kinter, 1956).

Overall, soil compaction has a negative impact on several soil chemical- and physical properties (Correa *et al.*, 2019). Some of the effects of soil compaction are explained in Sections 1.3.2.3.2, 1.3.3.1.2, 1.3.3.2.2, 1.3.5.1.1 and 1.3.5.2.1.

1.3.2.3 *Soil chemical properties*

The concept of soil nutrient availability can be viewed from two points. From a soil perspective, the flux of nutrient represents a nutrient supply rate (Binkley & Vitousek, 1989). Alternatively, the growth of plants can be affected by nutrient limitation or deficiencies. In agriculture, nutrient supply and nutrient limitation or deficiencies are closely linked, although some plant growth rates increase with increasing nutrient supply (Bray, 1961). In natural ecosystems, plant growth and water supply can survive with low nutrient supply rates. Several chemical properties of soil can give an insight into soil nutrient availability. Rehabilitated mines may have a close link between nutrient supply and nutrient deficiencies during the re-vegetation period, however, after the regular vegetation maintenance of 5–10 year, these systems may be similar to natural ecosystems.

In mine rehabilitation, soil acidity is not straightforward since coal discard or spoil contain large fractions of potential acidifying material which may influence the acidity of soil covers (Haigh, 1995). Acidity is a frequent occurrence in coal mines of South Africa due to high pyrite content of coal discard or spoil (Bell, 1996). Soil pH is a measure of soil acidity or alkalinity (Miller, 2016; U.S Department of Agriculture, 2006a) and can be used as an indicator for soil nutrient availability (Smith & Doran, 1996) to determine the soil's suitability for plant growth. The study of Peterson (1982) showed that if the pH increased from 4.32 to 7.83, the availability of phosphorus (P), iron (Fe), manganese (Mn), boron, zinc (Zn), and copper decreased. Peterson (1982) also found that the calcium (Ca) and magnesium increased in availability with increasing pH and nitrogen (N), and potassium (K) availability stayed relatively unaffected by pH differences. Härdtle *et al.* (2004) suggested that pH-values between 4–7 can be used as an indicator for optimal soil nutrient availability and can be associated with high CEC. In addition, a CEC close to zero may be associated with low or high pH-values (Härdtle *et al.*, 2004). The measurement of CEC is complicated and can be affected by clay and organic matter content, and pH (Robertson *et al.*, 1999). In soils high in acidity (pH < 4), CEC is likely dependant on the organic matter content and may differ considerably (Matschonat & Falkengren-Grerup, 2000; Ross *et al.*, 1991). In contrast, Smith & Doran (1996) reported that the optimum pH-values are between 5–8 for most soils. However, the optimum pH for grassland soils under semi-arid conditions are 6–8 (Troeh & Thompson, 1993). The Fertiliser Association of South Africa (2007) indicated that the optimum $pH_{(KCl)}$ for plant growth is between 6.5 to 7.4, whereas grasses can tolerant pH low as 4.1.

Another indicator for soil nutrient availability is EC (U.S Department of Agriculture, 2006b) that is a measure of the amount of salts in soils (Eigenberg *et al.*, 2000). A range of EC can be found in acid soil which is unsuitable for plant growth (Troeh & Thompson, 1993), therefore both pH and EC need to be measured. Soil salinity can greatly influence the soil physical properties and soils with EC in the saturated paste extract (EC_e) exceeding 200 $mS.m^{-1}$ are considered as slightly saline (Smith & Doran, 1996). According to Troeh & Thompson (1993), the EC_e value of 200 $mS.m^{-1}$ is equivalent to an EC for a 1:1 soil-to-water-mixture ($EC_{1:1}$) of 100–140 $mS.m^{-1}$ for coarse and fine-textured soils. Saline soils have EC_e of 400 $mS.m^{-1}$ with a pH less than 8.5. Micro-organisms vary in their tolerance to salt while microbial processes such as ammonification, nitrification and denitrification as well as chemical processes are sensitive to EC (Corwin & Lesch, 2003). A seven-year experiment at the US Meaty Animal Research Centre in the central USA, showed that EC effectively explained the dynamic changes in available N (Eigenberg *et al.*, 2002). McClung & Frankenberger (1987) reported that a non-saline soils had higher mineralisable N compared to saline soils.

Morgenthal (2003) used the $pH_{(H_2O)}$ guideline where it may not be outside the range of 5.5 to 7.5 for the soil covers of seven rehabilitated coal discard dumps at Mpumalanga Highveld. The EC_e must be lower than 200 $mS.m^{-1}$ and this threshold value for EC_e is specified by Cummings & Elliott (1991)

and Williamson *et al.* (1982) for normal grass growth. Outside these guidelines, nutrient deficiencies may become possible.

1.3.2.3.1 *Effect of soil texture on soil nutrient availability*

Soil texture can influence the soil nutrient availability. In sandy soils where the pores are large and the CEC is low and the nutrient availability is low (Zotarelli *et al.*, 2007). In contrast, clayey soils have high CEC and have higher nutrient availability (Don & Schulze, 2008; Kaiser & Zech, 2000). Duong *et al.* (2012) conducted a 77-day pot experiment in a glasshouse, South Australia, and one of the tests was soil texture effects on nutrient availability. They reported that loamy sand had greater P availability and on the other hand, sandy clay had more N availability. Moreover, they confirmed that the N availability increased when composts were incorporated into loamy sand. A study in Sulaymaniyah, Iraq, of Hamarashid *et al.* (2000) showed that total N content was high in fine-textured soils (clay loam, loam and silty clay), whereas it was lowest in coarse-textured soils (loamy sand). Fine-textured soils have more stable aggregates, which in turn may be the reason for greater total N contents (Raiesi, 2006). Gravel can greatly reduce the nutrient availability of soils. Qin *et al.* (2015) found that a soil with 2.58% gravel content had 2.41 $g.kg^{-1}$ total N, whereas a soil with 49.88% gravel content had 1.06 $g.kg^{-1}$ total N. Another study also found that a soil with 30% gravel content greatly reduced the accumulation and remobilisation of N and P (Masoni *et al.*, 2008).

1.3.2.3.2 *Effect of bulk density on soil nutrient availability*

There are numerous studies regarding the effect of soil compaction on nutrient availability. Alteration of strength properties and reduced soil porosity of compacted soil affects nutrient availability (Nawaz *et al.*, 2013) and indirectly reduces nutrient uptake with weaker root development (Kemper *et al.*, 1971). Sexstone *et al.* (1988) and Wolkowski (1990) showed that nutrient availability is dependent on soil porosity. In an experiment, a silt loam was compacted from 1.1 to 1.5 $g.cm^{-3}$ to establish a range of bulk density and a significant trend was observed where total N in soil reduced with increase in bulk density (Tan & Chang, 2007). Due to soil compaction, denitrification increases (Arah & Smith, 1989) that results in an increased emission of nitrous oxide to the air (Douglas & Crawford, 1993). According to Stepniewski *et al.* (1994), in compacted soil, denitrification is probably the most important process affecting N balance. Tan *et al.* (2008) reported a reduced available N and Douglas & Crawford (1991) found reduced N uptake by roots in compacted soils. However, the available N can be increased by N fertilisers applications in compacted soil.

Table 1.9 summarises the effect of bulk density on P and K concentration. A number of studies have shown that there is a relationship between reduced soil porosity and decreased availability of K. In compacted conditions, it may be difficult to determine whether decreased K is caused by diffusion or uptake by root or if the K availability is lower (Lawton, 1946).

Table 1.9: Effect of soil bulk density on phosphorous and potassium concentration on an unfertilised soil.

ρ_b (g.cm^{-3})	P[a] %	K[b]
1.25	-	1.68
1.40	0.13	
1.45	-	1.48
1.50	0.14	
1.60	0.13	
1.80	0.18	

Note: ρ_b = soil bulk density, P = phosphorous, K = potassium.
[a]After Mu'azu & Skopp (1986).
[b]After Hallmark & Barber (1981) and the silt loamy soil was in Purdue Agronomy Farm, USA.

Silberbush *et al.* (1983) further concluded that availability of K and total K uptake in unfertilised and compacted soil is lower. Parlak & Parlak (2011) found that macro elements N and K decreased while P increased with increasing bulk density in soil. While diffusion of P may increase with increasing bulk density, the P uptake may lessen due to weaker root growth (Barley & Rovira, 1970). Kristoffersen & Riley (2005) observed that the relative degree of compaction of 75% decreased the total P uptake (mg P root^{-1}) of all three soil textures, namely loam, clay loam and silt, while the P uptake increased at degree of compaction of 90% which can attributed to higher P diffusion.

1.3.3 Soil hydraulic properties

Since SRCs strive to work with the forces of nature rather than control them, these covers rely on evapotranspiration and WHC. One of the main criteria of SRCs is to hold enough water to minimise water movement (Zornberg *et al.*, 2003) and meet the requirements of the site. As soil texture, SOM (Nemes *et al.*, 2005) and bulk density can influence the soil hydraulic properties, ageing of covers is also a factor. Hydraulic properties are often used to determine the long-term performance of soil covers (Fayer *et al.*, 1992). However, these hydraulic properties are measured on laboratory-compacted samples and may not reflect the conditions of soil covers in the field with long exposure to environmental conditions. Post-construction processes *viz.* wetting and drying, root growth and worms burrowing holes can create preferential water flow and alter the hydraulic properties of soil (Buol *et al.*, 1997). Changes of soil formation over time can reduce the bulk density with increasing soil porosity and in turn, increasing soil hydraulic properties (Othman & Benson, 1993). A limited amounted of research has been done on changes in hydraulic properties of SCRs over time (Benson *et al.*, 2007; Khire *et al.*, 2000; Waugh *et al.*, 1994; Zornberg *et al.*, 2003). Table 1.10 summarises the changes of soil hydraulic properties of SRCs over time.

1.3.3.1 *Saturated hydraulic conductivity*

Saturated hydraulic conductivity is one of the most important hydraulic properties that determine water flow in soil (Hao *et al.*, 2019). In particular, K_{sat} regulates the precipitation portioning processes between surface runoff and recharge water, water uptake and plant growth, and the risk of seepage impact on groundwater (Jarvis *et al.*, 2013). Understanding K_{sat} is critical during SRC design and

whether the SRC system meets the objective over long term performance. A well-constructed SRC is considered as a massive soil structure hierarchy that can minimise the environmental pollution arising from preferential flow of water (Jarvis *et al.*, 2012). Under agricultural conditions, Jarvis *et al.* (2013) found a weak correlation of K_{sat} with soil texture in the 0–300 mm soil layer, but a strong correlation with bulk density and SOM. However, García-Gutiérrez *et al.* (2018), Papanicolaou *et al.*, 2015 and Singh *et al.* (2014) found that soil texture significantly affects K_{sat} and may differ under different climate and field conditions

1.3.3.1.1 *Effect of soil texture on saturated hydraulic conductivity*

Table 1.11 shows the effect of soil texture on K_{sat} of soils reported on by several authors. Only the K_{sat} of loamy fine sand, sandy loam, loam, sandy clay loam, clay loam and clay is reported since they are considered relevant to SRCs in this study. Soil texture strongly control K_{sat} (Hacke *et al.*, 2000) since K_{sat} is a function of pore size (Hultine *et al.*, 2006). Coarse-textured soils with larger pores have higher K_{sat} than fine-textured soils. Reynolds *et al.* (2000) concluded that the K_{sat} of sandy soils was 300 times higher than clayey soils. Karki *et al.* (2018) noted a significant trend between K_{sat} and soil texture. High gravel content can increase the K_{sat} due to a higher amount of larger pores than in sandy soils and may create preferential flow (Abrahams & Parsons, 1991).

Ferrer Julià *et al.* (2004) found a significant strong and positive relationship between K_{sat} and sand content, while K_{sat} had a significant moderate, negative relationship with silt and clay content. A strong and negative relationship between K_{sat} and clay content was reported by Gülser & Candemir (2008). In contrast, Gamie & De Smetd (2018); Li *et al.*, 2007 and Wang *et al.* (2012) found no relation between K_{sat} and particle-size distribution.

1.3.3.1.2 *Effect of bulk density on saturated hydraulic conductivity*

Numerous studies indicate that increased bulk density is associated with decreased macroporosity in coarser soils and consequently decreased $K_{sat.}$ Variations of K_{sat} will occur since bulk density has an interaction with soil texture, structure and SOM. A study evaluated the effects of three levels of compaction on soil hydraulic conductivities of two silty loam soil from the Loess Plateau, China and found that as the soil compaction increased, K_{sat} decreased (Zhang *et al.*, 2006). Dec *et al.* (2008) reported that as the bulk density increased from 1.2 to 1.6 g.cm^{-3}, K_{sat} decreased in identical soil textures. From a loose to compacted soils range, the K_{sat} with bulk density relationship ranges from high to low (Guérif *et al.*, 2001). Olorunfemi & Fasinmirin (2011) found a Pearson correlation coefficient (r) of 0.94 between K_{sat} and bulk density of different soils.

Assouline (2006) reported that the effect of compaction on K_{sat} is more pronounced for sandy soils. According to Lipiec & Hatano (2003), active macropores have a significant effect on the water infiltration, where more macropores can increase the infiltration rate. Approximately 10% of macropores and mesopores contributed about 98% of water flux under saturated flow in soil (Lin *et al.*, 1996). In an experiment of Håkansson & Lipiec (2000), the volume of active macropores decreased significantly with increasing soil compaction by wheeled traffic.

Table 1.10: Effect of ageing on soil hydraulic properties of store-and-release covers in United States (after Benson *et al.*, 2007)

Site location	Soil texture	Particle size distribution				Initial		After two years		After three years		After four years	
		Gravel (%)	Sand (%)	Silt (%)	Clay (%)	K_{sat}	θ_s	K_{sat}	θ_s	K_{sat}	θ_s	K_{sat}	θ_s
Altamont, Calif.	SiCL	1.449	3.623	67.391	27.536	4.579×10^{-4}	0.36	-	-	6.186×10^{-2}	0.37	-	-
Boardman, Ore.	SiL	0.000	14.286	75.000	10.714	1.037×10^{-2}	0.39	2.419×10^{-2}	0.39	3.110×10^{-2}	0.41	-	-
Helena, Mont.	L	1.538	41.538	33.846	23.077	1.300×10^{-4}	0.34	-	-	7.214×10^{-5}	0.44	4.842×10^{-2}	0.49
Marina, Calif.	SL	6.957	52.174	27.826	13.043	7.430×10^{-5}	0.31	-	-	2.678×10^{-1}	0.43	-	-
Sacramento, Calif.	SiL	1.681	18.487	63.866	15.966	2.678×10^{-4}	0.29	-	-	-	-	3.974×10^{-2}	0.43

Note: SL = Sandy loam, L = Loam, SiL = Silt loam, SiCL = Silty clay loam, K_{sat} = saturated hydraulic conductivity in $m.d^{-1}$, θ_s = saturated volumetric water content in $m^3.m^{-3}$.

Table 1.11: Effect of soil texture on saturated hydraulic conductivity ($m.d^{-1}$) of soils adapted from several authors.

Soil texture	Clapp & Hornberger (1978)	Bouma *et al.* (1979)	Rawls *et al.* (1982)	Rawls *et al.* (1998)	Bagarello *et al.* (1999)	Reynolds *et al.* (2000)	Shwetha & Varija (2015)	García-Gutiérrez *et al.* (2018)
Loamy fine sand	3.499	-	1.466	1.492	-	-	-	2.362
Sandy loam	1.058	-	0.622	1.339	-	-	1.376	1.181
Loam	0.620	-	0.317	0.094	-	-	-	1.361
Sandy clay loam	0.214	-	0.103	0.185	-	-	-	0.782
Clay loam	0.062	0.050	0.055	0.101	-	0.0218	-	0.379
Clay	0.048	0.001–5.000[a]	0.014	0.048	0.402[b]	-	-	0.977

[a]Different saturated hydraulic conductivities of clayey soils are due to swelling and shrinkage.
[b]The clayey soils were characterised with a vertical shrinkage cracks developed at the soil surface.

Moreover, a regression equation with macroporosity explained the variation in K_{sat}, where K_{sat} decreased with decreasing in macroporosity (Kim *et al.,* 2010).

1.3.3.2 *Soil water retention curves*

In general, SWRCs are the other key hydraulic property used in many applications in the field of soil science and geotechnical engineering (Too *et al.*, 2014). Soil water retention curves are important for soil and water management practices during cultivation (Seema Dahiya & Phogat, 2019) or designing SRCs (Hauser, 2009). Soil water retention curves are usually used (1) to determine the AWC of soil, *e.g.*, for soil cover design (Khire *et al.*, 1997) or irrigation purposes (Gradwell & Rijkse, 1988); (2) to ascertain the relation between SWRCs and other soil properties (Rawls *et al.*, 1991); (3) to observe changes in soil structure caused by ripping, mixing soil layers, etc. (Ferreira *et al.*, 2019); and (4) to determine the drainable pore space for a drainage design/modelling (Zhang *et al.*, 2018b). Soil water retention curves characterised by soil water content and potential are not unique and can be affected by several environmental and soil factors.

While the SWRCs are central to the application of unsaturated flow, the following characteristics of a SWRC are used for unsaturated flow modelling: (1) Soil water retention to retain infiltrated rain in the water retention layer (sublayer) of SRCs for evapotranspiration (water retention increases considerably with increasing silt- and clay content and SOM, and gravel and medium- and coarse sand content have low water retention capacities); (2) WHC to store infiltrated rain in the soil cover during wet periods for evapotranspiration during dry periods (WHC increases with increasing soil water retention, but can decrease with soil compaction); (3) capillary potential required for (deep) infiltrated rain to move upwards to the surface under evaporative demand for evaporation (capillary potential increases with increasing soil water retention); and (4) AWC which increases with increasing WHC of growth medium (top layer). In general, water ingress rates into a facility decreases with increasing soil water retention, WHC, capillary potential and AWC. A number of parameters can be determined from a water retention curve, which are shown in Figure 1.2.

1.3.3.2.1 *Effect of texture on soil water retention curves*

Table 1.12 summarises the effect of soil texture on WHC. Water holding capacity is strongly related to the size of soil particles. The water molecules hold more tightly to the finer particles of clayey soil than to coarser particles of sandy soils. Since soil texture influences the SWRCs, Chestworth (2008) stated that at field capacity (FC) sandy soils retain less water than clayey soils. Olorunfemi & Fasinmirin (2011) concluded that WHC increases with increasing finer fraction in soil. Soils with clay content and SOM have higher WHC according to Kar *et al.* (2017). Soil organic matter can influence the SWRCs, where increases in SOM led to an increase in WHC in sandy soils (Rawls *et al.*, 2003). Nath (2014) found that sand content had a negative correlation coefficient (r = -0.78), whereas clay content and SOM had a positive coefficient correlation of 0.80 and 0.82 with WHC, respectively.

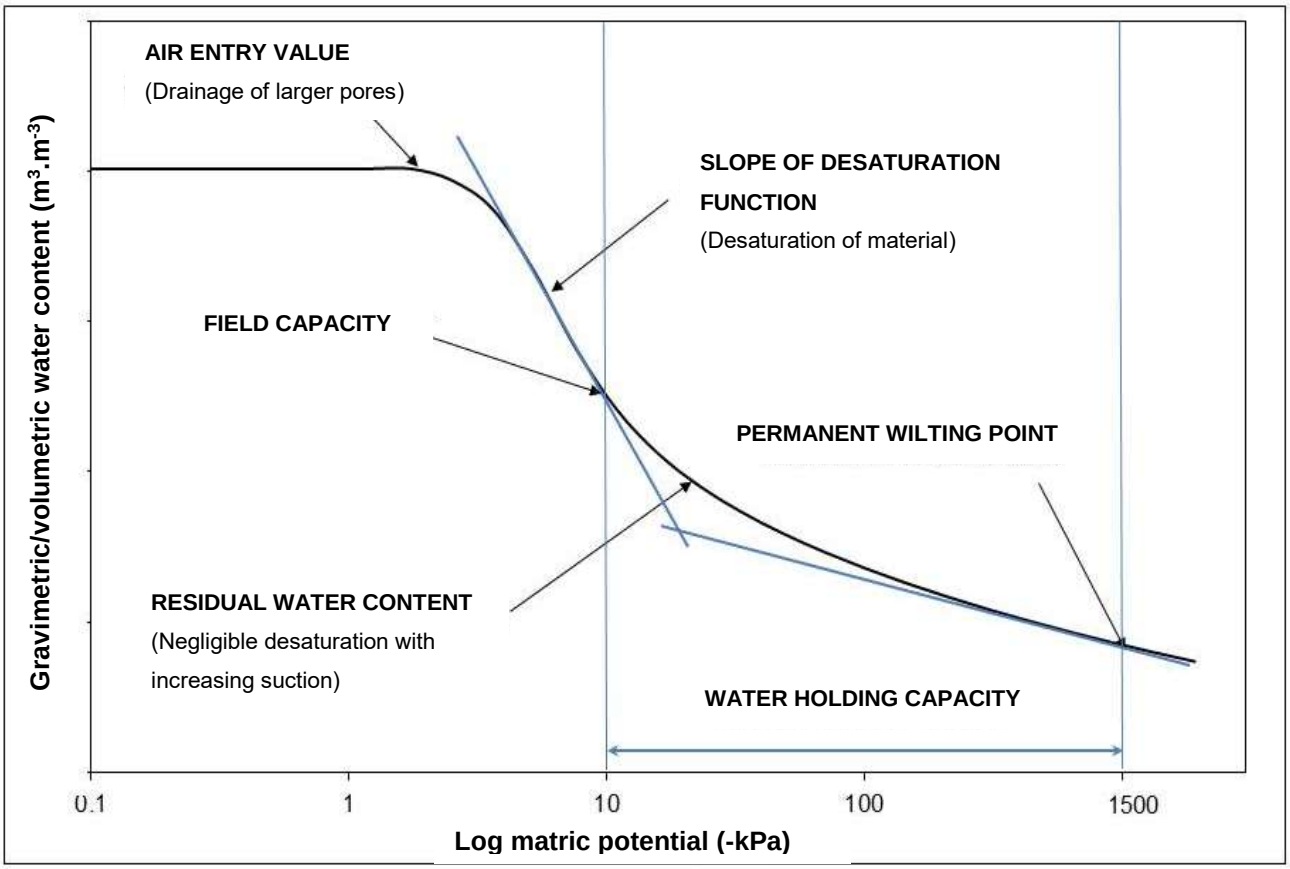

Figure 1.2: Number of parameters that can be determined from a soil water retention curve (Hillel, 2004).

Therefore, it is expected that the permanent wilting point (PWP) and WHC of sandy soils are lower than in clayey soils (Bandaranayake *et al.*, 2007).

1.3.3.2.2 *Effect of bulk density on soil water retention curves*

Soil compaction can significantly change the SWRCs (Van Wesenbeeck & Kachanoski, 1988). According to Dec *et al.* (2008), the increasing bulk density reduces soil porosity and affects the ability of soil to conduct water under unsaturated conditions.

Increasing bulk density can decrease the soil water content at low matric potentials (Kojima *et al.*, 2018; Singh *et al.*, 2015). The effect of soil compaction on SWRCs is illustrated in Figure 1.3. Smith *et al.* (2001) observed a flattened S-shaped SWRC in all cases of soil compaction. Croney & Coleman (1954) stated the following: (1) at high matric potential, the amount of water held decreases; (2) the amount of water held decreases at air-entry level; and (3) at low matric potential, the amount of water held increases. Similar observations are also reported by Gupta *et al.* (1989) and O'Sullivan & Ball (1993). Hill & Summer (1967) further explained that soil compaction has the greatest effect at high matric potentials in sandy soils, while having an effect at low matric potentials in clayey soils. Since soil compaction decreased soil macroporosity at high matric potentials, the air-entry value increased according to Aschonitis *et al.* (2012). In contrast, Reeve *et al.* (1973) noticed increased soil compaction with decreasing air-entry value. It is important to note that in some cases, the increased bulk density may increase the volumetric water content, but reduce the gravimetric water content (Archer & Smith, 1973).

Table 1.12: List of studies of disturbed soils of different textures and their water holding capacity (WHC) in the 0–60 cm soil layer.

Author(s)	Soil texture	ρ_b (g.cm^{-3})	Sand (%)	Silt (%)	Clay (%)	WHC (% Vol.Vol^{-1})
Mohamed *et al*. (2016)	Loamy sand	1.57	76.8	18.1	4.8	14
Olorunfemi & Fasinmirin (2011)	Sandy loam	-	-	-	-	25
Basso *et al*. (2013)		1.41	68.2	25.1	6.7	16
Deb *et al.* (2014)	Loam	1.22–1.45	48.0–50.0	31.0–36.5	21.0–13.5	33.0–65.7
Olorunfemi & Fasinmirin (2011)	Sandy clay loam	-	-	-	-	37
Deb *et al.* (2014)		1.08–1.36	47.0–60.0	24.0–34.0	14.0–27.0	42.8–63.7
Viji & Rajesh (2012)	Clay loam	1.19	35.4	35.5	14.0	29.3
		1.19	46.9	25.3	21.3	30.7
Deb *et al.* (2014)		1.09–1.14	30.0–40.0	30.0–41.5	28.5–34.0	56.0–72.6
Sun & Lu (2014)	Clay	-	26.0	30.7	43.3	30

Furthermore, the AWC can respond to soil compaction in three ways: (1) in most soils, increased soil compaction causes decreased AWC; (2) in some sandy and clayey soils, increased soil compaction can increase AWC; and (3) increased soil compaction with increasing AWC can progress to a point after which it declines (Smith *et al.*, 2001). Agrawal (1991) observed that soil compaction in sandy soils can have favourable effects on SWRCs, however, the compaction in the sublayer is less effective than in the top layer.

1.3.4 Pedotransfer functions for soil hydraulic properties

Since variations of soil texture and bulk density influence the soil hydraulic properties, the variability of soil factors can increase the uncertainty of predictions. As a result, soil scientists or geotechnical engineers developed models for defining soil hydraulic properties using mathematical or soil physical properties (Carsel & Parrish, 1988). This information can be used to determine the probability of potential long-term soil cover performance. To determine soil hydraulic properties are expensive and time-consuming, therefore inexpensive and rapid methods are needed (Alvarez-Acosta *et al.*, 2012). For these reasons, pedotransfer functions (PTFs), such as multiple linear regression (MLR), calculated from easily measured soil physical properties (Bouma, 1989) will be discussed in the section below.

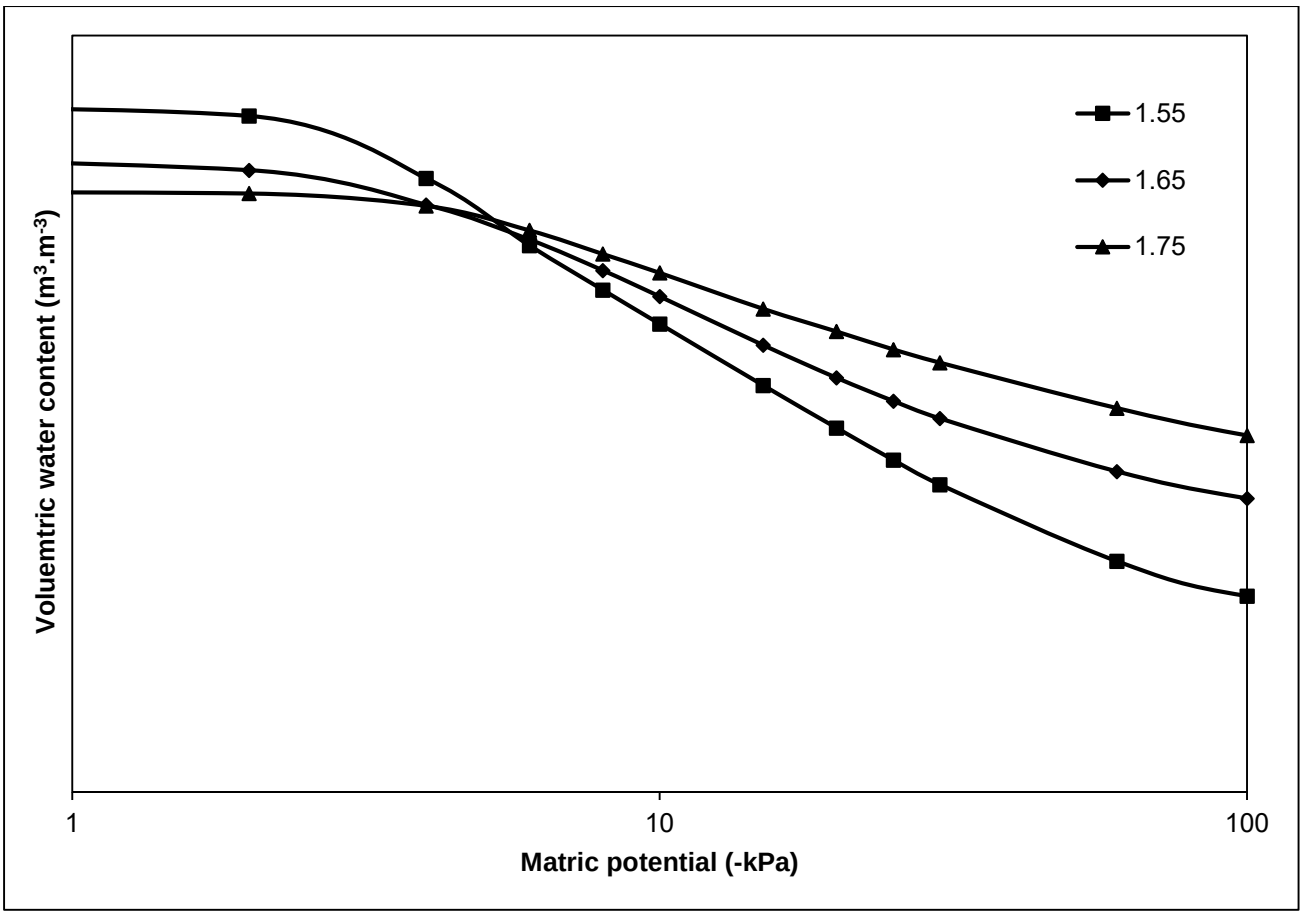

Figure 1.3: The effect of soil compaction on the soil water retention curve of fine sandy loam soil at different soil bulk density values in g.cm^{-3} (after Bennie & Burger, 1979).

There are several reports on PTF development all over the globe and consistent research interest exist in PTFs (Givi *et al.*, 2004; Zhang *et al.*, 2019). Pedotransfer functions can be empirical in nature and therefore force researchers to develop site-specific PTFs for different applications (Patil & Singh, 2016). Methods of PTF development can be grouped into two types: (1) mechanistic and (2) empirical approaches (Patil & Singh, 2016). In the latter type, the general form of MLR is:

Predicted K_{sat} or θ_p = a*Sand + b*Silt + c*Clay + d*Soil organic matter + e*Soil bulk density + … + x*variable X [Eq. 1.1]

where predicted K_{sat} is predicted saturated hydraulic conductivity, θ_p is predicted water content at selected matric potential and a, b, c, d, e and x are regression coefficients. Variable X is any other soil property that can be easily be measured and which is not time-consuming. The empirical approaches also attempt to develop a relationship between the hydraulic properties and soil properties. In addition, Minasny *et al.* (1999) used different approaches such as MLR, nonlinear regression and artificial neural network, but found MLR and nonlinear regression the appropriate tools to predict soil hydraulic properties.

1.3.4.1 *Saturated hydraulic conductivity*

The most commonly used input parameters to express the relationship with K_{sat} are sand-, silt- and clay content. Because the large amount of PTFs is based on soil texture information, only the commonly used as well as some recently developed MLR models, are listed in Table 1.13. The relation between particle-size distribution and K_{sat} may be imperfect as Wösten *et al.* (2001) mentioned that strongly structured soil can determine the soil properties in predicting K_{sat}. Tomasella & Hodnett (1997) and Romero-Ruiz *et al.* (2018) mentioned that bulk density or soil porosity provide limited information regarding soil structure. The MLR models of Gamie & De Smedt (2018) showed that soil structure was more related to K_{sat} than soil texture was, and Griffiths *et al.* (1999) and Lilly (2000) reported similar results. However, soil covers are man-made soils and in general, the soil structure for monolithic or duel-layered SRC at Mpumalanga Highveld, South Africa is characterised as massive or moderate soil structure, where structure does not have a big effect on K_{sat}.

Since the bulk density is negatively correlated with K_{sat}, Zhang *et al.* (2018a) have shown that with bulk density is an additional input parameter, the coefficient of determination (R^2) increased between predicted and measured K_{sat} from ~0.45 to 0.55. Pachepsky & Park (2015) further suggested that splitting the data sets into high and low bulk density groups may be advantageous in data-poor environments or large-scale projects. Pedotransfer functions that used bulk density or soil porosity as an input parameter were developed by Rawls & Brakensiek (1985), Vereecken *et al*. (1990), Jabro (1992), Salchow *et al.* (1996), Wösten *et al.* (1999), Li *et al.* (2007), Gülser & Candemir (2008) and Arshad *et al.* (2013). Bulk density has sometimes a negative correlation with SOM (Heuscher *et al.*, 2005) and Wagner *et al.* (2001) showed that the PTFs with SOM as an input parameter performed better than PTFs without SOM. The PTFs using SOM are those recommended by Wösten *et al.* (1999) and Li *et al.* (2007).

Regions with similar soil physical properties can have good results using PTFs developed from regional data sets. For example, the PTF of Dane & Puckett (1994) predicted accurate K_{sat} values for sandy soils in Australia (Minasny & McBartney, 2000). Pedotransfer functions developed for soils in the southern regions of USA (Jabro, 1992) were applicable for the soils in Naghadeh country, Azarbaijanegharbi province, Iran (Rasoulzadeh, 2011). However, Schaap & Leji (1998) mentioned that the use of PTFs under different environmental conditions must be exercised with caution.

1.3.4.2 *Soil water retention curves*

When the parameters of SWRC or conductivity functions are estimated, it is termed parametric PTFs (Børgesen & Schaap, 2005), whereas predicting water content at selected matric potential points in the SWRC is termed point PTFs (Ghanbarian-Alavijeh & Millán, 2010). According to Patil & Singh (2016), the point PTFs can give a good insight into the relevance of soil properties. Another advantage of point PTFs is that a fairly accurate prediction can be made at specific points of a SWRC.

Table 1.13: Pedotransfer functions of several authors using the multiple linear regression models from easily determined soil physical properties to predict saturated hydraulic conductivity.

Author(s)		Multiple linear regression model	R^2
Cosby *et al.* (1984)	K_{sat}	$= 25.4\times10^{(-0.600 + 0.013*Sand - 0.006*Clay)}$	0.81~0.87
Rawls & Brakensiek (1985)	K_{sat}	$= 10*exp(-8.938 + 19.525*p - 0.028*Clay + 1.811\times10^{-4}*Sand^2 - 9.143\times10^{-2}*Clay^2 - 8.395*p^2 + 0.078*Sand*p - 0.003*Sand^2*p^2 - 0.019*Clay^2*p^2 + 1.730\times10^{-5}*Sand^2*Clay + 0.027*Clay^2*p + 0.014*Sand^2*p)$	0.43
Saxton *et al.* (1986)	K_{sat}	$= 2.778\times10^{-3}\{exp[A + (B/\theta_s)]\}$	0.95
	A	$= 12.012 - 0.076*Sand$	
	B	$=-3.895 + 0.037*Sand - 0.110*Clay + 8.755\times10^{-4}*Clay^2$	
	θ_s	$= 0.332 - 7.251\times10^{-4}*Sand + 0.128*log(Clay)$	
Vereecken *et al.* (1990)	K_{sat}	$= 0.417*exp[20.620 - 0.960*ln(Clay) - 0.660*ln(Sand) - 0.460*ln(SOM) - 8.430*ln(\rho_b)]$	0.26
Jabro (1992)	K_{sat}	$= 10*10^{[9.650 - 0.810*\log(Silt) - 1.090*\log(Clay) - 4.640*\rho_b]}$	0.68
Dane & Puckett (1992)	K_{sat}	$= 4.660\times10^{-3}exp(-0.198*Clay)$	0.72~0.77
Campbell & Shiozawa (1992)	K_{sat}	$= 54exp(-0.070*Sand - 0.167*Clay)$	0.75
Salchow *et al.* (1996)	K_{sat}	$= 10^{0.070*Sand + 0.073*Silt + 0.043*Clay + 0.334*SOM - 4.694*\rho_b}$	0.58
Wösten *et al.* (1999)	K_{sat}	$= 0.417*exp[8.685 + 0.035*Silt - 0.967*\rho_b^2 - 0.001*Clay^2 - 0.0003*Silt^2 + 0.001Silt^{-1} - 0.075*SOM^{-1} - 0.064*ln(Silt) - 0.014*\rho_b*Clay -0.167*\rho_b*SOM + 0.030*Clay - 0.033*Silt]$	0.19
Li *et al.* (2007)	K_{sat}	$= 0.422*[2.718^{13.626 - 1.914*\ln(Sand) - 0.974*\ln(Silt) - 0.058*Clay - 1.709*\ln(SOM) + 2.885*SOM - 18.026*\ln(\rho_b)}]$	0.58~0.74
Gülser & Candemir (2008)	K_{sat}	$= 10*(11.200 + 0.026*Silt - 0.282*Clay + 26.500*\rho_b - 0.002*Silt^2 + 0.003*Clay^2 - 12.800*\rho_b^2)$	0.87
Arshad *et al.* (2013)	K_{sat}	$= 0.422*[2.718^{14.660 - 0.440*\ln(Sand) - 1.370*\ln(Silt) - 1.250*\ln(Clay) - 2.800*\ln(\rho_b)}]$	0.50

Note: R^2 = coefficient of determination, K_{sat} = saturated hydraulic conductivity ($mm.hr^{-1}$), Sand = % of sand content, Silt = % of silt content, Clay = % of clay content, SOM = % of soil organic matter, ρ_b = soil bulk density in $g.cm^{-3}$, p = fraction of porosity.

The disadvantages of point PTFs are that a large number of regression equations are required to complete a SWRC and outputs may be tabular (Wösten *et al.,* 2001). The empirical approach of Eq. 1.1 for predicting SWRC requires prior knowledge about the relationship between input parameters and soil water content at selected matric potential.

The PTFs for predicting SWRC are shown in Table 1.14. Using particle-size distribution as input parameters, Husz (1967) developed relationships that describe SWRC between -33 and -1500 kPa. Soil water content at high matric potentials is dominated by sand- and silt content (Chen, 2018), while clay is more dominant at lower matric potentials (Abrol *et al.*, 1968). Rawls *et al.* (1982) also found these typical trends in their regression equations at selected matric potentials. In contrast,

Gupta & Larson (1979) and Puckett *et al.* (1985) used sand- and clay content from -4 to -1500 kPa in their regression equations. However, Puckett *et al.* (1985) found that total soil porosity and bulk density played important roles at 0 and -1 kPa matric potentials. Moreover, Gupta & Larson (1979) utilised SOM and bulk density for all 12 matric potentials, whereas the PTFs of Rawls *et al.* (1982) only had bulk density at -4 and -7 kPa matric potentials. Only the commonly and well-developed MLR models are discussed in this current study which also include high matric potentials near saturation. These PTFs have matric potentials of up to 10 or more that are needed to have a fully described SWRC. The most recently MLR models as point PTFs have more or less matric potentials at -10, -33, -100, -300, -500, -100, -1500 kPa (Babaeian *et al.*, 2015; Ghanbarian-Alavijeh & Millán, 2010; Phuong *et al.*, 2014; Shwetha & Varija, 2013) which were not included. Furthermore, some of these recent PTFs also included other soil properties which may not be easily available.

Parametric PTFs have gained more popularity due to the fact that the SWRC can be depicted as continuous curves (Scheinost *et al.*, 1997). However, Tomasella *et al.* (2003) and Shwetha & Varija (2013) compared point and parametric PTFs and found that the approach to estimate soil water content at certain matric potential provided better results. Ghanbarian-Alavijeh & Millán (2010) also found that the root mean square value of point PTFs are lower than the parametric approach. A possible explanation is that the soil water content is controlled by different independent soil variables at different matric potential ranges of SWRC. Another feasible explanation is that the relationship between water retention parameters and soil physical properties is too complex to be described by the parametric method. Predicting SWRC by using published PTFs are not recommended when the soils that are outside the range of those soils from which the PTFs were derived. Consequently, caution must be exercised when using the published PTFs.

1.3.5 Vegetation properties

During soil cover construction, the upper layer or growth medium of a SRC is usually been ripped and seeded with a mixture of native grasses or trees. Store-and-release covers are depending on evapotranspiration and the objectives of good vegetation covers are: (1) well-adapted to the ecosystem; (2) capable of high transpiration rates; (3) limit soil erosion and prevent soil loss; and (4) functionally resilient (Chamber of Mines of South Africa / Coaltech, 2007; Waugh *et al.*, 2008). Rehabilitated soils are often inferior to the natural profile due to compaction and mixing the growth medium with the subsoil horizon and therefore fertilisation is important. The University of Queensland (2012) observed that when the total vegetation cover is below 50%, the changes in vegetation composition have less influence on soil cover performance. They further concluded that vegetation densities are not likely to exceed 30% under semi-arid conditions. A good ground cover will optimise evapotranspiration with a well-developed root system optimising the water uptake (Tracy *et al.*, 2013) and improve the soil cover's performance.

Table 1.14: Point pedotransfer functions of several authors using the multiple linear regression models from easily soil physical properties to predict soil water content ($mm^{1}.mm^{-1}$) at selected matric potentials.

Author(s)	Matric potential (-kPa)	Parameter estimates								R^2
		Intercept	Sand	Fine sand	Silt	Clay	SOM	ρ_b	p	
Gupta & Larson (1979)[a]	4		7.053		10.242	10.070	6.330	-32.120		0.95
	7		5.678		9.228	9.135	6.103	-26.960		0.96
	10		5.018		8.548	8.833	2.966	-24.230		0.96
	20		3.890		7.066	8.408	2.817	-18.780		0.96
	33		3.075		5.886	8.039	2.208	-14.340		0.96
	60		2.181		4.557	7.557	2.191	-9.276		0.96
	100		1.563		3.620	7.154	2.388	-5.759		0.97
	200		0.932		2.643	6.636	2.717	-2.214		0.97
	400		0.483		1.943	6.128	2.925	-0.204		0.96
	700		0.214		1.538	5.908	2.855	1.530		0.95
	1000		0.076		1.334	5.802	2.653	2.145		0.95
	1500		-0.059		1.142	5.766	2.228	2.671		0.95
Rawls *et al.* (1982)	4	0.790	-0.004				0.010	-0.134		0.58
	7	0.715	-0.003			0.002		-0.169		0.74
	10	0.412	-0.003			0.002	0.032			0.81
	20	0.312	-0.002			0.003	0.031			0.86
	33	0.258	-0.002			0.004	0.030			0.87
	60	0.207	-0.002			0.004	0.028			0.87
	100	0.035			0.001	0.006	0.025			0.87
	200	0.028			0.001	0.005	0.020			0.86
	400	0.024			0.001	0.005	0.019			0.84
	700	0.022			0.001	0.005	0.018			0.81
	1000	0.021			0.001	0.005	0.016			0.81
	1500	0.026				0.005	0.016			0.80
Puckett *et al.* (1985)[a]	0	-0.706						0.264	1.600	0.79
	1	-0.834						0.318	1.690	0.79
	5	0.410	-3.570	1.930		1.820				0.92
	10	0.415	-3.830	0.712		2.430				0.94
	30	0.365	-3.480	0.059		3.210				0.93
	60	0.330	-3.190	0.003		3.510				0.92
	100	0.310	-3.020	0.019		3.620				0.92
	500	0.265	-2.620	0.140		3.750				0.93
	1000	0.264	-2.440	0.197		3.780				0.93
	1500	0.239	-2.390	0.254		3.800				0.93

Note: R^2 = coefficient of determination, Sand = % of sand content, Fine sand = % of fine sand (0.25–0.106 mm), Silt = % of silt content, Clay = % of clay content, SOM = % of soil organic matter, ρ_b = soil bulk density in $g.cm^{-3}$, p = fraction of porosity.

[a]The parameter estimates of sand-, fine sand-, silt-, clay content, SOM and ρ_b are $\times 10^{-3}$.

A poor vegetation cover results in low transpiration as well as a decrease in the soil-plant conductance (Botha *et al.*, 1983). Vegetation covers do not only increase the long-term soil cover performance, but also decrease runoff and erosion (Harris *et al.*, 1996). Luo *et al.* (2020) found a strong and positive correlation coefficient between surface runoff and annual sediment yield and recommend a good vegetation cover to reduce the surface runoff. O'Kane & Ayres (2012) reported that the vegetation cover of SRC needs to mimic or replicate the existing native vegetation in the surrounding areas. In the South African guideline, "Guidelines for the Rehabilitation of Mined Land" (Chamber of Mines of South Africa / Coaltech, 2007), highlighted that species selected should meet the ecosystem objectives which are usually grasslands. Based on practical considerations, planting should be done when climatic conditions will likely ensure rehabilitation success. This guideline further explains the methods of establishing vegetation and vegetation monitoring.

1.3.5.1 *Root development*

A deep or thicker soil layers provide an ideal opportunity for deep rooting depth (Lopes & Reynolds, 2010). Rooting in thinner soil layers can often be restricted by subsurface compaction or non-uniform compaction (Bengough *et al.*, 2006). Botha & Bennie (1982) observed a deeper root system in thicker soils than in thinner soils and thinner soils have lower AWC. Venkatraman & Ashwath (2010) found that a thicker SRC perform better with deeper rooting systems than a thinner SRC. Another observation by White & Kirkegaard (2010) showed that deep roots were found where bulk density throughout in the soil profile is uniform.

1.3.5.1.1 *Interacting effect of soil texture and bulk density on root development*

Under prolonged water infiltration, a severely compacted soil layer can cause anaerobic conditions and may lead to ethylene production causing severe root damage (Campbell & Moreau, 1979). The elongation rate of root growth is determined by which extent the root pressure exceeds the mechanical resistance of soil. Soil resistance increases with increasing bulk density (Stošić *et al.*, 2020) and Figure 1.4 illustrates how soil compaction affects the root growth of plants. In compacted soils, the root volume was 27.8% less than in non-compacted soils (Tracy *et al.*, 2012). Taylor & Brar (1991) stated that changes in soil compaction may not directly affect root development, but indirectly through changes in structural arrangements and root volume. Głab (2013) conducted a field experiment of soil compaction on meadow-grass root development and found that the soil compaction significantly changed the root arrangements, *e.g.* distortion, in the upper 0–50 mm soil layer.

A pot trial filled with clay loam soils and grass plants showed that, as the bulk density increased, the root length and root surface area decreased (Parlak *et al.*, 2011). A compacted soil can increase in the root diameters (thicker roots) and higher root density in the upper/top layer (Materechera *et al.*, 1992; Popova *et al.*, 2016). Twum & Nii-Annang (2015) studied the effect of soil compaction on root density in Lusatia, Germany and found that the root density in the upper/top layer of a compacted soil was two-fold greater compared to the uncompacted soil.

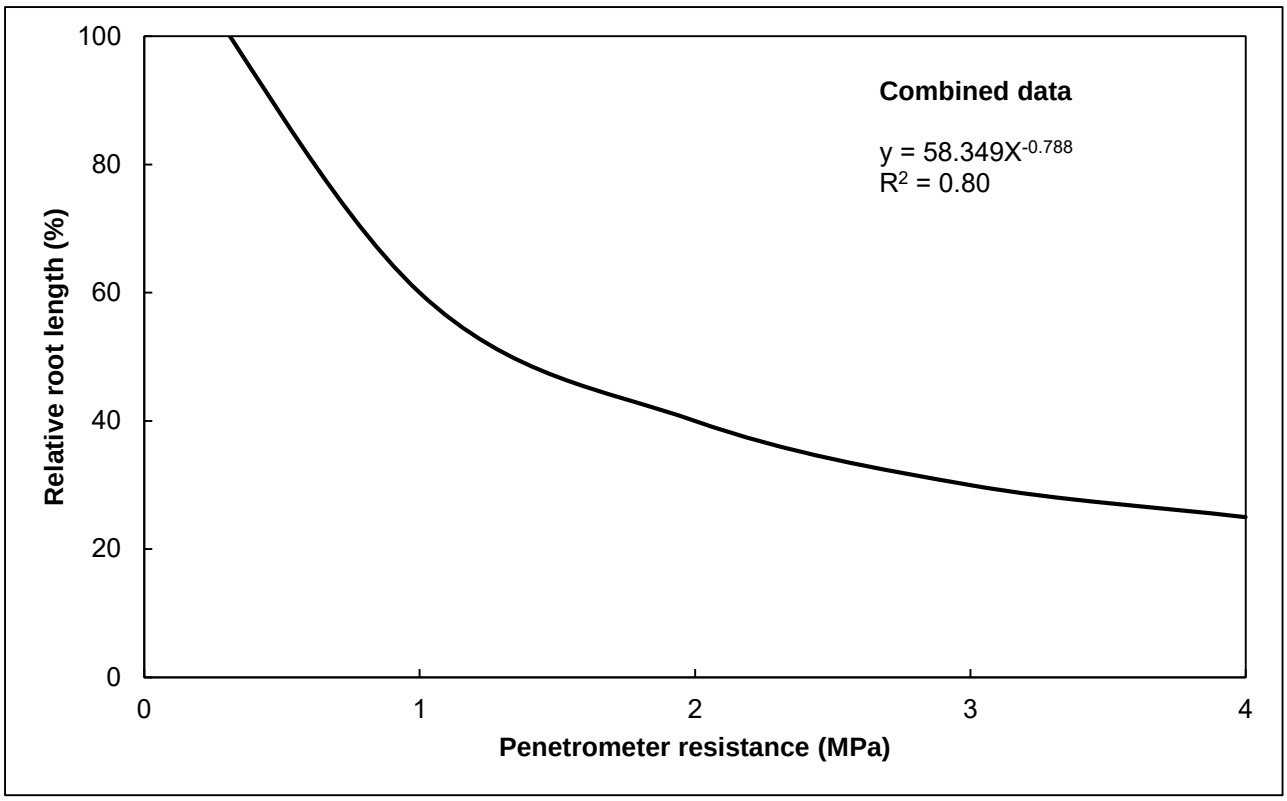

Figure 1.4: The effect of soil compaction on several relative plant root lengths (after Bennie & Burger, 1981).

Clark *et al.* (2003) concluded that if the roots hit a compacted layer, there are three probabilities: (1) horizontal growth; (2) penetration through the strong soil or/and (3) growth stops. An experiment in Western Australia showed that roots grew horizontal and root density increased in a compacted soil (Chen *et al.*, 2014).

High bulk density does not only affect the root development, but also the ability of roots to penetrate deeper soil layers to absorb water and nutrients (Elfadil & Salih, 2017). Weaker root growth in presence of compacted soil may cause a reduction in nutrient uptake of major elements N, P, K and Ca and minor elements Fe, Mn and Zn (Bennie & Laker, 1975). In a study of Shierlaw & Alston (1984), ryegrass absorbed twice as much P from an uncompacted soil than from to a compacted soil. Moreover, the interaction between soil texture and bulk density can influence root growth (Tracy *et al.*, 2013) and is summarised in Table 1.15. These authors found that root growth was the greatest at 1.3 g.cm^{-3} in loamy sand soil and at 1.5–1.6 g.cm^{-3} in clay loam soil. Pierce *et al.* (1983) reported that root growth stated to decrease at bulk density of ~1.47–1.58 g.cm^{-3} and 1.85 g.cm^{-3} in sandy and clayey soils, respectively.

However, soils with high clay content may be less sensitive to soil compaction due to their having higher soil strength (Atwell, 1993). According to Busscher & Lichier (1993) the effect of soil compaction on root growth in sandy soils was less inhibited compared to clayey soil, although the soil resistance was higher in the former. This implies the preferential root growth in macropores.

1.3.5.2 *Above-ground biomass and leaf area index*

The vegetation in the rehabilitated Highveld of Mpumalanga is characterised as Highveld grasslands, a ubiquitous single-layered (or fine-leaved) herbaceous community (Tainton, 1999). The peak

Table 1.15: Effect of bulk density on root development and penetration (after USDA, 1996; Vepraskas, 1988).

Soil texture	ρ_b	
	Restriction on root development initiated	Root penetration limiting
Loamy sand	1.690	1.850
Sandy loam, loam	1.630	1.800
Sandy clay loam, clay loam	1.600	1.780
Clay	1.390	1.470

Note: ρ_b = soil bulk density in g.cm^{-3}.

photosynthetic active LAI is being commonly used in the soil cover design or long-term performance modelling. Few studies have been done on the total biomass, active vegetation biomass, total LAI and photosynthetic active LAI of grasslands on rehabilitated mines, particularly in Mpumalanga Highveld. Vermaak *et al*. (2004) used LAI values of 3 and 1 m^2.m^{-2} for good and poor vegetation covers, respectively for SRCs in KwaZulu-Natal, South Africa. However, the climatic condition of KwaZulu-Natal is subtropical with high mean annual rainfall of ~845 mm (OpenStreetMap contributors, 2021), whereas the climate of Mpumalanga Highveld is semi-arid. Some consultants or geo-engineers use the published LAI values (personal observation) which may be problematic due to climatic differences between KwaZulu-Natal and Mpumalanga, and different grasses with different leaf area and shapes.

The following research was carried out on LAI of grasslands under semi-arid conditions, but not at rehabilitated mines. In the study of Friedl *et al.* (1994), they found that the total LAI of grasslands was ~0.5–2.3 m^2.m^{-2}and Darvishzadeh *et al.* (2011) reported values ranged between 0.72–2.87 m^2.m^{-2}. In addition, in the Haupt (2018) study, the peak photosynthetic LAI of natural grasses was 1.29 m^2.m^{-2}. Flanagan *et al.* (2015) found a peak photosynthetic active LAI of ~1.20–1.50 m^2.m^{-2} of northern Great Plains grassland. Some grasslands may be classified as bushed grassland and Kisambo *et al.* (2016) observed that the total LAI for bushed grassland was 2.52 m^2.m^{-2} and for grassland only 0.76 m^2.m^{-2}. Li & Guo (2010) found that the photosynthetic active LAI during the growing season of grasses was 0.92 m^2.m^{-2} and it reached the minimum in the senescence season of 0.14 m^2.m^{-2}. Moreover, the authors found that dead vegetation covers accounted for 47.4% of the variance of total LAI while photosynthetic active vegetation covers accounted for 43.8%. The observations of Asner *et al.* (1998) showed that litter and dead matter often dominate the above-ground biomass of grasslands. Wever *et al.* (2002) found that the dead LAI can contribute about 1.2 m^2.m^{-2} in total LAI. A large amount of dead matter can lead to an inaccurate LAI (Duncan *et al.*, 1993), which in turn generate higher inaccuracy in the soil cover long-term performance modelling (Tucker *et al.*, 1980). Therefore, it is important to study the seasonal LAI to understand the plant growth. Correlation is high between photosynthetic active LAI and active vegetation biomass. This observation has been reported by several investigators. Petcu *et al.* (2003) found several positive and linear relationships from r = 0.66 to 0.82 between total LAI and total above-ground biomass.

Goswami *et al.* (2015) also reported a positive and linear relationship between photosynthetic active LAI and active vegetation biomass of r = 0.92 for common vascular plant species had. Another study found a strong coefficient correlation of 0.74 between the same parameters for grassland species under semi-arid conditions in Southern Ethiopia (Kisambo *et al.*, 2016).

1.3.5.2.1 *Effect of bulk density on vegetation active biomass and photosynthetic active leaf area index*

Plant growth is strongly related with the extent and function of the root system. Nawaz *et al.* (2013) mentioned that root growth in highly compacted soil is reduced and had low photosynthesis rates. According to Grzesiak (2009), the active vegetation biomass and photosynthetic active LAI with poor root growth decreased with increasing bulk density. Lipiec *et al.* (1991) observed a significantly reduced plant growth and lower LAI when degree of soil compaction exceeded ~88%. A poor plant growth with low active vegetation biomass and photosynthetic active LAI in highly compacted soil is attributed to reduced infiltration (Radford *et al.*, 2001), reduced soil porosity (Kubota & Williams, 1967) or bad weather conditions.

1.4 Conclusion

Soil covers as an alternative mitigation methods are cost-effective and effective in long term. Soil covers may have more or less similar physical properties to natural soils, however modification of soil cover-, soil hydraulic- and vegetation properties can happen during soil cover construction if not done properly. Poorly constructed soil covers can have many problems which include compaction (high bulk density) and poor vegetation growth. High bulk density reduces soil nutrient availability, K_{sat}, WHC and plant growth. In addition, if the soil texture of the growth medium or water retention layer contains high gravel amount, *i.e.*, K_{sat} increases with a decrease in WHC. Consequently, the long-term performance of poorly constructed SRCs is poor with a higher risk of high oxygen- and water ingress or of erosion and runoff.

Due to the nature of soil covers, the published PTFs may not be applicable and therefore more suitable PTFs need to developed for predicting soil hydraulic properties of SRCs. Additionally, to use the published LAI values of 3 and 1 $m^2.m^{-2}$ for good and poor vegetation covers, respectively in Highveld Mpumalanga can be problematic. Considering these shortcomings of available information, the effect of soil cover-, soil hydraulic- and vegetation properties on long-term soil cover performance were investigated in the current study. Most importantly, PTFs for SRCs at Mpumalanga Highveld will be developed and photosynthetic active LAI values for good and poor vegetation covers will be established. With regard to this study, the hypothesis is: (1) well-designed and constructed soil covers will perform better in terms of optimum K_{sat} and WHC with good vegetation cover; (2) developed PTFs will perform better compared to published PTFs for predicting soil hydraulic properties of SRCs due to the particular soil-forming factors and pedogenesis on the Highveld; and (3) photosynthetic active LAI at Mpumalanga Highveld may be lower compared to the LAI at KwaZulu-Natal due to differences in climatic condition and vegetation species.

1.5 References

Abrahams, A.D. & Parsons, A.J. 1991. Relation between infiltration and stone cover on a semi-arid hillslope, southern Arizona. *Journal of Hydrology*. 122(1–4):49–59.

Abrol, I.P., Khosla, B.K. & Bhumbla, D.R. 1968. Relationship of texture to some important soil moisture constants. *Geoderma*. 2(1):33–39.

Adler, R. & Rascher, J. 2007. A strategy for management of acid mine drainage from gold mines in Gauteng. Pretoria.

Agrawal, R.P. 1991. Water and nutrient management in sandy soils by compaction. *Soil and Tillage Research*. 19(2–3):121–130.

Akcil, A. & Koldas, S. 2006. Acid Mine Drainage (AMD): Causes, treatment and case studies. *Journal of Cleaner Production*. 14:1139–1145.

Albright, W.H., Benson, C.H. & Waugh, W.J. 2009. *Water Balance Covers for Waste Containment: Principles and Practice*. Reston, VA: American Society of Civil Engineers.

Alvarez-Acosta, C., Lascano, R.J. & Stroosnijder, L. 2012. Test of the Rosetta pedotransfer function for saturated hydraulic conductivity. *Open Journal of Soil Science*. 02(03):203–212.

Apiwantragoon, P., Benson, C.H. & Albright, W.H. 2014. Field hydrology of water balance covers for waste containment. *Journal of Geotechnical and Geoenvironmental Engineering*. 141(2):1–20.

Arah, J.R.M. & Smith, K.A. 1989. Steady-state denitrification in aggregated soils: A mathematical model. *Journal of Soil Science*. 40(1):139–149.

Archer, J.R. & Smith, P.D. 1973. The relation between bulk density, available water capacity and air capacity of soils. *Journal of Terramechanics*. 10(4):61.

Arshad, R.R., Sayyad, G., Mosaddeghi, M. & Gharabaghi, B. 2013. Predicting saturated hydraulic conductivity by artificial intelligence and regression models. *ISRN Soil Science*. 2013:1–8.

Aschonitis, V.G., Kostopoulou, S.K. & Antonopoulos, V.Z. 2012. Methodology to assess the effects of rice cultivation under flooded conditions on van Genuchten's model parameters and pore size distribution. *Transport in Porous Media*. 91(3):861–876.

Asner, G.P., Wessman, C.A., Schimel, D.S. & Archer, S. 1998. Variability in leaf and litter optical properties: Implications for BRDF model inversions using AVHRR, MODIS, and MISR. *Remote Sensing of Environment*. 63(3):243–257.

Assouline, S. 2006. Modeling the relationship between soil bulk density and the hydraulic conductivity function. *Vadose Zone Journal*. 5(2):697–705.

Assouline, S., Tessier, D. & Tavares-Filho, J. 1997. Effect of compaction on soil physical and hydraulic properties: Experimental results and modeling. *Soil Science Society of America Journal*. 61(2):390.

Atwell, B.J. 1993. Response of roots to mechanical impedance. *Environmental and Experimental Botany*. 33(1):27–40.

Australian Alternative Cover Assessment Program. 2011. *Guidelines for the Assessment, Design, Construction and Maintenance of Phytocaps as Final Covers for Landfilss*. Waste Management Association of Australia.

Babaeian, E., Homaee, M., Vereecken, H., Montzka, C., Norouzi, A.A. & van Genuchten, M.T. 2015. A comparative study of multiple approaches for predicting the soil water retention curve: Hyperspectral information vs. basic soil properties. *Soil Science Society of America Journal*. 79(4):1043–1058.

Babalola, O. & Lal, R. 1977. Subsoil gravel horizon and maize root growth: Gravel concentration and bulk density effects. *Plant and Soil*. 46(2):337–346.

Bagarello, V., Iovino, M. & Reynolds, W.D. 1999. Measuring hydraulic conductivity in a cracking clay soil using the Guelph permeameter. *Transactions of the ASAE*. 42(4):957–964.

Bandaranayake, W.M., Parsons, L.R., Borhan, M.S. & Holeton, J.D. 2007. Performance of a capacitance-type soil water probe in a well-drained sandy soil. *Soil Science Society of America Journal*. 71(3):993–1002.

Banks, V.J., Palumbo-Roe, B., van Tonder, D., Fleming, C. & Chevrel, S. 2011. *Earth observation for monitoring and observing environmental and societal impacts of mineral resources exploration and exploitation xonceptual models of Witbank coalfield*. Project no: 244242. South Africa.

Banning, N.C., Lalor, B.M., Grigg, A.H., Phillips, I.R., Colquhoun, I.J., Jones, D.L. & Murphy, D. V. 2011. Rehabilitated mine-site management, soil health and climate change. In Berlin, Heidelberg: Springer-Verlag. *Soil Health and Climate Change*. 287–314.

Barley, K.P. & Rovira, A.D. 1970. The influence of root hairs on the uptake of phosphate. *Communications in Soil Science and Plant Analysis*. 1(5):287–292.

Bartoli, F., Begin, J.C., Burtin, G. & Schouller, E. 2007. Shrinkage of initially very wet soil blocks, cores and clods from a range of European Andosol horizons. *European Journal of Soil Science*. 58(2):378–392.

Basso, A.S., Miguez, F.E., Laird, D.A., Horton, R. & Westgate, M. 2013. Assessing potential of biochar for increasing water-holding capacity of sandy soils. *Global Change Biology Bioenergy*.

5(2):132–143.

Basson, M.S., van Niekerk, P.H. & van Rooyen, J.A. 1997. *Overview of water resources availability and utilisation in South Africa*. Report P RSA/00/0197. Pretoria.

Bell, F.G. 1996. Dereliction: Colliery spoil heaps and their rehabilitation. *Environmental & Engineering Geoscience*. II(1):85–96.

Bell, L.C. 2001. Establishment of native ecosystems after mining - Australian experience across diverse biogeographic zones. *Ecological Engineering*. 17(2–3):179–186.

Bengough, A.G., Bransby, M.F., Hans, J., McKenna, S.J., Roberts, T.J. & Valentine, T.A. 2006. Root responses to soil physical conditions; growth dynamics from field to cell. *Journal of Experimental Botany*. 57(2 SPEC. ISS.):437–447.

Bennie, A.T.P. & Burger, R.D.T. 1979. *Grondverdigting onder besproeiing op die Vaalhartsbesproeiingskema. Volume II: Die invloed van grondverdigting op die grond-plant sisteem*. Report No. 79/2. Bloemfontein: University of the Orange Free State.

Bennie, A.T.P. & Burger, R.D.T. 1981. Root characteristics of different crops as affected by mechanical resistance in fine sandy soils. In East London *Proceedings of the 10th National Congress of Soil Science Society of South Africa*. 29–32.

Bennie, A.T.P. & Krynauw, G.N. 1985. Causes, adverse effects and control of soil compaction. *South African Journal of Plant and Soil*. 2(3):109–114.

Bennie, A.T.P. & Laker, M.C. 1975. The influence of soil strength on plant growth in red apedal soils. In Blydepoort *Proceedings of the 6th Soil Science Society of South Africa Congress*.

Benson, C., Abichou, T., Albright, W., Gee, G., Roesler, A. & Abichou, T. 2001. Field evaluation of alternative earthen final covers. *International Journal of Phytoremediation*. 3(1):105–127.

Benson, C.H., Albright, W.H., Roesler, A.C. & Abichou, T. 2002. Evaluation of final cover performance: Field data from the alternative cover assesment program (ACAP). In Tucson, Arizona *Waste Management Conference*. 1–16.

Benson, C.H., Sawangsuriya, A., Trzebiatowski, B. & Albright, W.H. 2007. Post-construction changes in the hydraulic properties of water balance cover soils. *Journal of Geotechnical and Geoenvironmental Engineering*. 133(4):349–359.

Binkley, D. & Vitousek, P. 1989. Soil nutrient availability. In R.W. Pearcy et al. (eds.). Dordrecht: Springer Netherlands. *Plant Physiological Ecology*. 75–96.

Blackwell, P.S., Graham, J.P., Armstrong, J. V., Ward, M.A., Howse, K.R., Dawson, C.J. & Butler, A.R. 1986. Compaction of a silt loam soil by wheeled agricultural vehicles. I. Effects upon soil conditions. *Soil and Tillage Research*. 7(1–2):97–116.

Blackwell, P.S. & Soane, B.D. 1981. A method of predicting bulk density changes in field soils resulting from compaction by agricultural traffic. *Journal of Soil Science*. 32(1):51–65.

Bodman, G.B. & Constantin, G.K. 1965. Influence of particle size distribution in soil compaction. *Hilgardia*. 36(15):567–591.

Børgesen, C.D. & Schaap, M.G. 2005. Point and parameter pedotransfer functions for water retention predictions for Danish soils. *Geoderma*. 127(1–2):154–167.

Bossé, B., Bussière, B., Hakkou, R., Maqsoud, A. & Benzaazoua, M. 2013. Assessment of phosphate limestone wastes as a component of a store-and-release cover in a semiarid climate. *Mine Water and the Environment*. 32(2):152–167.

Botha, F.J.P. & Bennie, A.T.P. 1982. The effect of tillage on water-use efficiency of maize under irrigation. *Crop Production*. 11:26–29.

Botha, F.J.P., Bennie, A.T.P. & Burger, R.D.T. 1983. *Water use efficiency of irrigated crops as influenced by varying cultivation practices and root configurations*. Report to Water Research Commission. Bloemfontein: University of the Orange Free State.

Bouma, J. 1989. Using soil survey data for quantitative land evaluation. In Vol. 9. New York: Springer-Verlag. *Advances in Soil Science*. 177–213.

Bouma, J., Jongerius, A. & Schoonderbeek, D. 1979. Calculation of saturated hydraulic conductivity of some pedal clay soils using micromorphometric data. *Soil Science Society of America Journal*. 43(2):261–264.

Brakensiek, D.L. & Rawls, W.J. 1994. Soil containing rock fragments: Effects on infiltration. *Catena*. 23(1–2):99–110.

Bray, R.H. 1961. You can predict fertilizer needs with soil tests. *Better Crops with Plant Food*. 45:18–27.

Buol, S., Hole, F., McCracken, F. & Southard, R. 1997. *Soil genesis and classification*. 4th ed. Ames, Iowa: Iowa State University Press.

Busscher, W. & Lipiec, J. 1993. Early growth of maize in compacted soil with fine and coarse structure. *International Agrophysics*. 7(1):77–83.

Cadle, A.B., Cairncross, B., Christie, A.D.M. & Roberts, D.L. 1993. The Karoo Basin of South Africa: type basin for the coal-bearing deposits of southern Africa. *International Journal of Coal Geology*. 23:117–157.

Cairncross, B. 2001. An overview of the Permian (Karoo) coal deposits of southern Africa. *African Earth Sciences*. 33:529–562.

Campbell, G.S. & Shiozawa, S. 1992. Prediction of hydraulic properties of soils using particle-size distribution and bulk density data. In M.T. van Genuchten et al. (eds.). Riverside, CA: University of California. *Indirect methods for estimating the hydraulic properties of unsaturated soils*. 317–328.

Campbell, R.B. & Moreau, R.A. 1979. Ethylene in a compacted field soil and its effect on growth, tuber quality, and yield of potatoes. *American Potato Journal*. 56(4):199–210.

Cannell, R.Q., Davies, D.B. & Pigeon, J.D. 1979. The suitablity of soils for sequential direct drilling of combine- harvested crops in Britain: a provisional classification. *United Kingdom, Soil Survey England & Wales, Technical Monograph*. 13:1–23.

Carsel, R.F. & Parrish, R.S. 1988. Developing joint probability distributions of soil water retention characteristics. *Water Resources Research*. 24(5):755–769.

Chamber of Mines of South Africa. 2018. *National coal strategy for South Africa*. South Africa. [Online], Available: www.chamberofmines.org.za.

Chamber of Mines of South Africa / Coaltech. 2007. *Guidelines for the Rehabilitation of Mined Land*. J. Beukes (ed.). Johannesburg: Coaltech Research Assocation.

Chaudhari, P.R., Ahire, D. V, Ahire, V.D., Chkravarty, M. & Maity, S. 2013. Soil bulk density as related to soil texture, organic matter content and available total nutrients of Coimbatore soil. *International Journal of Scientific and Research Publications*. 3(1):2250–3153.

Chen, Y. 2018. Soil water retention curves derived as a function of soil dry density. *GeoHazards*. 1(1):3–19.

Chen, Y.L., Palta, J., Clements, J., Buirchell, B., Siddique, K.H.M. & Rengel, Z. 2014. Root architecture alteration of narrow-leafed lupin and wheat in response to soil compaction. *Field Crops Research*. 165:61–70.

Chestworth, W. 2008. *Encyclopedia of soil science*. Dordrecht: The Netherlands: Springer.

Chinkulkijniwat, A., Man-Koksung, E., Uchaipichat, A. & Horpibulsuk, S. 2010. Compaction characteristics of non-gravel and gravelly soils using a small compaction apparatus. *Journal of ASTM International*. 7(7):1–15.

Clapp, R.B. & Hornberger, G.M. 1978. Empirical equations for some soil hydraulic properties. *Water Resources Research*. 14(4):601–604.

Clark, L.J., Whalley, W.R. & Barraclough, P.B. 2003. How do roots penetrate strong soil? *Plant and Soil*. 255(1):93–104.

Correa, J., Postma, J.A., Watt, M. & Wojciechowski, T. 2019. Soil compaction and the architectural plasticity of root systems. *Journal of Experimental Botany*. 70(21):6019–6034.

Corwin, D.L. & Lesch, S.M. 2003. Application of soil electrical conductivity to precision agriculture: Theory, principles, and guidelines. *Agronomy Journal*. 95(3):455–471.

Cosby, B.J., Hornberger, G.M., Clapp, R.B. & Ginn, T.R. 1984. A statistical exploration of the relationships of soil moisture characteristics to the physical properties of soils. *Water Resources Research*. 20(6):682–690.

Croney, D. & Coleman, J.D. 1954. Soil structure in relation to soil suction (pF). *Journal of Soil Science*. 5(1):75–84.

Cummings, R.W. & Elliott, G.L. 1991. Soil chemical properties. In Sydney, Australia: Sydney University Press *Soils: Their properties and management. A soil conversation handbook for New South Wales*. 193–205.

Dane, J.H. & Puckett, W.E. 1992. Field soil hydraulic properties based on physical and mineralogical information. In M.T. van Genuchten et al. (eds.). Riverside, CA: University of California *Indirect methods for estimating the hydraulic properties of unsaturated soils*. 463–466.

Darvishzadeh, R., Atzberger, C., Skidmore, A. & Schlerf, M. 2011. Mapping grassland leaf area index with airborne hyperspectral imagery: A comparison study of statistical approaches and inversion of radiative transfer models. *ISPRS Journal of Photogrammetry and Remote Sensing*. 66(6):894–906.

Da Silva, S.R., De Barros, N.F., Da Costa, L.M. & Leite, F.P. 2008. Soil compaction and eucalyptus growth in response to forwarder traffic intensity and load. *Revista Brasileira de Ciencia do Solo*. 32(3):921–932.

Davies, R., Younger, A. & Chapman, R. 1992. Water availability in a restored soil. *Soil Use and Management*. 8(2):67–73.

Deb, P., Debnath, P. & Pattanaaik, S.K. 2014. Physico-chemical properties and water holding capacity of cultivated soils along altitudinal gradient in South Sikkim, India. *Indian Journal of Agricultural Research*. 48(2):120–126.

Dec, D., Dörner, J., Becker-Fazekas, O. & Horn, R. 2008. Effect of bulk density on hydraulic properties of homogenized and structured soils. *Revista de la Ciencia del Suelo y Nutricion Vegetal*. 8(1):1–13.

de Lima, R.P., da Silva, A.P., Giarola, N.F.B., da Silva, A.R. & Rolim, M.M. 2017. Changes in soil compaction indicators in response to agricultural field traffic. *Biosystems Engineering*. 162(October):1–10.

Department of Water Affairs and Forestry. 2007. *Best Practice Guideline H2: Pollution prevention and minimasation of impacts*. Pretoria: Department of Water Affairs and Forestry.

Department of Water Affairs and Forestry. 2008. *Best Practise Guidelines for Water Resource Protection in the South African Mining Industry*. Pretoria: Department of Water Affairs and Forestry.

Diamond, S. & Kinter, E.B. 1956. Surface areas of clay minerals as derived from measurements of glycerol retention. *Clays and Clay Minerals*. 5(1):334–347.

Dodd, M.B. & Lauenroth, W.K. 1997. The influence of soil texture on the soil water dynamics and vegetation structure of a shortgrass steppe ecosystem. *Plant Ecology*. 133(1):13–28.

Don, A. & Schulze, E.D. 2008. Controls on fluxes and export of dissolved organic carbon in grasslands with contrasting soil types. *Biogeochemistry*. 91(2–3):117–131.

Douglas, J.T. & Crawford, C.E. 1991. Wheel-induced soil compaction effects on ryegrass production and nitrogen uptake. *Grass and Forage Science*. 46(4):405–416.

Douglas, J.T. & Crawford, C.E. 1993. The response of a ryegrass sward to wheel traffic and applied nitrogen. *Grass and Forage Science*. 48(2):91–100.

Duncan, J., Stow, D., Franklin, J. & Hope, A. 1993. Assessing the relationship between spectral vegetation indices and shrub cover in the Jornada Basin, New Mexico. *International Journal of Remote Sensing*. 14(18):1–2.

Duong, T.T.T., Penfold, C. & Marschner, P. 2012. Amending soils of different texture with six compost types: Impact on soil nutrient availability, plant growth and nutrient uptake. *Plant and Soil*. 354(1–2):197–209.

Durkin, T. V. & Herrmann, J.C. 1994. Focusing on the problem of mining wastes: An introduction to acid mine drainge. In Canada *EPA Seminar Publication*.

Eigenberg, R.A., Doran, J.W., Nienaber, J.A. & Woodbury, B.L. 2000. Soil conductivity maps for monitoring temporal changes in an agronomic field. In Des Moines, IA *Proceedings of the 8th International Symposium on Animal Agriculture and Food Processing Wastes*. 249–265. [Online], Available: file:///C:/Users/youhe/Downloads/kdoc_o_00042_01.pdf.

Eigenberg, R.A., Doran, J.W., Nienaber, J.A., Ferguson, R.B. & Woodbury, B.L. 2002. Electrical conductivity monitoring of soil condition and available N with animal manure and a cover crop. *Agriculture, Ecosystems and Environment*. 88(2):183–193.

El-Swaify, S.A. & Emerson, W.W. 1975. Changes in the physical properties of soil clays due to precipitated aluminum and iron hydroxide : 1. Swelling and aggregate stability after drying. *Soil Science Society of America Journal*. 39(6):1056–1063.

Elfadil, A.D. & Salih, H.A. 2017. Effect of soil compaction on shoot and root development and nutrients uptake of sesame plant. *European Academic Research*. 5(7):3054–3064.

Elhakeem, M., Papanicolaou, A.N.T., Wilson, C.G., Chang, Y.-J., Burras, L., Abban, B., Wysocki, D.A. & Wills, S. 2018. Understanding saturated hydraulic conductivity under seasonal changes in climate and land use. *Geoderma*. 315:75–87.

Eskom. 2018. *Coal Power*. [Online], Available: http://www.eskom.co.za/AboutElectricity/ElectricityTechnologies/Pages/Coal_Power.aspx [2018, October 11].

Fabiola, N., Giarola, B., Da Silva, A.P., Imhoff, S. & Dexter, A.R. 2003. Contribution of natural soil compaction on hardsetting behavior. *Geoderma*. 113(1–2):95–108.

Fayer, M.J., Rockhold, M.L. & Campbell, M.D. 1992. Hydrologic modeling of protective barriers: Comparison of field data and simulation results. *Soil Science Society of America Journal*. 56(3):690–700.

Fernandez-illescas, C.P., Porporato, A. & Rodriguez-iturbe, I. 2001. The ecohydrological role of soil texture in a water-limited ecosystem. *Water Resources Research*. 37(12):2863–2872.

Ferreira, T.R., Pires, L.F., Auler, A.C., Brinatti, A.M. & Ogunwole, J.O. 2019. Water retention curve to analyze soil structure changes due to liming. *Anais da Academia Brasileira de Ciencias*. 91(3):1–12.

Ferrer Julià, M., Estrela Monreal, T., Sánchez Del Corral Jiménez, A. & García Meléndez, E. 2004. Constructing a saturated hydraulic conductivity map of Spain using pedotransfer functions and spatial prediction. *Geoderma*. 123(3–4):257–277.

Flanagan, L.B., Sharp, E.J. & Gamon, J.A. 2015. Application of the photosynthetic light-use efficiency model in a northern Great Plains grassland. *Remote Sensing of Environment*. 168:239–251.

Flint, A.L. & Childs, S. 1984. Physical properties of rock fragments and their effect on available water in skeletal soils. In J.D. Nichols et al. (eds.). (SSSA Special Publications). Madison, WI, USA: Soil Science Society of America *Erosion and productivity of soils containing rock fragments*. 91–103.

Franzluebbers, A.J. & Hons, F.M. 1996. Soil-profile distribution of primary and secondary plant-available nutrients under conventional and no tillage. *Soil & Tillage Research*. 39(3–4):229–239.

Friedl, M.A., Michaelsen, J., Davis, F.W., Walker, H. & Schimel, D.S. 1994. Estimating grassland biomass and leaf area index using ground and satellite data. *International Journal of Remote Sensing*. 15(7):1401–1420.

Gamie, R. & De Smedt, F. 2018. Experimental and statistical study of saturated hydraulic

conductivity and relations with other soil properties of a desert soil. *European Journal of Soil Science*. 69(2):256–264.

García-Gutiérrez, C., Pachepsky, Y. & Ángel Martín, M. 2018. Saturated hydraulic conductivity and textural heterogeneity of soils. *Hydrology and Earth System Sciences*. 22(7):3923–3932.

Garga, V.K. & Madureira, C.J. 1985. Compaction characteristics of river terrace gravel. *Journal of Geotechnical Engineering*. 111(8):987–1007.

Ghanbarian-Alavijeh, B. & Millán, H. 2010. Point pedotransfer functions for estimating soil water retention curve. *International Agrophysics*. 24(3):243–251.

Givi, J., Prasher, S.O. & Patel, R.M. 2004. Evaluation of pedotransfer functions in predicting the soil water contents at field capacity and wilting point. *Agricultural Water Management*. 70(2):83–96.

Głab, T. 2013. Impact of soil compaction on root development and yield of meadow-grass. *International Agrophysics*. 27(1):7–13.

Google Earth 2.7. 2020. [Online], Available: http://www.google.com/earth/index.html.

Gorakhki, M.H. & Bareither, C.A. 2017. Sustainable reuse of mine tailings and waste rock as water-balance covers. *Minerals*. 7(7):128.

Goswami, S., Gamon, J., Vargas, S. & Tweedie, C. 2015. Relationships of NDVI, biomass, and leaf area index (LAI) for six key plant species in Barrow, Alaska. *PeerJ PrePrints*. 3(e913v1).

Gradwell, M.W. & Rijkse, W.C. 1988. An evaluation of the physical properties of some Gisborne Plains soils for irrigation purposes. *New Zealand Journal of Experimental Agriculture*. 16(3):286–294.

Greco, R. 2002. Preferential flow in macroporous swelling soil with internal catchment: Model development and applications. *Journal of Hydrology*. 269(3–4):150–168.

Griffiths, E., Webb, T.H., Watt, J.P.C. & Singleton, P.L. 1999. Development of soil morphological descriptors to improve field estimation of hydraulic conductivity. *Soil Research*. 37(5):971.

Grzesiak, M.T. 2009. Impact of soil compaction on root architecture, leaf water status, gas exchange and growth of maize and triticale seedlings. *Plant Root*. 3:10–16.

Guérif, J., Richard, G., Dürr, C., Machet, J.M., Recous, S. & Roger-Estrade, J. 2001. A review of tillage effects on crop residue management, seedbed conditions and seedling establishment. *Soil and Tillage Research*. 61(1–2):13–32.

Gülser, C. & Candemir, F. 2008. Prediction of saturated hydraulic conductivity using some moisture constants and soil physical properties. In Ohrid: Republic of Macedonia *BALWOIS 2008*.

Gupta, S.C. & Larson, W.E. 1979. Estimating soil water retention characteristics from particle size

distribution, organic matter percent, and bulk density. *Water Resources Research*. 15(6):1633–1635.

Gupta, S.C., Sharma, P.P. & DeFranchi, S.A. 1989. Compaction effects on soil structure. *Advances in Agronomy*. 42(C):311–338.

Hacke, U.G., Sperry, J.S., Ewers, B.E., Ellsworth, D.S., Schäfer, K.V.R. & Oren, R. 2000. Influence of soil porosity on water use in Pinus taeda. *Oecologia*. 124(4):495–505.

Haigh, M. 1995. Soil quality standards for reclaimed coal-mine disturbed lands: A discussion paper. *International Journal of Surface Mining, Reclamation and Environment*. 9(4):187–202.

Håkansson, I. & Lipiec, J. 2000. A review of the usefulness of relative bulk density values in studies of soil structure and compaction. *Soil and Tillage Research*. 53(2):71–85.

Hallmark, W.B. & Barber, S.A. 1981. Root growth and morphology, nutrient uptake, and nutrient status of soybeans as affected by soil K and bulk density. *Agronomy Journal*. 73(5):779–782.

Hamarashid, N.H., Othman, M.A. & Hussain, M.-A.H. 2000. Effects of soil texture on chemical compositions, microbial populations and carbon mineralization in soil. *The Egyptian Society of Experimental Biology Introduction*. 6(1):59–64.

Hao, M., Zhang, J., Meng, M., Chen, H.Y.H., Guo, X., Liu, S. & Ye, L. 2019. Impacts of changes in vegetation on saturated hydraulic conductivity of soil in subtropical forests. *Scientific Reports*. 9(1):1–9.

Härdtle, W., Von Oheimb, G., Friedel, A., Meyer, H. & Westphal, C. 2004. Relationship between pH-values and nutrient availability in forest soils: The consequences for the use of ecograms in forest ecology. *Flora*. 199(2):134–142.

Harris, J.A., Birch, P. & Palmer, J.P. 1996. *Land restoration and reclamation: Principles and practice*. Essex, London: Longman.

Haupt, S.A. 2018. *Satellite monitoring of post-mining rehabilitation and the quantification of backfill dynamics using differential SAR interferometry*. Degree of Master of Science, Stellenbosch University.

Hauser, V.K. 2009. *Evapotranspiration covers for landfills and waste sites*. New York: Taylor & Francis Goup, LLC.

Herbauts, J., El Bayad, J. & Gruber, W. 1996. Influence of logging traffic on the hydromorphic degradation of acid forest soils developed on loessic loam in middle Belgium. *Forest Ecology and Management*. 87(1–3):193–207.

Heuscher, S.A., Brandt, C.C. & Jardine, P.M. 2005. Using soil physical and chemical properties to estimate bulk density. *Soil Science Society of America Journal*. 69(1):51–56.

Hill, J.N.S. & Summer, M.E. 1967. Effect of bulk density on moisture characteristics of soils. *Soil Science*. 103(4):234–238.

Hillel, D. 2004. *Introduction to environmental soil physics*. New York: Academic Press.

Hobbs, P., Oelofse, S.H.H. & Rascher, J. 2008. Management of environmental impacts from coal mining in the upper Olifants River Catchment as a function of age and scale. *Internation Journal of Water Resources Development*. 24(3):417–431.

Hobday, D.K. 1987. Gondwana coal basins of Australia and South Africa: Tectonic setting, depositional systems and resources. *Geological Society, London, Special Publications*. 32(1):219–233.

Hodgson, F.D.I. & Krantz, R.M. 1998. *Goundwater quality deterioration in the Olifants River Cathment above the Loskop Dam with specialised invesitgations in the Witbank Dam Sub-Catchment*. Report 291/1/98. Pretoria: Water Research Commision.

Hultine, K.. R., Koepke, D.F., Pockman, W.T., Fravolini, A., Sperry, J.S. & Williams, D.G. 2005. Influence of soil texture on hydraulic properties and water relations of a dominant warm-desert phreatophyte. *Tree Physiology*. 26:313–323.

Hultine, K.R., Koepke, D.F., Pockman, W.T., Fravolini, A., Sperry, J.S. & Williams, D.G. 2006. Influence of soil texture on hydraulic properties and water relations of a dominant warm-desert phreatophyte. *Online*. 313–323.

Husz, G. 1967. Determination of the pF curve from texture, using multiple regressions. *Journal of Plant Nutrition and Soil Science*. (116):115–125.

INAP. 2014. *The International Network for Acid Prevention: Global Acid Rock Grainage Guide*. Melbourne, Victoria: International Network for Acid Protection.

INAP. 2017. *Global Cover System Deisng - Technical guidance document*. International Network for Acid Protection.

Jabro, J.D. 1992. Estimation of saturated hydraulic conductivity of soils from particle size distribution and bulk density data. *Transactions of the American Society of Agricultural Engineers*. 35(2):557–560.

Jarvis, N.J., Koestel, J. & Hollis, J.M. 2012. Preferential flow in a pedological perspective. In H.S. Lin (ed.). San Diego: Synergistic Integration of Soil Science and Hydrology. Elsevier Academic Press *Hydropedology*. 75–120.

Jarvis, N., Koestel, J., Messing, I., Moeys, J. & Lindahl, A. 2013. Influence of soil, land use and climatic factors on the hydraulic conductivity of soil. *Hydrology and Earth System Sciences*. 17(12):5185–5195.

Kaiser, K. & Zech, W. 2000. Dissolved organic matter sorption by mineral constituents of subsoil clay fractions. *Journal of Plant Nutrition and Soil Science*. 163(5):531–535.

Kar, G., Kumar, A., Panigrahi, S., Dixit, P.R. & Sahoo, H.N. 2017. Particle size distribution, soil organic carbon stock and water retention of some upland use system of odisha and assessing their interrelationship. *Journal of the Indian Society of Soil Science*. 65(1):48.

Karahan, G. & Erşahin, S. 2016. Predicting saturated hydraulic conductivity using soil morphological properties. *Eurasian Journal of Soil Science*. 5(1):30.

Karki, J., Mandal, U.K., Chidi, C.L., Dahal, J., Khanal, N.R. & Pantha, R.H. 2018. An analysis of hydraulic properties of soil based on soil texture in Chiti areas of Lamjung District in Nepal. *Geographical Journal of Nepal*. 11:63–76.

Kemper, W.D., Stewart, B.A. & Porter, L.K. 1971. Effects of compaction on soil nutrient status. In K.K. Barnes et al. (eds.). St. Joseph, MI: American Society of Agrlcultural Engineers *Compaction of Agricultural Soils*. 178–189.

Khire, M. V., Benson, C.H. & Bosscher, P.J. 1997. Water balance modeling of earthen final covers. *Journal of Geotechnical Engineering*. 123(8):744–754.

Khire, M. V., Benson, C.H. & Bosscher, P.J. 2000. Capillary barriers: Design variables and water balance. *Journal of Geotechnical and Geoenvironmental Engineering*. 126(8):695–708.

Kim, H., Anderson, S.H., Motavalli, P.P. & Gantzer, C.J. 2010. Compaction effects on soil macropore geometry and related parameters for an arable field. *Geoderma*. 160(2):244–251.

King, J.A. 1988. Some physical features of soil after opencast mining. *Soil Use and Management*. 4(1):23–30.

Kisambo, B.K., Pfister, J., Schaffert, A. & Asch, F. 2016. Leaf area dynamics and aboveground biomass of specific vegetation types of a semi-arid grassland in southern Ethiopia. *Tropical and Subtropical Agroecosystems*. 19(3):253–262.

Kojima, Y., Heitman, J.L., Sakai, M., Kato, C. & Horton, R. 2018. Bulk density effects on soil hydrologic and thermal characteristics: A numerical investigation. *Hydrological Processes*. 32(14):2203–2216.

Kristoffersen, A.Ø. & Riley, H. 2005. Effects of soil compaction and moisture regime on the root and shoot growth and phosphorus uptake of barley plants growing on soils with varying phosphorus status. *Nutrient Cycling in Agroecosystems*. 72(2):135–146.

Kubota, T. & Williams, R.J.B. 1967. The effects of changes in soil compaction and porosity on germination, establishment and yield of barley and globe beet. *The Journal of Agricultural Science*. 68(2):227–233.

Lawton, K. 1946. The influence of soil aeration on the growth and absorption of nutrients by corn plants. *Soil Science Society of America Journal*. 10(C):263–268.

Li, Y., Chen, D., White, R.E., Zhu, A. & Zhang, J. 2007. Estimating soil hydraulic properties of Fengqiu County soils in the North China Plain using pedo-transfer functions. *Geoderma*. 138(3–4):261–271.

Li, Z. & Guo, X. 2010. A suitable vegetation index for quantifying temporal variation of leaf area index (LAI) in semiarid mixed grassland. *Canadian Journal of Remote Sensing*. 36(6):709–721.

Lilly, A. 2000. The relationship between field-saturated hydraulic conductivity and soil structure: Development of class pedotransfer functions. *Soil Use and Management*. 16(1):56–60.

Limpitlaw, D., Aken, M., Kilani, J., Mentis, M., Nell, J.P. & Tanner, P.D. 1997. Rehabilitation and soil characterization. *Proceedings of the 11th International conference on coal research.* 297–309.

Lin, H.S., McInnes, K.J., Wilding, L.P. & Hallmark, C.T. 1996. Effective porosity and flow rate with infiltration at low tensions into a well-structured subsoil. *Transactions of the American Society of Agricultural Engineers*. 39(1):131–133.

Lipiec, J. & Hatano, R. 2003. Quantification of compaction effects on soil physical properties and crop growth. *Geoderma*. 116(1–2):107–136.

Lipiec, J.I., Tarkiewicz, S. & Kossowski, J. 1991. Soil physical properties and growth of spring barley as related to the degree of compactness of two soils. *Soil and Tillage Research*. 19(2–3):307–317.

Lloyd, P. 2002. Coal mining and the environment. *Energy Research Centre*. 228455347.

Logsdon, S.D. & Karlen, D.L. 2004. Bulk density as a soil quality indicator during conversion to no-tillage. *Soil and Tillage Research*. 78(2):143–149.

Lopes, M.S. & Reynolds, M.P. 2010. Partitioning of assimilates to deeper roots is associated with cooler canopies and increased yield under drought in wheat. *Functional Plant Biology*. 37(2):147–156.

Luo, J., Zhou, X., Rubinato, M., Li, G., Tian, Y. & Zhou, J. 2020. Impact of multiple vegetation covers on surface runoff and sediment yield in the small basin of Nverzhai, Hunan Province, China. *Forests*. 11(3).

Malaya, C. & Sreedeep, S. 2011. Critical review on the parameters influencing soil-water characteristic curve. *Journal of Irrigation and Drainage Engineering*. 138(1):55–62.

Mamedov, A.I., Levy, G.J., Shainberg, I. & Letey, J. 2001. Wetting rate, sodicity, and soil texture effects on infiltration rate and runoff. *Soil Research*. 39(6):1293.

Masoni, A., Ercoli, L., Mariotti, M. & Pampana, S. 2008. Nitrogen and phosphorus accumulation and remobilization of durum wheat as affected by soil gravel content. *Cereal Research Communications*. 36(1):157–166.

Materechera, S.A., Alston, A.M., Kirby, J.M. & Dexter, A.R. 1992. Influence of root diameter on the penetration of seminal roots into a compacted subsoil. *Plant and Soil*. 144(2):297–303.

Mathu, K. & Chinomona, R. 2013. South African coal mining industry: Socio-economic attributes. *Mediterranean Journal of Social Sciences*. 4(14):347–358.

Matschonat, G. & Falkengren-Grerup, U. 2000. Recovery of soil pH, cation-exchange capacity and the saturation of exchange sites from stemflow-induced soil acidification in three Swedish beech (*Fagus sylvatica* L.) forests. *Scandinavian Journal of Forest Research*. 15(1):39–48.

McCarthy, T.S. 2011. The impact of acid mine drainage in South Africa. *South African Journal of Science*. 107:1–7.

Mccartney, J.S. & Zornberg, J.G. 2002. Design and performance criteria for evapotranspirative cover systems. In Rio de Janeiro, Brazil: A.A. Balkema *Proceedings of the Fifth International Conference on Environmental Geotechnics*. 195–200.

McClung, G. & Frankenberger, W.T. 1987. Nitrogen mineralization rates in saline vs. salt-amended soils. *Plant and Soil*. 104(1):13–21.

McGuire, P.E. & England, J.A. 2000. The design of an evapotranspiration lanfdill cover for a semi-arid site. *Journal American Society of Mining and Reclamation*. (1):178–187.

McNabb, D.H., Startsev, A.D. & Nguyen, H. 2001. Soil wetness and traffic effect levels on bulk density and air-field porosity of compacted boreal forest soils. *Soil Science Society of America Journal*. 65(4):1238–1247.

Miller, J. 2016. Soil pH affects nutrient availability. *University of Maryland Extension*. (July):1–5.

Minasny, B. & McBratney, A.B. 2000. Evaluation and development of hydraulic conductivity pedotransfer functions for Australian soil. *Soil Research*. 38(4):905.

Minasny, B., McBratney, A.B. & Bristow, K.L. 1999. Comparison of different approaches to the development of pedotransfer functions for water retention curves. *Geoderma*. 93(3–4):225–253.

Mohamed, B.A., Ellis, N., Kim, C.S., Bi, X. & Emam, A.E. 2016. Engineered biochar from microwave-assisted catalytic pyrolysis of switchgrass for increasing water-holding capacity and fertility of sandy soil. *Science of the Total Environment*. 566–567:387–397.

Moolman, J.H. 1981. Soil textural properties influencing compactibility. *Agrochemophysica*. 13:13–19.

Morgenthal, T.L. 2003. *Assessment of topsoil degradation on rehabilitated coal discard dumps*. B.Sc. Ph.D., North-West University.

Mu'azu, S. & Skopp, J. 1986. *The influence of soil bulk density, soil water regime, and fertilization on the uptake of P and K by corn*. University of Nebraska (ed.). Soil Science Research Report.

Nath, T.N. 2014. Soil texture and total organic matter content and its influences on soil water holding capacity of some selected tea growing soils in Sivasagar District of ASSAM, India. *International Journal of Chemical Sciences*. 12(4):1419–1429.

Nawaz, M.F., Bourrié, G. & Trolard, F. 2013. Soil compaction impact and modelling. A review. *Agronomy for Sustainable Development*. 33(2):291–309.

Needham, P., Scholz, G. & Moore, G. 2004. Hard layers in soils. In G. Moore (ed.). Western Australia: Department of Agriculture *Soil guide: A handbook for understanding and managing agricultural soils*. 111–115.

Nemes, A., Rawls, W.J. & Pachepsky, Y.A. 2005. Influence of organic matter on the estimation of saturated hydraulic conductivity. *Soil Science Society of America Journal*. 69(4):1330–1337.

Neves, C.S.V.J., Feller, C., Guimarães, M.F., Medina, C.C., Tavares Filho, J. & Fortier, M. 2003. Soil bulk density and porosity of homogeneous morphological units identified by the Cropping Profile Method in clayey Oxisols in Brazil. *Soil and Tillage Research*. 71(2):109–119.

O'Kane, M. & Ayres, B. 2012. Cover systems that utilise the moisture store-and-release concept – do they work and how can we improve their design and performance? In A.B. Fourie et al. (eds.). Perth: Australian Centre for Geomechanics *Mine Closure*. 1–9.

O'Sullivan, M.F. 1992. Uniaxial compaction effects on soil physical properties in relation to soil type and cultivation. *Soil and Tillage Research*. 24(3):257–269.

O'Sullivan, M.F. & Ball, B.C. 1993. The shape of the water release characteristic as affected by tillage, compaction and soil type. *Soil and Tillage Research*. 25(4):339–349.

Olorunfemi, I.E. & Fasinmirin, J.T. 2011. Hydraulic conductivity and infiltration of soils of Tropical Rain Forest Climate of Nigeria. In Abeokuta, Nigeria: Federal University of Agriculture *Proceedings of the Environmental Management Conference*. 397–413.

OpenStreetMap contributors. 2021. *KwaZulu-Natal climate (South Africa)*. [Online], Available: https://en.climate-data.org/africa/south-africa/kwazulu-natal-569/.

Othman, M.A. & Benson, C.H. 1993. Effect of freeze-thaw on the hydraulic conductivity and morphology of compacted clay. *Canadian Geotechnical Journal*. 30(2):236–246.

Pachepsky, Y. & Park, Y. 2015. Saturated hydraulic conductivity of US soils grouped according to textural class and bulk density. *Soil Science Society of America Journal*. 79(4):1094–1100.

Panayiotopoulos, K.P., Papadopoulou, C.P. & Hatjiioannidou, A. 1994. Compaction and penetration resistance of an Alfisol and Entisol and their influence on root growth of maize seedlings. *Soil and Tillage Research*. 31(4):323–337.

Papanicolaou, A.T.N., Elhakeem, M., Wilson, C.G., Lee Burras, C., West, L.T., Lin, H.H., Clark, B. & Oneal, B.E. 2015. Spatial variability of saturated hydraulic conductivity at the hillslope scale: Understanding the role of land management and erosional effect. *Geoderma*. 243–244:58–68.

Parlak, M. & Parlak, A.Ö. 2011. Effect of soil compaction on root growth and nutrient uptake of forage crops. *Journal of Food, Agriculture and Environment*. 9(3–4):275–278.

Patil, N.G. & Singh, S.K. 2016. Pedotransfer functions for estimating soil hydraulic properties: A review. *Pedosphere*. 26(4):417–430.

Peng, S. & Jiang, H. 2009. A review on soil cover in waste and contaminant containment: Design monitoring and modeling. 3(3):303–311.

Peng, X. & Horn, R. 2005. Modeling soil shrinkage curve across a wide range of soil types. *Soil Science Society of America Journal*. 69(3):584–592.

Petcu, E., Petcu, G., Lazar, C. & Vintila, R. 2003. Relationship between leaf area index, biomass and winter wheat yield obtained at Fundulea, under conditions of 2001 year. *Romanian Agricultural Research, Vol. 19-20, pp. 21-29*. 21–29. [Online], Available: http://www.incda-fundulea.ro/rar/nr1920/19.4.pdf.

Peterson, J.C. 1982. Effects of pH upon nutrient availability in a commercial soilless root medium utilized for floral crop production. In Wooster, Ohio: Ohio Agricultural Research and Development Center *Ornamental Plants - 1982: A summary of research*. 16–19.

Phuong, N.M., Le Khoa, V. & Cornelis, W. 2014. Predicting soil water retention characteristics for Vietnam Mekong Delta soils. *IAHS-AISH Proceedings and Reports*. 363(October):392–398.

Pierce, F.J., Larson, W.E., Dowdy, R.H. & Graham, W.A.P. 1983. Productivity of soils: Assessing long-term changes due to erosion. *Journal of Soil and Water Conservation*. 38:39–44.

Popova, L., Van Dusschoten, D., Nagel, K.A., Fiorani, F. & Mazzolai, B. 2016. Plant root tortuosity: An indicator of root path formation in soil with different composition and density. *Annals of Botany*. 118(4):685–698.

Puckett, W.E., Dane, J.H. & Hajek, B.F. 1985. Physical and mineralogical data to determine soil hydraulic properties. *Soil Science Society of America Journal*. 49(4):831–836.

Qin, Y., Yi, S., Chen, J., Ren, S. & Ding, Y. 2015. Effects of gravel on soil and vegetation properties of alpine grassland on the Qinghai-Tibetan plateau. *Ecological Engineering*. 74:351–355.

Rademeyer, B., Wates, J., Bezuidenhout, N., Jones, G., Rust, E., Lorentz, S., Van Deventer, P.,

Pulles, W., 2008. *Preliminary Decision Support System for the Sustainable Design , Operation and Closure of Metalliferous Mine Residue Disposal Facilities*. Gezina: Water Research Commission.

Radford, B.J., Yule, D.F., McGarry, D. & Playford, C. 2001. Crop responses to applied soil compaction and to compaction repair treatments. *Soil and Tillage Research*. 61(3–4):157–166.

Raiesi, F. 2006. Carbon and N mineralization as affected by soil cultivation and crop residue in a calcareous wetland ecosystem in Central Iran. *Agriculture, Ecosystems & Environment*. 112(1):13–20.

Ramsay, W.J.H. 1986. Bulk soil handling for quarry restoration. *Soil Use and Management*. 2(1):30–39.

Rao, S.M. & Revanasiddappa, K. 2000. Role of matric suction in collapse of compacted clay soil. *Journal of Geotechnical and Geoenvironmental Engineering*. 126(1):85–90.

Rasoulzadeh, A. 2011. Estimating hydraulic conductivity using pedotransfer functions. *Hydraulic Conductivity - Issues, Determination and Applications*. (December).

Rawls, W.J. & Brakensiek, D.L. 1985. Prediction of soil water properties for hydrologic modeling. In E.E. Jones et al. (eds.). New Yo: ASCE Convention *Proceedings of Symposium on Watershed Management in the Eighties*. 293–299.

Rawls, W.J., Brakensiek, D.L. & Saxton, K.E. 1982. Estimation of soil water properties. *Transactions of the ASAE*. 25(5):1316--1320 & 1328.

Rawls, W.J., Gish, T.J. & Brakensiek, D.L. 1991. Estimating soil water retention from soil physical properties and characteristics. In Vol. 16. B.A. Stewart (ed.). New York: Springer-Verlag *Advances in Soil Science*. 213–234.

Rawls, W.J., Gimenez, D. & Grossman, R. 1998. Use of soil texture, bulk density, and slope of the water retention curve to predict saturated hydraulic conductivity. *American Society of Agricultural Engineers*. 41(4):983–988.

Rawls, W.J., Pachepsky, Y.A., Ritchie, J.C., Sobecki, T.M. & Bloodworth, H. 2003. Effect of soil organic carbon on soil water retention. *Geoderma*. 116(1–2):61–76.

Reeve, M.J., Smith, P.D. & Thomasson, J. 1973. The effect of density on water retention properties of field soils. *Journal of Soil Science*. 24(3):355–367.

Reynolds, W.D., Bowman, B.T., Brunke, R.R., Drury, C.F. & Tan, C.S. 2000. Comparison of tension infiltrometer, pressure infiltrometer, and soil core estimates of saturated hydraulic conductivity. *Soil Science Society of America Journal*. 64(2):478–484.

Richard, G., Cousin, I., Sillon, J.F., Bruand, A. & Guérif, J. 2001. Effect of compaction on the porosity

of a silty soil: Influence on unsaturated hydraulic properties. *European Journal of Soil Science*. 52(1):49–58.

Robertson, G.P., Sollins, P., Elllis, B.G. & Lajtha, K. 1999. Exhangeable ions, pH, and cation exchange capacity. In G.P. Robertson et al. (eds.). New York, Oxford: Oxford University Press, Inc. *Standard soil methods for long-term ecological research*. 106–114.

Romero-Ruiz, A., Linde, N., Keller, T. & Or, D. 2018. A review of geophysical methods for soil structure characterization. *Reviews of Geophysics*. 56(4):672–697.

Ross, D.S., Bartlett, R.J. & Magdoff, F.R. 1991. Exchangeable cations and the pH-independent distribution of cation exchange capacities in Spodosols of a forested watershed. *Plant-Soil Interactions at Low pH*. 81–92.

Rücknagel, J., Götze, P., Hofmann, B., Christen, O. & Marschall, K. 2013. The influence of soil gravel content on compaction behaviour and pre-compression stress. *Geoderma*. 209–210:226–232.

Salchow, E., Lal, R., Fausey, N.R. & Ward, A. 1996. Pedotransfer functions for variable alluvial soils in southern Ohio. *Geoderma*. 73(3–4):165–181.

Saxton, K.E., Rawls, W.J., Romberger, J.S. & Papendick, R.I. 1986. Estimating generalised soil-water characteristics from texture. *Soil Science Society of America Journal*. 50(4):1031–1036.

Schaap, M.G. & Leij, F.J. 1998. Using neural networks to predict soil water retention and soil hydraulic conductivity. *Soil and Tillage Research*. 47(1–2):37–42.

Scheinost, A.C., Sinowski, W. & Auerswald, K. 1997. Regionalization of soil water retention curves in a highly variable soilscape, I. Developing a new pedotransfer function. *Geoderma*. 78(3–4):129–143.

Schneider, A., Baumgartl, T., Doley, D. & Mulligan, D. 2010. Store and release cover systems: A suitable preventive for acid mine drainage in semi-arid monsoonal Queensland? In *19th World Congress of Soil Science, Soil Solutions for a Changing World*. 77–80.

Seema Dahiya, R. & Phogat, V. 2019. Investigation of hydraulic properties of soils varying in texture, organic carbon and soluble salt contents of arid and semi-arid regions. *International Journal of Current Microbiology and Applied Sciences*. 8(04):2827–2838.

Sexstone, A.J., Parkin, T.B. & Tiedje, J.M. 1988. Denitrification response to soil wetting in aggregated and unaggregated soil. *Soil Biology and Biochemistry*. 20(5):767–769.

Shierlaw, J. & Alston, A.M. 1984. Effect of soil compaction on root growth and uptake of phosphorus. *Plant and Soil*. 77(1):15–28.

Shwetha, P. & Varija, K. 2013. Soil water retention prediction from pedotransfer functions for some Indian soils. *Archives of Agronomy and Soil Science*. 59(11):1529–1543.

Shwetha, P. & Varija, K. 2015. Soil water retention curve from saturated hydraulic conductivity for sandy loam and loamy sand textured soils. *Aquatic Procedia*. 4(Icwrcoe):1142–1149.

Silberbush, M., Hallmark, W.B. & Barber, S.A. 1983. Simulation of effects of soil bulk density and P addition on K uptake by soybeans. *Communications in Soil Science and Plant Analysis*. 14(4):287–296.

Singh, A., Phogat, V.K., Dahiya, R. & Batra, S.D. 2014. Impact of long-term zero till wheat on soil physical properties and wheat productivity under rice-wheat cropping system. *Soil and Tillage Research*. 140:98–105.

Singh, J., Salaria, A. & Kaul, A. 2015. Impact of soil compaction on soil physical properties and root growth: A review. *International Journal of Food*. 5(1):23–32.

Smith, J.L. & Doran, John W. 1996. Measurement and use of pH and electrical conductivity for soil quality analysis. In J.W. Doran et al. (eds.). Madison, WI: Soil Science Society of America *Methods for Assessing Soil Quality*. 169–185.

Smith, C.W., Johnston, M.A. & Lorentz, S.A. 2001. The effect of soil compaction on the water retention characteristics of soils in forest plantations. *South African Journal of Plant and Soil*. 18(3):87–97.

Soane, B.D. 1990. The role of organic matter in soil compactibility: A review of some practical aspects. *Soil and Tillage Research*. 16(1–2):179–201.

Soane, B.D., Blackwell, P.S., Dickson, J.W. & Painter, D.J. 1980. Compaction by agricultural vehicles: A review I. Soil and wheel characteristics. *Soil and Tillage Research*. 1(C):207–237.

Stepniewski, W., Gliński, J. & Ball, B.C. 1994. Effects of compaction on soil aeration properties. *Developments in Agricultural Engineering*. 11(C):167–189.

Stewart, V.I., Adams, W.A. & Abdulla, H.H. 1970. Quantitative pedological studies on soils derived from Silurian mudstones. II: The relationship between stone content and the apparent density of the fine earth. *Journal of Soil Science*. 21(2):248–255.

Stošić, M., Brozović, B., Vinković, T., Ravnjak, B., Kluz, M. & Zebec, V. 2020. Soil resistance and bulk density under different tillage system. *Poljoprivreda*. 26(1):17–24.

Sun, F. & Lu, S. 2014. Biochars improve aggregate stability, water retention, and pore-space properties of clayey soil. *Journal of Plant Nutrition and Soil Science*. 177(1):26–33.

Tainton, N.M. 1999. The ecology of the main grazing lands of South Africa. In N.M. Tainton (ed.). South Africa University of Natal Press *Veld management*.

Tan, X. & Chang, S.X. 2007. Soil compaction and forest litter amendment affect carbon and net nitrogen mineralization in a boreal forest soil. *Soil and Tillage Research*. 93(1):77–86.

Tan, X., Chang, S.X. & Kabzems, R. 2008. Soil compaction and forest floor removal reduced microbial biomass and enzyme activities in a boreal aspen forest soil. *Biology and Fertility of Soils*. 44(3):471–479.

Taylor, H.M. & Brar, G.S. 1991. Effect of soil compaction on root development. *Soil and Tillage Research*. 19(2–3):111–119.

The Fertiliser Association of South Africa. 2007. *Fertilisation manual*. 7th ed. Lynnwoodrif: FSSA-MVSA.

The Mine Manager of Landau Colliery. 2001. *Landdua Colliery South African coal estates*. Clewer.

The University of Queensland. 2012. Designing effectvie store-and-release covers for the long-term containement of mine waste: The role of vegetation (stage 2). Queensland.

Tomasella, J. & Hodnett, M.G. 1997. Estimating unsaturated hydraulic conductivity of Brazilian soils using soil-water retention data. *Soil Science*. 162(10):703–712.

Tomasella, J., Pachepsky, Y., Crestana, S. & Rawls, W.J. 2003. Comparison of two techniques to develop pedotransfer functions for water retention. *Soil Science Society of America Journal*. 67(4):1085–1092.

Tomlinson, P. 1984. Evaluating the success of land reclamation schemes. *Landscape Planning*. 11(3):187–203.

Too, V.K., Omuto, C.T., Biamah, E.K. & Obiero, J.P. 2014. Review of soil water retention characteristic (SWRC) models between saturation and oven dryness. *Open Journal of Modern Hydrology*. 04(04):173–182.

Torri, D., Poesen, J., Monaci, F. & Busoni, E. 1994. Rock fragment content and fine soil bulk density. *Catena*. 23(1–2):65–71.

Tracy, S.R., Black, C.R., Roberts, J.A., Sturrock, C., Mairhofer, S., Craigon, J. & Mooney, S.J. 2012. Quantifying the impact of soil compaction on root system architecture in tomato (*Solanum lycopersicum*) by X-ray micro-computed tomography. *Annals of Botany*. 110(2):511–519.

Tracy, S.R., Black, C.R., Roberts, J.A. & Mooney, S.J. 2013. Exploring the interacting effect of soil texture and bulk density on root system development in tomato (*Solanum lycopersicum* L.). *Environmental and Experimental Botany*. 91:38–47.

Troeh, F.R. & Thompson, L.M. 1993. *Soils and soil fertility*. 6th ed. New York: Oxford University Press, Inc.

Trouse, A.C. 1966. Alteration of the infiltration permeability capacity of tropical soils by vehicular traffic. In Sao Paulo, Brazil *1st Pan-American Congress of Soil Conversation*. 1103–1109.

Tucker, C.J., Holben, B.N., Elgin, J.H. & McMurtrey, J.E. 1980. Relationship of spectral data to grain yield variation. *Photogrammetric Engineering & Remote Sensing*. 46(5):657–666.

Twum, E.K.A. & Nii-Annang, S. 2015. Impact of soil compaction on bulk density and root biomass of *Quercus petraea* L. at reclaimed post-lignite mining site in Lusatia, Germany. *Applied and Environmental Soil Science*. 2015(October 2015):1–5.

U.S Department of Agriculture. 2006a. Soil pH. *U.S Department of Agriculture Natural Resources Conservation Service*. 1–7.

U.S Department of Agriculture. 2006b. Soil electrical conductivity. *U.S Department of Agriculture Natural Resources Conservation Service*. 1–7.

U.S. Department of Agriculture. 1996. Soil quality indicators: Bulk Density. *Natural Resources Conservation Service*. 192(April):1836–41.

U.S. Department of Agriculture. 1998. *Inherent factors affecting bulk density and available water capacity*. [Online], Available: https://www.nrcs.usda.gov/Internet/FSE_DOCUMENTS/nrcs142p2_053260.pdf.

Van der Watt, H.v.H. 1972. Influence of particle size distribution on soil compactibility. *Journal of Terramechanics*. 8(3):118.

Van Wesenbeeck, I.J. & Kachanoski, R.G. 1988. Spatial and temporal distribution of soil water in the tilled layer under a corn crop. *Soil Science Society of America Journal*. 52:363–368

Van Zyl, B. 2002. *Challenges for industry in reaching mine closure*. In Randfontein WISA Mine Water Division, Mine Closure Conference.

Venkatraman, K. & Ashwath, N. 2007. Phytocapping: An alternative technique to reduce leachate and methane generation from municipal landfills. *Environmentalist*. 27(1):155–164.

Venkatraman, K. & Ashwath, N. 2010. Field performance of a phytocap at Lakes Creek landfill, Rockhampton, Australia. *Management of Environmental Quality: An International Journal*. 21(2):237–252.

Vepraskas, M.J. 1988. Bulk density values diagnostic of restricted root growth in coarse-textured soils. *Soil Science Society of America Journal*. 52(4):1117–1121.

Verburg, R., Bezuidenhout, N., Chatwin, T. & Ferguson, K. 2009. *The global acid rock drainage guide (GARD Guide)*. Vol. 28. The International Network for Acid Prevention.

Vereecken, H., Maes, J. & Feyen, J. 1990. Estimating unsaturated hydraulic conductivity from easily measured soil properties. *Soil Science*. 149(1):1–12.

Vermaak, J.J.G., Wates, J.A., Bezuidenhout, N. & Kgwale, D. 2004. *The evaluation of soil covers*

used in the rehabilitation of coal mines. Vol. 1002/1/04. Water Research Commission.

Viji, R. & Rajesh, P.P. 2012. Assessment of water holding capacity of major soil series of Lalgudi, Trichy, India. *J.Environ.Res.Develop*. 7(1):393–398.

Wagner, B., Tarnawski, V.R., Hennings, V., Müller, U., Wessolek, G. & Plagge, R. 2001. Evaluation of pedo-transfer functions for unsaturated soil hydraulic conductivity using an independent data set. *Geoderma*. 102(3–4):275–297.

Wang, Y., Shao, M. & Liu, Z. 2012. Pedotransfer functions for predicting soil hydraulic properties of the Chinese loess plateau. *Soil Science*. 177(7):424–432.

Waugh, W.J., Petersen, K.L., Link, S.O., Bjornstad, B.N. & Gee, G.W. 1994. Natural analogs of the long-term performance of engineered covers. In G.W. Gee et al. (eds.). Battelle, Columbus, Ohio *In-Situ remediation: Scientific basis for current and future technolgies*. 379–409.

Waugh, W.J., Kastens, M.K., Sheader, L.R.L., Benson, C.H., Albright, W.H. & Mushovic, P.S. 2008. Monitoring the performance of an alternative landfill cover at the Monticello, Utah, Uranium Mill Tailings Disposal Site. In Phoenix: Wessex Institute of Technology *Waste Management*.

Wels, C., Fortin, S. & Loudon, S. 2002. Assessment of store-and-release cover for Questa Tailings Facility, New Mexico. In Fort Collins, Colorado: A.A. Balkema *Proceedings of the 9th International Conference on Tailings and Mine Waste*. 459–468.

Wever, L.A., Flanagan, L.B. & Carlson, P.J. 2002. *Seasonal and inter-annual variation in evapotranspiration energy balance and surface conductance in a northern temperate grassland*. Agricultural and Forest Meteorology (in press).

White, R.G. & Kirkegaard, J.A. 2010. The distribution and abundance of wheat roots in a dense, structured subsoil - Implications for water uptake. *Plant, Cell and Environment*. 33(2):133–148.

Williamson, N.A., Johnson, M.S. & Bradshaw, A.D. 1982. *Mine waste reclamation*. London, UK: Mineral Industry Research Organisation.

Winter, M.G., Hólmgeirsdóttir, T. & Suhardi. 1998. The effect of large particles on acceptability determination for earthworks compaction. *Quarterly Journal of Engineering Geology*. 31(3 Part 3):247–268.

Wolkowski, R.P. 1990. Relationship between wheel-traffic-induced soil compaction, nutrient availability, and crop growth: A review. *Journal of Production Agriculture*. 3(4):460–469.

Wösten, J.H.M., Lilly, A., Nemes, A. & Le Bas, C. 1999. Development and use of a database of hydraulic properties of European soils. *Geoderma*. 90(3–4):169–185.

Wösten, J.H.M., Pachepsky, Y.A. & Rawls, W.J. 2001. Pedotransfer functions: Bridging the gap between available basic soil data and missing soil hydraulic characteristics. *Journal of*

Hydrology. 251(3–4):123–150.

Yanful, E.K., Mousavi, S.M. & Yang, M. 2003. Modeling and measurement of evaporation in moisture-retaining soil covers. 7:783–801.

Yuen, S.T.S., Salt, M., Sun, J., Zhu, G.X., Jaksa, M., Ashwath, N. & Fourie, A.B. 2011. Phytocapping as a sustainable cover for waste containment systems: Experience of the A-ACAP study. In Cagliari, Italy: Envirmental Sanitary Engineering Centre *Thirteenth International Waste Management and Landfill Symposium*.

Zhan, G., Keller, J., Milczarek, M. & Giraudo, J. 2014. 11 Years of evapotranspiration cover performance at the AA Leach Pad at Barrick Goldstrike Mines. *Mine Water and the Environment*. 33(3):195–205.

Zhang, J., Wang, Z. & Luo, X. 2018a. Parameter estimation for soil water retention curve using the salp swarm algorithm. *Water (Switzerland)*. 10(6):1–11.

Zhang, S., Grip, H. & Lövdahl, L. 2006. Effect of soil compaction on hydraulic properties of two loess soils in China. *Soil and Tillage Research*. 90(1–2):117–125.

Zhang, Y. & Schaap, M.G. 2019. Estimation of saturated hydraulic conductivity with pedotransfer functions: A review. *Journal of Hydrology*. 575(May):1011–1030.

Zhang, Y., Schaap, M.G. & Zha, Y. 2018b. A high-resolution global map of soil hydraulic properties produced by a hierarchical parameterization of a physically-based water retention model. *Water Resources Research*. 54(12):9774–9790.

Zornberg, J.G., LaFountain, L. & Caldwell, J.A. 2003. Analysis and design of evapotranspirative cover for hazardous waste landfill. *Journal of Geotechnical and Geoenvironmental Engineering*. 129(5):427–438.

Zotarelli, L., Scholberg, J.M., Dukes, M.D. & Muñoz-Carpena, R. 2007. Monitoring of nitrate leaching in sandy soils: Comparison of three methods. *Journal of Environmental Quality.* 36(4):953–962.

Chapter 2: Soil cover properties of old store-and-release covers

2.1 Introduction

Currently, coal discard or spoil is being compacted and covered with a soil cover layer, and thereafter the soil cover is seeded with an indigenous grass pasture. Direct revegetation on coal discard or spoil is seldom done since it is not feasible and sustainable. The primary function of the soil covers is to preserve the environment, particularly groundwater. In semi-arid environments, it is often proposed to use store-and-release covers (SRCs) to prevent oxygen- and water ingress into coal discard or spoil and inhibits seeping impact (Fourie & Tibbett, 2007). This natural approach is more likely to be effective over the long term because it is congruent with nature (Wels *et al.*, 2002) together with the primary aim of mine rehabilitation namely, establishing a self-sustaining ecosystem. Annual fertilisation for about 5–10 years is essential to increase root growth and thereby, increasing nutrient recycling. Kent (1982) stated that the rate of nutrient supply during early rehabilitation is critical, since vegetation will most likely be self-sustainable later on if nutrient cycling is effective. With the advantages of SRCs, field data describing its long-term performance are limited in South Africa. The cost-effectiveness and success of long-term performance are important to prevent business losses. Nevertheless, to achieve a self-sustainable ecosystem is challenging because properties of soil covers can be easily affected by several factors during rehabilitation. High bulk densities on rehabilitated mines were reported by Limpitlaw *et al.* (1997). Nell & Steenekamp (1998) mentioned unfavourable soil texture and high bulk densities as the main physical problems during soil cover constructions.

Typically, SRCs consist of a coarse-textured soil layer placed on top of finer medium. The textural contrast can control the vertical infiltration by capillary forces (Parent & Cabral, 2005). Store-and-release covers depend on soil cover properties as well as hydraulic and vegetation properties for their proper functioning (Qian *et al.*, 2010). Some critical soil cover properties indicated by Schafer (1979) include soil texture, bulk density and soil nutrient availability. The book of Williamson *et al.* (1982) can be used for mine rehabilitation and use critical threshold values to evaluate the soil nutrient availability, while Haigh (1995) proposed to use only bulk density and pH. In the current study, however, the soil texture with soil organic matter (SOM), bulk density, $pH_{(H_2O)}$, $pH_{(KCl)}$, electrical conductivity of saturated paste extract (EC_e) and cation exchange capacity (CEC) were evaluated. These parameters are being usually used for designing soil covers or modelling long-term soil cover performance and to determine the success of rehabilitation.

Mostly rehabilitated soil covers are viewed as inferior to natural soil profiles due to mixing or compaction, but proper soil cover construction with good management of revegetation and fertilisation on rehabilitated mines can establish a self-sustainable ecosystem. The objectives of this Chapter were (1) to evaluate the impact of configurations and soil cover properties on the long-term

performance of SRCs; and (2) to determine if the bulk density and soil nutrient availability guidelines can be used as critical threshold values for SRCs.

2.2 Materials and methods

2.2.1 General site descriptions

The regional climate of Mpumalanga Highveld is semi-arid characterised by a mild to warm summer rainfall and cool to cold winters according to Kottek *et al.* (2006). Frost is a common occurrence during winter. The mean annual minimum and maximum temperatures are 7.15°C and 23.91°C, respectively (OpenStreetMap contributors, 2020). The mean annual precipitation is around 683 mm and occurs from October to April with gross mean A-pan evaporation approximately 2000–2200 mm (Schulze *et al.*, 2007).

Vegetation in rehabilitated mining areas is primarily grassland (Mills *et al.*, 2013). Rutherford *et al.* (2006) describes the vegetation in these mining areas as “Eastern Highveld Grassland”. The soil types primarily used for the SRCs were soil types for arable land capability.

2.2.2 Soil cover selection criteria

Emails were sent to environmental representatives at selected mining companies with background information on the Water Research Commission of South Africa and Coaltech Research Association research project. The emails included a table of information regarding soil cover type and age, and soil cover design, construction, and care and maintenance. They were followed up with telephonic communication to maximise the amount of candidate covers available from which research sites could be selected. The number of soil covers were limited to as old covers with moderately- and very dense soil cover conditions at Mpumalanga Highveld coalfields, South Africa (Figure 2.1). Three profile pits were identified at Discard Dump 1 (26°05'14"S, 29°19'55"E), two profile pits at Discard Dump 2 (26°05'14"S, 29°19'55"E), four profile pits were identified at Opencast Backfilled Pit 1 (25°45'55"S, 29°04'51"E) and three profile pits at Opencast Backfilled Pit 2 (26°00'36"S, 29°12'26"E). Particulars of the profile pits are summarised in Table 2.1. An additional research site at Discard Dump 3 (26°07'13"S, 29°23'46"E) with two profile pits similar to Discard Dump 1 & 2 were included for obtaining a data-set to validate the saturated hydraulic conductivity and soil water retention curve models (Table 2.1).

Other aspects that were also considered in the site selection process include:

- Logistical support that the mine was prepared to provide, such as site health and induction and site access requirements and providing a tractor loader backhoe (TLB),
- Relatively easy access to field investigation sites was required for equipment to be transported or carried to the research sites, and
- Available information on soil cover design and construction.

Table 2.1: Particulars of four research sites and one additional research site in the Highveld of Mpumalanga, South Africa.

Facility	Age (yrs)[a]	Profile pit	Soil cover type	Soil cover condition
Discard Dump 1	26	D1-1 D1-2 D1-3	Dual-layered store-and-release	Good construction Moderately dense
Discard Dump 2	22	D2-1 D2-2	Dual-layered store-and-release	Poor construction Very dense
Opencast Backfilled Pit 1	27	P1-1 P1-2	Monolithic store-and-release	Very dense
	27	P1-3 P1-4	Monolithic store-and-release	Moderately dense
Opencast Backfilled Pit 2	18	P2-1	Dual-layered store-and-release	Poor construction Very dense
	18	P2-2	Dual-layered store-and-release	Good construction Moderately dense
	18	P2-3	Monolithic store-and-release	Good construction Moderately dense
Discard Dump 3	18	D3-1 D3-2	Dual-layered store-and-release	Good construction Moderately dense

[a]Soil covers age are at 2020.

Figure 2.1: Aerial photo showing the location of Discard Dump 1, 2 & 3 and Opencast Backfilled Pit 1 & 2 taken on 09 September 2020 (Google Earth 2.7, 2020).

2.2.3 Soil cover configurations

The access was approved to Discard Dump 1, 2 & 3, and Opencast Backfilled Pit 1 & 2 to conduct the field investigation on 29 August 2018. As a result, the field investigation on the earliest could be conducted during 03-14 September 2018 based on the permit that allowed only 20 days (10 + 10 days) conducting all the fieldwork required for this study. At the Discard Dump 1 & 2, the profile pits were dug by spade into the discard and the TBL was used to dug the profile pits at Opencast Backfilled Pit 1 & 2. The profile pits at Discard Dump 3 were not examined because of the limited time since only a 10-day Permit was granted to conduct the field investigation. After the fieldwork and samples were taken, the materials were backfilled and compacted by hand in 100 mm layers according to the sequence of the cover layers (Figure 2.2). The configuration of SRCs for the various soil cover layers was investigated and characterised in terms of thickness, material morphological characteristics (colour and soil structure), cover density, root occurrence and preferential flows. Due to limited time, the field investigation focussed on Discard Dump 1 & 2 in order to obtain the information and data required for the project and was completed one day ahead of schedule. The last day was used to conduct selected fieldwork at Discard Dump 3 that excluded time consuming field investigation such as the excavation of profile pits that would not be feasible in a day. Moreover, a 10-day Permit was also given for Backfilled Opencast Pit 1 & 2 and all the configuration of SRCs could be done.

Figure 2.2: Hand compaction of 100 mm layers during pit in-filling according to cover layering on the lefthand side. On the righthand side is the surface of in-filled pit.

2.2.4 Soil cover properties

Duplicate undisturbed core samples were collected with a soil core sampler at the surface (0–10 mm), and in the growth medium and water retention layer of dual-layered covers as well as at the surface, upper- and lower section of monolithic covers of SRC to determine SWRCs and soil physical properties. Due to a limited number of core rings, not all the surfaces of profile pits were sampled. A total of 49 core samples were obtained with a diameter of 65 mm and 20 mm in height. In addition, a total of 37 disturbed soil samples were taken at the locations where the infiltrometer tests on each SRC were carried out in order to determine soil chemical properties: $pH_{(H_2O)}$, $pH_{(KCl)}$, EC_e and CEC. Before the disturbed soil samples were analysed by analytical laboratories of the Western Cape Department of Agriculture, Elsenburg, the soil samples were air dried, crushed and sieved through a 2 mm mesh sieve. Atterberg limits were also determined by using the disturbed samples. Standard test methods for liquid limit and plasticity index were followed as described in ASTM D4318-00 (1989) and the shrinkage limit was determined by the method of ASTM D4943-08 (1989). The swelling potential of the soil cover layers were determined by using the approaches proposed to predict the soil expansion by Holtz & Gibbs (1956) and Chen (1988), as well as the swelling potential chart proposed by Van der Merwe (1964).

Before the soil texture, SOM, bulk density and porosity of the undisturbed core samples were determined, the SWRCs were determined as explained in Chapter 4. Bulk density was determined by the core method of Blake & Hartge (1986) after the core samples were oven-dried at 105°C. Thereafter, sand content of the core samples was determined using sieving separation (ASTM D6913-04, 2004), while silt- and clay content were determined by the pipette method as described by Gee & Or (2002). The textural class was classified according to a textural triangle USDA, 1987) and is presented in Table 2.2. Gravel content was determined as described by ASTM D5519-94 (1994) using the specific ranges of the textural fractions of Udden-Wentworth gravel-size scale (Wentworth, 1922) in Table 2.2. The total SOM was determined during the pre-treatment of the soil texture. Total SOM was equal to the weight loss of oven-dried soil after the sample (40g) was treated with hydrogen peroxide (30%). The soil porosity was calculated from soil particle density and bulk density (Flint & Flint, 2002b). The particle density was determined using the pycnometer (Flint & Flint, 2002a). The probability level for statistical analysis was 0.05 with a null hypothesis that there is no relationship or difference between two groups.

Finally, the soil covers were divided into moderately- and very dense soil cover conditions (Table 2.1) based on differences in bulk density, soil hydraulic- and vegetation properties, and construction status. However, the soil cover layer, 0–500 mm, of P2-2 was classified as a very dense soil cover condition, however, the overall soil cover condition of P2-2 was classified as moderately dense (Table 2.1). These results are being used to evaluate the long-term performance between moderately- and very dense SRCs.

It is important to note that the major- and minor elements of SRCs and the seeping impact of well and poorly constructed soil covers were not included in this project.

Table 2.2: The specific ranges of textural fractions for gravel (Wentworth, 1922) and soil (USDA, 1987).

Name of textural fraction	Diameter limits (mm)
Very coarse gravel	64.00–32.00
Coarse gravel	32.00–16.00
Medium gravel	16.00–8.00
Fine gravel	8.00–4.00
Very fine gravel	4.00–2.00
Very coarse sand	2.00–1.00
Coarse sand	1.00–0.50
Medium sand	0.50–0.25
Fine sand	0.25–0.106
Very fine sand	0.106–0.053
Coarse silt	0.053–0.0063
Fine silt	0.0063–0.002
Clay	<0.002

2.3 Results and discussion

2.3.1 Soil cover configurations

The cover layer properties of each profile pit are summarised in Tables 2.3–2.14. The description of categories and ratings of soil cover properties on field sheets are described in Tables A.1 & A.2 in Appendix A. The Atterberg limits and swelling potentials of moderately- and very dense SRCs are shown in Table 2.15. The following inferences were made from the information collated on the soil covers profiles described: (1) the soil covers were classified as monolithic and dual-layered SRC with long exposure to climatic conditions and environmental processes; and (2) the dual-layered SRCs were described as consisting of a growth medium (top layer), underlaid by a lower water retention layer (sublayer). The growth medium was mainly constructed using apedal-B soil layers and orthic soil horizons which are suitable as growth medium material. Little mixing of the stripped apedal soil horizons did occur with less suitable subsoils such as gleyed- and plinthic subsoil, or weathered rock and coralliferous material, resulting in high quality soil that was used for the growth medium. The sublayers were constructed from sandy clay loam to clayey plinthic soil layers, which is suitable as cover material for the water retention layer.

The plasticity of the soil cover layers was rated as acceptable (Table 2.15). The plasticity index for the growth medium- and moisture retention layers was rated as slightly- to medium plastic according to the plasticity index guideline in “Minimum requirements for handling, classification and disposal of hazardous waste” (DWAF, 1998), excluding the water retention layer of D2-2. The plasticity index of more clayey layers at D2-2 was unsuitable which marginally exceeded the plasticity index guideline of 15 specified in the minimum requirements of DWAF (1998) for the clay layer in a soil cover.

The clay activity (Table 2.15) was rated as inactive since all the indices were under 0.75 according to the guideline of clay activity of Skempton (1984). This indicated a low fraction of swelling clays. In the line with this, the swelling potential (Table 2.15) was rated as low for the growth medium layer for both soil cover conditions, excluding the growth medium of D1-1 and P2-1 which was rated medium. The water retention layers for both soil cover conditions was rated low and medium. The clay activity indices and swelling potentials indicated that the orthic, apedal and soft plinthic (mixed with the apedal) soil horizons were suitable borrow materials for soil covers due to the low probability for desiccation crack development and associated preferential flows through the cracks. Apedal soil horizons are widely distributed and are typically the bulk of non-wetland soils at Mpumalanga Highveld. It is important that the plasticity index and swelling potential of clayey non-apedal soil horizons are determined as an indication of the susceptibility to desiccation crack development.

No surface cracks were observed (Tables 2.3–2.14), which can be ascribed to the apedal soil horizons that were used for the surface layer, except for D2-1 & 2-2 (Tables 2.6 & 2.7). Apedal soils are characterised by massive soil structure *viz.* large, solid, featureless mass with little or no structure (Soil Classification Working Group, 1991). Soft plinthic material can be sometimes weakly structured as was observed at D1-3 (Table 2.5), but it was not a concern. Therefore, the concern in terms of soil structure to develop pedotransfer functions for saturated hydraulic conductivity and soil water retention curves was negligible. Note that the platy structure of P2-1 (Table 2.12) was caused by compaction by heavy machinery. Overall, relatively low erosion rates were expected for the apedal soil surface layer characterised by good infiltration and relatively low runoff potential for vegetated surfaces. Observed surface crusts were rated as weak indicating that it should not be of a concern in significantly increasing runoff and erosion damage, except D2-1 & 2-2 (Tables 2.6 & 2.7) which were rated as moderate. The substantial sheet (interrill) and rill erosion of D2-1 & 2-2 at localised runoff areas can be ascribed to high bulk density. In addition, the higher bulk densities caused vertical cracks in the soil cover layers of D2-1 & 2-2 (Tables 2.6 & 2.7 and Figure 2.2) and P2-1 (Table 2.12). These cracks can increase the oxygen- and water ingress into the coal discard or spoil which can enhance by lowering the pH and a higher seeping impact. Lateral cracks were also observed in D2-2 and P2-1 which can prevent evaporation due to a created capillary break that prevents infiltrated water from moving upwards. Poorly constructed soil covers, D2-1 & 2-2 (Tables 2.6 & 2.7), P1-1 &1-2 (Tables 2.8 & 2.9) and P2-1 (Table 2.12), with poor root distribution and poor or moderate vegetation covers pose a risk for high erosion damage and landform design should account for the increased runoff and erosion damage with consideration of the sustainable function of these SRCs in the long term. Limpitlaw *et al.* (1997) and Steffen Robertson & Kirsten (1989) addressed the same issue of soil covers with high bulk density that are more susceptible to erosion and runoff. Keep in mind, if the plintic water retention layer is not properly constructed or mixed with apedal, oxidisation may occurs because the soft plinthic are sensitive for redox changes. This means that if the soft plinthic water retention layer gets dry, it will oxidised and the pH decreases, where D2-2 is possibly the example of this occurrence.

Table 2.3: Soil cover profile of D1-1.

Profile pit		D1-1	**Terrain unit**	0	**Surface cracks**	None	**Effective soil depth (mm)**	900	**Cover profile**
Slope (%)		0	**Surface crust**	Weak	**Vegetation cover**	Good	**Effective root depth**	900	
Layer	**Depth (mm)**	**Colour**	**Soil material**	**Soil structure**	**Soil quality**	**Soil homogeneity**	**Soil density**	**Root occurrence**	
Ob1	0–500	Red	Apedal	Massive	High	Slighty mixed	Slight	Many	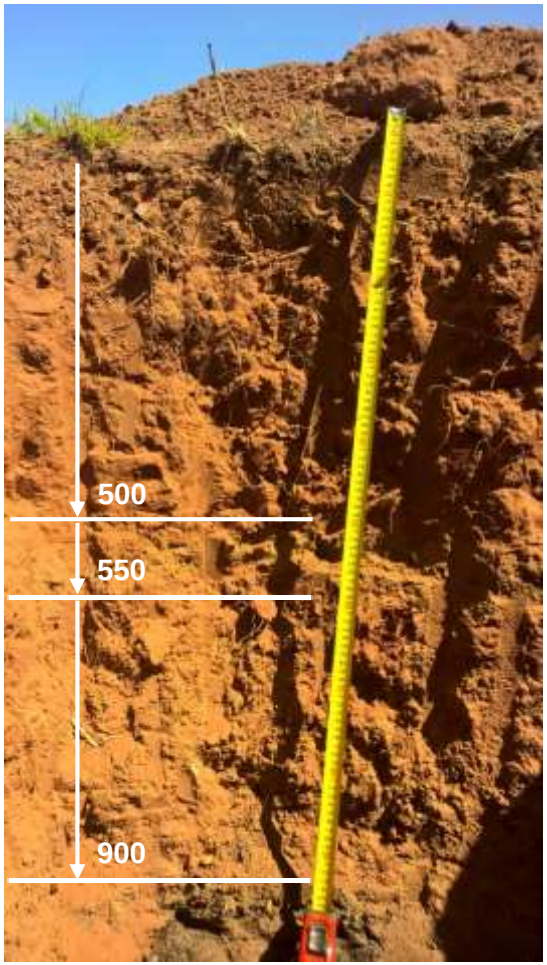
Ob2	500–550	Yellow brown	-	Massive	High	Slighty mixed	Slight	Common	
Sub3	550–900	Red	Soft plinthic	Massive	Medium	Moderately mixed	Slight	Common	
Discard	900+	Black	-	-	-	-	-	-	
Land capability (Slope, depth, soil quality)			Arable						

Comments:

Erosion: Some sheet erosion between grass tussocks.

Ob1: High quality, red apedal material, good growth medium and suitable for surface layer. Good root distribution with 55% amount of roots in this layer.

Ob2: A thin layer (50-100 mm), yellow brown, high quality, good growth medium and suitable for surface layer. Purpose and origin of layer unknown. It appears if Ob3 was placed and exposed for a long period and later covered with Ob2 and Ob1. Poor root distribution with few roots that grew through fine cracks.

Sub3: Medium quality, red plinthic material with small concretions occupying approximately 10% of the matrix. Low suitability for a surface layer, but high suitability for a slower permeable second layer (water retention layer). Good root distribution with 45% of the total amount of roots.

Discard: Fine and medium grained, black discard material.

General: *The typical store-and-release cover for optimise soil cover performance although this store-and-release cover had a thin layer between growth medium and water retention layer.*

Table 2.4: Soil cover profile of D1-2

Profile pit		D1-2	**Terrain unit**	3	**Surface cracks**	None	**Effective soil depth (mm)**	600	**Cover profile**
Slope (%)		15	**Surface crust**	Weak	**Vegetation cover**	Good	**Effective root depth**	600	
Layer	**Depth (mm)**	**Colour**	**Soil material**	**Soil structure**	**Soil quality**	**Soil homogeneity**	**Soil density**	**Root occurrence**	
Ob1	0–400	Yellow brown	Apedal	Massive	High	Slighty mixed	Slight	Common	
Sub2	400–600	Yellow red	Soft plinthic	Massive	Medium	Moderately mixed	High	Few	
Discard	600+	Black	-	-	-	-	-	-	
Land capability (Slope, depth, soil quality)		Grazing							

Comments:

Erosion: Some sheet erosion between grass tussocks.

Ob1: High quality, pale yellow brown apedal material, good growth medium and suitable for surface layer. Many roots of 40% in the upper 100 mm, but sparse of 20% in the remainder of the layer.

Sub2: Yellowish red plinthic material with concretions occupying 5-10% of the matrix. Low suitability for a surface layer, but high suitability for a slower permeable second layer (water retention layer). Moderately well root distribution of 34% root amount in this layer.

Discard: A mixture of fine, medium and coarse grained, highly compacted, black discard material.

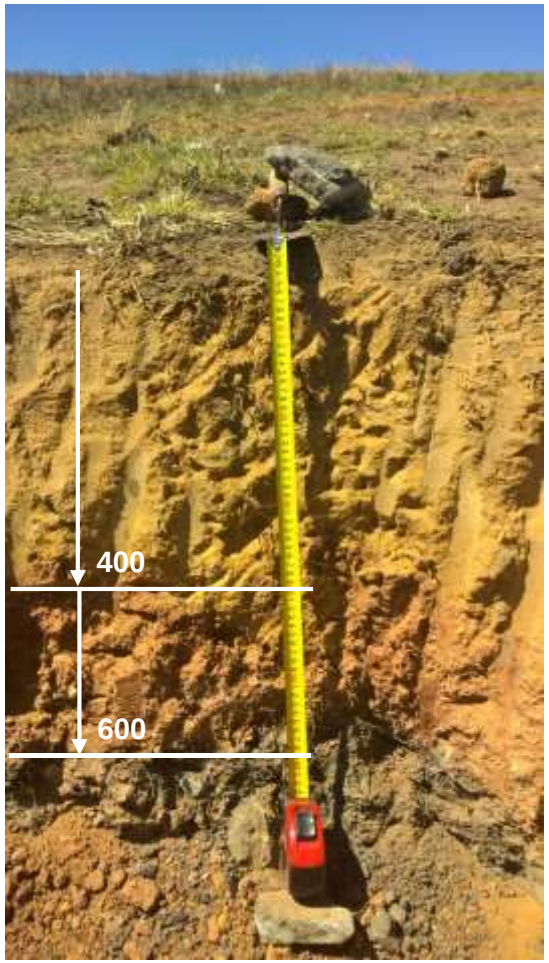

Table 2.5: Soil cover profile of D1-3.

Profile pit		D1-3	**Terrain unit**	3	**Surface cracks**	None	**Effective soil depth (mm)**	550
Slope (%)		12	**Surface crust**	Weak	**Vegetation cover**	Good	**Effective root depth (mm)**	550
Layer	**Depth (mm)**	**Colour**	**Soil material**	**Soil structure**	**Soil quality**	**Soil homogeneity**	**Soil density**	**Root occurrence**
Ob1	0–250	Red	Apedal	Massive	High	Slighty mixed	Slight	Few
Sub2	250–550	Yellow red	Soft plinthic	Weak structured	Medium	Moderately mixed	Slight	Common
Discard	550+	Grey	-	-	-	-	-	-
Land capability (Slope, depth, soil quality)			Grazing					

Cover profile

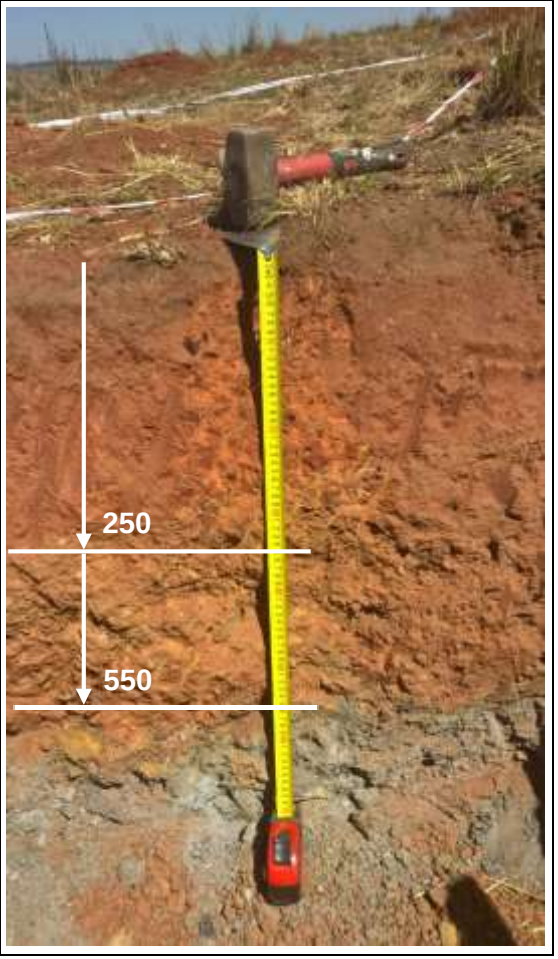

Comments:

Erosion: Some sheet erosion between grass tussocks.

Ob1: High quality, red apedal material, good growth medium and suitable for surface layer. Moderately root distribution with 40% roots in the upper 100 mm, but sparse roots of 20% in the remainder of the layer.

Sub2: Yellowish red plinthic material with concretions occupying 15% of the matrix with few fine cracks. Low suitability for a surface layer and high suitability for a slower permeable second layer (water retention layer). Moderately well root distribution with 40% of roots in this layer.

Discard: A mixture of fine, medium and coarse grained, highly compacted, grey discard material.

Table 2.6: Soil cover profile of D2-1.

Profile pit		D2-1	**Terrain unit**	1	**Surface cracks**	Few	**Effective soil depth (mm)**	850
Slope (%)		0	**Surface crust**	Moderate	**Vegetation cover**	Poor	**Effective root depth (mm)**	100
Layer	**Depth (mm)**	**Colour**	**Soil material**	**Soil structure**	**Soil quality**	**Soil homogeneity**	**Soil density**	**Root occurrence**
Ob1	0–450	Brown	Orthic	Weak structured	High	Slighty mixed	Moderate	Few
Ob2	450–650	Yellow brown	Apedal	Massive	High	Slighty mixed	High	None
Ob3	650–850	Red	Apedal	Massive	High	Slighty mixed	High	None
Sub4	850–1100	Yellow red	Soft plinthic	Massive	Medium	Moderately mixed	Moderate	None
Discard	1100+	Black	-	-	-	-	-	-
Land capability (Slope, depth, soil quality)			Arable					

Cover profile

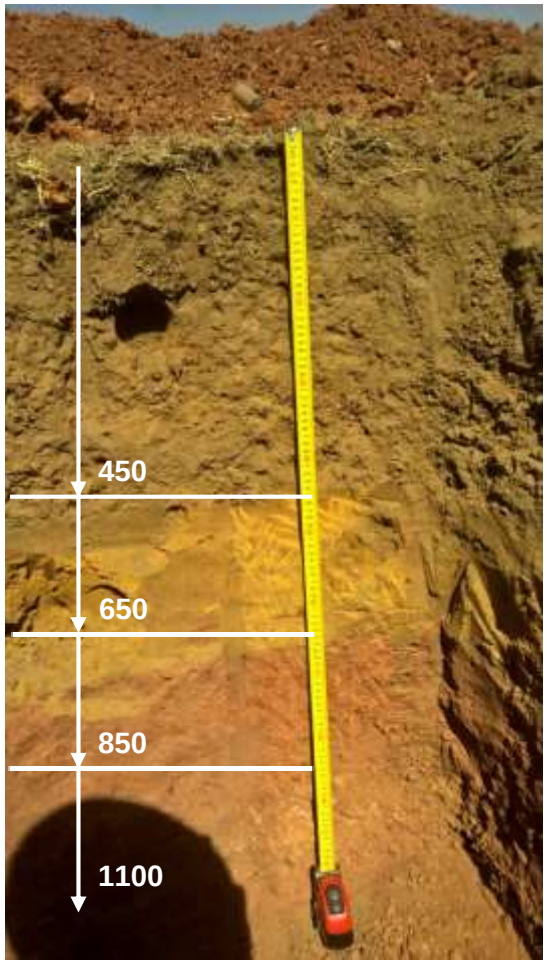

Comments:

Erosion: Severe sheet erosion between grass tussocks.

Ob1: High quality, greyish brown orthic material with concretions occupying 10-20% of the matrix. Fairly good growth medium and suitable for surface layer. Poor root distribution with 95% roots in the upper 100 mm, but very few in the remainder of the layer.

Ob2: High quality, yellow brown apedal material, good growth medium and suitable for surface layer. Hardly any roots in the layer.

Ob3: High quality, red apedal material with hardly any roots in the layer. Good growth medium and suitable for surface layer. Hardly any roots in the layer.

Sub4: Yellowish red, material with concretions occupying 5-10% of the matrix. Low suitability for a surface layer, but high suitability for a slower permeable second layer (water retention layer). No roots in the layer.

General: The profile pit had several vertical cracks which can promote preferential flow. No discard reached within 1100 mm.

Table 2.7: Soil cover profile of D2-2.

Profile pit		D2-2	**Terrain unit**	3	**Surface cracks**	Few	**Effective soil depth (mm)**	300	**Cover profile**
Slope (%)		8	**Surface crust**	Moderate	**Vegetation cover**	Poor	**Effective root depth (mm)**	100	
Layer	**Depth (mm)**	**Colour**	**Soil material**	**Soil structure**	**Soil quality**	**Soil homogeneity**	**Soil density**	**Root occurrence**	
Ob1	0–300	Red	Apedal	Massive	High	Slighty mixed	Extreme	Very few	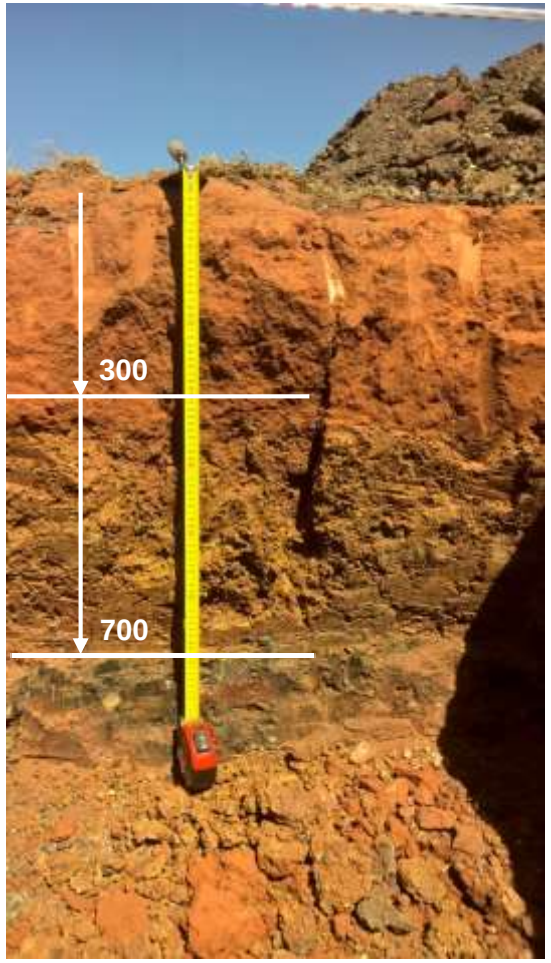
Sub2	300–700	Yellow red	Soft plinthic	Massive	Low	Moderately mixed	High	None	
Discard	700+	Black	-	-	-	-	-	-	
Land capability (Slope, depth, soil quality)			Grazing						

Comments:

Erosion: Severe sheet erosion with rills at localised runoff areas.

Ob1: High quality, red apedal material, good growth medium and suitable for surface layer. Poor root distribution with 95% roots in the upper 100 mm, but very few in the remainder of the layer.

Sub2: Yellowish brown, plinthic material with concretions occupying 10% of the matrix. Low suitability for a surface layer and high suitability for a slower permeable second layer (water retention layer). Hardly any roots in this layer.

Discard: Predominantly fine grained, very dense, black discard material.

General: The profile pit had several vertical cracks which can promote preferential flow.

Table 2.8: Soil cover profile of P1-1.

Profile pit		P1-1	**Terrain unit**	3	**Surface cracks**	None	**Effective soil depth (mm)**	1000
Slope (%)		4	**Surface crust**	Weak	**Vegetation cover**	Poor	**Effective root depth (mm)**	200
Layer	**Depth (mm)**	**Colour**	**Soil material**	**Soil structure**	**Soil quality**	**Soil homogeneity**	**Soil density**	**Root occurrence**
Ob1A	0–200	Yellow brown	Apedal	Massive	High	Slighty mixed	Severe	Few
Ob1B	200–700	Yellow brown	Apedal	Massive	High	Slighty mixed	Extreme	Few
Spoil	700+	Dark grey	-	-	-	-	-	-
Land capability (Slope, depth, soil quality)			Arable					

Cover profile

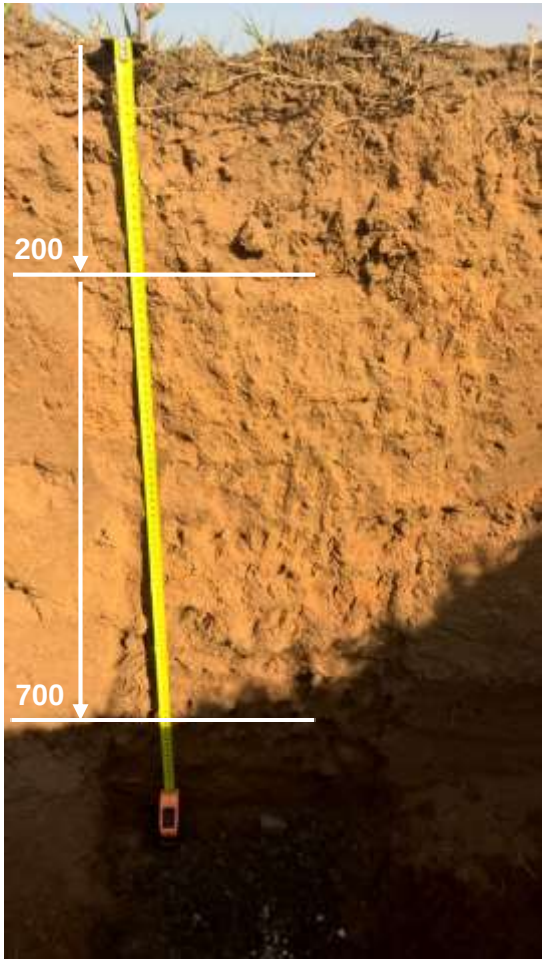

Comments:

Erosion: Sheet erosion with rills at localised runoff areas.

Ob1A: High quality, yellow brown apedal material, good growth medium and suitable for surface layer. Poor root distribution with 97% roots in the 200 mm upper layer.

Ob1B: High quality, yellow brown apedal material, good growth medium, and suitable for surface layer. Root occurrence was poor.

Spoil: A mixture of fine, medium and coarse grained (fine grained dominant), dark grey carbonaceous material (pulverized shale and sandstone).

General: The profile consists basically of a single, fairly homogeneous layer of soil material and was only subdivided based on variation in compaction and root distribution. No frequent visible cracks.

Table 2.9: Soil cover profile of P1-2.

Profile pit		P1-2	**Terrain unit**	1	**Surface cracks**	None	**Effective soil depth (mm)**	400	**Cover profile**
Slope (%)		1	**Surface crust**	Weak	**Vegetation cover**	Moderate	**Effective root depth (mm)**	100	
Layer	**Depth (mm)**	**Colour**	**Soil material**	**Soil structure**	**Soil quality**	**Soil homogeneity**	**Soil density**	**Root occurrence**	
Ob1	0–400	Yellow brown	Apedal	Weak structured	Moderate	Moderately mixed	High / severe	Few	
Spoil	400+	Dark grey	-	-	-	-	-	-	
Land capability (Slope, depth, soil quality)		Grazing							

Comments:

Erosion: Sheet erosion with rills at localised runoff areas.

Ob1: Moderate quality, yellow brown apedal material, coarse grained, good growth medium and suitable for surface layer. Root development mainly in the upper 100 mm and restricted by high bulk density. No visible cracks.

Spoil: A mixture of fine, medium and coarse grained (fine grained dominant), dark grey carbonaceous material (pulverized shale and sandstone).

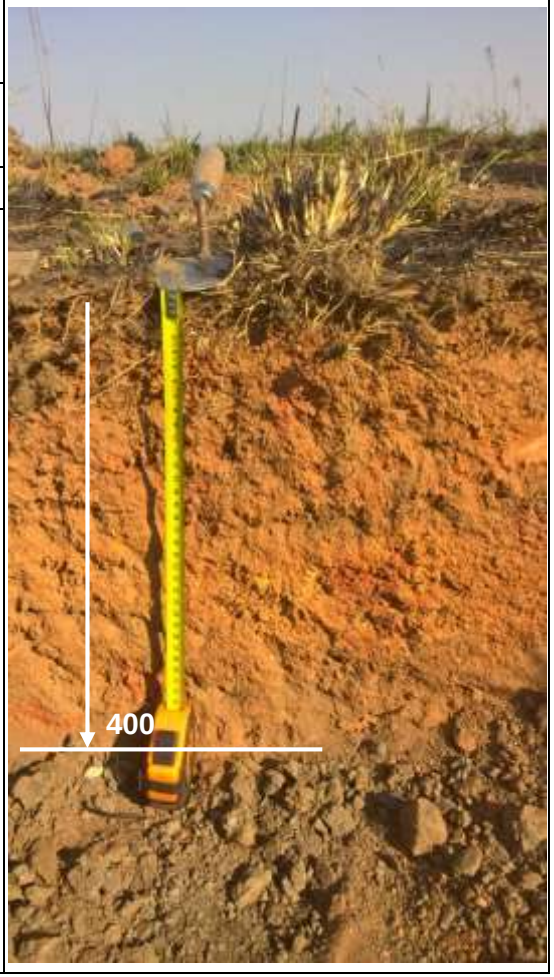

Table 2.10: Soil cover profile of P1-3.

Profile pit		P1-3	**Terrain unit**	3	**Surface cracks**	None	**Effective soil depth (mm)**	400	**Cover profile**
Slope (%)		3	**Surface crust**	Weak	**Vegetation cover**	Good	**Effective root depth (mm)**	400	
Layer	**Depth (mm)**	**Colour**	**Soil material**	**Soil structure**	**Soil quality**	**Soil homogeneity**	**Soil density**	**Root occurrence**	
Ob1A	0–400	Yellow brown	Apedal	Massive	High	Slighty mixed	High	Common	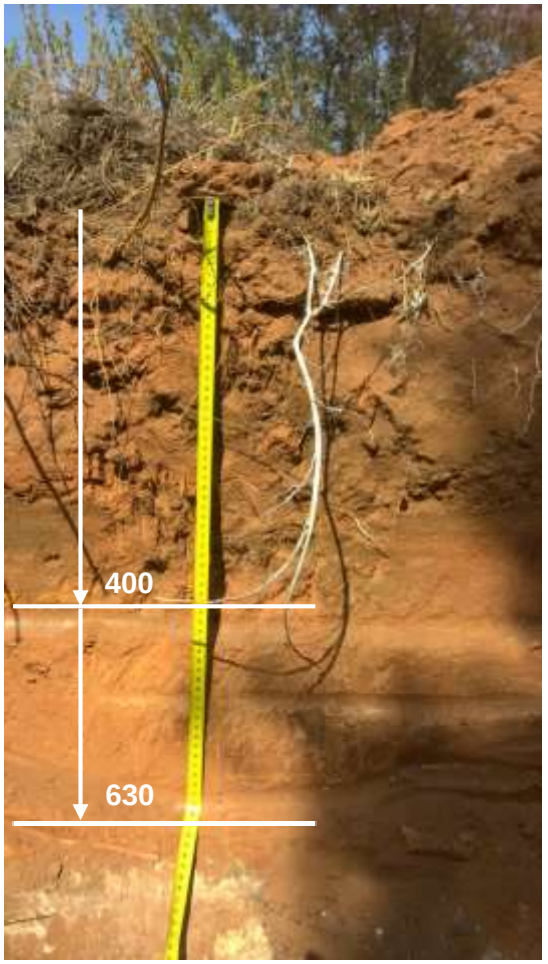
Ob1B	400–630	Yellow brown	Apedal	Massive	Moderate	Moderately mixed	Moderate	Few	
Spoil	630+	Grey	-	-	-	-	-	-	
Land capability (Slope, depth, soil quality)			Grazing						

Comments:

Erosion: Some sheet erosion with rills at localised runoff areas.

Ob1A: High quality, yellow brown apedal, good growth medium and suitable for surface layer. Good root distribution with 80% number of roots.

Ob1B: Moderate quality, yellow brown apedal, possibly suitable for surface layer. Few isolate vertical cracks. Poor root distribution with 20% number of roots.

Spoil: A mixture of fine, medium and coarse grained (fine grained dominant), grey carbonaceous material (pulverized shale and sandstone).

Table 2.11: Soil cover profile of P1-4.

Profile pit		P1-4	**Terrain unit**	3	**Surface cracks**	None	**Effective soil depth (mm)**	350	**Cover profile**
Slope (%)		3	**Surface crust**	Weak	**Vegetation cover**	Good	**Effective root depth (mm)**	350	
Layer	**Depth (mm)**	**Colour**	**Soil material**	**Soil structure**	**Soil quality**	**Soil homogeneity**	**Soil density**	**Root occurrence**	
Ob1	0–350	Yellow brown	Apedal	Massive	High	Slighty mixed	Moderate	Common	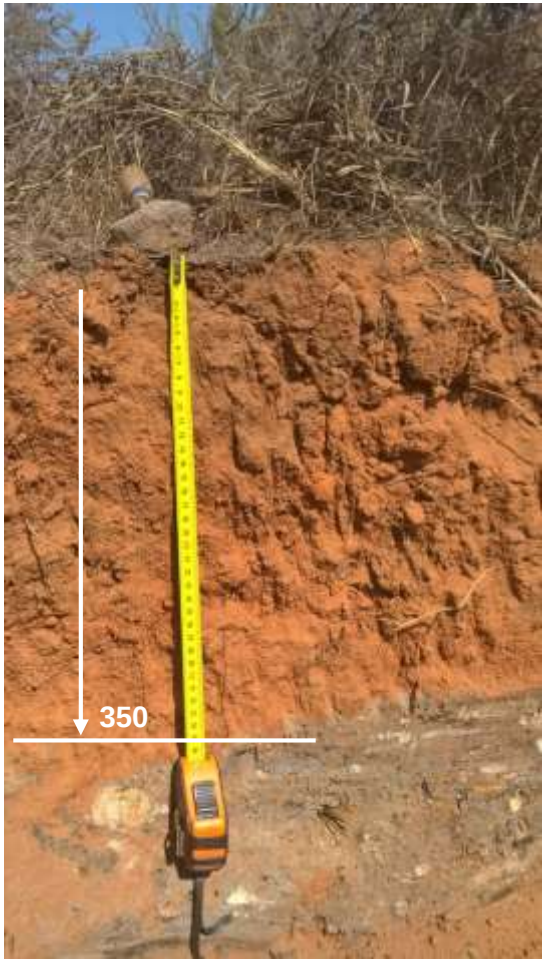
Spoil	350+	Grey	-	-	-	-	-	-	
Land capability (Slope, depth, soil quality)			Grazing						

Comments:

Erosion: Some sheet erosion with rills at localised runoff areas.

Ob1: High quality, yellow brown apedal material, good growth medium and suitable for surface layer. Moderate root distribution with 78% roots in the 300 mm upper layer and 22% in the lower layer. No frequent cracks.

Spoil: A mixture of fine, medium and coarse grained (fine grained dominant), grey carbonaceous material (pulverized shale and sandstone).

Table 2.12: Soil cover profile of P2-1.

Profile pit		P2-1	**Terrain unit**	3	**Surface cracks**	None	**Effective soil depth (mm)**	300	**Cover profile**
Slope (%)		4	**Surface crust**	Weak	**Vegetation cover**	Moderate	**Effective root depth (mm)**	100	
Layer	**Depth (mm)**	**Colour**	**Soil material**	**Soil structure**	**Soil quality**	**Soil homogeneity**	**Soil density**	**Root occurrence**	
Ob1	0–100	Grey brown	Orthic	Platy	High	Slighty mixed	High	Many	
Ob2	100–300	Red yellow	Apedal	Platy	High	Slighty mixed	Extreme	None	
Ob3	300–400	Brown red	Apedal	Platy	High	Slighty mixed	Severe	None	
Sub4	400+	Brown red	Soft plinthic	Platy	High	Slighty mixed	-	None	
Land capability (Slope, depth, soil quality)			Grazing						

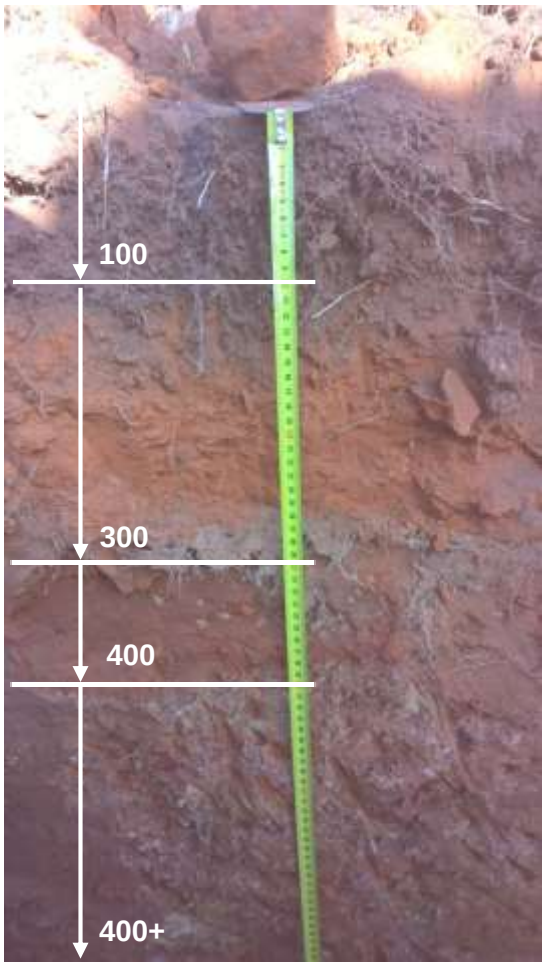

Comments:

Erosion: Some sheet erosion between grass tussocks.

Ob1: High quality, greyish brown orthic material, good growth medium and suitable for surface layer. No visible cracks. Poor root distribution with 95% roots in the upper 100 mm, but very few in the remainder of the layer.

Ob2: High quality, reddish yellow apedal material. Roots consist of compressed mats restricted to isolated fine vertical cracks or in-between thin, horizontal plates caused by compaction. Possibly suitable for surface layer if not compacted. Poor root development caused by severe compaction. Prominent compressed horizontal root mat occurred at interface of Ob2 and Ob3.

Ob3: High quality, brownish red apedal material. Possibly suitable for surface layer if not compacted. Poor root development caused by severe compaction. Prominent compressed horizontal root mat at interface of Ob3 and Sub4.

Sub4: Brown red plinthic material that appear to have a restricting effect on root penetration and distribution. No visible cracks.

Table 2.13: Soil cover profile of P2-2.

Profile pit		P2-2	**Terrain unit**	1	**Surface cracks**	None	**Effective soil depth (mm)**	700	**Cover profile**
Slope (%)		0	**Surface crust**	Weak	**Vegetation cover**	Good	**Effective root depth (mm)**	700	
Layer	**Depth (mm)**	**Colour**	**Soil material**	**Soil structure**	**Soil quality**	**Soil homogeneity**	**Soil density**	**Root occurrence**	
Ob1	0–500	Red brown	Apedal	Massive	High	Slighty mixed	High	Many	
Sub2	500–700	Red brown	Soft plinthic	Massive	High	Slighty mixed	Slight	Common	
Sub3	700–1100	Grey red	Saprolite	Weak structered	Poor	Moderately mixed	Slight	None	
Spoil	1100+	Black	-	-	-	-	-	-	
Land capability (Slope, depth, soil quality)			Grazing						

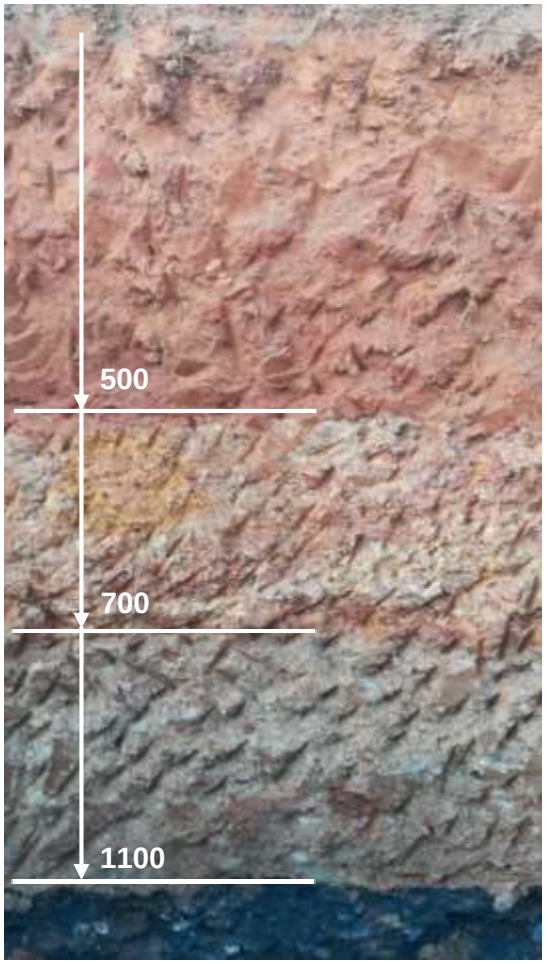

Comments:

Erosion: Some sheet erosion between grass tussocks.

Ob1: High quality, reddish brown apedal material, good growth medium and suitable for surface layer. No visible cracks. Good root distribution with 82% roots in this layer although soil density was high.

Sub2: High quality, red brown apedal material with concretions occupying 5-10% of the matrix. Low suitability for a surface layer, but high suitability for a slower permeable second layer (water retention layer). No visible cracks. Fairly few root distribution with 18% roots in this layer.

Sub3: Poor quality, greyish red saporlite material. No visible cracks and hardly any roots in this layer.

Spoil: Black, non-carbonaceous material (pulverized shale and sandstone) consisting of compacted (dense), fine grained, soft overburden material that appear to have a restricted effect on root penetration and distribution. No visible cracks.

General: *The typical store-and-release cover with a saprolite layer to optimise soil cover performance, although Ob1 suffered from high soil density. The deep soil cover with three soil cover layers can also be an indication that there were enough borrow materials in surrounding areas for store-and-release cover construction.*

Table 2.14: Soil cover profile of P2-3

Profile pit		P2-3	**Terrain unit**	3	**Surface cracks**	None	**Effective soil depth (mm)**	500	**Cover profile**
Slope (%)		1	**Surface crust**	Weak	**Vegetation cover**	Good	**Effective root depth (mm)**	500	
Layer	**Depth (mm)**	**Colour**	**Soil material**	**Soil structure**	**Soil quality**	**Soil homogeneity**	**Soil density**	**Root occurrence**	
Ob1	0–500	Yellow red	Apedal	Massive	High	Slighty mixed	Slight	Common	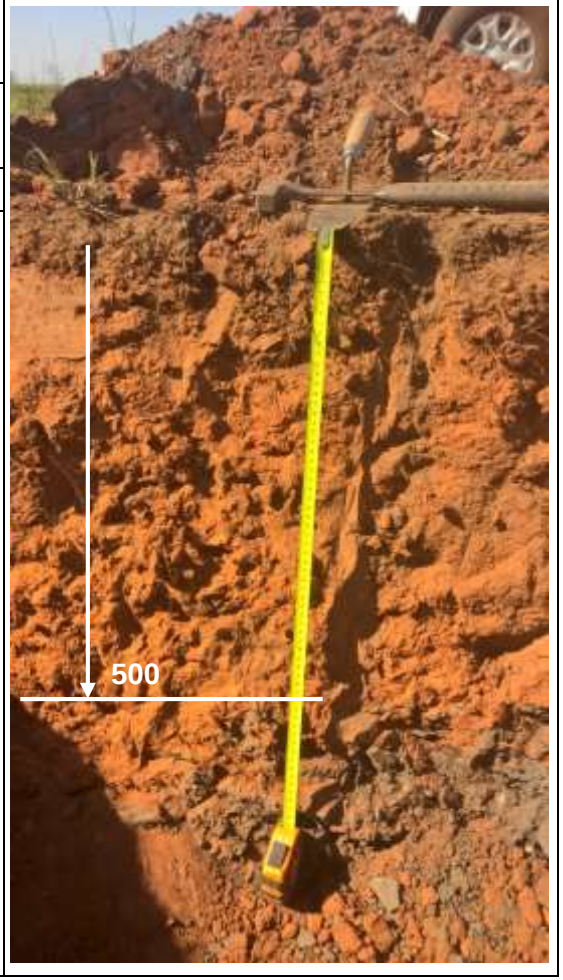
Spoil	500+	Dark grey	-	-	-	-	-	-	
Land capability (Slope, depth, soil quality)			Grazing						

Comments:

Erosion: Some sheet erosion with rills at localised runoff areas.

Ob1: High quality, yellowish red apedal material, good growth medium and suitable for surface layer. Good root distribution in this layer. No visible cracks.

Spoil: A mixture of fine, medium and coarse grained, dark grey carbonaceous material (pulverized shale and sandstone).

Figure 2.3: Vertical cracks through severely compacted layers at D2-1 (A) and, vertical and lateral cracks in severely compacted layers at D2-2 (B). Cracks can act as preferential flow paths for (nearly) saturated flows. Soil cover layers with high bulk density may not effectively function as water retention layer due to potential preferential flows through vertical and lateral cracks. Little water losses through plant transpiration will occur as no roots have penetrated and developed in the soil cover layers of D1-2 & 2-2 with high bulk density.

Table 2.15: Plasticity index, clay activity and swelling potential for soil cover layers.

Soil cover condition	Profile pit	Soil cover layer (mm)	Plasticity index[a,b] %	Clay activity	Swelling potential
Moderately dense	D1-1	0–500	14.40	0.609	L/M
		550–900	14.98	0.577	M
	D1-2	0–400	5.89	0.338	L
		400–600	10.37	0.339	L
	D1-3	Surface	-	-	-
		0–200	13.78	0.635	L
		200–550	13.23	0.358	L
	P1-3	Surface	2.84	0.367	L
	P1-4	Surface	6.00	0.777	L
		0–350	0.56	0.041	L
	P2-2	Surface	4.01	0.368	L
		500–700	14.01	0.740	L
	P2-3	0–500	2.45	0.104	L
	D3-1	0–300	0.59	0.068	L
		>300	14.25	0.501	L/M
	D3-2	Surface	2.40	0.179	L
		0–400	3.11	0.202	L
		>400	13.93	0.566	L/M
Very dense	D2-1	0–450	5.67	0.600	L
		450–650	4.02	0.199	L
		650–850	7.10	0.284	L
		850–1100	15.00	0.347	L
	D2-2	0–300	11.30	0.742	L
		300–700	16.26	0.396	L/M
	P1-1	Surface	0.16	0.030	L
		200–700	3.39	0.343	L
	P1-2	Surface	1.83	0.359	L
		0–400	6.38	0.377	L
	P2-1	0–100	13.41	0.596	L/M
		100–300	-	-	-
	P2-2	0–500	2.21	0.136	L

Note: L = Low, M - Medium.
[a]Plasticity index classification based on minimum requirements of DWAF (1998).
[b] Rating colours: Green: Suitable, Brown: Moderately suitable, Red: Unsuitable.

2.3.2 Soil cover properties

2.3.2.1 *Soil texture*

Hydraulic properties (Chapter 3 & 4) of soil cover layers are mainly influenced by the size of the individual particles and the distribution of the particle sizes. The average particle-size distribution and average SOM results for the profile pits are included in Table 2.16.

The moderately dense SRCs had clay content with average of 19.61 % and ranged between 7.72–39.94%. The silt content ranged between 9.18–35.87% with an average of 18.03%, and sand content was 27.37–81.70% with an average of 57.10% of the moderately dense SRCs. The clay content of very dense SRCs ranged between 3.59–43.34% and the average was 17.73%. Very dense SRCs had silt content values of 7.77–31.58% with an average of 18.96% and the sand content values were 32.65–75.30% with an average of 57.31%. The soil cover layers of both moderately- and very dense SRCs had low gravel (>4.75 mm) contents, which is beneficial to the performance of the soil covers. The soil layers, 500–700 mm of P2-2, > 400 mm of D3-2, 0–450 mm of D2-1, surface of P1-1, and surface and 0–400 mm of P1-2 were between 10% < gravel content < 20%. The gravel content at the surface of P2-2 was the highest with the value of 26.07%. The effect of gravel content of these profile pits are negligible on hydraulic and vegetation properties as explained in Section 1.3.2.2.1 of Chapter 1 and shown in Section 3.2.2 of Chapter 3.

There was a significant difference in soil texture (P = 0.008) of the duel-layered SRCs of both soil cover conditions. The soils of moderately- and very dense SRCs are poorly graded (relatively even distribution of the various particle fractions) and characterised by a fine sand grade, excluding the surface of P1-3 & 1-4, 500–700 mm of P2-2 and 0–300 mm of D3-1. The higher fine sand fraction compared to the coarse- and medium sand fraction is favourable for cover performance. Additionally, there was a significant difference of SOM (P = 0.088) between the moderately- and very dense SRCs.

The following inferences were made on soil texture of moderately- and very dense SRCs: (1) the soil texture of the growth medium layers varied between loamy sand and sandy clay loam, excluding D3-1; and (2) the soil texture of the water retention layers were loam, sandy clay loam, clay loam and clay. These soil textures for dual-layered SRCs are the preferred texture for growth medium and moisture retention layer. The soil texture at the D3-1 was loamy sand for the growth medium and sandy clay loam for the water retention layers, where the soil texture of the growth medium was a marginally suitable texture due to the high sand fraction. The soil texture of monolithic SRCs of moderately- and very dense SRCs was sandy loam or sandy clay loam. The results correspond well with the results of the Nell & Steenekamp (2016) study, where the monolithic soil covers were predominantly fine to medium sandy loam at Mpumalanga Highveld and Northern Province. In the case of monolithic SRCs, the soil cover depth and bulk density of soil covers may play a role in good long-term performance.

Table 2.16: Soil texture, average particle-size distribution and average soil organic matter of moderately- and very dense store-and-release covers.

Soil cover condition	Profile pit	Soil cover layer	Texture	Gravel		Sand						Silt		Clay	Soil organic matter
				Medium	Fine gravel	Very fine	Very coarse	Coarse	Medium	Fine	Very fine	Coarse	Fine		
		(mm)		(%)	(%)	(%)	(%)	(%)	(%)	(%)	(%)	(%)	(%)	(%)	(%)
Moderately dense	D1-1	0–500	SCL	0.00	1.01	1.44	2.36	5.56	14.60	24.54	9.19	15.35	2.30	23.66	0.16
		550–900	SCL	0.00	0.56	1.73	2.04	5.42	13.03	18.76	10.48	13.11	8.94	25.94	0.01
	D1-2	0–400	SL	0.00	0.00	0.12	1.95	7.40	21.12	28.66	8.85	10.16	4.32	17.42	0.51
		400–600	SCL	0.00	0.48	2.96	2.47	5.75	11.78	19.05	9.40	12.43	5.13	30.56	0.09
	D1-3	Surface	SCL	0.00	0.27	0.83	1.86	4.57	14.06	21.42	10.18	17.03	6.37	23.40	0.48
		0–200	SCL	0.00	0.00	0.27	1.85	6.85	18.74	26.24	10.76	10.50	3.09	21.71	0.18
		200–550	CL	0.57	1.22	3.48	1.71	4.55	8.59	11.40	6.89	20.86	3.77	36.94	0.31
	P1-3	Surface	SL	0.00	0.00	1.42	10.09	12.60	22.97	18.39	7.25	15.38	4.16	7.73	0.50
	P1-4	Surface	SL	0.00	0.00	2.25	4.95	11.51	28.07	22.33	8.04	7.42	7.72	7.72	2.87
		0–350	SL	0.00	0.12	8.07	6.90	8.02	19.41	21.50	9.24	11.69	1.19	13.85	0.56
	P2-2	Surface	SL	0.00	0.00	26.07	2.44	6.25	12.69	18.52	7.40	11.68	4.09	10.89	2.14
		500–700	L	6.34	3.51	7.98	2.01	2.68	4.03	9.24	9.41	27.69	8.18	18.93	0.43
	P2-3	0–500	SCL	0.00	0.19	3.95	3.90	6.37	12.59	19.03	11.27	16.23	2.85	23.62	0.31
	D3-1	0–300	LFS	0.00	0.00	0.44	1.94	14.02	34.98	25.55	5.21	5.55	3.63	8.69	0.96
		>300	SCL	1.89	1.34	3.79	1.54	4.49	10.84	18.59	7.63	16.97	4.45	28.46	0.80
	D3-2	Surface	SL	0.00	0.00	0.20	1.65	9.47	26.04	32.39	7.60	6.51	2.72	13.42	1.09
		0-400	SL	0.00	0.00	0.00	1.38	8.64	23.69	33.42	7.49	8.07	1.90	15.41	0.24
		>400	SCL	8.17	0.59	3.53	1.46	3.98	9.96	16.60	8.05	19.27	3.80	24.60	0.95
Very dense	D2-1	0–450	SL	3.35	2.64	4.26	1.65	4.47	6.59	23.03	15.77	29.62	1.96	6.67	0.07
		450–650	SCL	0.00	0.00	0.57	2.11	6.77	19.56	27.74	8.78	10.95	3.28	20.24	0.09
		650–850	SCL	0.00	0.81	3.75	1.78	3.38	10.50	26.43	7.72	19.24	1.38	25.02	0.05
		850–1100	C	0.00	0.91	2.23	1.41	3.61	8.51	11.90	7.22	12.44	8.43	43.34	0.40
	D2-2	0–300	SL	0.00	0.00	0.23	1.79	5.22	18.99	30.20	9.78	6.62	11.95	15.22	0.18
		300–700	C	1.41	0.00	2.37	2.12	4.99	8.28	13.98	6.84	15.72	3.25	41.05	0.04
	P1-1	Surface	SL	0.00	0.23	14.10	10.12	8.68	13.66	18.10	6.98	19.81	3.03	5.32	0.66
		200–700	SL	0.00	0.00	5.45	3.80	8.89	19.41	25.75	12.17	11.60	3.03	9.90	0.29
	P1-2	Surface	SL	0.00	1.03	14.05	11.65	7.81	12.31	15.83	8.19	23.07	0.95	5.11	0.36
		0–400	SL	0.00	0.00	14.12	14.48	8.08	12.75	19.57	6.45	18.96	2.01	3.59	0.87
	P2-1	0–100	SCL	1.75	0.50	2.89	2.20	6.41	13.15	20.49	9.68	15.99	4.46	22.49	0.13
		100–300	SL	0.00	0.00	0.62	2.98	8.85	20.10	27.78	15.59	6.78	0.99	16.31	0.03
	P2-2	0–500	SL	0.00	0.00	0.88	3.77	9.11	19.80	28.87	10.44	7.25	3.66	16.21	0.93

Note: LS = loamy sand, SL= sandy loam, L = Loam, SCL = sandy clay loam, CL = clay loam, and C = clay.

2.3.2.2 *Bulk density*

The bulk densities and porosities determined from intact core samples collected from moderately- and very dense SRCs layers are summarised in Table 2.17. Bulk densities of moderately dense SRCs ranged from 1.460–1.841 g.cm^{-3} and between 1.700–2.286 g.cm^{-3} for very dense SRCs. The porosity ranged between 30.54–44.81% and 13.72–40.71% for moderately- and very dense SRCs, respectively. If the bulk densities of moderately dense SRCs were grouped according to soil textural classes, the following resulted: (1) loamy sand: 1.840 g.cm^{-3}, (2) sandy loam: 1.465–1.841 g.cm^{-3}, (3) loam: 1.548 g.cm^{-3}, (4) sandy clay loam: 1.460–1.810 g.cm^{-3} and (5) clay loam: 1.610 g.cm^{-3}. For very dense SRCs, the following results were obtained: (1) sandy loam: 1.600–2.286 g.cm^{-3}, (2) sandy clay loam: 1.700–1.770 g.cm^{-3} and (3) clay: 1.680–1.740 g.cm^{-3}.

Between moderately- and very dense SRCs, there was a significant difference in bulk density (P = 0.001) and porosity (P = 0.001) values. There was no significant difference between the growth medium and water retention layer (duel-layered SRCs) of moderately dense SRCs regarding bulk density (P = 0.468) and porosity (P = 0.878). Between growth medium and water retention layer of very dense SCRS, no significant difference in bulk density (P = 0.479) and porosity (P = 0.571) was observed.

If bulk densities were grouped according to soil textural classes and compared to the critical threshold values for limiting root penetration (Table 1.13 after USDA, 1996 and Vepraskas, 1988 in Chapter 1), the following results were obtained: (1) all the bulk density values of moderately dense SRCs were below the critical threshold values, except 400–600 mm of D1-2 and the surface of P1-3 and P2-2; and (2) all the bulk density values of very dense SRCs were higher than the critical threshold value, except 0–450, 450–650 & 650–850 mm of D2-1, 0–400 mm of P1-2 and 0–100 mm of P2-1. In addition, a strong and negative correlation was found between bulk density and porosity with a Pearson correlation coeffient value of -0.786, but no correlation existed between bulk density and SOM (data not shown). The high bulk density of 400–600 mm of D1-2 was not a concern since it is the water retention layer and did not affect the WHC (Table 4.3 in Chapter 4). The high bulk densities of P1-3 and P2-2 did not affect the root development in the growth medium (Tables 2.5 & 2.13). It is noteworthing that the surface of P2-2 had a SOM content of 2.14% (Table 2.16). High bulk density is a problem and is attributed to poorly constructed SRCs. Nell & Steenekamp (2016) evaluated the soil covers of several coal mines in Mpumalanga Highveld and Northern Province and encountered a similar problem, where the median bulk density exceeded 1.820 g.cm^{-3} with the minimum bulk density of 1.747 g.cm^{-3}. High bulk density is due to equipment compaction or heavy machinery. Generally, these high bulk densities were caused during the construction period if *e.g.* by traffic on wet soils (at optimum water content). In addition, during revegetation, ripping techniques are required for loosening the soils (Limpitlaw *et al.* 1997) and if wrong implements were used or poor ripping techniques followed, this can result in high bulk densities in growth medium or water retention layer. Goosen (2015) also discussed the effect of heavy machinery on bulk density in soil covers and how poor management can quickly degrade the soil covers.

Table 2.17: Average bulk density, porosity and void ratio of moderately-and very dense store-and-release covers.

Soil cover condition	Profile pit	Soil cover layer (mm)	Bulk density ($g.cm^{-3}$)	Porosity (%)
Moderately dense	D1-1	0–500	1.630	38.47
		550–900	1.460	44.81
	D1-2	0–400	1.570	40.92
		400–600	1.810	31.73
	D1-3	Surface	1.680	36.75
		0–200	1.570	40.91
		200–550	1.610	39.13
	P1-3	Surface	1.813	31.59
	P1-4	Surface	1.785	32.65
		0–350	1.643	37.99
	P2-2	Surface	1.841	30.53
		500–700	1.548	41.58
	P2-3	0–500	1.465	44.73
	D3-1	0–300	1.840	40.87
		>300	1.550	41.41
	D3-2	Surface	1.690	36.47
		0–400	1.580	40.44
		>400	1.730	34.86
Average			1.660	38.10
Very dense	D2-1	0–450	1.700	36.39
		450–650	1.870	36.58
		650–850	1.700	35.70
		850–1100	1.680	40.71
	D2-2	0–300	2.030	23.52
		300–700	1.740	30.54
	P1-1	Surface	1.848	30.26
		200–700	2.197	17.08
	P1-2	Surface	1.859	29.84
		0–400	1.741	34.30
	P2-1	0–100	1.703	35.75
		100–300	2.286	13.73
	P2-2	0–500	1.872	29.35
Average			1.864	30.29

Most importantly, Guidelines for the Rehabilitation of Mined Land (Chamber of Mines of South Africa / Coaltech, 2007), acknowledges that compaction is the biggest problem during cover construction and summarised several steps how to minimise compaction. In this case of the study, there were growth medium of moderately- and very dense SRCs that had higher bulk density than the bulk density value of water retention layer or *vice versa*. Seemingly, the construction or management and maintenance periods are the important stages during rehabilitation which can determine the bulk densities of SRCs. Another reason for high bulk density is the soil texture which was dominated by a high medium or fine sand content in all SRCs (Table 2.16). Sandy loam soils were more sensitive to compaction than sandy clay loam soils if the bulk densities and porosities were compared between moderately- and very dense SRCs, excluding D1-2 and D3-2. These results indicated that a well-designed and constructed soil cover with good maintenance and management is highly important for sustainability.

2.3.2.3 *Soil chemical properties*

The $pH_{(H_2O)}$, $pH_{(KCl)}$, EC_e and CEC are summarised in Table 2.18 with moderately- and very dense SRCs. In Section 1.3.2.3 of Chapter 1, the critical threshold values for $pH_{(H_2O)}$, $pH_{(KCl)}$ and EC_e were 5.5–7.5, > 4.1, and > 200 $mS.m^{-1}$, respectively. The $pH_{(H_2O)}$ of moderately dense SRCs ranged between 5.5–7.5. All the $pH_{(H_2O)}$ of very dense SRCs were below 5.5, except the soil cover layer, 0–500 mm of P2-2 which was between the critical threshold values. The $pH_{(KCl)}$ of moderately- and very dense SRCs were above 4.1. Only the soil cover layer, 300–700 mm, of D2-2 had a $pH_{(KCl)}$ lower than 4.1. The EC_e values of moderately dense SRCs were below 200 $mS.m^{-1}$, whereas some very dense SRCs were higher than 200 $mS.m^{-1}$ *viz*. D2-2 and 0–400 mm of P2-1. Cation exchange capacity of moderately- and very dense SRCs ranged between 0.8–6.8 and 0.4–7.0 $cmol_c.kg^{-1}$, respectively.

The $pH_{(H_2O)}$ and $pH_{(KCl)}$ difference between moderately- and very dense SRCs was statistical significant ($P = 1.081\times10^{-4}$ and P = 0.022, respectively), where the $pH_{(H_2O)}$ and $pH_{(KCl)}$ of very dense SRCs was lower compared to moderately dense SRCs. Furthermore, there were significant differences in EC_e ($P = 0.040$), but no difference in CEC ($P = 0.066$) between the two soil cover conditions. Comparison of $pH_{(H_2O)}$ and CEC between growth medium and water retention layer of moderately SRCs, showed significant difference in $pH_{(H_2O)}$ ($P = 0.004$) and no difference in CEC ($P = 0.376$). These was also no significant difference in $pH_{(H_2O)}$ ($P = 0.524$) and CEC ($P = 0.443$) between the growth medium and water retention layer of very dense SRCs.

The low $pH_{(H_2O)}$ and $pH_{(KCl)}$ values of very dense SRCs was due to high bulk density and led to lower nutrient availability for plants. Comparison between the growth medium and water retention layer showed that the $pH_{(H_2O)}$ values of the growth medium of the moderately dense SRCs were higher than the water retention layers and Mentis (2006) reported similar results where the nutrient availability was higher in the growth medium than in the water retention layer and saprolite. Higher

$pH_{(H_2O)}$ of growth medium can be attributed to higher SOM in the growth medium (Table 2.16). This can be expected since Chamber of Mines of South Africa / Coaltech (2007) mentioned that regular vegetation maintenance is required after plants were established, where fertilisers needs to be applied until the natural soil fertility have been restored. Such maintenance is necessary to ensure a good vegetation cover.

The EC_e values of the moderately dense SRCs were lower compared to very dense SRCs. Soil salinity was not a problem in moderately dense SRCs, but for very dense SRCs and can ascribed to poor constructed soil cover conditions which led to higher bulk density, cracks and low pH. In turns, the soil nutrient availability is lower and vegetation covers may be poor (see Chapter 5).

The CEC values of both soil cover conditions are in good argument with CEC of 2.16–2.81 $cmol_c.kg^{-1}$ reported by Mentis (2006) on research done on rehabilitated soil cover in Naauwpoort pit, Mpumalanga Highveld, South Africa. Some CEC values of water retention layer were higher than 2.81 $cmol_c.kg^{-1}$ reported by Mentis (2006) study, which may point to well-constructed soil covers. In addition, in the study of Nell & Steenekamp (2016), a median CEC value of 4.36 $cmol_c.kg^{-1}$ was found at rehabilitated coal mines in Mpumalanga Highveld and Limpopo Province, where some coal mines had high CEC of 22.93–55.86 $cmol_c.kg^{-1}$. Although there was no significant difference in CEC between the growth medium and water retention layer of both soil cover conditions, the CEC values tended to be higher in the water retention layer compared to the growth medium. This may be attributed to the higher clay content in the water retention layers of both soil cover conditions (Table 2.16). Worth to mention that the CEC value of the surface of P1-4 was higher than the 0–350 mm soil layer due to higher SOM (Table 2.16). Nell & Steenekamp (2016) observed a similar trend where the CEC was slightly higher in the 0–200 mm soil cover layer than at 200–600 mm soil cover layer and ascribed it to an increase in the accumulation of SOM in the 0–200 mm of the soil cover. Anderson (1977), Hallberg *et al.* (1978) and Schafer *et al.* (1980) found similar results. These authors mentioned that SOM in the growth medium may reach levels that can be found in natural soils over 30 years.

Overall, bulk density had a negative influence on nutrient availability, where moderately dense SRCs had higher soil nutrient availability than the very dense SRCs. Soil texture had an influence on CEC as expected where the water retention layer had higher CEC.

Table 2.18: Average $pH_{(H_2O)}$, $pH_{(KCl)}$, electrical conductivity of saturated paste (EC_e) and cation exchange capacity (CEC) of moderately- and very dense store-and-release covers.

Soil cover condition	Profile pit	Soil cover layer (mm)	$pH_{(H_2O)}$	$pH_{(KCl)}$	EC_e ($mS.m^{-1}$)	CEC ($cmol_c.kg^{-1}$)
Moderately dense	D1-1	0–500	5.9	5.0	35	2.0
		550–900	5.6	4.8	47	5.4
	D1-2	0–400	6.1	4.9	49	2.3
		400–600	5.6	5.4	70	3.4
	D1-3	Surface	-	-	-	-
		0–200	6.9	6.2	68	5.5
		200–550	5.6	4.9	156	4.8
	P1-3	Surface	6.9	6.2	29	0.8
	P1-4	Surface	7.0	6.0	32	3.0
		0–350	5.9	4.5	62	0.9
	P2-2	Surface	5.6	4.4	58	2.7
		500–700	5.6	4.9	44	-
	P2-3	0–500	5.6	4.5	48	2.8
	D3-1	0–300	6.2	4.3	22	5.1
		>300	5.5	5.2	45	5.1
	D3-2	Surface	6.0	5.0	27	2.8
		0–400	6.8	4.1	107	6.8
		>400	5.7	4.6	-	-
Average			6.0	5.0	56	3.6
Very dense	D2-1	0–450	5.3	4.8	88	1.9
		450–650	5.2	4.8	-	1.7
		650–850	5.1	4.4	-	-
		850–1100	5.1	4.3	-	-
	D2-2	0–300	5.3	4.8	223	1.2
		300–700	3.5	3.4	832	7.2
	P1-1	Surface	5.4	4.1	92	1.2
		200–700	4.8	4.3	38	0.7
	P1-2	Surface	5.1	4.9	89	4.5
		0–400	4.5	4.1	260	0.4
	P2-1	0–100	4.7	4.1	61	1.1
		100–300	-	-	-	0.9
	P2-2	0–500	6.3	5.4	55	3.8
Average			5.0	4.5	193	2.2

2.4 Conclusions

Traditionally, mine rehabilitation aspires to restore the ecosystem with sustainable soil covers. Criteria for measuring the success of long-term performance can be based on the quality of soil cover properties or vegetation covers. The dual-layered SRCs in this study consisted of a sandy loam or sandy clay loam growth medium with a finer soil texture water retention layer. Monolithic SRCs were predominantly sandy loam and sandy clay loam soils. These soil textures are preferable for SRCs design. The critical threshold values of natural soils are suitable to use for evaluating the long-term performance of SRCs. High bulk density is a problem at some research sites caused by heavy equipment during the process of grading and soil cover construction or ripping, and construction during optimum water content. Due to compaction, surface crusts, sheet and rill erosion and vertical cracks in cover layer were observed together with poor root distribution and vegetation covers. Lateral root development occurred in the very dense SRCs. Higher bulk densities also caused higher runoff, which resulted in erosion of the SRCs and oxygen- and water ingress directly into the coal discard or spoil. Furthermore, the very dense SRCs had low $pH_{(H_2O)}$ and high EC_e. The low nutrient availability of poorly constructed SRCs can also result in poorer vegetation growth and lowering the success of rehabilitation.

Preventing poorly constructed SRCs with high bulk density is preferable to alleviating problems after they have occurred. Many possibilities exist to reduce high bulk density in SRCs cause of by heavy machines. The most important is to avoid traffic on wet soil, but this may require a major change in the rehabilitation process. Correcting soil preparation for revegetation are important for optimum root development. If SRCs have been constructed correctly, vegetation growth and root development will be stimulated as is noticed at the moderately dense SRCs. Well-constructed SRCs will have less erosion and higher evapotranspiration with less oxygen- and water ingress which is a desirable long-term performance.

Dramatic or gradual changes in soil cover properties, vegetation growth and erosion rates could increase or decrease the success of rehabilitated mines. The negative outlook that rehabilitated mines is inferior to natural soil can be encourage to change if the SRCs have been correctly constructed.

2.5 References

Anderson, D.W. 1977. Early stages of soil formation on glacial till mine spoils in a semi-arid climate. *Geoderma*. 19(1):11–19.

ASTM D4318-00. 1989. Standard test methods for liquid limit, plastic limit and plasticity index for soils. *ASTM International, West Conshohocken, PA*. (Reapproved 2000):1–14.

ASTM D4943-08. 1989. Test method for shrinkage factors of soils by the wax method. *ASTM International, West Conshohocken, PA*. (Reapproved 2008):1–6.

ASTM D5519-94. 1994. Standard test method for particel size analysis of natural and man-made riprap materials. *ASTM International, West Conshohocken, PA*. 04(Reapproved 2001):1–6.

ASTM D6913-04. 2004. Standard test methods for particle-size distribution (gradation) of soils using sieve analysis. *ASTM International, West Conshohocken, PA*. 04(Reapproved 2017):1–35.

Blake, G.R. & Hartge, K.H. 1986. Bulk density. In A. Klute (ed.). Madison, WI: American Society of Agronomy/Soil Science Society of America *Methods of soil analysis: Part 1 – Physical and Mineralogical Methods*. 364–367.

Chamber of Mines of South Africa / Coaltech. 2007. *Guidelines for the Rehabilitation of Mined Land*. J. Beukes (ed.). Johannesburg: Coaltech Research Assocation.

Chen, F.H. 1988. *Foundations on expansive soils*. Amsterdam: Elsevier.

DWAF. 1998. *Minimum requirements for the handling, classification and disposal of hazardous waste*. 2nd ed. K. Langmore (ed.). Pretoria: Department of Water Affairs and Forestry.

Flint, A.L. & Flint, L.E. 2002a. Soil particle density. In J.H. Dane et al. (eds.). Madison, WI: Soil Science Society of America *Methods of soil analysis: Part 4 Physical Methods*. 229–240.

Flint, L.E. & Flint, A.L. 2002b. Porosity. In J.H. Dane et al. (eds.). Madison, USA: Soil Science Society of America *Methods of soil analysis: Part 4 Physical Methods*. 241–254.

Fourie, Andy & Tibbett, Mark. 2007. Post-mining landforms — Engineering a biological system. In A. Fourie et al. (eds.). Santiago de Chile: Australian Centre for Geomechanics *Second International Seminar on Mine Closure 2007*.

Gee, G.W. & Or, D. 2002. Particle-size analysis. In J.H. Dane et al. (eds.). Madison, WI: SSSA Book Ser. 5.4. SSSA *Methods of soil analysis: Part 4 – physical methods*. 255–293.

Google Earth 2.7. 2020. [Online], Available: http://www.google.com/earth/index.html.

Goosen, J. 2015. Topsoil stripping and management for mine rehabilitation. *Mining and the Environment.*

Haigh, M. 1995. Soil quality standards for reclaimed coal-mine disturbed lands: A discussion paper.

International Journal of Surface Mining, Reclamation and Environment. 9(4):187–202.

Hallberg, G.R., Wollenhaupt, N.C. & Miller, G.A. 1978. A century of soil development in spoil derived from loess in Iowa. *Soil Science Society of America Journal*. 42(2):339–343.

Holtz, W.G. & Gibbs, H.J. 1956. Engineering properties of expansive clays. *Transactions of the American Society of Civil Engineers*. 121(1):641–663.

Kent, M. 1982. Plant growth problems in colliery spoil reclamation: A review. *Applied Geography*. 2(2):83–107.

Kottek, M., Grieser, J., Beck, C., Rudolf, B. & Rubel, F. 2006. World Map of the Köppen-Geiger climate classification updated. *Meteorologische Zeitschrift*. 15(3):259–263.

Limpitlaw, D., Aken, M., Kilani, J., Mentis, M., Nell, J.P. & Tanner, P.D. 1997. Rehabilitation and soil characterization. *Proceedings of the 11th International Conference on Coal Research.* 297–309.

Limpitlaw, D., Aken, M. & Lodewijks, H. 2005. Post-mining rehabilitation, land use and pollution at collieries in South Africa. *Presented at the Colloquium: Sustainable Development in the Life of Coal Mining, Boksburg, 13 July, 2005*. (July):1–10. [Online], Available: http://www.csmi.co.za/papers/2005/Post_mining_landuse_Collieries_jul05.pdf.

Mentis, M.T. 2006. Restoring native grassland on land disturbed by coal mining on the Eastern Highveld of South Africa. *South African Journal of Science*. 102(5–6):193–197.

Mills, A.J., Milewski, A. V., Rogers, K.H., Witkowski, E.T.F. & Stalmans, M. 2013. Boundary of treeless grassland in relation to nutrient content of soils on the Highveld of South Africa. *Geoderma*. 200–201:165–171.

Nell, J.P. & Steenekamp, P.I. 1998. *Final report: Establishment of a soil profile database for rehabilitates opencast coal mined land*. Report GWIA198ff8. Pretoria.

Nell, J.P. & Steenekamp, P.I. 2016. *Establishing a soil profile database for rehabilitated opencast coal mined land in South Africa*. GWA/98/78. Pretoria.

OpenStreetMap contributors. 2020. *Middelburg climate (South Africa)*. [Online], Available: https://en.climate-data.org/africa/south-africa/mpumalanga/middelburg-10646/.

Parent, S.-É. & Cabral, A. 2005. Material selection for the design of inclined covers with capillary barrier effect. *GSP 142 Waste Containment and Remediation*. 40789(September 2015):1–5.

Qian, T., Huo, L. & Zhao, D. 2010. Laboratory investigation into factors affecting performance of capillary barrier system in unsaturated soil. *Water Air Soil Pollution*. 206:295–306.

Rutherford, M.C., Bredenkamp, G.J., Powrie, L.W. & Province, N.W. 2006. Grassland biome. In L.

Mucina et al. (eds.). Pretoria: South African Biodiversity Institute *The vegetation of South Africa, Lesotho and Swaziland*. 348–437.

Schafer, W.M. 1979. Guides for estimating cover soil quality and mine soil capability for use in coal strip mine reclamation in western United States. *Reclamation Review*. 2:67–74.

Schafer, W.M., Nielsen, G.A. & Nettleton, W.D. 1980. Minesoil genesis and morphology in a spoil cchronosequence in Montana. *Soil Science Society of America Journal*. 44(4):802–807.

Schulze, R.E. & Maharaj, M. 2007. A-Pan equivalent reference potential evaporation. In R.E. Schulze (ed.). Pretoria, RSA: Water Research Commission *South African Atlas of Climatology and Agrohydrology*. 1–11.

Skempton, A.W. 1984. The colloidal "activity" of clays. *Selected Papers on Soil Mechanics*. 60–64.

Soil Classification Working Group. 1991. *Soil classification - a taxonomic system for South Africa*. Pretoria: Department of Agricultural Development.

Steffen Robertson & Kirsten (B.C.) Inc. 1989. *Draft acid rock drainage technical guide. Volume I – Technical guide*.

The Fertiliser Association of South Africa. 2007. *Fertilisation manual*. 7th ed. Lynnwoodrif: FSSA-MVSA.

U.S. Department of Agriculture. 1987. USDA textural soil classification. *Soil Mechanics Level I Module 3 - USDA Textural Soil Classification*. 1–53.

U.S. Department of Agriculture. 1996. Soil quality indicators: Bulk Density. *Natural Resources Conservation Service*. 192:1836–41.

Van der Merwe, D.H. 1964. The prediction of heave from the plasticity index and percentage clay fraction. *The South African Institution of Civil Engineering*. 6(12):103–107.

Vepraskas, M.J. 1988. Bulk density values diagnostic of restricted root growth in coarse-textured soils. *Soil Science Society of America Journal*. 52(4):1117–1121.

Vermaak, J.J.G., Wates, J.A., Bezuidenhout, N. & Kgwale, D. 2004. *The evaluation of soil covers used in the rehabilitation of coal mines*. Vol. 1002/1/04. Water Research Commission.

Wels, C., Fortin, S. & Loudon, S. 2002. Assessment of store-and-release cover for Questa Tailings Facility, New Mexico. In Fort Collins, Colorado: A.A. Balkema *Proceedings of the 9th International Conference on Tailings and Mine Waste*. 459–468.

Wentworth, C.K. 1922. A scale of grade and class terms for clastic sediments. *The Journal of Geology*. 30(5):377–392.

Williamson, N.A., Johnson, M.S. & Bradshaw, A.D. 1982. *Mine waste reclamation*. London, UK:

Mineral Industry Research Organisation.

Chapter 3: Predicting saturated hydraulic conductivity of old store-and-release covers from soil physical properties

3.1 Introduction

Among soil hydraulic properties, several authors reported that saturated hydraulic conductivity (K_{sat}) has the greatest statistical variability and takes time at large scales (Biggar & Nielsen, 1976; Deb & Shukla, 2012; Webb *et al.*, 2000). The variability of K_{sat} is greatly influenced by external factors associated with land use and management, soil depth, instruments and methods of measurement as well as internal factors of soil formation (Stockton & Warrick, 1971).

In the investigation of SRCs, it is important to analyse or predict the long-term soil cover performance considering that the cover material properties can be impacted by ageing (Albright *et al.*, 2010). INAP (2017) stated that significant changes in the soil hydraulic properties may occur with the ageing of covers. In the study of Benson *et al.,* (2007), the fine-textured SRCs have a K_{sat} of 10^{-3}–10^{-1} m.d^{-1} after two to four years. Saturated hydraulic conductivity is an indispensable criterion of soil cover performance over the long term, and to overcome the lack of measured K_{sat} data indirect methods such as pedotransfer functions (PTFs) have been developed to predict soil hydraulic properties. According to De Souza *et al.* (2016), multiple linear regression (MLR) models are the simplest way to estimate the data by means of PTFs. Moreover, easily available soil physical properties can be used to develop MLR models (Salchow *et al*., 1996). Suriya & Jayalakshmi (2015) found that soil texture, soil organic matter (SOM), and soil bulk density influence K_{sat}. There are a number of PTFs to use, however Li *et al.* (2007) warned that extrapolating PTFs from one region to other regions must be exercised with caution. Another study, Ryczek *et al.* (2017), found that regarding their variability, the PTFs cannot be used as a universal method for soils in engineering works. Zhang & Schaap (2019) suggested that a large and completely independent data-set is needed for a universal use of PTFs and to assess their reliability and accuracy.

The objectives of this Chapter were (1) to evaluate the K_{sat} of SRCs by using threshold critical values of natural soils; and (2) to use soil physical properties as input parameters to develop models for predicting K_{sat} of old SRCs.

3.2 Materials and methods

3.2.1 Data collection

Water was pumped to two 210 l drums at Discard Dump 1 & 2 (Figure 3.1), where a water tank was used for the infiltrometer tests at Opencast Backfilled Pit 1 & 2. The falling head permeability test was used to measure the K_{sat} on the surface, top- and sublayers using a large and standard double-ring infiltrometer (ASTM D3385-0903, 2003), a single-ring infiltrometer (Johnson, 1963) and a constant-head permeameter as shown in Figure 3.1.

Figure 3.1: The water tank used to store water for infiltrometer tests (A) and conducting infiltrometer tests and excavate test pit (B). Pipe and drum system was used to provide water at Discard Dump 1 & 2. The infiltrometer tests were conducted with a constant-head permeameter (C) and in the picture at the bottom right-hand side (D), single-ring infiltrometer in front, large double-ring ring infiltrometer at right and standard double-ring infiltrometer at left were also used for infiltrometer tests.

Two types of ring infiltrometer double-ring infiltrometers were used *viz*., a large double-ring infiltrometer with an inner ring of 600 mm diameter and outer ring of 900 mm diameter, and standard double-ring with an inner ring of 300 mm diameter and outer ring of 600 mm diameter. The single-ring infiltrometer was 600 mm in diameter. These rings were sealed with bentonite clay powder at the ring outer circumference. No vegetation was removed for the infiltrometer tests at the surface.

The growth medium of dual-layered covers and the upper section of monolithic covers were removed by hand digging to expose a 1000 mm diameter area of the water retention layer of dual-layered covers and the lower section of monolithic covers. The rings were filled with water and the rate of infiltration was measured over a period of 3–6 hours. The constant-head permeameter tests were conducted where a shallow hole of 75 mm depth was augered. Permeameter tests were run for 1–3 hours depending on the time required to reach constant infiltration rates. A total of 74 infiltration tests were done and the average K_{sat} was calculated for each soil layer of every profile pit.

On the additional research site, Discard Dump 3, the same procedures used for K_{sat} measurement of the previous research sites were followed. Only five infiltration tests were conducted using the constant-head permeameter due to limited time. The K_{sat} values of old SRCs were grouped according to soil textural classes to compare the average K_{sat} values of SRCs to the K_{sat} values of soils in Table 3.1. The initial K_{sat} values at the time of SRCs construction were unknown, therefore the K_{sat} changes over time could not be evaluated

3.2.2 Data and regression analyses

Coefficient of variation (CV) was used to test the variability and Shapiro-Wilk (SW) normality test (Mishra *et al.* 2019) was used to verify the normal distribution of the total SRC data-set, and also the moderately- and very dense SRCs data sets separately. The data were divided into moderately- and very dense SRC data sets due to changes in porosity. The relationship between K_{sat} and soil physical properties were determined using the Pearson coefficient correlation (r) analysis.

Pedotransfer functions as K_{sat} model and, moderately- and very dense K_{sat} models were developed using MLR. The training sets for moderately- and very dense K_{sat} models are shown in Tables B.1 & B.2 in Appendix B. Sand-, silt- and clay content, SOM and soil bulk density were used as input parameters in MLR. Gravel content was not one of the input parameters because Shelley & Daniel (1993) reported that gravel content less than 50–60% did not considerably change K_{sat}. Furthermore, K_{sat} increased significantly at gravel content higher than 60%.

Table 3.1: Saturated hydraulic conductivity (K_{sat}) threshold criteria ranges for different soil textures (after Clapp & Hornberg, 1978; García-Gutiérrez *et al.,* 2018; Rawls *et al*., 1982, 1998).

Soil texture	$\boldsymbol{K_{sat}}$ **m.d^{-1}**
Loamy fine sand	1.466–3.499
Sandy loam	0.622–1.399
Loam	0.094–1.361
Sandy clay loam	0.103–0.782
Clay loam	0.055–0.379
Clay	0.014–0.977

Similar results were found by Shakoor & Cook (1990) that fine and very fine gravel content less of than 50% did not affect the K_{sat} of a compacted silty clay. The gravel content of all the SRCs consisted of medium to very fine gravel with lower than 26.07% gravel contents in this study (Table 2.16 in Chapter 2). Only some of the very dense SRCs had medium gravel content lower than 3.45%, whereas P2-2 of moderately dense SRCs had a medium gravel content of 6.34% (Table 2.16 in Chapter 2). The equation of K_{sat} model, moderately- and very dense K_{sat} models had the form:

$$Y = a + b*\text{Sand} + c*\text{Silt} + d*\text{Clay} + e*\text{SOM} + f*\rho_b \quad \text{[Eq. 3.1]}$$

where Y is predicted K_{sat}, and b, c, d, e and f are the regression coefficients of sand-, silt-, clay content, SOM and soil bulk density (ρ_b), respectively. Variance inflation factors and eigenvalues of centered correlations for multicollinearity was checked. The relative influence of each independent variable's regression coefficient was reported at the probability level of 0.05 (Salchow *et al.*, 1996). A second set of K_{sat} model, moderately- and very dense K_{sat} models were developed where the backward stepwise method was selected to simplify Eq. 3.1. The adjusted determination of coefficient (adjusted R^2) and predicted determination of coefficient (predicted R^2) between predicted and observed values of moderately- and very dense K_{sat} models were determined. The adjusted R^2, root mean square error (RMSE), and predicted R^2 were used to assess how well Eq. 3.1 and the simplified equation represented the moderately- and very dense SRCs data sets.

3.2.3 Model validation

3.2.3.1 *Moderately- and very dense store-and-release covers data sets*

After the SRC data-set was divided into moderately- and very dense SRCs data sets, the additional data-set (testing set) of Discard Dump 3 was used (Table 3.2) to validate the moderately dense K_{sat} models. The SRCs of Discard Dump 3 were similar to the very dense SRCs of Discard Dump 1, P1-3 & 1-4 and P2-2 & 2-3. A second additional facility with high bulk densities comparable to that of Discard Dump 2, Opencast Backfilled Pit 1 & 2 was not available. Consequently, the data-set of very dense SRCs was divided into separate data sets: training set (60%) and testing set (40%) using R software. The training set was to develop the very dense K_{sat} model, whereas the testing set (Table 3.1) was used to verify the accuracy and effectiveness of the model. The performance of the models was tested using the adjusted R^2, RMSE, and student's t-test. All analyses were performed using NCSS 12 Statistical Software (NCSS 12: Data Analysis & Graphics, 2019).

3.2.4 Pedotransfer functions compiled from literature

3.2.4.1 *Moderately- and very dense store-and-release covers data sets*

Twelve published K_{sat} PTFs were chosen to compare the predicted and average observed K_{sat} values of the moderately- and very dense SRCs. The twelve models are in Table 1.13 (Refer to Section 1.3.4.1 in Chapter 1). Model performance was evaluated using the adjusted R^2, RMSE and one-tail student's t-test between the predicted and observed K_{sat} values. The 1:1 line was used to determine how uniformly the data points were scattered.

3.3 Results and discussion

3.3.1 Data collection

The K_{sat} of the three infiltrometer tests and permeameter tests with the average K_{sat} are shown in Table 3.2. The average K_{sat} of moderately-and very dense SRCs ranged between 0.066–0.420 m.d^{-1} and 0.003–0.092 m.d^{-1}, respectively. If the average K_{sat} of moderately dense SRCs were grouped into soil textural classes, the results were as follows: (1) loamy sand: 0.328 m.d^{-1}, (2) sandy loam: 0.160–0.420 m.d^{-1}, (3) loam: 0.300 m.d^{-1}, (4) sandy clay loam: 0.066–0.290 m.d^{-1} and (5) clay loam: 0.077 m.d^{-1}. For very dense SRCs, the average K_{sat} values were: (1) sandy loam: 0.003–0.090 m.d^{-1}, (2) sandy clay loam: 0.040–0.092 m.d^{-1} and (3) clay: 0.024–0.049 m.d^{-1}.

Between moderately- and very dense SRCs, there was a significant difference in average K_{sat} (P = 3.120×10^{-6}). There was no significant difference between growth medium and water retention layer average K_{sat} values of either moderately- (P = 0.107) or very dense (P = 0.321) SRCs.

The following inferences were made on the K_{sat} values of moderately SRCs. The K_{sat} values were in the range between 10^{-3}–10^{-1} m.d^{-1} of the study by Benson *et al.* (2007) about the K_{sat} values of SRCs over ~4 years. Although, there was no difference between growth medium and water retention layer K_{sat} values, the K_{sat} values of the water retention layer were lower compared to the growth medium. The K_{sat} values of the water retention layer were favourable because according to Vermaak *et al.* (2004), the K_{sat} should be between 0.009–0.864 m.d^{-1}. After the average K_{sat} values were grouped accordingly to the soil textural classes, the following results were obtained: (1) the low K_{sat} values of loamy fine sand and sandy loam soils were likely due to compactness/hardsetting phenomenon and (2) the K_{sat} values of loam, sandy clay loam and clay loam were in the criteria range (Table 3.1). However, the K_{sat} values of the sandier soils were higher compared to the clayey soils, as was expected.

The following inferences were made on the K_{sat} values of very dense SRCs. The reduction in K_{sat} for the SRCs with high bulk density was lower than expected. Drumm *et al.* (1997) indicated that the K_{sat} values will be greater than 0.864 m.d^{-1} in a compacted clay layer with preferential flow paths. Saturated hydraulic conductivity determined from an area without cracks or preferential flow could be more than an order of magnitude lower as it only accounts for flows through the soil matrix and not through vertical cracks. The lowest K_{sat} determined for the very dense SRCs could be an indication of the K_{sat} for the flows through the cover matrix. The sandy loam and sandy clay loam K_{sat} values of very dense SRCs were lower than the criteria threshold values. The K_{sat} values of clayey soils were more or less similar to the natural soils and were less likely affected by compactness.

Overall, bulk density has a significant influence on $K_{sat,}$ since the K_{sat} values of very dense SRCs were lower compared to the K_{sat} values of moderately dense SRCs. Very dense SRCs can be problematic because SRCs rely on water-holding capacity rather than *significantly* decreasing the infiltration rate (Gorakhki & Bareither, 2017; Khire *et al.*, 2000). It can be assumed that the old SRCs with moderately dense soil cover conditions will have K_{sat} values similar to natural soils and have higher rehabilitation success.

Table 3.2: The saturated hydraulic conductivity ($m.d^{-1}$) of the three different infiltrometer tests and permeameter tests with average saturated hydraulic conductivity of moderately- and very dense store-and-release covers.

Soil cover condition	Profile pit name	Soil layer depth	Soil texture	Double-ring infiltrometer		Single-ring infiltrometer	Constant-head permeameter	Average K_{sat}
				Standard 600 mm	Large 900 mm			
		mm						
Moderately dense	D1-1	0–500	SCL	0.100	0.160	0.100	0.110	0.120
		550–900	SCL	0.046	0.061	0.092	0.065	0.066
	D1-2	0–400	SL	0.140	0.160	0.150	0.190	0.160
		400–600	SCL	0.130	0.140	0.116	0.154	0.135
	D1-3	Surface	SCL	0.140	0.160	0.190	0.150	0.160
		0–200	SCL	0.089	0.097	-	0.264	0.150
		200–550	CL	0.067	0.086	-	-	0.077
	P1-3	Surface	SL	0.260	-	0.420	-	0.330
	P1-4	Surface	SL	0.440	-	0.400	-	0.420
		0–350	SL	-	-	-	-	0.400
	P2-2	Surface	SL	0.310	0.330	0.029	-	0.310
		500–700	L	-	-	-	-	0.300
	P2-3	0–500	SCL	0.130	0.220	0.520	-	0.290
	D3-1	0–300	LFS	-	-	-	0.328	0.328
		>300	SCL	-	-	-	0.196	0.196
	D3-2	Surface	SL	-	-	-	0.275	0.275
		0–400	SL	-	-	-	0.372	0.372
		>400	SCL	-	-	-	0.141	0.141
Very dense	D2-1	0–450	SL	-	-	0.090	-	0.090
		450–650	SCL	0.081	0.030	0.090	0.047	0.062
		650–850	SCL	0.064	0.015	0.060	0.229	0.092
		850–1100	C	0.020	0.012	0.040	-	0.024
	D2-2	0–300	SL	0.061	0.042	0.040	0.105	0.062
		300–700	C	0.050	0.090	0.050	0.006	0.049
	P1-1	Surface	SL	0.081	-	0.085	-	0.083
		0–1100	SL	0.025	-	0.035	-	0.030
	P1-2	Surface	SL	0.051	-	-	-	0.060
		0–400	SL	-	-	-	-	0.040
	P2-1	0–100	SCL	0.036	0.040	0.044	-	0.040
		100–300	SL	0.003	0.004	0.002	-	0.003
	P2-2	0–500	SL	0.010	0.008	0.012	-	0.010

Note: LFS = loamy fine sand, SL = sandy loam, Loam = loam, SCL = sandy clay loam, CL = clay loam, and C = clay.

3.3.2 Data analysis

3.3.2.1 *Store-and-release covers data-set*

Basic summary statistics of average soil physical properties and K_{sat} of SRCs are presented in Table 3.3. According to Mishra *et al.* (2019), the SW normality test is more favourable to use for soil samples lower than 50 (26 soil samples in total). Therefore, SW normality test was used to verify whether the observations are normally distributed.

In Table 3.3, the CV for soil physical properties were large, indicating low to high variability. Bulk density was the least variable, whereas sand- and silt content were low to moderately variable. The variability of clay content and SOM were moderate to high and for gravel content, the variability was high. It was therefore expected that the variability of avg. K_{sat} would be high. Similar results were found by the Mulla & MacBratney (2002) study, where the CV of bulk density ranged between 3–26%, and sand- and silt content was between 3–37%. Moreover, the authors found that the variability of SOM and clay content were moderate to high ranging between 21–41%, and 16–53%, respectively. K_{sat} was the highest variable with 48–352% in the Mulla & MacBratney (2002) study. The variability of K_{sat} can be affected by the cross-section area of the flow domain (Bagarello, 1997). Das Gupta *et al.* (2006) performed infiltration tests in a field near College Station, Texas, USA using disk infiltrometers with disk sizes of 10, 15, 17, 20 and 24 cm. In the aforementioned study, minor differences in K_{sat} were reported, however, larger variability of bigger disks was due to an increase in heterogeneity and macropore network by increasing the sample volume.

Sand-, silt- and clay content, SOM and soil bulk density were normally distributed (Table 3.3). Gravel content and avg. K_{sat} were not normally distributed, but log-normal distributed. The gravel content had high positive skewness value of 1.387 with a right tail where most values ranged between 0.00–5.00% (Figure 3.2A).

Table 3.3: Descriptive statistics of soil physical properties of store-and-release covers data-set. Average soil physical properties are gravel (%), sand (%), clay (%), soil organic matter (SOM in %), soil bulk density (ρ_b in g.cm^{-3}), and saturated hydraulic conductivity (K_{sat} in m.d^{-1}).

Variable	Minimum	Maximum	Mean	CV	Skewness	SW test[a]
Gravel	0.12	26.07	6.21	99.73	1.387	*0.815*
$\log_{10}$(Gravel)	-0.936	1.250	0.430	140.00	-0.654	0.938
Sand	27.38	75.30	55.00	22.88	-0.406	0.929
Silt	7.78	35.87	19.53	31.41	0.718	0.945
Clay	3.59	43.34	20.70	52.74	0.533	0.930
SOM	0.01	2.87	0.90	40.48	0.983	0.895
ρ_b	1.460	2.286	1.786	11.21	0.627	0.940
K_{sat}	0.003	0.420	0.137	90.77	1.040	*0.841*
$\log_{10}(K_{sat})$	-2.553	-0.377	-1.076	-	-0.925	0.931

Note: CV = coefficient of variance in %, SW-test = Shapiro-Wilk normality test.
[a]A probability value smaller than 0.05 of SW normality test indicating the observation is non-normally distributed, is in italic.

The surface of P2-2 at Opencast Backfilled Pit 2 had a high gravel content (26.07%) compared to the other 25 soil samples that ranged between 0.12–17.83% (Table 2.16 in Chapter 2). Figure 3.2B showed the that log-normal distribution of avg. K_{sat} was skewed to right with most values ranging between 0.000–0.100 m.d^{-1}. This high positive skewness of avg. K_{sat} was expected due to preferential flow phenomenon and high bulk density.

Gravel content and avg. K_{sat} values were transformed into common logarithm ($\log_{10}$) to ensure a normal distribution, but there were still outliers for avg. $\log_{10}(K_{sat})$. To remove the outliers of avg. K_{sat} was not possible since it will exclude the high K_{sat} values (> 0.07 m.d^{-1}) of moderately dense SRCs and low K_{sat} values (< 0.09 m.d^{-1}) of very dense SRCs. Therefore, in this study, K_{sat} models were developed for moderately- and very dense SRCs at rehabilitated discard dumps and backfilled opencast pits.

3.3.2.2 *Moderately- and very dense store-and-release covers data sets*

Basic summary statistics of soil physical properties and avg. K_{sat} of moderately- and very dense SRCs are presented in Table 3.4. Bulk density of moderately- and very dense SRCs was the least variable, whereas sand- and silt content were low to moderately variable. The clay content of moderately dense SRCs was moderate to highly variable compared to the clay content of very dense SRCs which was high (Table 3.4). The high variability of SOM can be explained by veld fires (personal observation). There was a veld fire at Opencast Backfilled Pit 1 & 2 before samples were taken on August 2018. Therefore, some surface samples had higher SOM than others. After the SRCs been grouped into moderately- and very dense SRCs data sets, the variability of avg. K_{sat} decreased from 90.77% (Table 3.3) to 53.44% and 58.74%, respectively (Table 3.4).

Sand-, clay content, and bulk density were normally distributed in moderately- and very dense SRCs (Table 3.4). Gravel content was non-normally distributed because of the outliers *viz*., 17.82% and 26.07% in moderately dense SRCs, and 14.16%, 14.32% and 15.08% in very dense SRCs (Table 2.16 in Chapter 2). The effect of gravel content is negligible as explained in Section 3.2.2 and therefore, the gravel content as one of the input parameters was removed in Eq. 3.1.

The silt content was non-normally distributed in moderately dense SCRs, but normally distributed in very dense SCRs (Table 3.4). To remove the silt content of 35.87% (Table 2.16 in Chapter 2) from the moderately dense SRCs data-set wasn't possible because high silt content is desirable for SRCs. High silt content reduces the K_{sat} and increases the water holding capacity (WHC) (Libohova *et al.*, 2018). Greater WHC lowers the potential for oxygen- and water ingress through the SRC (Venkatraman *et al.*, 2010).

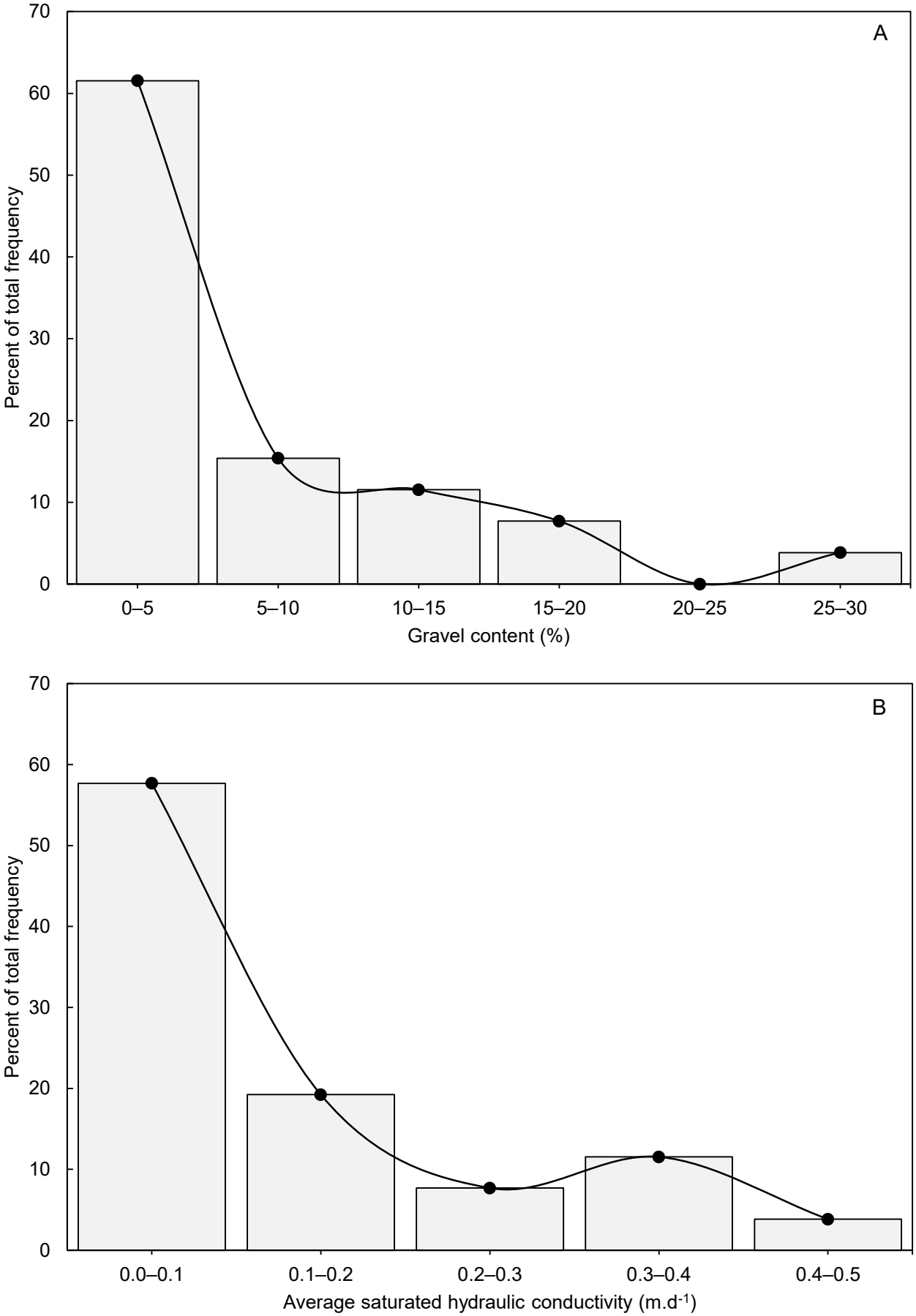

Figure 3.2: Total percentage frequency of percentage average gravel content (A), and average saturated hydraulic conductivity (B) of the store-and-release covers at rehabilitated coal discard dumps and opencast backfilled pits.

Table 3.4: Descriptive statistics of soil physical property variables of moderately- and very dense store-and-release covers (SRCs) data sets. Average soil physical properties are gravel (%), sand (%), clay (%), soil organic matter (SOM in %), soil bulk density (ρ_b in g.cm^{-3}) and saturated hydraulic conductivity (avg. K_{sat} in m.d^{-1}).

Data-set	Variable	Minimum	Maximum	Mean	CV	Skewness	SW test[a]
Moderately	Gravel	0.12	26.07	6.70	81.51	1.415	*0.765*
dense	Sand	27.38	74.90	52.13	27.90	-0.164	0.947
SRCs	Silt	12.88	35.86	19.09	31.99	1.500	*0.881*
	Clay	7.72	41.63	23.57	48.86	0.374	0.962
	SOM	0.01	2.87	0.94	57.32	1.408	0.945
	ρ_b	1.460	1.841	1.647	7.87	0.101	0.881
	K_{sat}	0.070	0.420	0.225	53.44	0.274	0.912
Very	Gravel	0.23	15.08	5.32	90.21	0.881	*0.849*
dense	Sand	32.64	75.30	57.29	23.69	-0.488	0.911
SRCs	Silt	7.77	31.58	18.63	33.46	0.185	0.956
	Clay	3.59	43.34	18.43	72.62	0.839	0.887
	SOM	0.03	2.14	0.87	80.77	0.679	0.953
	ρ_b	1.700	2.286	1.925	15.56	0.587	0.882
	K_{sat}	0.003	0.090	0.049	58.73	-0.025	0.950

Note: CV = coefficient of variance in %, SW-test = Shapiro-Wilk normality test.
[a]A probability value smaller than 0.05 of SW normality test indicating the observation is non-normally distributed, is in italic.

3.3.3 Relations between saturated hydraulic conductivity and soil physical properties

3.3.3.1 *Store-and-release covers data-set*

Pearson correlation coefficients (r) between soil physical properties and avg. K_{sat} of SRCs are presented in Table 3.5. The indicator for strong correlations are r ≥ 0.70 and moderate correlations are 0.40 ≤ r ≤ 0.70 (Gamie *et al.*, 2018). Table 3.5 shows that the avg. $\log_{10}(K_{sat})$ was weakly correlated with sand-, silt-, clay content, and SOM. The negative moderate correlation of avg. $\log_{10}(K_{sat})$ with bulk density indicated dependence of K_{sat} on the presence of macropores. In the agreement of the current investigation, the study of Li *et al.* (2007) also found weak correlations between K_{sat} with sand-, silt- and clay content, and SOM of seven soil profiles in Fengqiu County in the North China Plain. Moreover, a negative and significant correlation (r = -0.370) between K_{sat} and bulk density was found in aforementioned study.

3.3.3.2 *Moderately- and very dense store-and-release covers data sets*

Pearson coefficient correlation for moderately- and very dense SRCs between soil physical properties and avg. K_{sat} is presented in Table 3.6. The correlations between soil physical properties and avg. K_{sat} of moderately dense SRCs were as expected, except for bulk density. One would expect a negative correlation, *i.e.*, a decrease in K_{sat} with increasing bulk density. Nemes *et al.* (2005) found that K_{sat} of European data-set soils had a positive correlation, albeit not significant, with sand content, SOM, and bulk density. However, the Hungarian, and U.S. data-set soils from the

Table 3.5: Pearson correlation coefficients between soil physical variables and average common logarithm of saturated hydraulic conductivity of store-and-release covers.

	Sand	Silt	Clay	SOM	ρ_b
Silt	*-0.714*[a]				
Clay	*-0.694*	0.051			
SOM	*0.469*	0.467	-0.392		
ρ_b	*0.557*	*0.557*	-0.341	0.287	
avg. $\log_{10}(K_{sat})$	-0.142	0.377	-0.126	0.020	*-0.407*

Note: SOM = soil organic matter, ρ_b = soil bulk density, Avg. K_{sat} = average common logarithm of saturated hydraulic conductivity
[a]Significant at $P < 0.05$, indicated in italic.

Nemes *et al.* (2005) study had a negative correlation between K_{sat} and bulk density where the average bulk density of the three data-set soils was 1.46–1.50 g.cm^{-3}.

Normally, decreasing bulk density and increasing soil porosity, specifically macroporosity, cause an increase in K_{sat} and *vice versa* (Ahuja *et al.*, 1984). Another study found a strong negative correlation (r = -0.921) between bulk density and porosity (Kakaire *et al.*, 2016). This led to a strong positive correlation (r = 0.918) between porosity and K_{sat}. In the current study, the correlation between bulk density and porosity of moderately dense SRCs was r = -0.999 (data not shown), but the correlation between porosity and K_{sat} was r = -0.120 (data not shown). Furthermore, the significant correlations of K_{sat} with silt- and clay content, respectively, were both negative which is in the line with expectations.

Only sand- and silt content, and bulk density of very dense SRCs had a strong correlation with avg. K_{sat} (Table 3.6). As expected, bulk density had a negative correlation with K_{sat}. Kim *et al.* (2010) found similar results, namely that soil compaction significantly increased bulk density while porosity decreased. The negative correlation between sand content and avg. K_{sat} was possibly due to decreased macroporosity (Table 3.6). Silt content had a positive relationship with K_{sat} due to higher soil microporosity. This finding is supported by Bergamin *et al.* (2015) who studied a clayey soil (64.4% clay, 20.3% silt, and 15.3% sand); and observed a strong positive correlation (r = 0.70) between bulk density and soil microporosity. The study of Kooistra & Tovey (1995) also showed that greater bulk density of sandy loam soils caused higher soil microporosity.

3.3.4 Pedotransfer functions

3.3.4.1 *K_{sat} models*

To develop K_{sat} model 1, the data-set in Table B.1 in Appendix B (moderately- and very dense SRCs data-set combined as SRCs data-set) was used. Soil physical parameter estimates from sand-, silt-, clay content, SOM and bulk density are presented in Table 3.7. The backward stepwise MLR of K_{sat} model 2 is also presented in Table 3.7.

In Table 3.7, all the model input parameters of K_{sat} model 1 were not significant ($P \leq 0.05$) except bulk density ($P = 0.005$). Therefore, the other four variables were excluded and backward MLR was

Table 3.6: Pearson correlation coefficients between soil physical property variables and average saturated hydraulic conductivity of moderately- and very dense store-and-release covers (SRCs).

		Sand	Silt	Clay	SOM	ρ_b
Moderately dense SCRs	**Silt**	*-0.736*[a]				
	Clay	*-0.687*	0.311			
	SOM	0.439	-0.301	-0.020		
	ρ_b	0.500	*-0.436*	-0.587	0.378	
	Avg. K_{sat}	0.445	-0.285	*-0.810*	-0.164	0.375
Very dense SCRs	**Silt**	*-0.846*				
	Clay	0.050	-0.461			
	SOM	-0.096	0.228	-0.496		
	ρ_b	*0.964*	*-0.732*	-0.037	0.084	
	Avg. K_{sat}	*-0.905*	*0.787*	0.159	-0.022	*-0.823*

Note: SOM = soil organic matter, ρ_b = soil bulk density, Avg. K_{sat} = average saturated hydraulic conductivity.
[a]Significant at $P < 0.05$, indicated in italic.

performed to develop K_{sat} model 2 (Eq. 3.1). The adjusted R^2 was 0.343 in K_{sat} model 1 which was low, but significant ($P = 0.024$) with a RMSE of 0.426 $m.d^{-1}$. Furthermore, the predicted R^2 was low with a value of 0.486. The regression analysis of K_{sat} model 2 gave an adjusted R^2 = 0.304 ($P = 0.002$), RMSE = 0.424 $m.d^{-1}$, and the predicted R^2 was 0.332. Multicollinearity for both models was not a problem. These K_{sat} models weren't analysed further for model validation because for good predictions $R^2 > 0.60$ (Alexander *et al.*, 2015).

3.3.4.2 *Moderately- and very dense K_{sat} models*

Details of moderately- and very dense K_{sat} model of Eq. 3.1 and simplified equation and performance are listed in Table 3.8 and 3.9, respectively. To develop moderately- and very dense K_{sat} models, the data sets in Table B.1 in Appendix B were used. After the moderately- and very dense K_{sat} models were developed, the regression equations were as follows:

Moderately dense K_{sat} = 1.015 - 9.884×10^{-05}*Sand - 0.003*Silt - 0.012*Clay - 0.028*SOM - 0.268*ρ_b [Eq. 3.2]

Very dense K_{sat} = -0.029 + 0.001*Sand + 0.005*Silt + 0.003*Clay + 0.009*SOM - 0.040* ρ_b [Eq. 3.3]

Multicollinearity for moderately dense K_{sat} model 1 was not a problem. The regression coefficient of clay content of moderately dense K_{sat} model 1 was significant, whereas the other four variables were not. Thereafter, backward stepwise MLR was performed and a simplified equation, moderately dense K_{sat} model 2 (Table 3.8), was developed as follows:

Moderately dense K_{sat} = 0.432 – 0.010*Clay [Eq. 3.4]

The adjusted R^2 and predicted R^2 of moderately dense K_{sat} model 2 decreased compared to moderately dense K_{sat} model 1 (Table 3.9). Moreover, RMSE value was higher than moderately dense K_{sat} model 1. No backward stepwise MLR for very dense SCRs data-set was performed because all the regression coefficients of very dense K_{sat} model were significant (Table 3.8). All the regression coefficients had an impact on the dependent variable, K_{sat}. Multicollinearity for the very dense K_{sat} model was not a problem. The adjusted R^2 and predicted R^2 of the very dense K_{sat} model were high and close to the value of 1. All the regression equations had a good predicted R^2 above 0.60, therefore further analyses could be done, namely model validation.

Table 3.7: Parameters estimate for saturated hydraulic conductivity models of store-and-release covers.

Variable	Parameter estimate	Standard error	Probability value[a]
K_{sat} model 1			
Intercept	-1.330	4.677	*0.780*
Sand (%)	0.035	0.044	*0.439*
Silt (%)	0.051	0.058	*0.393*
Clay (%)	0.014	0.039	*0.723*
SOM (%)	-1.792	0.120	*0.711*
ρ_b (g.cm^{-3})	0.074	0.555	0.005
K_{sat} model 2			
Intercept	1.538	0.762	0.049
ρ_b (g.cm^{-3})	-1.493	0.432	0.002

Note: SOM = soil organic matter, K_{sat} = saturated hydraulic conductivity, Soil organic matter, ρ_b = soil bulk density.
[a]Significant at $P < 0.05$, indicated in italic.

Table 3.8: Parameters estimate for saturated hydraulic conductivity of moderately- and very dense store-and-release covers.

Variable	Parameter estimate	Standard error	Probability value[a]
Moderately dense K_{sat} model 1			
Intercept	1.015	0.659	0.184
Sand (%)	-9.884×10^{-05}	0.004	0.981
Silt (%)	-0.003	0.006	0.690
Clay (%)	-0.012	0.004	*0.039*
SOM (%)	-0.028	0.069	0.698
ρ_b (g.cm^{-3})	-0.268	0.240	0.315
Moderately dense K_{sat} model 2			
Intercept	0.432	0.045	*0.000*
Clay (%)	-0.010	0.002	*0.001*
Very dense K_{sat} model			
Intercept	-0.092	0.0106	*0.013*
Sand (%)	0.001	0.001	*0.011*
Silt (%)	0.005	0.001	*0.001*
Clay (%)	0.003	8.367×10^{-05}	*0.001*
SOM (%)	0.009	0.001	*0.006*
ρ_b (g.cm^{-3})	-0.040	0.006	*0.004*

Note: K_{sat} = saturated hydraulic conductivity, SOM = Soil organic matter, ρ_b = soil bulk density.
[a]Significant at $P < 0.05$, indicated in italic.

Table 3.9: Summary of statistical analyses for saturated hydraulic conductivity models.

Regression model	Adjusted R^2	RMSE	P-value[a]	Predicted R^2
Moderately dense K_{sat} model 1	0.749	0.065	*0.028*	0.875
Moderately dense K_{sat} model 2	0.675	0.069	*0.001*	0.704
Very dense K_{sat} model	0.999	0.001	*0.007*	0.999

Note: Adjusted R^2 = Adjusted coefficient of determination, RMSE = Root mean square error in $m.d^{-1}$, Predicted R^2 = Predicted coefficient of determination, K_{sat} = saturated hydraulic conductivity.
[a]Significant at $P < 0.05$, indicated in italic.

3.3.5 Model validation of moderately- and very dense K_{sat} models

The three models were tested using the testing sets of moderately- and very dense SRCs in Table B.2 in Appendix B. Percentage of sand, silt and clay content, SOM and soil bulk density were inserted in Eq. 3.2 and 3.3. Only the percentage of clay content of the moderately dense SCRs data-set were inserted in Eq. 3.4. The adjusted R^2 and RMSE of the models are summarised in Table 3.10. The estimated moderately- and very dense K_{sat} were compared with the measured moderately- and very dense K_{sat} values (Figures 3.3–3.4).

A student's t-test was performed and there were no statistically significant differences between the measured and predicted moderately dense K_{sat} values of model 1 (t = -0.205, P = 0.842), and model 2 (t = 0.207, P = 0.841). The student's t-test was also performed with a null hypothesis of no difference between the mean of measured and predicted K_{sat} values at a probability level of 0.05 (Steel & Torrie, 1980). Between the two means, there was no statistically significant difference of the moderately dense K_{sat} model 1. Moreover, there was no statistically significant difference between the mean of measured and predicted K_{sat} of moderately dense model 2. Figure 3.3A of moderately dense K_{sat} model 1 showed that the data points were uniformly scattered around the 1:1 line. Compared to model 1, the data points of K_{sat} model 2 (Figure 3.3B) weren't as closely and uniformly scattered around the 1:1 line. The assessment of moderately dense K_{sat} model 1 showed a higher adjusted R^2 and lower RMSE compared to moderately dense K_{sat} model 2 (Table 3.10). These statistically reasonable agreements suggested that moderately dense K_{sat} model 1 (Eq. 3.2) performed well, therefore the model was satisfactorily validated.

The student's t-test of very dense K_{sat} model is t = -0.100 and P-value = 0.926. There was no statistically difference between the measured and predicted K_{sat} of the very dense K_{sat} model. Furthermore, there was no difference between the mean of measured and predicted K_{sat} at the probability level of 0.05. Figure 3.4 of very dense K_{sat} model 1 showed that the data points were uniformly scattered around the 1:1 line. The adjusted R^2 was close to the value of 1 and RMSE was low (Table 3.10). These statistically reasonable agreements suggested that very dense K_{sat} model (Eq. 3.3) performed well and the model was satisfactorily validated.

Table 3.10: Performance of saturated hydraulic conductivity models using the testing data sets.

Regression model	Adjusted R^2	RMSE
Moderately dense K_{sat} model 1	0.696	0.036
Moderately dense K_{sat} model 2	0.516	0.066
Very dense K_{sat} model	0.999	0.004

Note: Adjusted R^2 = Adjusted coefficient of determination, RMSE = Root mean square error in $m.d^{-1}$.

Note that the very dense K_{sat} model might have suffered from overfitting because the rule of thumb for the number of observations for each variable is 10–15 (Soper, 1990). Soper (1990) also mentioned that the shrinkage method to avoid overfitting is adjusted R^2, and bootstrapping. Only adjusted R^2 was used in this study. Nevertheless, the very dense SRCs data-set originated mostly from poorly constructed SRCs which isn't desirable for long-term soil cover performance. Poorly constructed and very dense SRCs are likely to fail over the long term. Several studies investigated the failure of very dense soil covers regarding their long-term performance and the main factors of failure were: the compaction was not uniform (Albrecht *et al.*, 1990; Benson *et al.*, 2007), insufficient water holding capacity (Warren *et al.*, 1996), and cracks (Albright *et al.*, 2006a; Albright *et al.*, 2006b). Another factor of poor performance is that the cover materials of poorly constructed covers do not meet the soil cover design which was optimised to meet required performance (Suter *et al.*, 1993).

Moderately dense K_{sat} model 1 and the very dense K_{sat} model may be useful for old SRCs with similar properties, the use of the PTFs from this study has a major advantage for rehabilitated mine land in the Mpumalanga Highveld because it provides an inexpensive and simple method to determine cover material hydraulic properties from easily available data.

3.3.6 Pedotransfer functions compiled from literature

3.3.6.1 *Modelling saturated hydraulic conductivity of moderately- and very dense store-and-release covers*

For the 12 published K_{sat} PTFs, the predicted K_{sat} and descriptive statistics for moderately- and very dense SRCs are presented in Table 3.11. Average K_{sat} predicted of moderately dense SRCs of the 12 K_{sat} PTFs ranged from 0.002 $m.d^{-1}$ with the Li *et al.* (2007) model to 4.153 $m.d^{-1}$ with the Gülser & Candemir (2008) model (Table 3.11). The average predicted K_{sat} of very dense SRCs of the 12 K_{sat} PTFs ranged from 7.351×10^{-5} $m.d^{-1}$ with the Li *et al*. (2007) model to 4.039 $m.d^{-1}$ with Gülser & Candemir (2008) model. All of the 12 moderately dense predicted K_{sat} were within a standard deviation (SD) of one. The Campbell & Shiozawa (1992) had the lowest SD of 0.002 $m.d^{-1}$ and the highest of 0.868 $m.d^{-1}$ was the Gülser & Candemir (2008) of the moderately dense predicted K_{sat} (Table 3.11). The SD of the very dense predicted K_{sat} of the 12 K_{sat} PTFs (Table 3.11) were lower than one, except the Dune & Puckett (1992) and Gülser & Candemir (2008) models. The SD of Li *et al.* (2007) was the lowest of 6.229×10^{-5} $m.d^{-1}$ and the highest SD (1.679 $m.d^{-1}$) was the Dane & Puckett (1992) model of the very dense SRCs (Table 3.12). The CV above 100% for both predicted K_{sat} data sets of the 12 K_{sat} PTFs, were Rawls & Brakensiek (1985), Campbell & Shiozawa (1992) and Salchow *et al.* (1996).

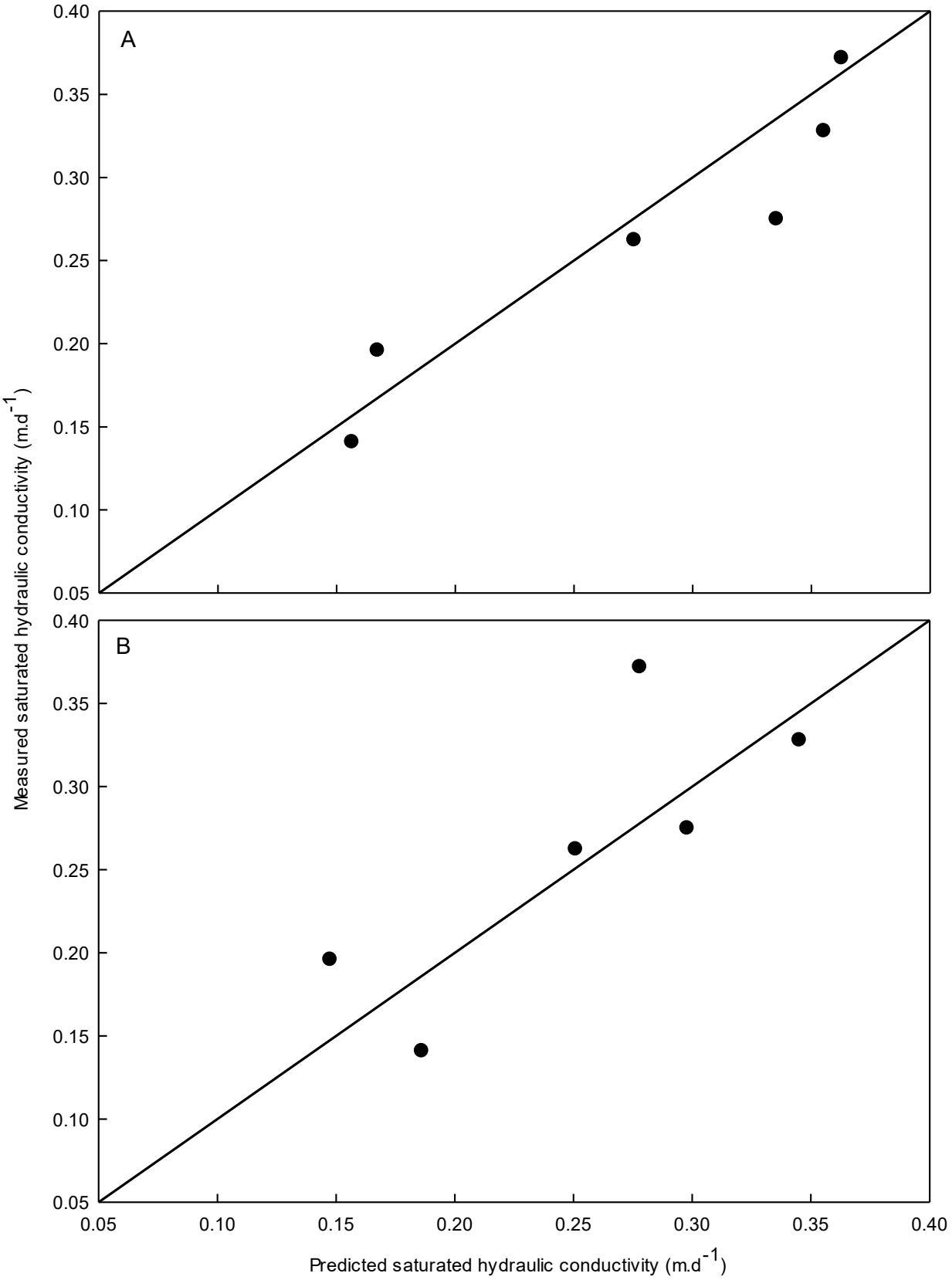

Figure 3.3: Measured versus predicted saturated hydraulic conductivity of moderately dense K_{sat} model 1 (A) & 2 (B).

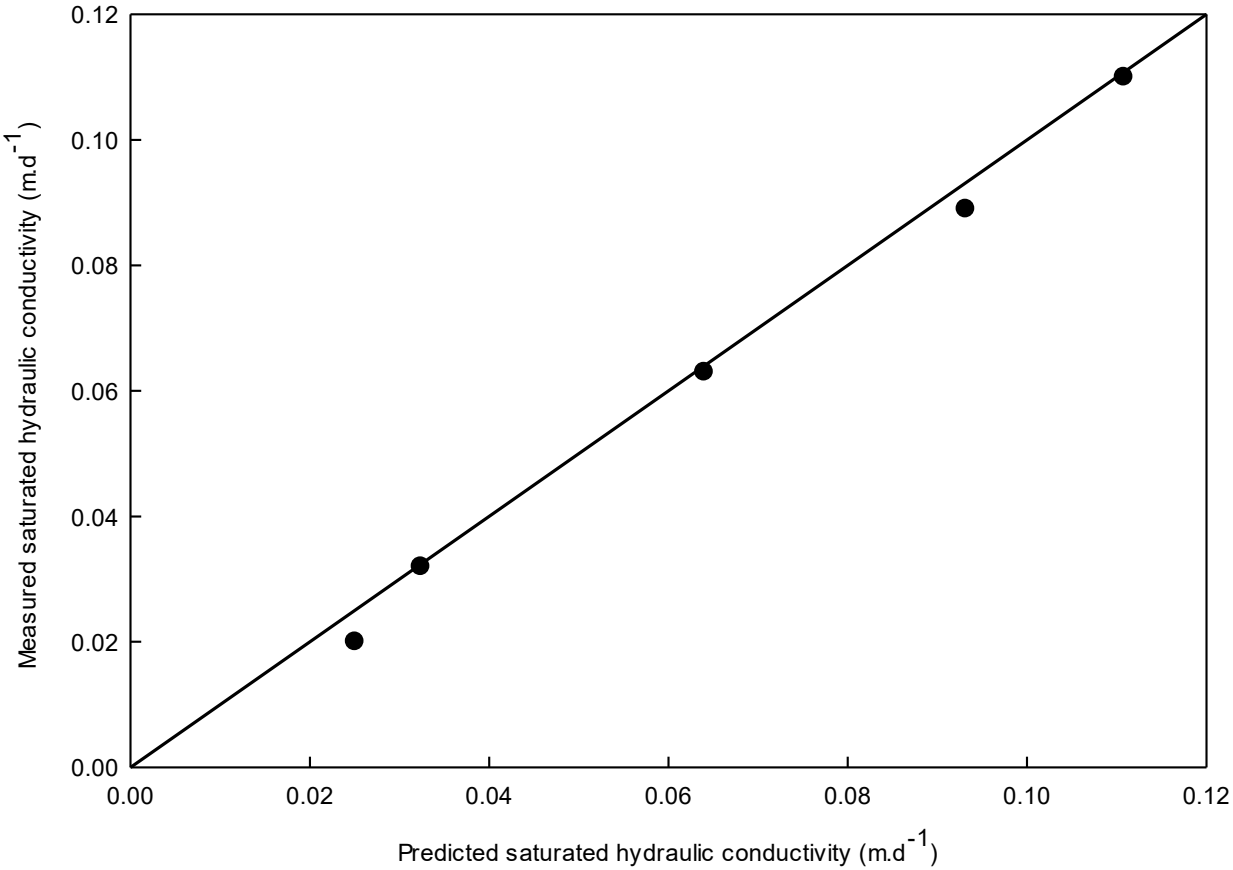

Figure 3.4: Measured versus predicted saturated hydraulic conductivity intervals of very dense K_{sat} model.

Rawls & Brakensiek (1985), Campbell & Shiozawa (1992) and Salchow *et al.* (1996) models had low K_{sat} values with high CV of both data sets (Table 3.11). The reason may due to Rawls & Brakensiek (1985) model has exponential and polynomial with sand- and clay content, and saturated water content as input parameters in the MLR model. Although, the K_{sat} database of Rawls & Brakensiek (1985) contain more than 1000 measurements and has 14 different soil textural classes. Some values of K_{sat} database of Rawls & Brakensiek (1985) were removed and may cause a bias: (1) soils greater than 1% gravel content; (2) ratio of SOM to clay greater than 0.2; and (3) K_{sat} greater than one order of magnitude and contained macropores. Campbell & Shiozawa (1992) model has only sand- and clay content as input parameters of an exponential equation. Whilst compared to Dane & Puckett (1992) model, the exponential equation has clay content as an input parameter. The soil textural classes, climatic conditions and how the database was selected play an important role when developing a K_{sat} model. Salchow *et al.* (1996) model has no intercept for a MLR model and may cause bias. The K_{sat} database of Salchow *et al.* (1996) contains 108 samples with sandy loam, loam, silty loam and silty clay loam soils. Li *et al.* (2007) model for both data sets had low K_{sat}, but the CV was under 100%. The low K_{sat} values of Li *et al.* (2007) model may due to the high regression coefficient for bulk density for a MLR model. Furthermore, the research of Li *et al.* (2007) contains 36 determined K_{sat} by using only the disk permeameter and has six soil textural classes *viz*. sand, loamy sand, sandy loam, silty loam, silty clay loam and silty clay.

3.3.6.2 *Model performance*

Model performance is shown in Figures 3.5–3.10 and summarised in Table 3.12. Two of the 12 K_{sat} PTFs of the moderately dense SRCs had moderately adjusted R^2 values which were Dane & Puckett (1992) and Arshad *et al*. (2013) models in Table 3.12. In contrast, the data points of Dane & Puckett (1992) and Arshad *et al.* (2013) models weren't uniformly scattered around the 1:1 line, but rather overestimated the K_{sat} values (Figures 3.6 & 3.7). Jabro (1992) model had a low adjusted R^2 value, but had the smallest student's t-test value of 2.697. Moreover, the data points were scattered around the 1:1 line, albeit not uniformly (Figure 3.7).

One of the 12 K_{sat} PTFs of the very dense SRCs had a high adjusted R^2 value of 0.784 was Cosby *et al.* (1984) model (Table 3.12). The data points weren't, however, uniformly scattered around the 1:1 line and overestimated the K_{sat} values (Figure 3.8). Similar to moderately dense SRCs, the Jabro (1992) model for very dense SRCs had the smallest student's t-test value of 2.655 (Table 3.12) and the data points were scattered around the 1:1 line, albeit also not uniformly (Figure 3.9). All the K_{sat} PTFs performed poorly either underestimating or overestimating the K_{sat} values for moderately- and very dense SRCs.

3.4 Conclusion

Although the initial K_{sat} values of SCRs during design and construction are unknown, the K_{sat} values, especially those of the moderately dense SRCs, were more or less similar to the K_{sat} values of the natural soils after >20 years. Despite that the K_{sat} values of loamy fine sand and sandy loam were low because of lower resistance to compaction. In this study, the sand- and clay content of moderately dense SRCs had a moderate to strong relationship with K_{sat}, while the bulk density had a positive weak relationship with K_{sat}. In contrast, bulk density, sand- and silt content of very dense SRCs had a strong relationship with K_{sat}, but opposite to those found in moderately dense SRCs. The reason is due to changes in porosity when bulk density increased. This result supported the decision to develop separate MLR models for moderately- and very dense SRCs.

The most suitable models for moderately- and very dense SRCs had the input parameters of sand-, silt- and clay content, SOM and bulk density. In general, it seems that the K_{sat} values of soil covers having a similar soil physical properties range to the old SRCs in Mpumalanga Highveld can be easily predicted using the basic soil physical properties in the MLR models. These predicted K_{sat} values can be used in soil cover design and modelling to evaluate the soil covers' long-term performance. The predicted K_{sat} values of the 12 published PTFs were not suitable to predict the K_{sat} values for SRCs on the Mpumalanga Highveld.

Table 3.11: Estimated saturated hydraulic conductivity (K_{sat} in m.d^{-1}) with descriptive statistics of moderately- and very dense store-and-release covers data-set using the 12 chosen K_{sat} models.

Descriptive statistics	**Author K_{sat} model**											
	Cosby *et al.* (1984)	**Rawls & Brakensiek (1985)**	**Saxton *et al.* (1986)**	**Vereecken *et al.* (1990)**	**Jabro (1992)**	**Dane & Puckett (1992)**	**Campbell & Shiozawa (1992)**	**Salchow *et al.* (1996)**	**Wösten *et al.* (1999)**	**Li *et al.* (2007)**	**Gülser & Candemir (2008)**	**Arshad *et al.* (2013)**
Moderately dense store-and-release covers												
Minimum	0.229	0.001	1.383	0.172	0.008	0.108	0.001	0.001	0.001	0.001	0.356	0.179
Maximum	1.419	0.332	1.875	1.546	0.407	3.026	0.028	0.336	3.787	0.016	4.153	1.956
Mean	0.681	0.050	1.597	0.712	0.130	1.114	0.005	0.036	1.827	0.002	3.411	0.720
SD	0.362	0.089	0.417	0.719	0.123	0.975	0.002	0.078	0.905	0.046	0.868	0.523
CV	50.32	158.90	22.84	53.21	99.61	81.45	143.55	203.30	51.06	97.27	24.73	32.60
Very dense store-and-release covers												
Minimum	0.205	0.001	1.438	0.058	0.001	0.052	0.001	0.001	0.023	2.293×10^{-4}	0.233	0.164
Maximum	1.053	0.029	3.312	1.806	0.097	4.842	0.042	0.120	1.764	2.905×10^{-6}	4.039	2.519
Mean	0.679	0.008	1.839	0.591	0.026	1.851	0.004	0.004	1.046	7.351×10^{-5}	2.770	0.711
SD	0.272	0.008	0.499	0.546	0.044	1.679	0.005	0.002	0.611	6.299×10^{-5}	1.074	0.641
CV	38.54	109.71	26.07	88.68	96.67	87.13	124.39	181.31	56.15	82.29	37.25	86.49

Note: SD = standard deviation in m.d^{-1}, CV = coefficient of variation in %.

Table 3.12: Model performance of the published pedotransfer functions for predicting saturated hydraulic conductivity of moderately- and very dense store-and-release covers (SRCs) data sets.

Author	Adjusted R^2	RMSE	Student's t-test[a]
Moderately dense SRCs data-set			
Cosby *et al.* (1984)	0.275	0.103	-4.974
Rawls & Brakensiek (1985)	0.064	0.117	5.593
Saxton *et al.* (1986)	0.091	0.115	-2.967
Vereecken *et al.* (1990)	0.050	0.123	-2.919
Jabro (1992)	0.075	0.125	2.697
Dane & Puckett (1992)	0.586	0.078	-3.926
Campbell & Shiozawa (1992)	0.149	0.111	8.834
Salchow *et al.* (1996)	0.002-	0.120	6.070
Wösten *et al.* (1999)	0.049	0.117	-7.910
Li *et al.* (2007)	0.066	0.124	7.817
Gülser & Candemir (2008)	0.030	0.119	-15.392
Arshad *et al.* (2013)	0.575	0.079	-3.841
Very dense SRCs data-set			
Cosby *et al.* (1984)	0.784	0.015	-8.177
Rawls & Brakensiek (1985)	0.069	0.033	5.325
Saxton *et al.* (1986)	0.281	0.027	-12.849
Vereecken *et al.* (1990)	0.013	0.032	-3.523
Jabro (1992)	0.054	0.031	2.655
Dane & Puckett (1992)	0.024	0.032	-3.853
Campbell & Shiozawa (1992)	0.090	0.034	5.876
Salchow *et al.* (1996)	0.028	0.032	6.050
Wösten *et al.* (1999)	0.168	0.029	-5.826
Li *et al.* (2007)	0.022	0.032	6.357
Gülser & Candemir (2008)	0.167	0.029	-9.105
Arshad *et al.* (2013)	0.075	0.031	-3.679

Note: Adjusted R^2 = Adjusted coefficient of determination, RMSE = Root mean square error in $m.d^{-1}$.
[a]All the probability levels were $P < 0.05$.

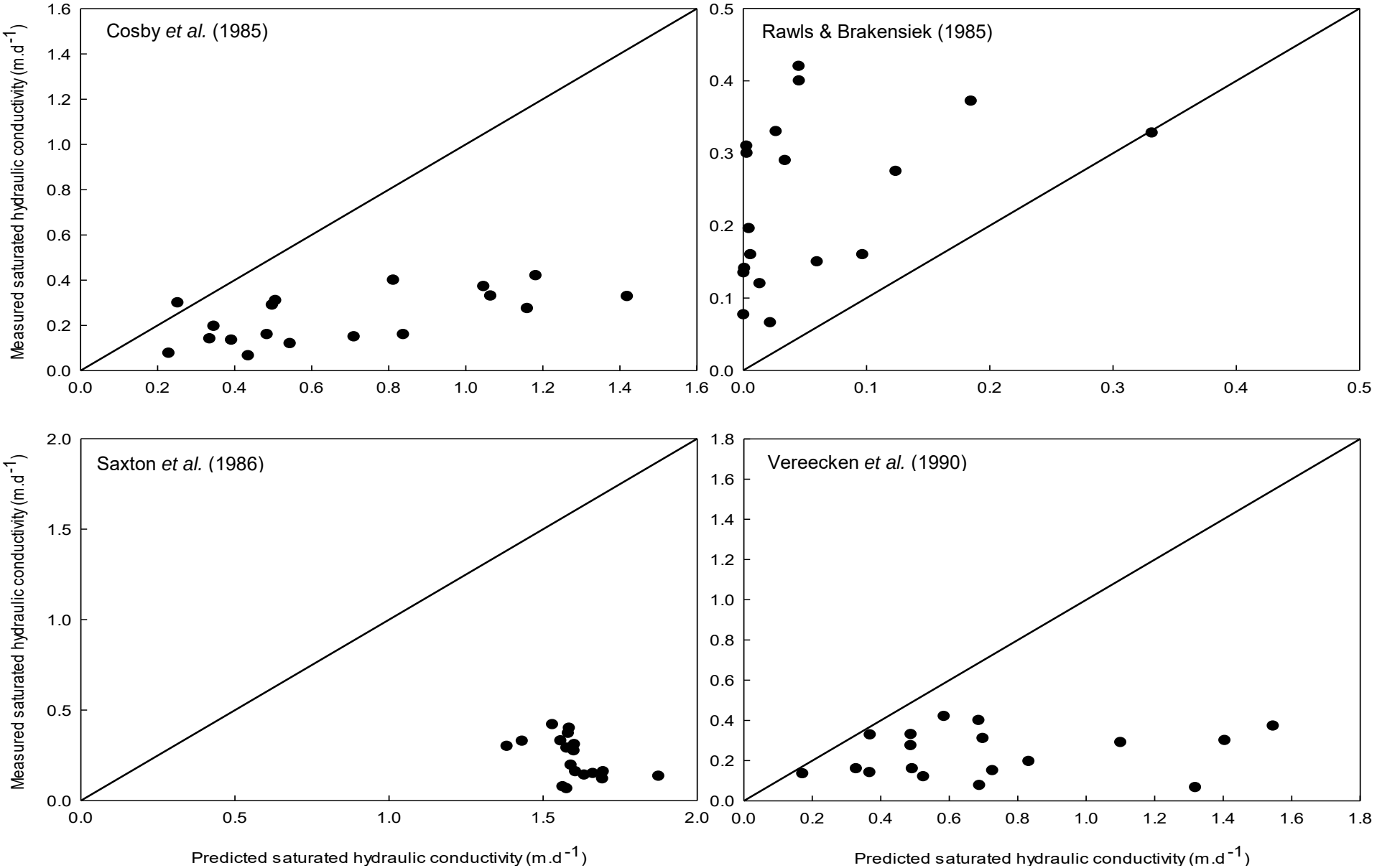

Figure 3.5: Measured saturated hydraulic conductivity versus Cosby *et al.* (1984) model, Rawls & Brakensiek (1985) model, Saxton *et al.* (1986) model and Vereecken *et al.* (1990) model predicted saturated hydraulic conductivity of moderately dense SRCs.

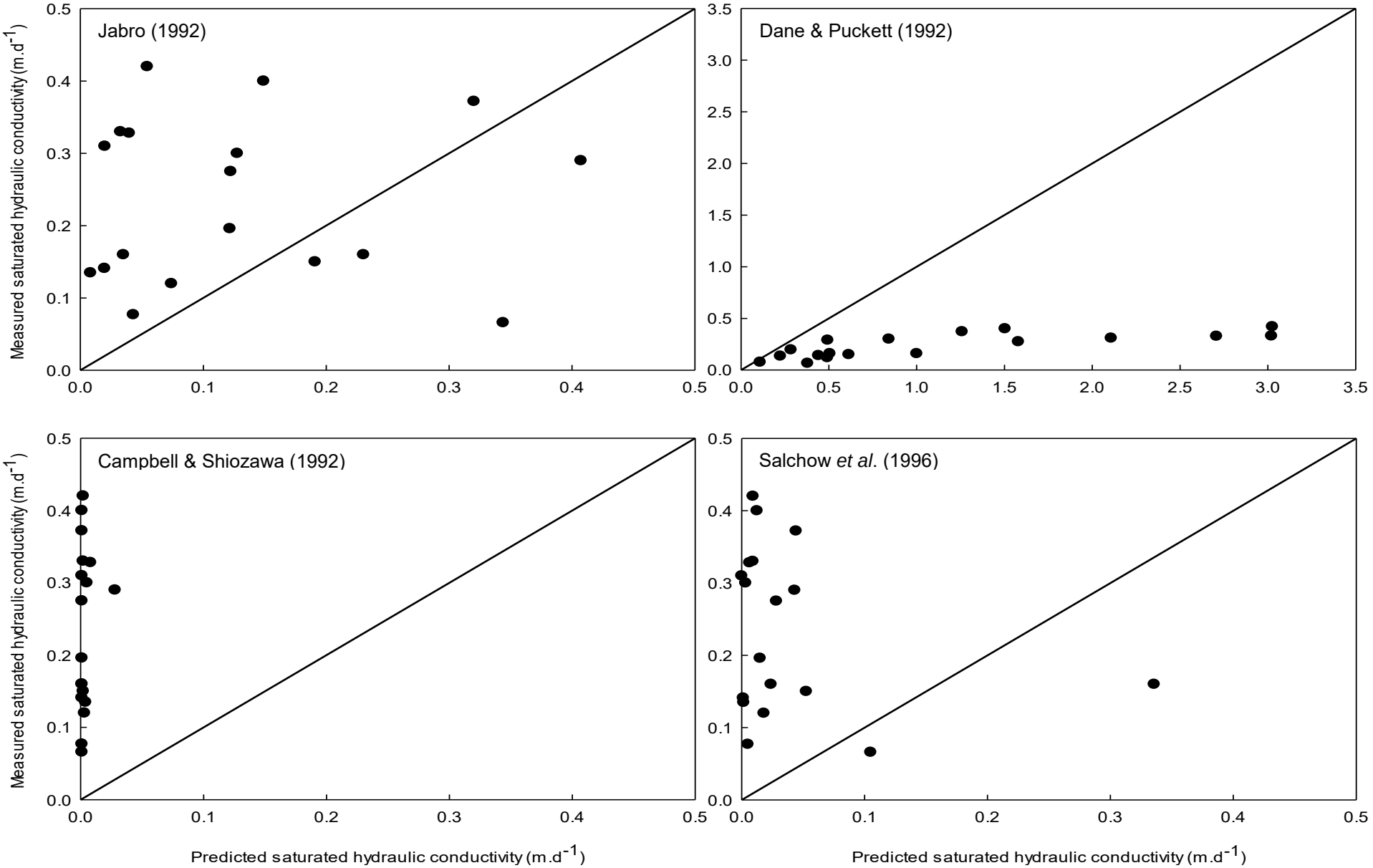

Figure 3.6: Measured saturated hydraulic conductivity versus Jabro (1992) model, Dane & Puckett (1992) model, Campebell & Shiozawa (1992) model and Salchow *et al.* (1996) model predicted saturated hydraulic conductivity of moderately dense SRCs.

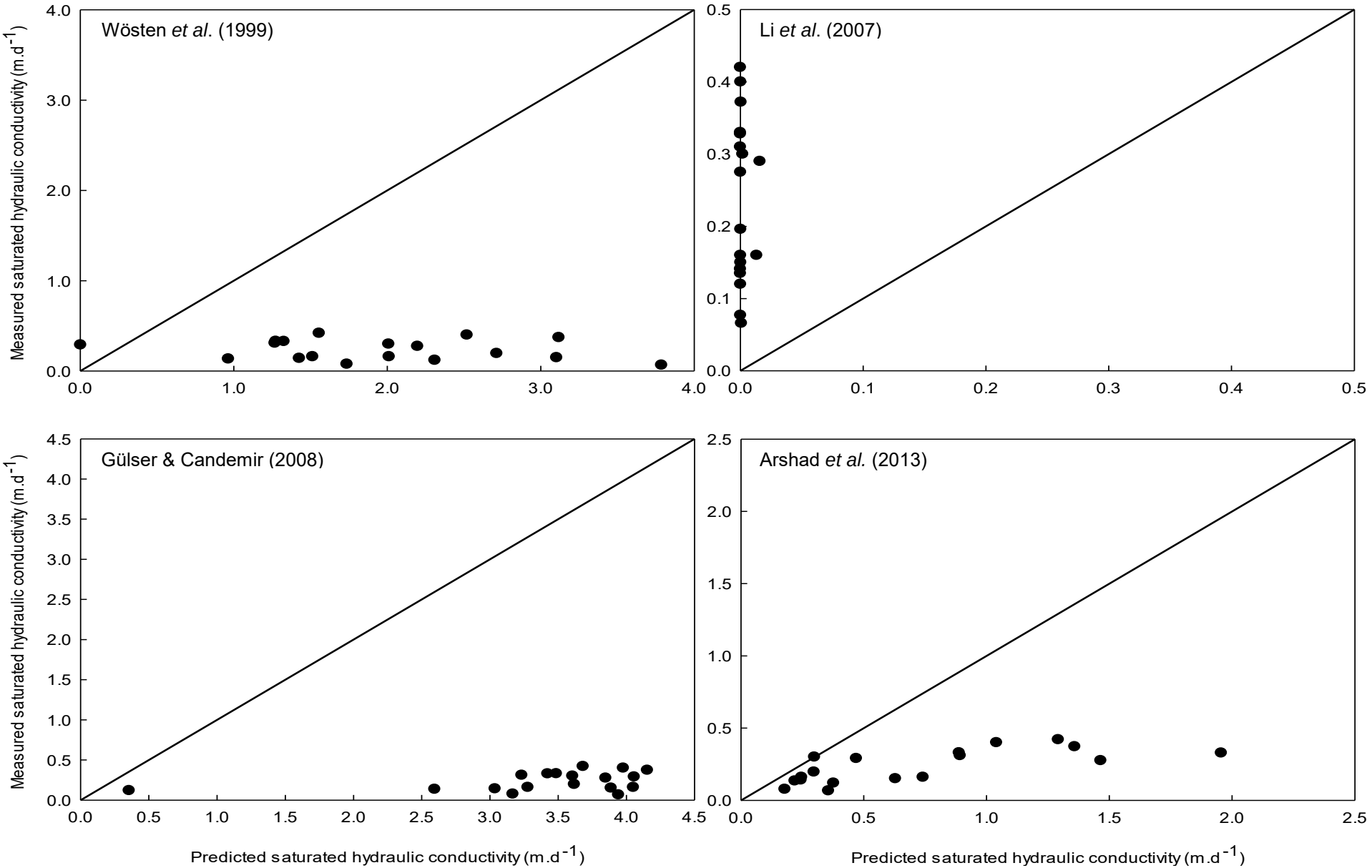

Figure 3.7: Measured saturated hydraulic conductivity versus Wösten *et al*. (1999) model, Li *et al*. (2007) model, Gülser & Candemir (2008) model and Arshad *et al.* (2013) model predicted saturated hydraulic conductivity of moderately dense SRCs.

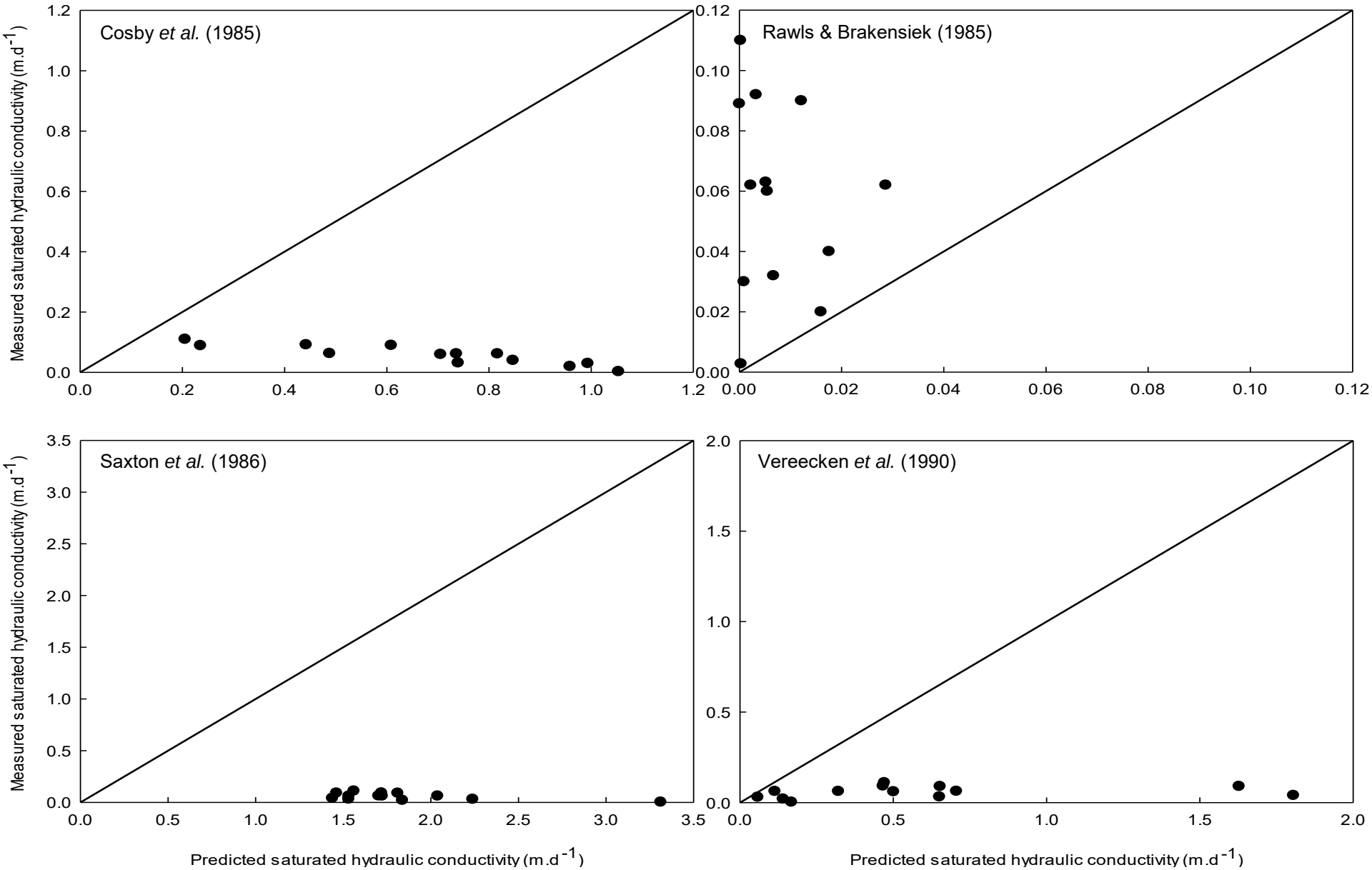

Figure 3.8: Measured saturated hydraulic conductivity versus Cosby *et al.* (1984) model, Rawls & Brakensiek (1985) model, Saxton *et al.* (1986) model and Vereecken *et al.* (1990) model predicted saturated hydraulic conductivity of very dense SRCs.

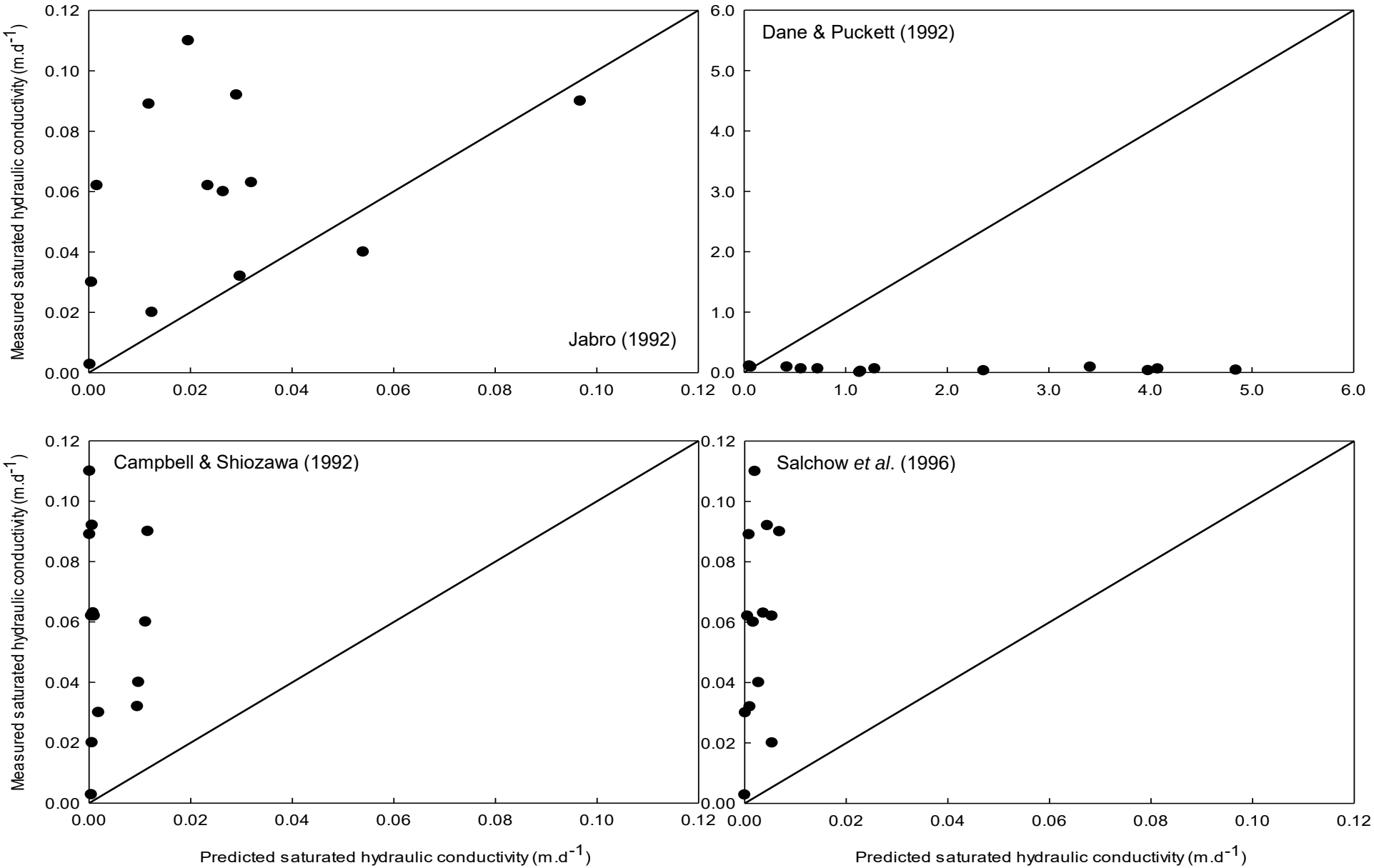

Figure 3.9: Measured saturated hydraulic conductivity versus Jabro (1992) model, Dane & Puckett (1992) model, Campebell & Shiozawa (1992) model and Salchow *et al.* (1996) model predicted saturated hydraulic conductivity of compacted SRCs.

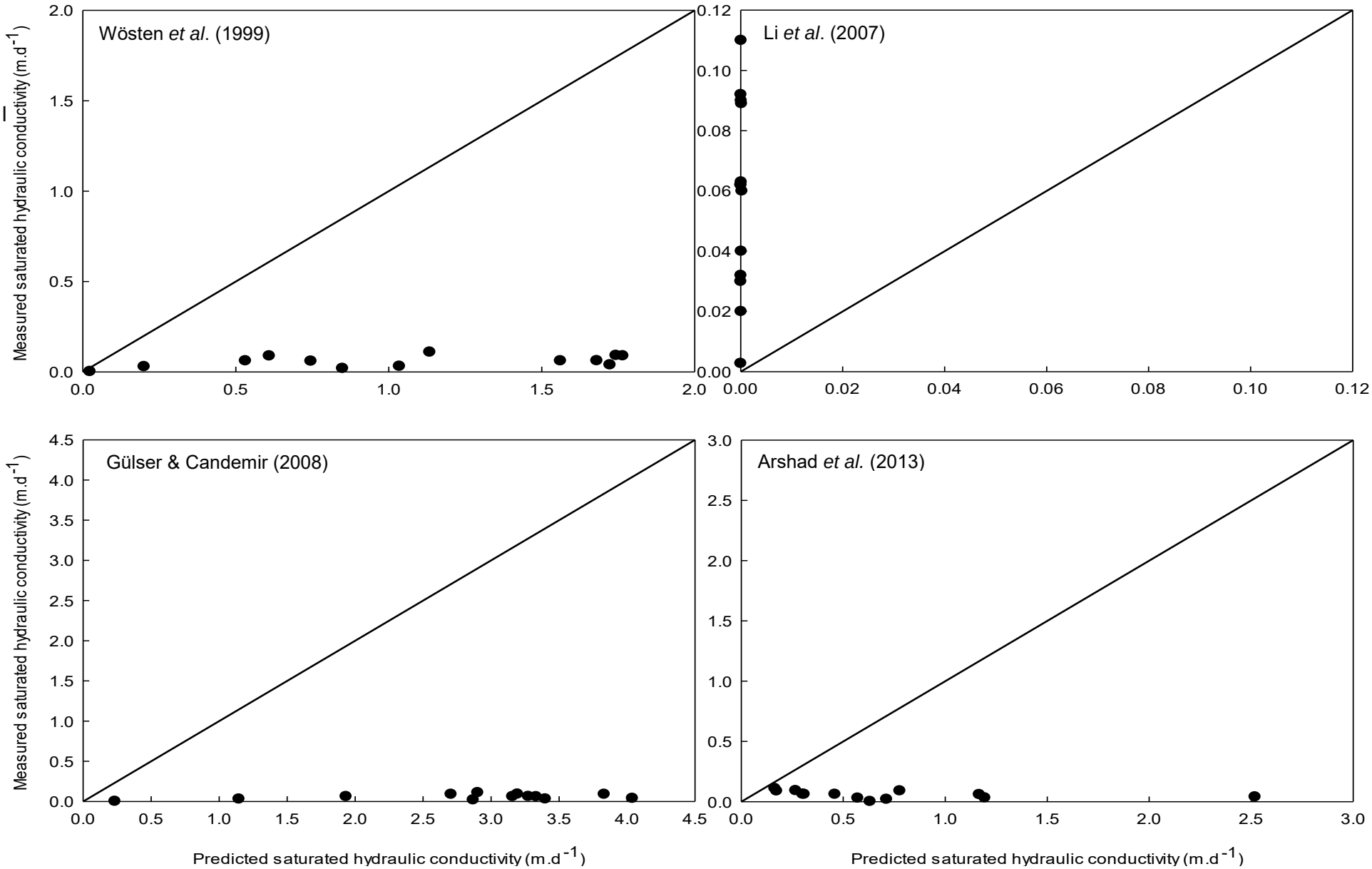

Figure 3.10: Measured saturated hydraulic conductivity versus Wösten *et al*. (1999) model, Li *et al*. (2007) model, Gülser & Candemir (2008) model and Arshad *et al.* (2013) model predicted saturated hydraulic conductivity of compacted SRCs.

3.5 References

Ahuja, L.R., Naney, J.W., Green, R.E. & Nielsen, D.R. 1984. Macroporosity to characterize spatial variability of hydraulic conductivity and effects of land management. *Soil Science Society of America Journal*. 48(4):699–702.

Albrecht, K.A., Herzog, B.L., Follmer, L.R., Krapac, I.G., Griffin, R.A. & Cartwright, K. 1990. Excavation of an instrumented earthen liner: Inspection of dyed flow paths and morphology. *Hazardous Waste and Hazardous Materials*. 7(2):222.

Albright, W.H., Benson, C.H., Gee, G.W., Abichou, T., Tyler, S.W. & Rock, S.A. 2006. Field performance of three compacted clay landfill covers. *Vadose Zone Journal*. 5(4):1157–1171.

Albright, W.H., Benson, C.H., Gee, G.W., Abichou, T., McDonald, E. V., Tyler, S.W. & Rock, S.A. 2006. Field performance of a compacted clay landfill final cover at a humid site. *Journal of Geotechnical and Geoenvironmental Engineering*. 132(11):1393–1403.

Albright, W.H., Benson, C.H. & Waugh, W.J. 2010. *Water Balance Covers for Waste Containment: Principles and practice*. Reston, VA: American Society of Civil Engineers.

Alexander, D.L.J., Tropsha, A. & Winkler, D.A. 2015. Beware of R2 : Simple, unambiguous assessment of the prediction accuracy of QSAR and QSPR Models. *Journal of Chemical Information and Modeling*. 55(7):1316–1322.

Arshad, R.R., Sayyad, G., Mosaddeghi, M. & Gharabaghi, B. 2013. Predicting saturated hydraulic conductivity by artificial intelligence and regression models. *ISRN Soil Science*. 2013:1–8.

ASTM D3385-0903. 2003. Standard test method for infiltration rate of soils in field using double-ring infiltrometer. *ASTM International, West Conshohocken, PA,*. 04.08(Reapproved 2004):1–8.

Bagarello, V. 1997. Influence of well preparation on field-saturated hydraulic conductivity measured with the Guelph Permeameter. *Geoderma*. 80(1–2):169–180.

Benson, C.H., Sawangsuriya, A., Trzebiatowski, B. & Albright, W.H. 2007. Post-construction changes in the hydraulic properties of water balance cover soils. *Journal of Geotechnical and Geoenvironmental Engineering*. 133(4):349–359.

Bergamin, A.C., Vitorino, A.C.T., Souza, F.R., Venturoso, L.R., Bergamin, L.P.P. & Campos, M.C.C. 2015. Relationship of soil physical quality parameters and maize yield in a Brazilian Oxisol. *Chilean journal of agricultural research*. 75(3):357–365.

Biggar, J.W. & Nielsen, D.R. 1976. Spatial variability of the leaching characteristics of a field soil. *Water Resources Research*. 12(1):78–84.

Campbell, G.S. & Shiozawa, S. 1992. Prediction of hydraulic properties of soils using particle-size distribution and bulk density data. In M.T. van Genuchten et al. (eds.). Riverside, CA: University

of California. *Indirect Methods for Estimating the Hydraulic Properties of Unsaturated Soils*. 317–328.

Clapp, R.B. & Hornberger, G.M. 1978. Empirical equations for some soil hydraulic properties. *Water Resources Research*. 14(4):601–604.

Cosby, B.J., Hornberger, G.M., Clapp, R.B. & Ginn, T.R. 1984. A statistical exploration of the relationships of soil moisture characteristics to the physical properties of soils. *Water Resources Research*. 20(6):682–690.

Das Gupta, S., Mohanty, B.P. & Köhne, J.M. 2006. Soil hydraulic conductivities and their spatial and temporal variations in a vertisol. *Soil Science Society of America Journal*. 70(6):1872–1881.

Dane, J.H. & Puckett, W.E. 1992. Field soil hydraulic properties based on physical and mineralogical information. In M.T. van Genuchten et al. (eds.). Riverside, CA: University of California. *Indirect Methods for Estimating the Hydraulic Properties of Unsaturated Soils*. 463–466.

Deb, S.K. & Shukla, M.K. 2012. Variability of hydraulic conductivity due to multiple factors. *American Journal of Environmental Sciences*. 8(5):489–502.

De Souza, E., Fernandes Filho, I., Gonçalves, C.E., Schaefer, R., Batjes, N.H., Rodrigues, G., Santos, D. & Pontes, L.M. 2016. Pedotransfer functions to estimate bulk density from soil properties and. *Scientia Agricola*. 73(6):525–534.

Drumm, E.C., Boles, D.R. & Wilson, G. V. 1997. Desiccation cracks result in preferential flow. *Environmental Geotechnics*. 15(2):22–16.

Gamie, R. & De Smedt, F. 2018. Experimental and statistical study of saturated hydraulic conductivity and relations with other soil properties of a desert soil. *European Journal of Soil Science*. 69(2):256–264.

García-Gutiérrez, C., Pachepsky, Y. & Ángel Martín, M. 2018. Saturated hydraulic conductivity and textural heterogeneity of soils. *Hydrology and Earth System Sciences*. 22(7):3923–3932.

Gorakhki, M.H. & Bareither, C.A. 2017. Sustainable reuse of mine tailings and waste rock as water-balance covers. *Minerals*. 7(7):128.

Gülser, C. & Candemir, F. 2008. Prediction of saturated hydraulic conductivity using some moisture constants and soil physical properties. In Ohrid: Republic of Macedonia *BALWOIS 2008*.

INAP. 2017. *Global Cover System Deisng - Technical guidance document*. International Network for Acid Protection.

Jabro, J.D. 1992. Estimation of saturated hydraulic conductivity of soils from particle size distribution and bulk density data. *Transactions of the American Society of Agricultural Engineers*. 35(2):557–560.

Johnson, A.I. 1963. Suggested method for determining infiltration rate. In Peck, D.L. ed. Washington DC: Geological Survey Water-Supply Paper 1544-F *A Field Method for Measurement of Infiltration*. 10–14.

Kakaire, J., Makokha, G.L., Mwanjalolo, M., Mensah, A.K. & Menya, E. 2016. Effects of mulching on soil hydro-physical properties in Kibaale Sub-catchment, South Central Uganda. *Applied Ecology and Environmental Sciences*. 3(5):127–135.

Khire, M. V., Benson, C.H. & Bosscher, P.J. 2000. Capillary barriers: Design variables and water balance. *Journal of Geotechnical and Geoenvironmental Engineering*. 126(8):695–708.

Kim, H., Anderson, S.H., Motavalli, P.P. & Gantzer, C.J. 2010. Compaction effects on soil macropore geometry and related parameters for an arable field. *Geoderma*. 160(2):244–251.

Kooistra, M.J. & Tovey, N.K. 1995. Effects of compaction on soil microstructure. *International Journal of Rock Mechanics and Mining Sciences & Geomechanics Abstracts*. 32(5):A219.

Li, Y., Chen, D., White, R.E., Zhu, A. & Zhang, J. 2007. Estimating soil hydraulic properties of Fengqiu County soils in the North China Plain using pedo-transfer functions. *Geoderma*. 138(3–4):261–271.

Libohova, Z., Seybold, C., Wysocki, D., Wills, S., Schoeneberger, P., Williams, C., Lindbo, D., Stott, D., et al. 2018. Reevaluating the effects of soil organic matter and other properties on available water-holding capacity using the National Cooperative Soil Survey Characterization Database. *Journal of Soil and Water Conservation*. 73(4):411–421.

Mishra, P., Pandey, C., Singh, U., Gupta, A., Sahu, C. & Keshri, A. 2019. Descriptive statistics and normality tests for statistical data. *Annals of Cardiac Anaesthesia*. 22(1):67.

Mulla, D.J. & MacBratney, A.D. 2002. Soil spatial varaibility. In A.W. Warrick (ed.). Boca Raton, FL: CRC Press *Soil Physics Companion*. 343–373.

NCSS 12: Data Analysis & Graphics. 2019. [Online], Available: https://www.ncss.com/software/ncss/.

Nemes, A., Rawls, W.J. & Pachepsky, Y.A. 2005. Influence of organic matter on the estimation of saturated hydraulic conductivity. *Soil Science Society of America Journal*. 69(4):1330–1337.

Rawls, W.J. & Brakensiek, D.L. 1985. Prediction of soil water properties for hydrologic modeling. In E.E. Jones et al. (eds.). New Yo: ASCE Convention *Proceedings of Symposium on Watershed Management in the Eighties*. 293–299.

Rawls, W.J., Brakensiek, D.L. & Saxton, K.E. 1982. Estimation of soil water properties. *Transactions of the ASAE*. 25(5):1316–1320 & 1328.

Rawls, W.J., Gimenez, D. & Grossman, R. 1998. Use of soil texture, bulk density, and slope of the

water retention curve to predict saturated hydraulic conductivity. *American Society of Agricultural Engineers*. 41(4):983–988.

Ryczek, M., Kruk, E., Malec, M. & Klatka, S. 2017. Comparison of pedotransfer functions for the determination of saturated hydraulic conductivity coefficient. *Ochrona Srodowiska i Zasobow Naturalnych*. 28(1):25–30.

Salchow, E., Lal, R., Fausey, N.R. & Ward, A. 1996. Pedotransfer functions for variable alluvial soils in southern Ohio. *Geoderma*. 73(3–4):165–181.

Saxton, K.E., Rawls, W.J., Romberger, J.S. & Papendick, R.I. 1986. Estimating generalised soil-water characteristics from texture. *Soil Science Society of America Journal*. 50(4):1031–1036.

Shakoor, A. & Cook, B.D. 1990. The effect of stone content, size, and shape on the engineering properties of a compacted silty clay. *Environmental & Engineering Geoscience*. xxvii(2):245–253.

Shelley, T.L. & Daniel, D.E. 1993. Effect of gravel on hydraulic conductivity of compacted soil liners. *International Journal of Rock Mechanics and Mining Sciences & Geomechanics Abstracts*. 30(4):A223.

Soper, M.E. 1990. What you see may not be what you get: A brief, nontechnical introduction to overfitting in regression-type models. *The Reference Librarian*. 12(27–28):185–213.

Steel, R.G.D. & Torrie, J.H. 1980. *Principles and procedures of statistics: A biometrical approach.* Auckland: McGraw-Hill International.

Stockton, J.G. & Warrick, A.W. 1971. Spatial variability of unsaturated hydraulic conductivity. *Soil Science Society of America Journal*. 35(5):847–848.

Suriya, P. & Jayalakshmi, R. 2015. Factors influences the soil water characteristic curve and its parameters. *International Journal of Engineering Research and General Science*. 3(4):741–748. [Online], Available: www.ijergs.org.

Suter, G.W., Luxmoore, R.J. & Smith, E.D. 1993. Compacted soil barriers at abandoned landfill sites are likely to fail in the long term. *Journal of Environment Quality*. 22(2):217–226.

Venkatraman, K. & Ashwath, N. 2010. Field performance of a phytocap at Lakes Creek landfill, Rockhampton, Australia. *Management of Environmental Quality: An International Journal*. 21(2):237–252.

Vereecken, H., Maes, J. & Feyen, J. 1990. Estimating unsaturated hydraulic conductivity from easily measured soil properties. *Soil Science*. 149(1):1–12.

Vermaak, J.J.G., Wates, J.A., Bezuidenhout, N. & Kgwale, D. 2004. *The evaluation of soil covers used in the rehabilitation of coal mines*. Vol. 1002/1/04. Water Research Commission.

Warren, R.W., Hakonson, T.E. & Bostick, K. V. 1996. Choosing the most effective hazardous waste landfill cover. *Remediation*. 6(2):23–41.

Webb, T.H., Claydon, J.J. & Harris, S.R. 2000. Quantifying variability of soil physical properties within soil series to address modern land-use issues on the Canterbury Plains, New Zealand. *Soil Research*. 38(6):1115.

Wösten, J.H.M., Lilly, A., Nemes, A. & Le Bas, C. 1999. Development and use of a database of hydraulic properties of European soils. *Geoderma*. 90(3–4):169–185.

Zhang, Y. & Schaap, M.G. 2019. Estimation of saturated hydraulic conductivity with pedotransfer functions: A review. *Journal of Hydrology*. 575(May):1011–1030.

Chapter 4: Predicting soil water retention curves of old store-and-release covers from soil physical properties

4.1 Introduction

Research interest in soil moisture dynamics as well as management of water and environment increased continuously over the years. Soil water retention is one of the fundamental hydraulic properties in modern agriculture, hydrology, geotechnical engineering, geoscience and environmental sciences. It is also a crucial input parameter to predict the long-term soil cover performance. Despite the progress that have been made in direct measurement of soil water retention curves (SWRCs), it is still relative expensive and extremely time-consuming. However, direct measurement of SWRCs may be cost-effective for site-specific problems (Patil & Chaturvedi, 2012), whilst predictive models such as indirect measurement will provide a viable and cost-effective means of characterising SWRCs of larger areas of land. Moreover, direct measurement may be less accurate due to spatial and temporal variabilities of soil properties. The major merit of the pedotransfer function (PTF) is that it involves widely available and easily measured soil physical properties that can be used as input parameters. In addition, according to Minasny *et al.* (1999), multiple linear regression (MLR) was the most appropriate method to develop PTFs. These PTFs, in practice, often prove to be good predictors of SWRCs.

Despite the large data sets for the development of PTFs for soils around the globe, there are few data sets for soil covers especially in South Africa (Vermaak *et al.*, 2004). This lack of availability challenges the development of PTFs predicting SWRCs for soil covers. Moreover, due to climate dependence of PFT, published PTFs based on soils should not be applied (Hodnett & Tomasella, 2002) for soil covers in South Africa. Therefore, PTFs should be used as an interpolation technique rather than as an extrapolation tool for estimating SWRCs of soils (Phuong *et al.*, 2014).

The objectives in this Chapter were (1) to evaluate the WHC values of the soils of SRCs from the current study by using critical threshold values of natural soils; (2) to develop and validate point PTFs as MLR predicting volumetric water content at selected matric potentials; and (3) compare the point PTFs against the published point PTFs.

4.2 Materials and methods

4.2.1 Data collection

Filter papers were glued on the one side of undisturbed core samples of the soil cover material layers sampled at Mpumalanga Highveld. Soil water retention curves data at 2, 4, 6, 8, 10, 15, 20, 25, 30, 60, 100, 300, 1000 and 1500 kPa pressure were determined using a pressure plate apparatus as described by Dane & Hopmans (2002). The 1 bar pressure plates were used for the low-pressure chambers (1–100 kPa), 5 & 15 bar pressure plates for medium-pressure chambers (300–600 kPa) and 15 bar plates for high-pressure chambers (1000–1500 kPa). After the cores attained equilibrium, the cores were weighed and before subjecting the cores to the next pressure, the pressure plates

and cores were saturated with normal water in a water bath. The equilibration periods varied in the pressure pots from 2–3 days at low pressure (high matric potentials) to 14–16 days at high pressure (low matric potentials). Figure 4.1 shows the steps of determining the water retention curves. Finally, the cores were oven-dried at 105°C for 24 hours and were cooled down for 30 minutes in a desiccator containing silica gel to reach a constant dry mass. Following this, the gravimetric water content, *i.e.* P_w, was determined as the percentage in the soil sample as follows (Hillel, 1980):

$$P_w\,(\%) = \frac{(\text{wet sample mass} - \text{dry sample mass})}{\text{dry sample mass}} \times 100 \qquad \text{[Eq. 4.1]}$$

The gravimetric water content was corrected with the amount of water the filter paper held at each matric potential. Volumetric water content was determined as m water per m soil depth as follows (Hillel, 1980):

$$\theta_V\,(m^3.m^{-3}) = \frac{P_W}{100} \times \frac{\rho_b}{\rho_w} \qquad \text{[Eq. 4.2]}$$

where:

θ_V	=	volumetric water content ($m^3.m^{-3}$)
P_w	=	gravimetric water content (%)
ρ_b	=	soil bulk density ($g.m^{-3}$)
ρ_w	=	density of water ($g.m^{-3}$)

Figure 4.1: Filter papers were glued at one side of the cores to ensure good contact between the cores and pressure plates (A), thereafter, the cores and the pressure plates were saturated in a water bath (B). The saturated cores were transferred on the pressure plates (C) and were inserted in a pressure chamber which ran for two to 16 days until the equilibrium was reached (D).

A total of 47 SWRCs were done and the average for each soil layer of every profile pit was calculated where applicable and the soil physical properties were determined as it was described in Section 2.2.4 in Chapter 2. The average WHC values were also grouped according to soil textural classes to compare the WHC values of SRCs to the WHC values of soils from Rawls *et al.* (1986, 1998) and the U.S. Department of Agriculture Bulletin 462 (1960). The threshold criteria range for different soil textural classes are shown in Table 4.1. Since the initial WHC values at the time of SRCs construction were unknown, the WHC changes over time were not evaluated.

4.2.2 Data and regression analyses

The SRCs data-set was used for SWRC model development, whereas the SRCs data-set was split into moderately- and very dense SRC data sets for moderately- and very dense SWRC models development. The soil cover layer, 0–500 mm, of the profile pit P2-2 was placed into the very dense SRC data-set due to high bulk density, but overall P2-2 was classified as moderately dense SRC. The data analysis and Pearson correlation coefficient (r) analysis for the SRC data-set, and moderately- and very dense SRC data sets were similar to the description in Section 3.2.2 of Chapter 3. Pedotransfer functions as input for the SWRC model and, moderately- and very dense SWRC models were developed using MLR. The very coarse-, coarse-, medium-, fine- and very fine sand, coarse- and fine silt, and clay content, soil organic matter (SOM) and soil bulk density were used as input parameters in MLR. Gravel content was not one of the input parameters as explained in Section 1.3.2.2.1 of Chapter 1 and Section 3.2.2 of Chapter 3.

The equation of the SWRC model as well as the moderately- and very dense SWRC models had the form:

$$Y = a + b*\text{Very coarse sand} + c*\text{Coarse sand} + d*\text{Medium sand} + e*\text{Fine sand} + f*\text{Very fine sand} + g*\text{Coarse silt} + h*\text{Fine silt} + i*\text{Clay} + j*\text{SOM} + k*\rho_b \quad \text{[Eq. 4.3]}$$

where Y is predicted volumetric water content at a selected matric potential in $m^3.m^{-3}$, and b, c, d, e, f, g, h, i, j and k are the regression coefficients of very coarse-, coarse-, medium-, fine- and very fine sand content (%), coarse- and fine silt content (%), clay content (%), SOM (%) and soil bulk density (ρ_b in $g.cm^{-3}$), respectively.

Table 4.1: Water holding capacity (WHC) threshold criteria ranges for different soil texture classes (after Rawls *et al.,* 1986, 1998; U.S. Department of Agriculture Bulletin 462, 1960).

Soil texture	WHC $mm.m^{-1}$
Loamy fine sand	62.25–103.75
Sandy loam	100.00–145.25
Loam	124.50–190.90
Sandy clay loam	80.00–150.00
Clay loam	90.00–207.5
Clay	80.00–150.00

Variance inflation factors and eigenvalues of centered correlations for multicollinearity were checked. The backward stepwise method was used to simplify Eq. 4.3 for the respective models. The adjusted determination of coefficient (adjusted R^2) and predicted determination of coefficient (predicted R^2) between predicted and observed values of SWRC model and, moderately- and very dense SWRC models were determined. The adjusted R^2, root mean square error (RMSE), and predicted R^2 were used to assess how well the simplified equation represented the SRCs data-set, and moderately- and very dense SRCs data sets.

4.2.3 Model validation

The testing sets of SRCs, and moderately- and very dense SRCs in Tables C.5 & C.6 in Appendix C were used to validate the SWRC model and the moderate- and very dense SWRC models. The data-set of SRCs was divided into two separate data sets namely a training set (70%) and testing set (30%) using R software. The training set was to develop SWRC model, whereas the testing set was used to verify the accuracy and effectiveness of the model.

The same model validation procedures in Section 3.2.3 of Chapter 3 were used for moderately- and very dense SWRC models. The performance of the models was tested using the adjusted R^2, RMSE, and student's t-test. All analyses were performed using NCSS 12 Statistical Software (NCSS 12: Data Analysis & Graphics, 2019)

4.2.4 Pedotransfer functions compiled from literature

Only the three well published PTFs in Table 1.14 (Refer to Section 1.3.4.2 of Chapter 1) were used to compare the observed SWRCs data of SWRC data-set. Although the parametric PTFs of Brooks & Corey (1966) and Van Genuchten (1980) models are the most popular to use for predicting SWRCs, but several authors showed these parametric PTFs performed poorly. Børgesen & Schaap (2005) observed that the root mean square residuals (RMSR) values of parametric PTFs were generally 0.011 $m^3.m^{-3}$ higher than the point PTFs with the same variables. Ghanbarian-Alavijeh & Millán (2010) developed three-point PTFs using MLR and backward stepwise method and found that RMSE values showed that the three point PTFs estimated the soil water content better than the parametric PTFs. Tomasella *et al.* (2003) supports the finding that the point PTFs was superior to the parametric PTFs for Brazilian soils. Du (2020) compared 22 models describing SWRCs and found that Brooks & Corey (1966) and Van Genuchten (1980) models had significantly the highest RMSE. These two models assume that the soil suction is infinite as soil water content decreases to residual water content. The second reason may be due to an imperfect fit of these two models to retention data at -1500 kPa. Madi *et al.* (2018) supports the finding that Brooks & Corey (1966) and Van Genuchten (1980) models describe the volumetric water content at high matric potentials rather than at low matric potentials of SWRCs. Although, in contrast, Merdun (2006) and Shwetha & Varija (2013) found no significant difference between the point and parametric PTFs performance, but the point PTFs were superior. Schaap & Bouten (1996) also found no significant difference between the two methods, however their data sets contained mostly coarse soils. On the other hand, no model

can perfectly describe the SWRCs of all soil types. Each PTF has its advantages for one or several soil types. Parametric PTFs may be less time-consuming, but point PTFs based on linear and also non-linear regressions can be used in most conditions (Das *et al.*, 2011). Therefore, only point PTFs were developed in the current study and the well published point PTFs were used for comparison.

Model performance was evaluated using the adjusted R^2, RMSE and one-tail student's t-test between the predicted and observed water content at selected matric potential values. The predicted volumetric water content was plotted against the measured volumetric water content to determine how well the data points were scattered.

4.3 Results and discussion

4.3.1 Data collection

The estimated field capacity (FC), permanent wilting point (PWP) and water holding capacity (WHC) are presented in Table 4.2. The measured SWRCs of SRCs are shown in Figures 4.2–4.5. Field capacity is commonly evaluated at -5, -6, -10 and -33 kPa matric potential, however Nemes *et al.* (2011) estimated a wide range of FC between -2.5 to -50 kPa. Filho *et al.* (2014) estimated FC at -6 kPa for sandy, loamy and clayey soils and Kern (2000) stated that the FC of sandy soils occurs between -5 kPa and -10 kPa. Therefore, in the current study, the FC was estimated at where the amount of water held in soil after excess water has drained away. The matric potential for permanent wilting point (PWP) is at -1 500 kPa according to Rawls *et al.* (1982). The average WHC of moderately- and very dense SRCs ranged between 81.00–180.83 $mm.m^{-1}$ and 60.90–121.85 $mm.m^{-1}$, respectively. If the average WHC of moderately dense SRCs were grouped into the soil textural classes, the following values obtained were: (1) loamy sand: 81.00 $mm.m^{-1}$, (2) sandy loam: 101.60–128.55 $mm.m^{-1}$, (3) loam: 92.81 $mm.m^{-1}$, (4) sandy clay loam: 115.59–180.83 $mm.m^{-1}$ and (5) clay loam: 147.75 $mm.m^{-1}$. For very dense SRCs, the WHC per textural class were: (1) sandy loam: 60.90–113.10 $mm.m^{-1}$, (2) sandy clay loam: 110.39–112.10 $mm.m^{-1}$ and (3) clay: 115.35–121.85 $mm.m^{-1}$.

There was a significant difference (P = 0.001) in WHC between the moderately- and very dense SRCs. The WHCs of the growth medium were significantly lower (P = 0.028) compared to the water retention layer (sandy clay loam, clay loam and clay) of moderately dense SRCs (Table 4.2), but this difference was not significant in the very dense SRCs (P = 0.066). The clayey soils of the dual-layered SRCs had higher WHC compared to the sandy soils for both soil cover conditions (P = 0.021).

The higher WHC of clayey soils of moderately dense SRCs can be ascribed to water molecules that like to hold tightly to the finer particle such as silt and clay (Table 2.16 in Chapter 2). Higher air entry values for the more clayey materials were found compared to the sandy materials (Figures 4.2–4.5). This can be ascribed to higher microporosity in silty and clayey soils compared to sandy soil, causing in clayey soils taking longer before it drains than sandy soils (Hillel, 2004). A more gradual slope in the desaturation function for more clayey soils were observed compared to sandy

soils (Figures 4.2–4.5). Due to higher macropores in sandy soils, clayey soils desaturate slower than sandy soils (Hillel, 2004). The high saturated volumetric water contents and air entry values, and gradual slope in the desaturation functions of the clayey soils can be attributed to their high water retention and WHC. This indicates that these layers are suitable as water retention layers. The high water retention also relates to high capillary potential (Hillel, 2004) that is required for water retention layers to minimise oxygen- and water ingress. The steep slope of the desaturation functions of the sandy soils indicates that soil water can easily be removed by plant roots as the soil dries, which is preferred for a growth medium. However, it is important that the growth medium has an acceptable plant available water capacity.

After the average WHC values of moderately- and very dense SRCs (Table 4.2) were grouped according to soil textural classes, the following inferences were made: (1) all the WHC values of all soil textural classes of moderately dense SRCs were in the threshold criteria range, excluding 550–900 mm soil cover layer of D1-1 and 500–700 mm soil cover layer of P2-2; (2) all the WHC values of sandy loam soil cover layers of very dense SRCs were below the threshold criteria range, excluding 0–400 mm and 0–500 mm soil cover layer of P1-2 and P2-2, respectively; and (3) the WHC values of sandy clay loam and clay of very dense SRCs were, however, in the threshold criteria range. The water retention layer's WHC of D1-1 was higher than the threshold criteria range. Higher WHC of sandy clay loam can be expected and the silt- and clay content was 22.05% and 25.94% (Table 2.16 in Chapter 2), respectively, with a low bulk density of 1.460 g.cm^{-3} (Table 2.17 in Chapter 2). The water retention layer of P2-2 had a lower WHC than the threshold criteria range for loam soil, but no clear reason can be given for this anomaly. If the average saturated hydraulic conductivity (K_{sat}) value (Table 3.2 in Chapter 3) of loam soil cover layer were higher than the threshold criteria range (Table 3.1 in Chapter 3), then the gravel content of 17.83 % (Table 2.16 in Chapter 3) could be the reason for higher K_{sat} value with lower WHC value. Unfortunately, the observations of K_{sat} and WHC of loam soil cover layer were in contrast and left an unexplainable result. However, P2-2 was also constructed with a saprolite cover layer (Table 2.13 in Chapter 2) which can has 35% of water storage capacity (Flinchum *et al.*, 2018) and can catch the infiltrated soil water that percolates through the loam soil cover layer during a heavy rain season. The good long-term performance of P2-2 was thereby not influenced by the low WHC of the loam water retention layer.

High bulk density had a marked effect on the sandier cover layers of very dense SRCs (Figures 4.2–4.4). The effect of bulk density on the clayey cover layers was less significant. The effect of high bulk density on SWRC of sandy loam cover layers was: (1) decreased volumetric water content at near saturation; (2) increased in the air entry values that relates to higher water retention; (3) more gradual (flattening) slope of the desaturation functions, which relates to higher water retention and capillary potential; and (4) increased volumetric water content below certain matric potential, although the effect was not significant (P = 0.155). This effect of high bulk density on SWRC is excluded for P1-1 and P2-1. The very high bulk densities of P1-1 (2.197 g.cm^{-3}) and P2-1 (2.286 g.cm^{-3}) caused a decrease in volumetric water content at high matric potential, lower volumetric water content at low

matric potential and *significant* lower WHC. Overall, high bulk density caused decreased FC and increased PWP. The high bulk density in the growth medium also decreased the plant available water capacity, and consequently a reduced sufficiency for plant use. Smith *et al.* (2001) observed similar trend of the effect of high bulk density on SWRCs of several soil textural classes.

Table 4.2: Estimated average field capacity, permanent wilting point and water holding capacity of store-and-release covers.

Soil cover condition	Profile pit	Soil cover layer (mm)	Soil texture	Field capacity ($mm.m^{-1}$)	Permanent wilting point ($mm.m^{-1}$)	Water holding capacity ($mm.m^{-1}$)
Moderately dense	D1-1	0–500	SCL	274.00	131.35	142.65
		550–900	SCL	376.53	215.70	160.83
	D1-2	0–400	SL	249.65	140.70	108.95
		400–600	SCL	373.20	247.30	126.70
	D1-3	Surface	SCL	315.00	194.40	120.60
		0–200	SCL	200.95	78.95	122.00
		200–550	CL	366.00	218.25	147.75
	P1-3	Surface	SL	177.60	51.50	126.10
	P1-4	Surface	SL	233.65	105.10	128.55
		0–350	SL	195.10	76.09	118.91
	P2-2	Surface	SL	165.22	43.74	121.48
		500–700	L	363.71	270.90	92.81
	P2-3	0–500	SCL	430.51	314.92	115.59
	D3-1	0–300	LFS	104.00	23.00	81.00
		>300	SCL	290.00	145.00	145.00
	D3-2	Surface	SL	197.50	88.35	109.15
		0–400	SL	196.00	94.40	101.60
		>400	SCL	315.00	181.40	133.60
Very dense	D2-1	0–450	SL	128.80	33.20	95.60
		450–650	SCL	236.00	124.60	111.40
		650–850	SCL	302.70	190.60	112.10
		850–1100	C	377.40	262.05	115.35
	D2-2	0–300	SL	160.25	88.15	72.10
		300–700	C	253.25	131.40	121.85
	P1-1	Surface	SL	193.50	109.30	84.20
		200–700	SL	125.30	67.40	60.90
	P1-2	Surface	SL	194.40	97.40	97.00
		0–400	SL	154.30	41.20	113.10
	P2-1	0–100	SCL	179.58	69.19	110.39
		100–300	SL	107.00	45.30	61.70
	P2-2	0–500	SL	211.38	106.78	105.60

Note: LFS = loamy fine sand, SL = sandy loam, Loam = loam, SCL = sandy clay loam, CL = clay loam, and C = clay.

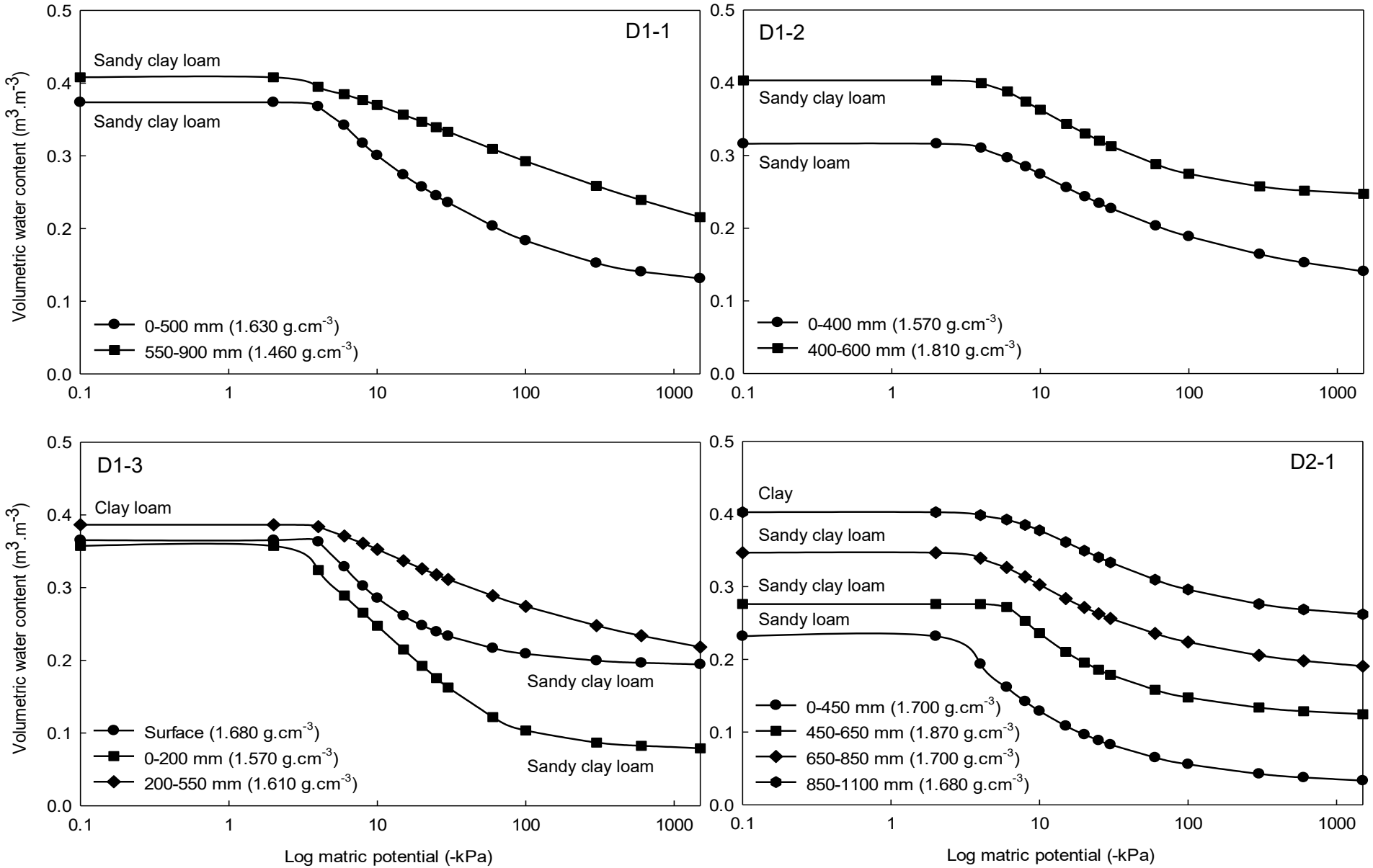

Figure 4.2: Measured soil water retention curves of D1-1, D1-2, D1-3, and D2-1.

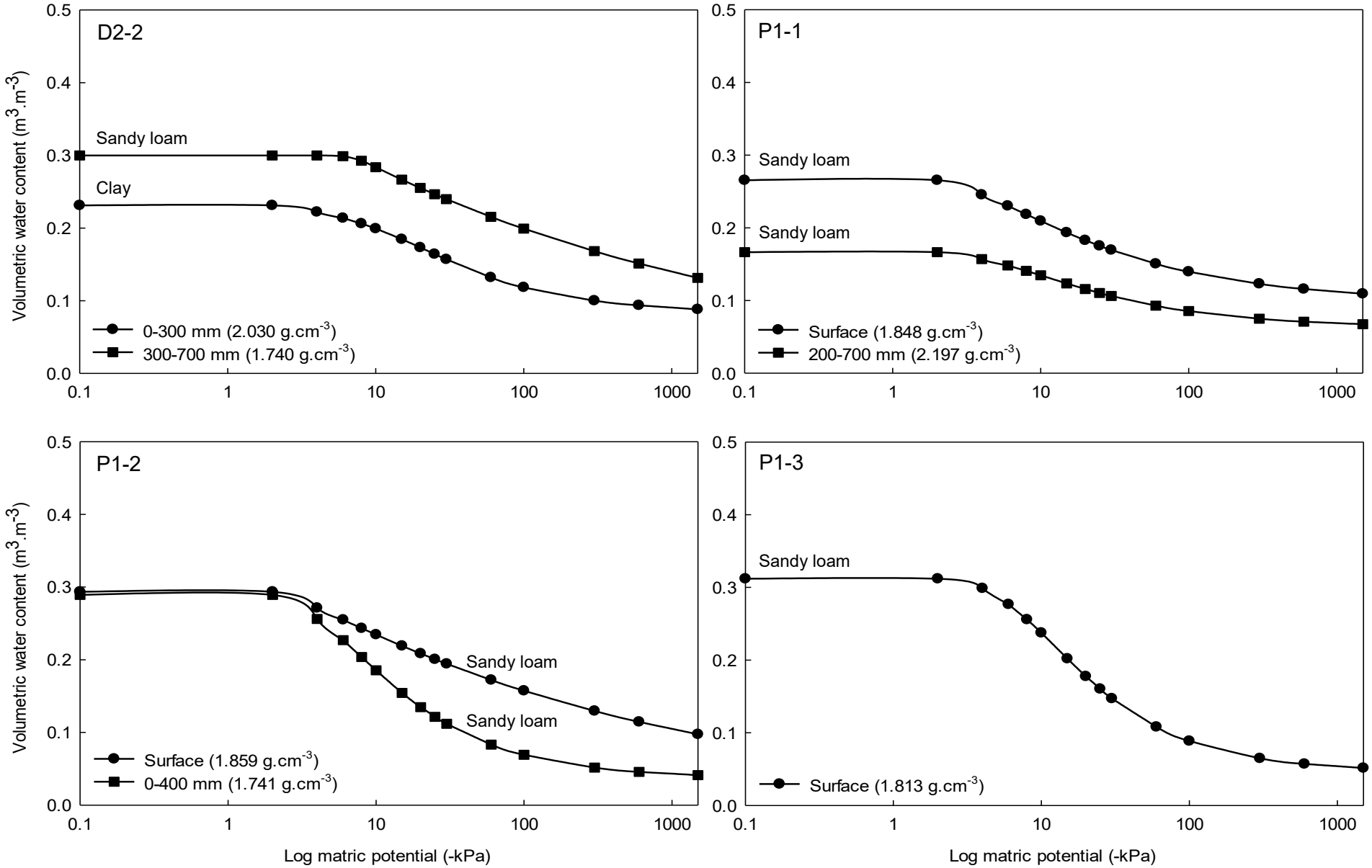

Figure 4.3: Measured soil water retention curves of D2-2, P1-1. P1-2 and P1-3.

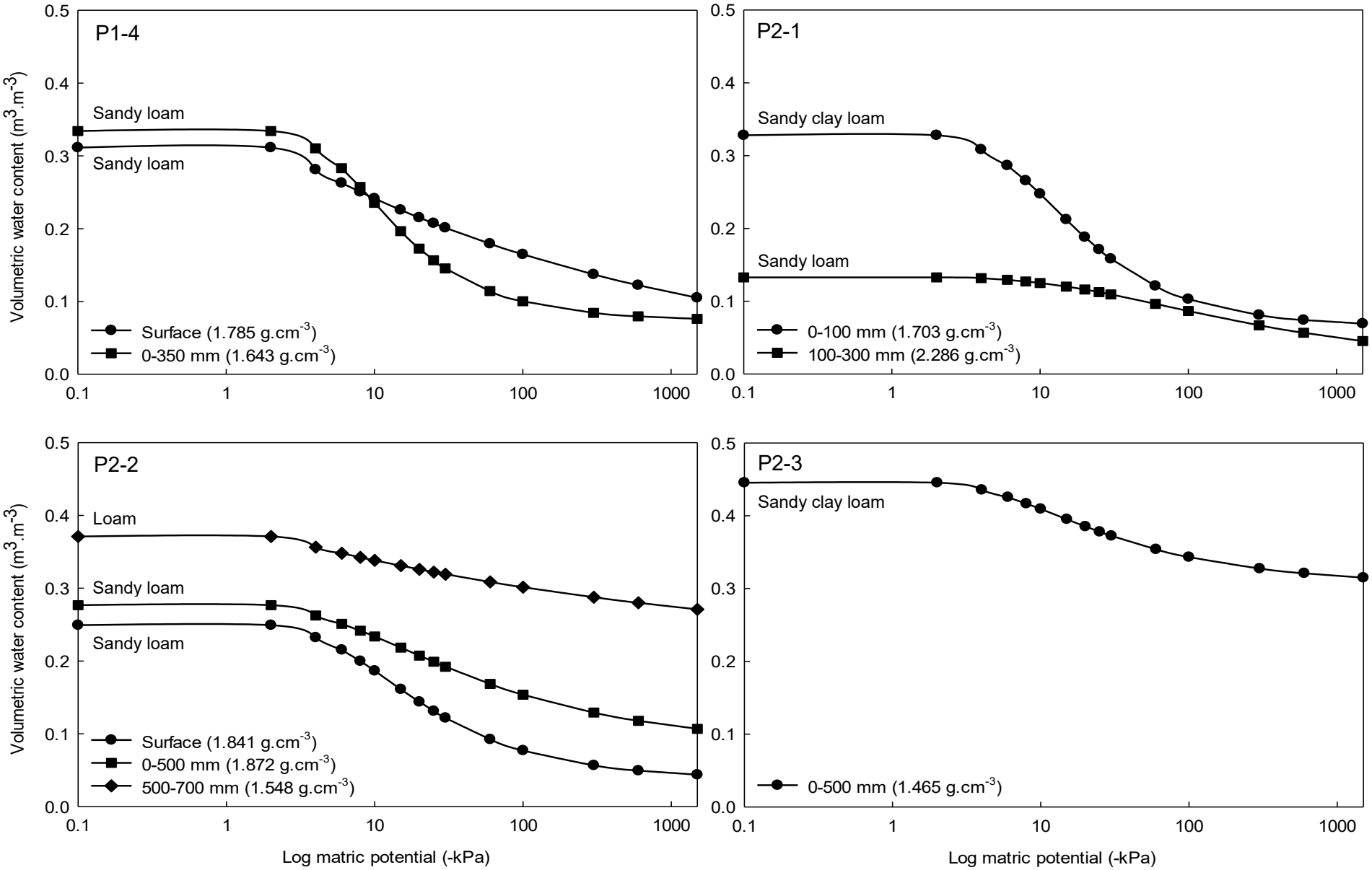

Figure 4.4: Measured soil water retention curves of P1-4, P2-1, P2-2 and P2-3.

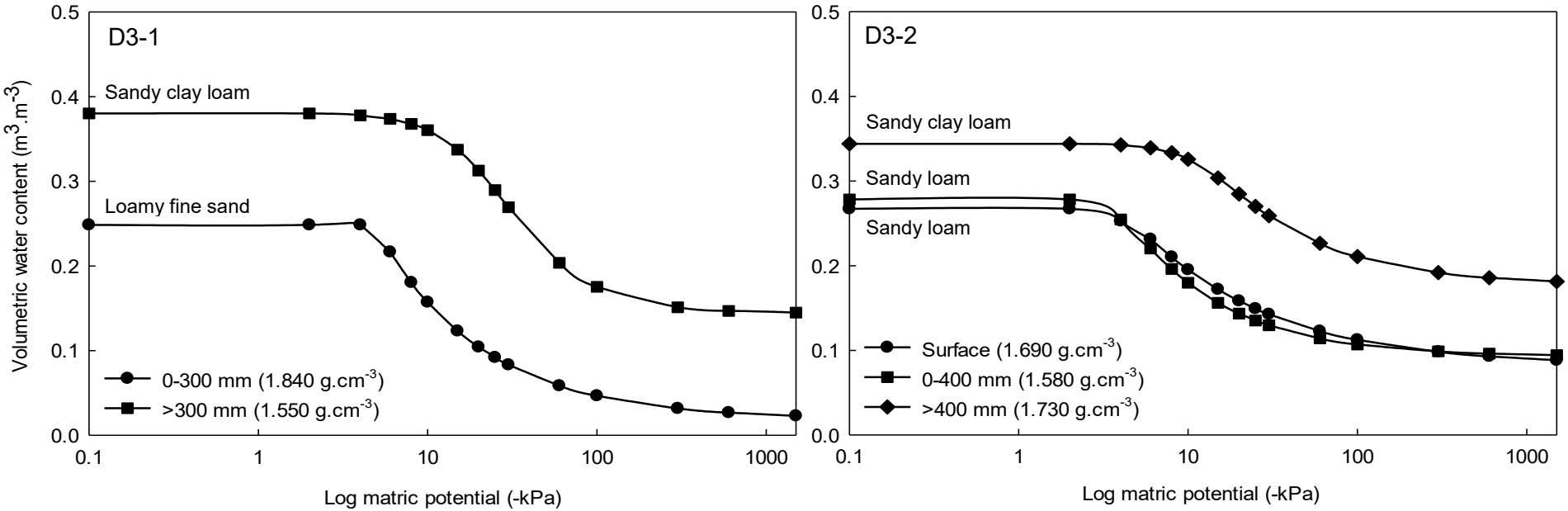

Figure 4.5: Measured soil water retention curves of D3-1 & 3-2.

4.3.2 Data analysis

4.3.2.1 *Store-and-release covers data-set*

Basic summary statistics of average soil physical properties determined from the core rings and volumetric water content at selected matric potentials for the SRCs data-set are presented in Table 4.3 & 4.4, respectively. In Table 4.3, the coefficient of variation (CV) for average soil physical properties ranged from low to high. The smallest CV values (< 10%) was found for bulk density, whereas the variability of very coarse-, coarse-, medium-, fine- and very fine sand content, coarse- and fine silt content, clay content and SOM were moderate to high. However, the variability of very fine sand content was higher compared to very coarse-, coarse-, medium- and fine sand contents. The variability of all three gravel fractions were the highest since most of the soil covers did not contain gravel. The CV of volumetric water content at selected matric potentials (Table 4.4) ranged from 19.19 to 49.78%, *i.e.* from low to high variability. It is noteworthy that the CV of volumetric water content increased proportionally as matric potential decreased. More or less similar performance was found in the study by Pan *et al.* (2019), where the CV of volumetric water content at selected matric potentials ranged between 5.50–34.56% with the use of the pressure plate apparatus method. In addition, the CV of volumetric water content increased from high to low matric potentials (-kPa) in the aforementioned study. Ceddia *et al.* (2009) observed a moderate CV of 36.4% at -10 kPa and high CV of 56.13% at -1500 kPa matric potential. This phenomena can be explained by the fact that water retention at low matric potential is caused by absorption (McQueen & Miller., 1974) rather than by capillarity, which can be more erratic due to its control by soil porosity (Lu, 2016). The results of the current study were higher compared to the study of Deka *et al.* (1995) who used the filter paper technique and obtained a CV of volumetric water content of 2–11%. Zhang *et al.* (2011) also found low CV values of volumetric water content of 8.25–14.39%.

Very coarse-, coarse-, medium- and fine sand-, coarse silt- and clay content, SOM and bulk density were normally distributed (Table 4.3). All three gravel content fractions, very fine sand- and fine silt content were log-normal distributed and had high positive skewness. The surface of P1-1 and 0–400 cm soil layer of P1-1 had total gravel content of 14.32% and 14.11%, respectively (Table 2.14 in Chapter 2). These values were higher compared to the rest of the core samples which ranged between 0.00–9.94% (Table 2.16 in Chapter 2). In Table 4.4, all the volumetric water contents at selected matric potential were normally distributed. All the independent variables to develop the SWRC model were transformed into square roots to had wider distributions. The dependent variable, volumetric water content, was not transformed into square roots for the SWRC model.

4.3.2.2 *Moderately- and very dense store-and-release covers data sets*

Basic summary statistics of average soil physical properties determined from the core samples and volumetric water content at selected matric potentials for moderately- and very dense SRCs data sets are presented in Tables 4.3 & 4.4, respectively. Only the CV of the bulk density of moderately dense SRCs data-set was smaller than 10%. All the other soil physical properties' CV of moderately

dense SRCs data-set ranged from moderate to high, whereas medium- and fine gravel content had the highest variability. The CV of all three gravel fractions, very fine sand and fine silt content, and SOM of very dense SRCs data-set were higher than 100%. The CV of rest of the soil physical properties of very dense SRCs data-set ranged from 11.86 to 59.99%. The CV of volumetric water content of moderately-and very dense SRCs data sets in Table 4.3 followed similar patterns as explained in Section 4.3.2.1.

As expected, the three gravel fractions of moderately- and very dense SRCs data sets had log-normal distribution (Table 4.4). Similar to SRCs data-set, the very fine sand content of moderately- and very dense SRCs data sets had log-normal distribution, however the fine silt content of moderately SRCs data-set had normal distribution. All the volumetric water contents of moderately- and very dense SRCs data sets were normally distributed. No outliers were removed, but all the soil physical properties for moderately- and very dense SWRC models were transformed into square roots.

4.3.3 Relations between volumetric water content at selected matric potentials and soil physical properties

4.3.3.1 *Store-and-release covers data-set*

Pearson correlation coefficients between soil physical properties and volumetric water content at selected matric potentials are presented in Table 4.5. The indicators for strong correlations are $|r| \geq 0.70$ and moderate correlations are $0.40 \geq |r| \geq 0.70$ (Gamie *et al.*, 2018).

As expected, negative correlations were found between volumetric water contents at selected matric potentials and all five sand fractions and bulk density in Table 4.5. Very coarse- and fine sand content had a moderate relationship with volumetric water content from -2 to -1500 kPa. From -8 to -1500 kPa, the medium sand content also had a moderate relationship with volumetric water content. The correlations between coarse- and very fine sand content with volumetric water content were poor. The results in Table 4.5 showed that the coarse- and fine silt content had non-significant, poor and positive correlations with volumetric water content, whereas the correlations with clay content were significant and strong from -4 to -1500 kPa. Botula *et al.* (2012) reported moderate/poor and positive correlations between silt content and volumetric water content. In addition, in the study of Dlapa *et al.* (2020), non-significant, poor and positive correlations between silt content and volumetric water content were found. Results similar to the current study were found by Van Den Berg *et al.* (1997), Ceddia *et al.* (2009) and Khlosi (2015), namely that the clay content had significant correlations with volumetric water content over the whole range of matric potentials. The strong negative correlation between clay content and volumetric water content is mainly caused by adsorption effects. These results of this current study confirmed why most PTFs use soil texture as the main parameter. Soil texture is the permanent, natural attribute of the soil and is often used to characterise its physical properties (Hillel, 2004). Arya & Paris (1981) converted the particle-size distribution data into a SWRC based on the notable similarity between the nonlinear shapes of

particle-size distribution and SWRC data. However, the Arya & Paris (1981) model only considered the capillary effect of the SWRC leaving the absorption of water on soil particles.

Soil organic matter was not a major factor regarding variations in SWRC at selected matric potentials (Table 4.5). At -2 kPa, the correlation between bulk density and volumetric water content was strong, but only moderate from -4 to -10 kPa and weak from -15 to -1500 kPa (Table 4.5). The strong, negative correlation between bulk density and volumetric water content at near saturation is due to higher soil porosity at lower bulk density and therefore, potentially, increase the conductive path of water of porosity. Moreover, soils with low bulk density are generally better structured which further increase the conductive path for water at high matric potentials (Reeve *et al.*, 1973). At low matric potential, the correlations between bulk density and volumetric water content became poor because the surface area becomes the main determinant for water retention rather than the available soil pore spaces.

4.3.3.2 *Moderately- and very dense store-and-release covers data sets*

Pearson correlation coefficients between soil physical properties and volumetric water content at selected matric potentials of moderately- and very dense SRC data-set are presented in Table 4.5. Pertaining to the moderately dense SRCs (Table 4.5), very coarse sand content had moderate and negative correlations with volumetric water content significant from -4 to -1500 kPa. Medium-, fine- and very fine sand content had moderate and negative correlations with volumetric water content from -2 to -1500 kPa. Coarse sand content had poor and positive correlations with volumetric water content, while coarse- and fine silt content, and clay content had moderate and positive relationships. Similar to the SRC data-set, the SOM did not have any major influence on variations in SWRC at selected matric potentials. Only bulk density had a significant strong and negative correlations with volumetric water content from -2 to -1500 kPa. After the SRC data-set was split into moderate- and very dense SRC data sets, the bulk density dominated the moderate dense SRCs.

In contrast to the moderately dense SRCs data-set, the coarse sand content of very dense SRC data-set (Table 4.5), had a significantly strong and negative correlation with volumetric water content from -2 to -15 kPa. Moderate and negative correlations were found between very coarse sand content and volumetric water content from -2 to -1500 kPa, while medium sand content had a moderate and negative correlation with volumetric water content from -2 to -4 kPa. Fine- and very fine sand content had little to no relationship with the volumetric water content at selected matric potentials. Coarse silt content had moderate and positive correlation with volumetric water content at -2 kPa, however, from -4 to -1500 kPa, the correlations were poor. The correlations between clay content and volumetric water content increased with decreasing matric potentials. As matric potential decreases, the quantity of water attached to the negatively charged clay particles increase relative to that retained in the soil pores by capillary forces. Minasny *et al.* (1999) found that volumetric water content from -10 to -1500 kPa had an exponentially increasing trend with increasing clay content.

Table 4.3: Descriptive statistics of average soil physical properties of store-and-release covers, moderately store-and-release covers and very dense store-and-release covers for the water retention curve modelling.

Data-set	Descriptive statistic	Variables												
		Medium gravel	**Fine gravel**	**Very fine gravel**	**Very coarse sand**	**Coarse sand**	**Medium sand**	**Fine sand**	**Very fine sand**	**Coarse silt**	**Fine silt**	**Clay**	**SOM**	**ρ_b**
Store-and-release covers	Minimum	0.00	0.00	0.11	3.61	4.37	6.59	21.37	1.40	6.41	0.95	3.59	0.03	1.565
	Maximum	8.17	2.64	14.11	12.63	15.76	35.59	32.38	14.48	29.62	11.95	43.34	0.92	2.197
	Mean	0.76	0.41	3.96	7.31	8.86	16.33	21.37	4.25	14.60	4.10	18.03	0.38	1.771
	CV	254.48	157.34	113.43	37.45	26.40	44.64	26.81	89.98	41.16	63.62	63.28	72.79	8.43
	Skewness	2.984	2.107	1.542	0.479	0.945	0.865	0.979	1.471	0.546	1.447	0.672	0.586	0.563
	SW-test[a]	*0.471*	*0.692*	*0.732*	0.929	0.929	0.936	0.901	*0.731*	0.947	*0.867*	0.925	0.922	0.911
Moderately dense store-and-release covers	Minimum	0.00	0.00	0.11	1.94	6.89	3.45	10.80	0.99	7.42	1.19	7.72	0.01	1.464
	Maximum	9.94	1.21	7.54	12.59	11.28	28.07	28.66	10.09	21.20	11.51	36.93	0.90	1.837
	Mean	0.80	0.37	2.32	6.86	9.34	15.83	20.65	3.41	14.12	4.87	21.37	0.34	1.628
	CV	339.80	120.52	83.81	41.99	14.03	40.79	25.73	74.17	28.78	53.27	38.27	64.08	7.52
	Skewness	3.157	1.839	1.455	0.531	-0.488	0.012	-0.512	1.602	0.334	0.889	-0.117	0.499	0.031
	SW-test	*0.335*	*0.803*	*0.863*	0.949	0.951	0.990	0.935	*0.789*	0.958	0.919	0.979	0.930	0.957
Very dense store-and-release covers	Minimum	0.00	0.00	0.22	3.38	6.45	6.58	15.82	1.65	6.41	0.95	3.59	0.03	1.685
	Maximum	3.34	2.64	14.11	8.88	15.76	20.17	30.20	14.48	29.62	11.95	25.02	0.87	2.286
	Mean	0.41	0.55	5.38	6.61	10.79	15.00	24.43	4.97	15.73	3.35	12.71	0.24	1.864
	CV	282.84	167.84	105.80	31.84	32.59	28.19	19.33	102.57	52.89	109.62	59.99	154.06	11.86
	Skewness	2.267	1.518	1.788	-0.300	0.395	-0.397	-0.725	1.156	0.358	1.840	0.291	1.451	0.547
	SW test	*0.418*	*0.690*	*0.805*	0.910	0.913	0.864	0.925	*0.704*	0.927	*0.689*	0.945	*0.772*	0.845

Note: CV = coefficient of variation, SOM = soil organic matter, ρ_b = soil bulk density.
[a]A probability value smaller than 0.05 of SW normality test indicating the observation is non-normally distributed, is in italic.

Table 4.4: Descriptive statistics of average measured volumetric water content at selected matric potentials of store-and-release covers, moderately- and very dense store-and-release covers for the water retention curve modelling.

Data-set	Descriptive statistic	Volumetric water content ($m^3.m^{-3}$) at selected matric potential (-kPa)													
		2	4	6	8	10	15	20	25	30	60	100	300	600	1500
Store-and-release covers	Minimum	0.166	0.156	0.148	0.140	0.128	0.108	0.096	0.088	0.082	0.058	0.046	0.031	0.026	0.023
	Maximum	0.402	0.398	0.392	0.384	0.377	0.361	0.349	0.340	0.333	0.156	0.296	0.276	0.268	0.262
	Mean	0.302	0.287	0.268	0.252	0.239	0.216	0.201	0.190	0.182	0.156	0.142	0.122	0.114	0.106
	CV	19.19	21.38	23.24	19.46	20.63	23.54	27.19	29.94	32.27	39.29	42.87	46.70	47.62	49.78
	Skewness	-0.278	-0.068	0.058	0.185	0.275	0.399	0.462	0.500	0.526	0.594	0.631	0.729	0.805	0.916
	SW test[a]	0.983	0.984	0.981	0.980	0.975	0.970	0.968	0.963	0.958	0.958	0.945	0.944	0.938	0.925
Moderately dense store-and-release covers	Minimum	0.249	0.232	0.215	0.199	0.18	0.161	0.143	0.131	0.121	0.092	0.076	0.056	0.049	0.043
	Maximum	0.445	0.435	0.425	0.416	0.409	0.395	0.385	0.377	0.372	0.353	0.343	0.335	0.332	0.330
	Mean	0.356	0.343	0.325	0.309	0.297	0.275	0.260	0.250	0.242	0.217	0.203	0.184	0.176	0.169
	CV	12.92	13.42	16.94	19.59	22.27	25.83	29.19	32.41	34.05	39.66	42.26	46.99	49.09	50.45
	Skewness	0.339	0.185	0.297	0.274	0.315	0.180	0.072	0.026	0.067	-0.098	-0.127	-0.007	0.139	0.141
	SW-test[a]	0.947	0.968	0.929	0.909	0.901	0.917	0.913	0.937	0.904	0.914	0.930	0.941	0.950	0.950
Very dense store-and-release covers	Minimum	0.133	0.131	0.129	0.127	0.125	0.108	0.096	0.088	0.082	0.064	0.055	0.042	0.037	0.033
	Maximum	0.346	0.339	0.326	0.313	0.302	0.283	0.271	0.262	0.256	0.235	0.223	0.205	0.197	0.190
	Mean	0.245	0.230	0.216	0.203	0.193	0.175	0.164	0.155	0.149	0.129	0.118	0.100	0.093	0.085
	CV	28.63	37.20	37.95	39.30	40.38	41.27	42.60	43.52	44.82	50.03	56.69	62.05	63.30	68.34
	Skewness	-0.315	0.008	0.196	0.196	0.430	0.475	0.524	0.520	0.402	0.525	0.737	0.605	0.577	0.628
	SW test[a]	0.970	0.956	0.933	0.920	0.915	0.915	0.900	0.925	0.919	0.926	0.919	0.919	0.917	0.929

Note: CV = coefficient of variation, SW test = Shapiro Wilk normality test.
[a]All the *P* values of the SW test were above 0.05 and indicated normal distribution.

Table 4.5: Relation between volumetric water content at selected matric potential and soil physical properties of store-and-release data-set, moderately- and very dense store-and-release covers data sets for SWRC model, and moderately- and very dense SWRC models development.

	Very coarse sand	Coarse sand	Medium sand	Fine sand	Very fine sand	Coarse silt	Fine silt	Clay	SOM	ρ_b
SRCs data-set										
-2 kPa	*-0.423*[a]	-0.303	-0.326	*-0.516*	-0.154	0.118	0.116	*0.630*	0.030	*-0.725*
-4 kPa	*-0.444*	-0.362	-0.314	*-0.535*	-0.230	0.076	0.173	*0.708*	0.006	*-0.665*
-6 kPa	*-0.482*	-0.381	-0.363	*-0.581*	-0.252	0.064	0.233	*0.767*	0.002	*-0.566*
-8 kPa	*-0.520*	-0.358	-0.417	*-0.608*	-0.258	0.074	0.276	*0.793*	0.009	*-0.481*
-10 kPa	*-0.540*	-0.339	*-0.443*	*-0.616*	-0.265	0.080	0.304	*0.801*	0.022	*-0.427*
-15 kPa	*-0.566*	-0.309	*-0.473*	*-0.618*	-0.280	0.087	0.344	*0.807*	0.046	-0.350
-20 kPa	*-0.576*	-0.293	*-0.484*	*-0.616*	-0.288	0.091	0.362	*0.805*	0.062	-0.310
-25 kPa	*-0.581*	-0.282	*-0.489*	*-0.613*	-0.293	0.095	0.372	*0.801*	0.074	-0.285
-30 kPa	*-0.583*	-0.275	*-0.492*	*-0.611*	-0.295	0.098	0.378	*0.797*	0.082	-0.268
-60 kPa	*-0.588*	-0.255	*-0.495*	*-0.603*	-0.302	0.108	0.388	*0.780*	0.106	-0.226
-100 kPa	*-0.593*	-0.245	*-0.496*	*-0.598*	-0.308	0.111	0.392	*0.773*	0.114	-0.214
-300 kPa	*-0.609*	-0.225	*-0.494*	*-0.582*	-0.327	0.109	0.400	*0.770*	0.113	-0.218
-600 kPa	*-0.620*	-0.214	*-0.492*	*-0.569*	-0.340	0.103	0.404	*0.771*	0.103	-0.227
-1500 kPa	*-0.630*	-0.200	*-0.486*	*-0.547*	-0.355	0.094	0.406	*0.770*	0.088	-0.240
Moderately dense SRCs data-set										
-2 kPa	-0.520	0.257	-0.381	-0.216	-0.405	0.341	0.178	0.414	-0.060	*-0.948*
-4 kPa	*-0.555*	0.219	-0.439	-0.244	-0.424	0.405	0.180	0.477	-0.117	*-0.893*
-6 kPa	*-0.551*	0.201	-0.470	-0.297	-0.426	0.410	0.236	0.494	-0.137	*-0.854*
-8 kPa	*-0.551*	0.198	-0.493	-0.342	-0.439	0.413	0.289	0.508	-0.145	*-0.823*
-10 kPa	*-0.556*	0.198	-0.508	-0.367	-0.455	0.415	0.328	0.519	-0.148	*-0.798*
-15 kPa	*-0.571*	0.203	-0.530	-0.397	-0.490	0.418	0.389	0.535	-0.146	*-0.735*
-20 kPa	*-0.582*	0.206	-0.542	-0.411	-0.510	0.421	0.422	0.542	-0.141	*-0.720*
-25 kPa	*-0.594*	0.208	-0.549	-0.421	-0.521	0.423	0.442	0.546	-0.136	*-0.709*
-30 kPa	*-0.607*	0.210	-0.554	-0.428	-0.527	0.425	0.456	0.548	-0.132	*-0.681*
-60 kPa	*-0.613*	0.220	-0.567	-0.445	-0.537	0.430	0.493	0.548	-0.119	*-0.675*
-100 kPa	*-0.623*	0.233	-0.571	-0.450	-0.540	0.431	0.509	0.545	-0.115	*-0.685*
-300 kPa	*-0.626*	0.273	-0.574	-0.440	-0.542	0.426	0.520	0.536	-0.121	*-0.694*
-600 kPa	*-0.627*	0.296	-0.572	-0.426	-0.541	0.421	0.517	0.529	-0.130	*-0.705*
-1500 kPa	*-0.633*	0.323	-0.569	-0.405	-0.536	0.416	0.508	0.519	-0.144	*-0.701*
Very dense SRCs data-set										
-2 kPa	-0.582	*-0.775*	-0.563	-0.388	0.285	0.487	-0.081	0.148	0.247	*-0.854*
-4 kPa	-0.579	*-0.782*	-0.414	-0.256	0.183	0.327	-0.031	0.319	0.183	*-0.751*
-6 kPa	-0.550	*-0.771*	-0.281	-0.159	0.109	0.193	0.014	0.431	0.151	-0.644
-8 kPa	-0.537	*-0.761*	-0.228	-0.115	0.074	0.133	0.033	0.482	0.152	-0.576
-10 kPa	-0.528	*-0.746*	-0.196	-0.087	0.048	0.097	0.042	0.513	0.156	-0.524
-15 kPa	-0.511	*-0.702*	-0.147	-0.041	-0.003	0.045	0.047	0.561	0.155	-0.438
-20 kPa	-0.498	-0.664	-0.120	-0.015	-0.038	0.018	0.040	0.589	0.149	-0.387
-25 kPa	-0.490	-0.637	-0.104	0.001	-0.080	0.003	0.031	0.606	0.143	-0.355
-30 kPa	-0.483	-0.616	-0.093	0.011	-0.134	-0.005	0.023	0.618	0.137	-0.333
-60 kPa	-0.471	-0.555	-0.070	0.044	-0.165	-0.024	-0.007	0.654	0.109	-0.284
-100 kPa	-0.473	-0.530	-0.061	0.065	-0.220	-0.030	-0.018	0.673	0.085	-0.270
-300 kPa	-0.500	-0.510	-0.049	0.116	-0.251	-0.044	-0.003	*0.710*	0.023	-0.271
-600 kPa	-0.524	-0.506	-0.044	0.152	-0.287	-0.053	0.018	*0.731*	-0.019	-0.281
-1500 kPa	-0.555	-0.504	-0.038	0.197	-0.290	-0.064	0.050	*0.752*	-0.076	-0.298

Note: SRCs = store-and-release covers, SOM = soil organic matter, ρ_b = soil bulk density.
[a]Significant at $P < 0.05$, indicated in italic.

Soil organic matter had poor correlations with the volumetric water content (Table 4.5). The correlations between bulk density and volumetric water content were negative and at near saturation, the relationship was strong. The reason of the strong correlation at near saturation is explained in Section 4.3.3.1

4.3.4 Pedotransfer functions

4.3.4.1 *SWRC model*

To develop a SWRC model for SRCs by using backward stepwise MLR, the data-set in Tables C.1 & C.2 in Appendix C was used. Soil physical parameters for regression equations, *viz.* medium-, fine- and very fine sand-, coarse- and fine silt-, clay content, SOM and bulk density were included and are presented in Table 4.6. The statistical analysis of the SWRC model is summarised in Table 4.7. All the variables were in square roots.

In Table 4.6, the very coarse- and coarse sand content had no impact on volumetric water content at selected matric potentials. Medium- and fine sand content affected volumetric water content at -2 and -4 kPa and very fine sand content from -2 to -25 kPa. Coarse- and fine silt content, clay content and SOM had a positive impact on volumetric water content over the whole range of the matric potentials. Rawls *et al.* (1982) and Tomasella *et al.* (2003) observed the same trend where sand content affects water contents at high matric potential and clay content at low matric potential. Since bulk density had a high correlation with volumetric water content at near saturation and according to backward stepwise MLR, it had a negative impact on volumetric water content from -2 to -10 kPa. Rawls *et al.* (1982) found the same results namely that bulk density had a negative impact on SWRC from -4 to -7 kPa. The model of Puckett *et al.* (1985) has bulk density as a parameter at saturation and -1 kPa matric potential. This observation indicates that bulk density can account for most of the variation in saturation or near saturation.

Multicollinearity for SWRC model was not a problem. The adjusted and predicted R^2 ranged between 0.882–0.943 at selected matric potentials (Table 4.7). The largest RMSE values were obtained in the drier range (low matric potentials), while RMSE for saturated water content yielded the lower values. These findings are in contrast to the findings by Babaeian *et al.* (2015) and Phuong *et al.*, (2014), where the lowest RMSE was in the low matric potential ranges. According to these authors, the low errors at low matric potentials is due to the inherent low water content retained in the soil. This can lead to less variation between measured and predicted values compared to the wetter range in a SWRC (Nemes *et al.*, 2006). Cornelis *et al.* (2001) also indicated that errors is usually low at low matric potentials. However, in the current study, the higher RMSE at the dry range of the SWRC may have been caused by lack of filter-plate contact which led to higher errors. It has been reported that at low matric potentials, the pressure plates are susceptible to substantial errors. Campbell (1985) and Cresswell *et al.* (2008) mentioned that two major causes of pressure plates errors are the filter-plate contact loss due to shrinkage on desaturation and soil dispersion that causes blocking the pores in the ceramic plate.

Table 4.6: Coefficients for multiple linear regression equations for prediction of volumetric water content at selected matric potentials of store-and-release covers, and moderately- and very dense store-and-release covers.

Model	Matric potential	Parameter estimate of variable								
		Intercept	Medium sand	Fine sand	Very fine sand	Coarse silt	Fine silt	Clay	SOM	ρ_b
	(-kPa)		(%)	(%)	(%)	(%)	(%)	(%)	(%)	(g.cm^{-3})
SWRC model	2	0.435	0.015	0.029	0.049	0.039	0.030	0.050	0.670	-0.650
	4	0.123	0.031	0.027	0.050	0.053	0.031	0.031	0.077	-0.539
	6	0.498			0.034	0.012	0.020	0.046	0.079	-0.459
	8	0.281			0.033	0.016	0.022	0.050	0.094	-0.339
	10	0.140			0.031	0.019	0.024	0.051	0.107	-0.260
	15	-0.261			0.021	0.026	0.021	0.054	0.137	
	20	-0.286			0.019	0.028	0.024	0.053	0.145	
	25	-0.302			0.017	0.030	0.026	0.053	0.150	
	30	-0.278				0.034	0.025	0.048	0.168	
	60	-0.317				0.036	0.028	0.046	0.174	
	100	-0.332				0.036	0.029	0.045	0.176	
	300	-0.340				0.035	0.029	0.043	0.172	
	600	-0.336				0.034	0.029	0.042	0.167	
	1500	-0.327				0.032	0.028	0.041	0.161	
Moderately dense SWRC model	2	1.600								-0.963
	4	1.636								-1.001
	6	1.649								-1.025
	8	1.664								-1.049
	10	1.587					0.031			-1.051
	15	1.597					0.041			-1.093
	20	1.605					0.048			-1.121
	25	1.611					0.053			-1.141
	30	1.614					0.056			-1.155
	60	1.624					0.066			-1.198
	100	1.637					0.070			-1.225
	300	1.681					0.073			-1.279
	600	1.708					0.073			-1.306
	1500	1.7407					0.071			-1.334
Very dense SWRC model	2	0.617			0.045	0.023	0.021	0.062	0.073	-0.598
	4	0.967						0.054	0.191	-0.725
	6	0.805						0.063	0.210	-0.674
	8	0.685						0.066	0.216	-0.578
	10	0.599						0.066	0.218	-0.525
	15	0.469						0.068	0.218	-0.447
	20	0.399						0.068	0.216	-0.404
	25	0.357						0.068	0.214	-0.378
	30	0.329						0.068	0.212	-0.363
	60	0.261						0.067	0.202	-0.324
	100	0.238						0.066	0.194	-0.311
	300	0.226						0.065	0.178	-0.306
	600	0.231						0.064	0.168	-0.309
	1500	0.245						0.062	0.155	-0.316

Note: SWRC = soil water retention curve, SOM = soil organic matter, ρ_b = soil bulk density.

Table 4.7: Summary of statistical analyses for soil water retention curve model, and moderately-and very dense soil water retention curve models.

Model	Matric potential (-kPa)	Adjusted R^2	RMSE	*P*-value[a]	Predicted R^2
SWRC model	2	0.909	0.017	0.000	0.943
	4	0.931	0.016	0.000	0.957
	6	0.909	0.018	0.000	0.935
	8	0.912	0.018	0.000	0.936
	10	0.908	0.019	0.000	0.919
	15	0.894	0.021	0.000	0.919
	20	0.899	0.021	0.000	0.923
	25	0.897	0.021	0.000	0.922
	30	0.882	0.023	0.000	0.905
	60	0.878	0.023	0.000	0.901
	100	0.878	0.023	0.000	0.901
	300	0.888	0.021	0.000	0.909
	600	0.890	0.021	0.000	0.911
	1500	0.882	0.021	0.000	0.905
Moderately dense SWRC model	2	0.890	0.017	0.000	0.899
	4	0.779	0.027	0.000	0.798
	6	0.707	0.033	0.000	0.732
	8	0.652	0.038	0.001	0.681
	10	0.683	0.038	0.001	0.736
	15	0.659	0.043	0.001	0.716
	20	0.648	0.047	0.002	0.706
	25	0.641	0.049	0.002	0.700
	30	0.636	0.051	0.002	0.697
	60	0.628	0.056	0.002	0.690
	100	0.634	0.058	0.002	0.695
	300	0.659	0.057	0.001	0.716
	600	0.670	0.057	0.001	0.725
	1500	0.675	0.056	0.001	0.729
Very dense SWRC model	2	0.999	0.001	0.006	1.000
	4	0.909	0.020	0.005	0.948
	6	0.900	0.021	0.005	0.943
	8	0.906	0.019	0.005	0.946
	10	0.908	0.019	0.005	0.947
	15	0.905	0.018	0.005	0.945
	20	0.898	0.018	0.006	0.942
	25	0.891	0.019	0.007	0.938
	30	0.885	0.019	0.007	0.934
	60	0.870	0.020	0.010	0.926
	100	0.871	0.020	0.009	0.926
	300	0.899	0.017	0.006	0.942
	600	0.917	0.015	0.004	0.953
	1500	0.928	0.014	0.003	0.959

Note: SWRC = soil water retention curve, Adjusted R^2 = Adjusted coefficient of determination, RMSE = Root mean square error in $m^3.m^{-3}$, Predicted R^2 = Predicted coefficient of determination.
[a]All *P* values are significant, $P < 0.05$.

Deka *et al.* (1995) and Skalová *et al.* (2011) found similar results namely that the errors at low matric potentials were higher compared to the errors at higher matric potentials. Their reason was that the filter paper tended to overestimate the volumetric water content at low matric potential, suggesting that longer equilibration periods may be required. Gee *et al.* (2002) observed that the water content at -1500 kPa did not reach equilibrium even after 10 days or longer of the equilibration periods and may be due to low conductivity of the plate. In the aforementioned study, soil water suction reduced when height of core rings increased from 1.5 to 3 cm, indicating a soil conductance effect. While the exact causes can't be confirmed, the RMSE values of the low matric potentials range were small enough (Table 4.7).

The R^2 ranged between 0.905–0.944 (data not shown) and is similar to the R^2 ranges of Puckett *et al*. (1985) PTFs at selected matric potentials. Similarly, Batjes (1996) developed PFTs at 10 different selected matric potentials and reported high R^2 values of 0.880–0.940. Such high values of R^2 in the current study suggest the appropriateness of the point PTFs in describing the behaviour of SWRCs. The predicted R^2 was above 0.60, therefore model validation of the SWRC model could be conducted.

4.3.4.2 *Moderately- and very dense SWRC models*

The training sets in Tables C.3 & C.4 in Appendix C were used to develop moderately- and very dense SWRC models by using backward stepwise MLR. The regression coefficients are summarised in Table 4.6 and the statistical analyses of moderately- and very dense SWRC models are presented in Table 4.7. The soil physical parameters that quantified for moderately dense SWRC model were fine silt content (-10 to -1500 kPa) and bulk density through the whole range of matric potentials.

At -2 kPa, six soil physical parameters, *viz*. very fine sand-, coarse and fine silt-, clay content, SOM and bulk density were included for the very dense SWRC model. After -2 kPa, only clay content, SOM and bulk density had an impact on the volumetric water content in the very dense SWRC model. All the parameters of moderately- and very dense SWRC models were in square roots.

In contrast to the SWRC model, the bulk density played a role from -2 to -1500 kPa in the moderately- and very dense SWRC models. Multicollinearity was a mild problem for both models due to a small number of samples. The adjusted R^2 for moderately dense SWRC model ranged between 0.628–0.890 and for very dense SWRC model ranged between 0.885–0.999 (Table 4.7). Compared to the adjusted R^2 values of the SWRC model (Table 4.7), the adjusted R^2 values of moderately dense SWRC model was lower and for the very dense SWRC model, it was higher. Due to a small number of samples, the models may be less accurate or suffer from overfitting. Model validation of the moderately- and very dense SWRC models was conducted in Section 4.3.5.2.

4.3.5 Model validation of SWRC model, and moderately- and very dense SWRC models

4.3.5.1 *SWRC model*

The testing set with the soil physical properties of SRCs in Table C.5 in Appendix C was used to test the SWRC model.

Square roots of medium sand-, fine sand-, very fine sand-, coarse and silt-, clay content, SOM and bulk density (Table C.5 in Appendix C) were inserted in the regression equations of SWRC model. The measured volumetric water content of SRCs testing set (Table C.6 in Appendix C) and predicted volumetric water contents from -2 to -1500 kPa were plotted in a 1:1 line and is presented in Figure 4.6. For each matric potential with the 1:1 line of measured and predicted volumetric water contents are shown separately in Figures C1–C4 in Appendix C. The adjusted R^2 and RMSE of the model validation are summarised in Table 4.8.

In Figure 4.6, according to the student's t-test that there was no statistically difference between measured and predicted volumetric water content values of SWRC model (t = 0.911, *P* = 0.363). Moreover, there was no difference between the mean of measured and predicted volumetric water contents at the 0.05 probability level. Figure 4.6 showed that the data points were uniformly scattered around the 1:1 line. For data uniformity at each separate matric potential, it was more or less uniform scattered around the 1:1 line as shown in Figures C1–C4 in Appendix C. The agreement between the measured and predicted values at selected matric potential was good with adjusted R^2 values range of 0.619–0.931 and low RMSE values (Table 4.8). The RMSE values of the current study are similar to those of Ghanbarian-Alavijeh & Millán (2010) and Phuong *et al.* (2014) PTFs for their testing sets which had RMSE of 0.040–0.060 $m^3.m^{-3}$ and 0.047–0.048 $m^3.m^{-3}$, respectively. The statistical analysis between predicted and measured values for the whole range of matric potentials showed that the SWRC model performed well and was satisfactorily validated.

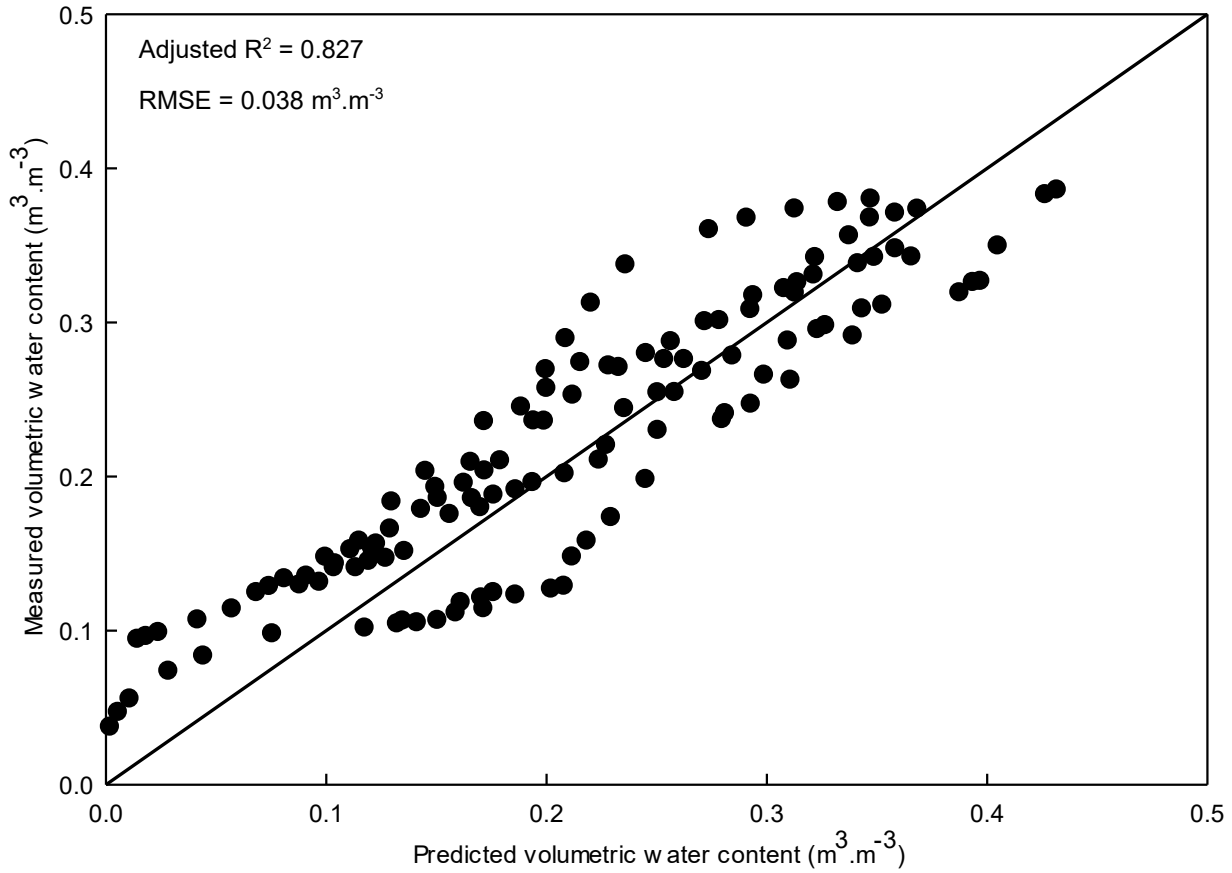

Figure 4.6: Measured versus predicted volumetric water content of SWRC model.

Table 4.8: Performance of soil water retention curve model, moderately- and very dense soil water retention curve models using the testing data sets.

Model	Matric potential (-kPa)	Adjusted R^2	RMSE	Student's t-test[a]
SWRC model	2	0.931	0.024	0.130
	4	0.921	0.025	0.357
	6	0.849	0.035	0.667
	8	0.819	0.039	0.848
	10	0.802	0.041	1.002
	15	0.696	0.050	1.434
	20	0.726	0.047	1.545
	25	0.741	0.045	1.616
	30	0.706	0.048	1.777
	60	0.682	0.049	1.846
	100	0.660	0.051	1.898
	300	0.635	0.053	1.954
	600	0.628	0.054	1.999
	1500	0.619	0.054	1.999
Moderately dense SWRC model	2	0.326	0.064	*2.216*
	4	0.307	0.069	1.895
	6	0.274	0.304	1.604
	8	0.264	0.097	1.465
	10	0.312	0.105	1.133
	15	0.278	0.108	1.073
	20	0.258	0.103	1.164
	25	0.255	0.097	1.285
	30	0.266	0.093	1.368
	60	0.316	0.079	1.726
	100	0.331	0.073	1.833
	300	0.333	0.070	1.769
	600	0.333	0.069	1.673
	1500	0.333	0.069	1.531
Very dense SWRC model	2	0.772	0.026	1.295
	4	0.748	0.029	1.368
	6	0.765	0.030	1.391
	8	0.770	0.030	1.369
	10	0.768	0.032	1.304
	15	0.750	0.035	1.349
	20	0.743	0.035	1.349
	25	0.719	0.037	1.376
	30	0.698	0.039	1.349
	60	0.629	0.044	1.333
	100	0.596	0.047	1.334
	300	0.555	0.049	1.403
	600	0.535	0.050	1.419
	1500	0.505	0.052	1.387

Note: SWRC = soil water retention curve, Adjusted R^2 = Adjusted coefficient of determination, RMSE = Root mean square error in $m^3.m^{-3}$.
[a]Significant at $P < 0.05$, indicated in italic.

4.3.5.2 *Moderately- and very dense SWRC models*

The testing sets containing the soil physical properties of moderately- and very dense SRCs (Table C.5 in Appendix C) were used to test the moderately- and very dense SWRC models, respectively.

For the moderately dense SWRC model, only the square roots of fine silt content and bulk density were inserted. At -2 kPa, square roots of very fine sand-, coarse and fine silt-, clay content, SOM and bulk density were inserted in the very dense SWRC model. Thereafter, from -4 to -1500 kPa, square roots of coarse and fine silt-, clay content, SOM and bulk density were inserted. The adjusted R^2 and RMSE of the moderately- and very dense model validations are summarised in Table 4.8. The data uniformity of moderately- and very dense SWRC models are shown Figures 4.7A & B, respectively. At each matric potential, the data uniformity of moderately dense- and very dense SWRC models is presented in Figures C5–C8 and Figures C9–C12 in Appendix C, respectively.

In Figures 4.7A & B, the student's test for moderately dense SWRC model was t = -1.480 and *P* = 0.140, and for very dense SWRC model it was t = -1.960 and *P* = 0.051. There was no statistical difference between measured and predicted volumetric water content for both models. However, at -2 kPa of moderately dense SWRC model, there was a significant difference between both volumetric water content values (Table 4.8). The mean difference of measured and predicted volumetric water contents of both models (mean difference > 0.02) was higher compared to the SWRC model with the difference of 0.008. The data values (Figures 4.7A & B) of both models were further away from the 1:1 line and not uniformly scattered. Both models may have suffered from overestimating the volumetric water contents at selected matric potentials. In Table 4.8, the adjusted R^2 at each matric potential of moderately dense SWRC model was lower than 0.4. The adjusted R^2 for very dense SWRC model was higher than 0.7 from -2 to -25 kPa and between 0.4 and 0.7 from -30 to -1500 kPa. Overall, the adjusted R^2 of both models were lower with higher RMSE and they performed weaker compared to the SWRC model with wider range of soil texture and bulk density.

4.3.6 Pedotransfer functions compiled from literature

4.3.6.1 *Modelling soil water retention curves of store-and-release covers, and moderately- and very dense covers*

The descriptive statistics of predicted volumetric water content at selected matric potentials for SRCs, moderately- and very dense SRCs data sets using the three PTFs in Table 1.14 (Refer to Section 1.3.4.2 in Chapter 1) are presented in Tables 4.9–4.11, respectively. All the standard deviation (SD) values at selected matric potentials of all three PTFs were < 1 for SRCs, moderately- and very dense SRCs data sets (Tables 4.10–4.12). Moreover, the SD values were more or less the same as the measured volumetric water content SD values (data not shown). For both data sets, Puckett *et al.* (1985) had higher SD values compared to the SD values of the other two PTFs. The CV of predicted volumetric water content of all three data sets varied between 3.94 and 44.29 starting with a low CV value at high matric potentials and increasing to higher values at low matric potentials.

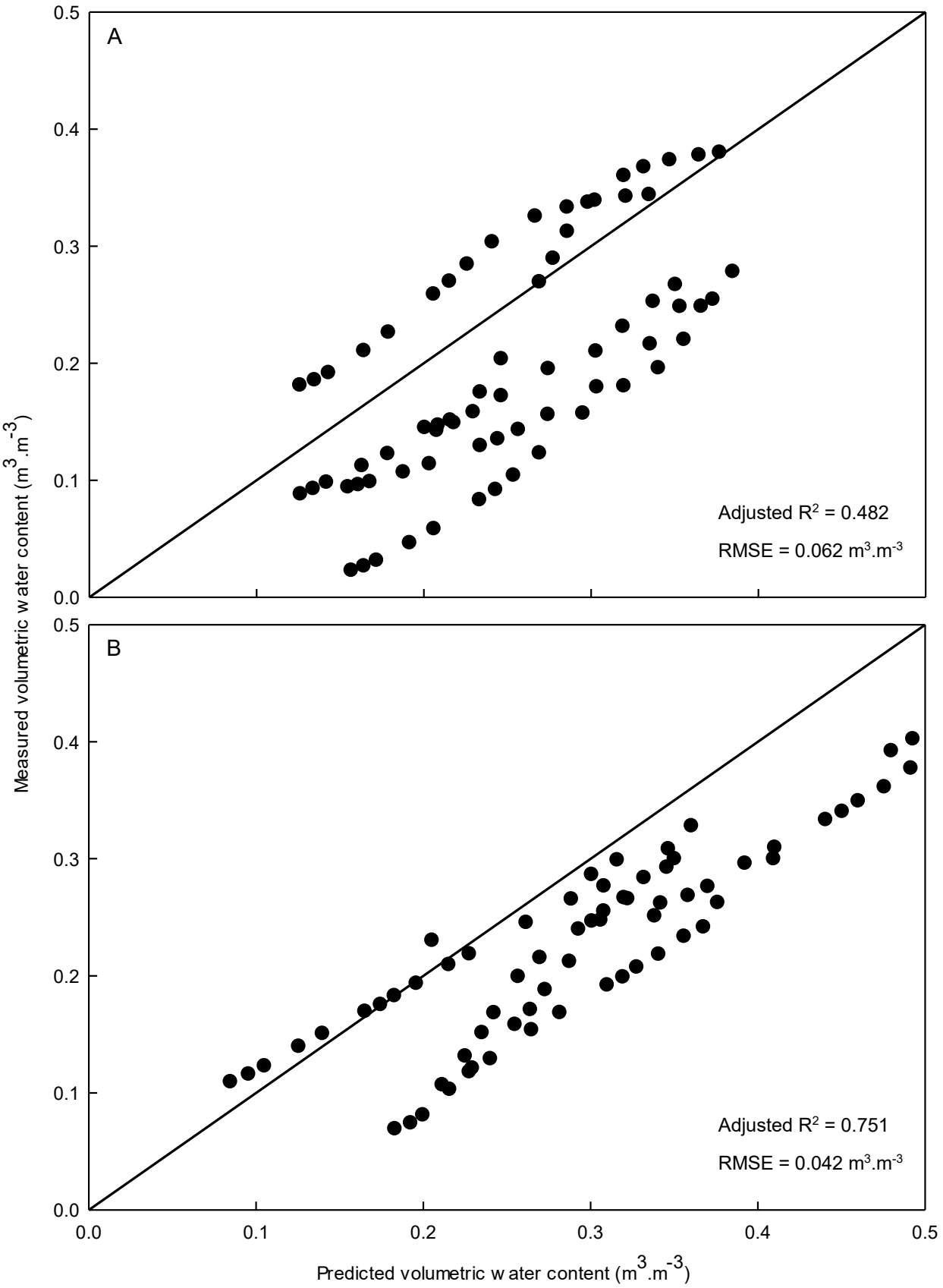

Figure 4.7: Measured versus predicted volumetric water content of moderately dense SWRC model (A) and very dense SWRC model (B).

The CV values of the predicted volumetric water content of the three PTFs for the moderately dense SRC data-set were lower compared to the CV values of the very dense SRC data-set. Moreover, the CV values of the predicted volumetric water content were more or less similar to the CV of the measured volumetric water contents of the three data sets (Table 4.4), although the CV at -1500 kPa (Tables 4.9–4.11) was lower compared to the CV of the measured volumetric water content of the three data sets.

4.3.6.2 *Model performance*

Model performance for the three data sets of the three PTFs is summarised in Table 4.12 and the plotted 1:1 line are shown in Figures 4.8–4.12. The adjusted R^2 values of Gupta & Larson (1979) model of the three data sets ranged from low to moderate with RMSE values of 0.042–0.066 $m^3.m^{-3}$, whereas, the adjusted R^2 of Rawls *et al*. (1982) model ranged from moderate to high and RMSE values ranged between 0.035–0.067 $m^3.m^{-3}$. The adjusted R^2 values of the Puckett *et al*. (1985) model were moderate with RMSE values of 0.042–0.065 $m^3.m^{-3}$ for the three data sets. Overall, for the whole range of matric potentials, the three PTFs of SRCs, moderately- and very dense SRCs data sets had moderately adjusted R^2 and the RSME ranged between 0.053 and 0.073 $m^3.m^{-3}$ (Figures 4.8–4.12).

For all three data sets, Rawls *et al*. (1982) performed the best to predict the volumetric water contents (Figures 4.8B, 4.10A & 4.11B). The data uniformity of Rawls *et al.* (1982) model were closer to and more uniform by distributed along the 1:1 line compared to the Gupta & Larson (1979) model (Figures 4.8A, 4.9B & 4.11A) and the Puckett *et al*. (1985) model (Figures 4.9A, 4.10B & 4.12). In the Rawls *et al.* (1982) model, the model development included 2 541 soils horizons with a wide range of sand (0.10–99.00%), silt (0.10–93.00%), clay (0.10–94.00%), SOM (0.1–12.5%) and bulk density (0.100–2.090 $g.cm^{-3}$). Moreover, most soils included both expanding (montmorillonite) and nonexpanding (koalinite, illite, chlorite, and vermiculite) type clay minerals. Considering the wide range of data and the model performance, it can be concluded that Rawls *et al.* (1982) model can predict volumetric water content for SRCs. Hodnett & Tomasella (2002) mentioned that the PTFs of Rawls *et al*., (1982) are valid for soils with sand content of 5-70% and clay content of 5–60%. The Gupta & Larson (1979) model performed the weakest when predicting the volumetric water content for moderately- and very dense SRCs data sets. This is due to the fact that the linear multiple regression equations did not have intercepts and may not be comparable. When removing the intercept, the data is forced to go through the origin and the other estimates may become biased (Hahn, 1977). This bias of Gupta & Larson (1979) model can also be caused to differences in experimental procedures. Gupta & Larson (1979) used 1 to 7.6 cm thick cores and estimated clay content by the hydrometer method rather than the pipette method. It should be noted that the adjusted R^2 of Gupta & Larson (1979) model at -4 kPa was low for the three data sets.

Table 4.9: The descriptive statistics of the volumetric water content predicted by the three published pedotransfer functions of store-and-release covers data-set.

Descriptive statistics	Selected matric potential (-kPa)																
	0	**1**	**4**	**5**	**7**	**10**	**22**	**30**	**33**	**60**	**100**	**200**	**400**	**500**	**700**	**1000**	**1500**
Gupta & Larson (1979)																	
Minimum			0.630		0.530	0.478	0.385		0.317	0.241	0.188	0.134	0.093		0.070	0.058	0.046
Maximum			0.829		0.731	0.686	0.609		0.549	0.479	0.428	0.371	0.323		0.299	0.286	0.277
Mean			0.735		0.628	0.575	0.484		0.416	0.340	0.285	0.227	0.182		0.158	0.145	0.134
SD			0.048		0.049	0.051	0.055		0.058	0.059	0.060	0.060	0.058		0.058	0.059	0.059
CV			6.49		7.75	8.86	11.37		13.82	17.52	21.12	26.40	32.09		36.99	40.31	44.29
Rawls *et al.* (1982)																	
Minimum			0.182		0.135	0.203	0.191		0.146	0.095	0.086	0.074	0.070		0.067	0.066	0.050
Maximum			0.466		0.421	0.413	0.389		0.378	0.326	0.326	0.274	0.269		0.267	0.265	0.249
Mean			0.329		0.285	0.288	0.265		0.230	0.178	0.177	0.149	0.145		0.142	0.141	0.127
SD			0.068		0.075	0.057	0.052		0.061	0.061	0.059	0.049	0.049		0.049	0.050	0.048
CV			20.79		26.17	19.72	19.60		26.61	34.41	33.15	33.06	34.10		34.68	35.25	37.60
Puckett *et al.* (1985)																	
Minimum	0.117	0.125		0.192		0.153		0.122		0.103	0.106			0.097		0.112	0.092
Maximum	0.426	0.433		0.395		0.404		0.387		0.374	0.369			0.344		0.351	0.329
Mean	0.313	0.311		0.282		0.257		0.226		0.208	0.206			0.189		0.201	0.180
SD	0.072	0.071		0.057		0.071		0.075		0.076	0.073			0.069		0.066	0.066
CV	23.10	22.87		20.29		27.67		33.23		36.77	35.63			36.33		33.14	36.53

Note: SD = standard deviation in $m^3.m^{-3}$, CV = coefficient of variation in %.

Table 4.10: The descriptive statistics of the volumetric water content predicted by the three published pedotransfer functions of moderately store-and-release covers data-set.

Descriptive	**Selected matric potential (-kPa)**																
statistics	**0**	**1**	**4**	**5**	**7**	**10**	**22**	**30**	**33**	**60**	**100**	**200**	**400**	**500**	**700**	**1000**	**1500**
								Gupta & Larson (1979)									
Minimum			0.713		0.593	0.534	0.434		0.360	0.279	0.222	0.162	0.117		0.092	0.079	0.067
Maximum			0.808		0.711	0.665	0.584		0.521	0.449	0.397	0.338	0.291		0.267	0.254	0.244
Mean			0.756		0.648	0.595	0.504		0.436	0.359	0.305	0.246	0.200		0.176	0.163	0.152
SD			0.030		0.034	0.037	0.041		0.044	0.046	0.048	0.048	0.047		0.048	0.048	0.049
CV			3.94		5.21	6.16	8.16		10.07	12.90	15.62	19.53	23.65		27.13	29.42	32.09
								Rawls *et al.* (1982)									
Minimum			0.258		0.220	0.203	0.191		0.146	0.095	0.109	0.091	0.087		0.085	0.083	0.077
Maximum			0.444		0.417	0.396	0.366		0.349	0.297	0.289	0.243	0.239		0.237	0.235	0.216
Mean			0.345		0.312	0.295	0.274		0.242	0.191	0.194	0.164	0.159		0.156	0.156	0.143
SD			0.057		0.057	0.057	0.049		0.056	0.057	0.047	0.040	0.040		0.040	0.041	0.036
CV			16.55		18.32	19.23	17.97		23.32	29.67	24.42	24.69	25.39		25.75	26.11	25.21
								Puckett *et al.* (1985)									
Minimum	0.215	0.200		0.192		0.153		0.122		0.103	0.106			0.097		0.112	0.092
Maximum	0.426	0.433		0.381		0.386		0.366		0.350	0.344			0.318		0.325	0.303
Mean	0.349	0.345		0.292		0.268		0.238		0.221	0.220			0.203		0.215	0.194
SD	0.054	0.057		0.055		0.070		0.073		0.074	0.070			0.065		0.062	0.061
CV	15.39	16.64		18.80		26.01		30.66		33.27	31.91			31.77		28.84	31.41

Note: SD = standard deviation in $m^3.m^{-3}$, CV = coefficient of variation in %.

Table 4.11: The descriptive statistics of the volumetric water content predicted by the three published pedotransfer functions of very dense store-and-release covers data-set

Descriptive statistics	Selected matric potential (-kPa)																
	0	**1**	**4**	**5**	**7**	**10**	**22**	**30**	**33**	**60**	**100**	**200**	**400**	**500**	**700**	**1000**	**1500**
Gupta & Larson (1979)																	
Minimum			0.700		0.600	0.547	0.448		0.374	0.291	0.233	0.172	0.127		0.102	0.089	0.076
Maximum			0.829		0.731	0.686	0.609		0.549	0.479	0.428	0.371	0.323		0.299	0.286	0.277
Mean			0.764		0.660	0.609	0.520		0.453	0.377	0.322	0.263	0.217		0.192	0.180	0.169
SD			0.041		0.045	0.048	0.057		0.062	0.067	0.069	0.071	0.070		0.070	0.071	0.072
CV			5.38		6.77	7.95	10.90		13.68	17.73	21.52	26.82	32.18		36.54	39.34	42.58
Rawls *et al.* (1982)																	
Minimum			0.256		0.205	0.250	0.231		0.184	0.133	0.108	0.094	0.090		0.088	0.087	0.061
Maximum			0.439		0.421	0.413	0.389		0.378	0.326	0.326	0.274	0.269		0.267	0.265	0.249
Mean			0.352		0.311	0.317	0.291		0.261	0.210	0.208	0.175	0.171		0.169	0.168	0.151
SD			0.065		0.074	0.063	0.063		0.075	0.075	0.076	0.063	0.063		0.063	0.063	0.064
CV			18.44		23.81	20.00	21.54		28.62	35.55	36.47	35.86	36.69		37.12	37.33	42.21
Puckett *et al.* (1985)																	
Minimum	0.205	0.208		0.260				0.221		0.166	0.166			0.153		0.167	0.147
Maximum	0.388	0.387		0.395				0.404		0.374	0.369			0.344		0.351	0.329
Mean	0.311	0.311		0.320				0.300		0.253	0.250			0.230		0.240	0.219
SD	0.061	0.061		0.054				0.073		0.083	0.081			0.077		0.075	0.074
CV	19.67	19.69		16.97				24.19		32.94	32.42			33.32		31.02	33.62

Note: SD = standard deviation in $m^3.m^{-3}$, CV = coefficient of variation in %.

Table 4.12: Model performance of the published pedotransfer functions for predicting soil water retention curves of moderately- and very dense store-and-release covers (SRCs) data sets.

Author's PTFs	Selected matric potential (-kPa)	Adjusted R^2	RMSE	Student's t-test[a]
SRCs data-set				
Gupta & Larson (1979)	**4**	0.385	0.058	*3.634*
	10	0.523	0.055	*2.342*
	20	0.554	0.055	1.847
	60	0.531	0.057	1.331
	100	0.514	0.059	1.203
	1500	0.480	0.060	1.001
Rawls *et al.* (1982)	**4**	0.596	0.047	1.035
	10	0.600	0.050	1.046
	20	0.653	0.048	1.069
	60	0.598	0.053	0.996
	100	0.546	0.057	1.010
	1500	0.467	0.061	0.994
Puckett *et al.* (1985)	**10**	0.567	0.052	0.989
	30	0.583	0.053	1.018
	60	0.552	0.056	1.023
	100	0.534	0.057	1.037
	1500	0.498	0.059	1.044
Moderately dense SRCs data-set				
Gupta & Larson (1979)	**4**	0.395	0.047	*2.497*
	10	0.551	0.051	1.763
	20	0.611	0.053	1.481
	60	0.566	0.060	1.184
	100	0.537	0.063	1.109
	1500	0.499	0.066	0.992
Rawls *et al*. (1982)	**4**	0.614	0.037	0.993
	10	0.642	0.046	0.998
	20	0.654	0.050	1.018
	60	0.578	0.059	0.987
	100	0.540	0.062	0.997
	1500	0.477	0.067	0.987
Puckett *et al.* (1985)	**10**	0.636	0.046	0.974
	30	0.615	0.054	0.999
	60	0.559	0.060	1.006
	100	0.533	0.063	1.014
	1500	0.512	0.065	1.018
Very dense SRCs data-set				
Gupta & Larson (1979)	**4**	0.275	0.061	*2.287*
	10	0.496	0.051	1.580
	20	0.547	0.047	1.423
	60	0.580	0.045	1.169
	100	0.562	0.045	1.107
	1500	0.581	0.042	1.008
Rawls *et al.* (1982)	**4**	0.642	0.043	1.037
	10	0.706	0.036	1.047
	20	0.753	0.035	1.055
	60	0.701	0.037	1.008
	100	0.659	0.039	1.013
	1500	0.583	0.041	1.006
Puckett *et al.* (1985)	**10**	0.627	0.044	1.015
	30	0.611	0.043	1.022
	60	0.595	0.043	1.022
	100	0.589	0.043	1.028
	1500	0.551	0.042	1.033

Note: Adjusted R^2 = Adjusted coefficient of determination, RMSE = Root mean square error in $m^3.m^{-3}$.
[a]Probability levels at $P < 0.05$ is indicated in italic.

For all three PTFs and the three data sets (Table 4.12), the t-values were in the range $-2 \leq t \leq 2$ for 0.05 probability level. However, at -4 kPa of Gupta & Larson (1979) model of all three data sets and -10 kPa of SRCs data-set, the t-values were higher than 2. Therefore, at each matric potential, there was no statistical difference between the measured and predicted volumetric water content of the three PTFs.

If the whole range of matric potential had been considered (Table 4.13), the results were as follows: (1) there was a statistical difference between the measured and volumetric water content of Gupta & Larson (1979) model for all three data sets; (2) no statistical difference between the volumetric water content values of Rawls *et al.* (1982) for all three data sets; (3) no statistical difference between the volumetric water content vales of Puckett *et al*. (1985) for moderately- and very dense SRCs data sets; and (4) the t-values of Rawls *et al.* (1982) model were the lowest with all three data sets. It is safe to conclude that the statistical analysis between predicted and measured values for the whole range of matric potentials showed agreement that the Rawls *et al.* (1982) model performed fairly well and was satisfactorily validated. Similar results were found by Abdelbaki & Youssef (2009), where Rawls *et al.* (1982) model performed the best to predict the volumetric water content with R^2 values of 0.538–0.563 for 2046 US soils.

Compared to the statistical analysis of the Rawls *et al*. (1982) model (Table 4.13 and Figure 4.8B) to the SWRC model of the current study (Table 4.8 and Figure 4.6) for a fully described SWRC, the SWRC model performed better due to higher validated adjusted R^2 value with lower RMSE value. Pedotransfer functions predicting soil or volumetric water content using soil texture, particle density, bulk density, porosity and pore-size distribution etc. have already been derived for different soil types and at different places. These PTFs are often developed from empirical observations and the applicability may be restricted to the data sets (Wösten *et al.*, 1999).

Table 4.13: Student's t-test and *P*-value of the three selected PTFs for the whole range of matric potentials.

Author's PTFs	Student's t-test	*P*-value[a]
SRCs data-set		
Gupta & Larson (1979)	12.26	*<0.05*
Rawls *et al.* (1982)	1.510	0.132
Puckett *et al.* (1985)	3.255	*0.001*
Moderately dense SRCs data-set		
Gupta & Larson (1979)	9.208	*<0.05*
Rawls *et al.* (1982)	0.099	0.291
Puckett *et al.* (1985)	0.818	*0.414*
Very dense SRCs data-set		
Gupta & Larson (1979)	9.218	*<0.05*
Rawls *et al.* (1982)	0.089	*0.275*
Puckett *et al.* (1985)	0.819	*0.410*

Note: PTFs = Pedotransfer functions.
[a]Probability levels at $P < 0.05$ is indicated in italic.

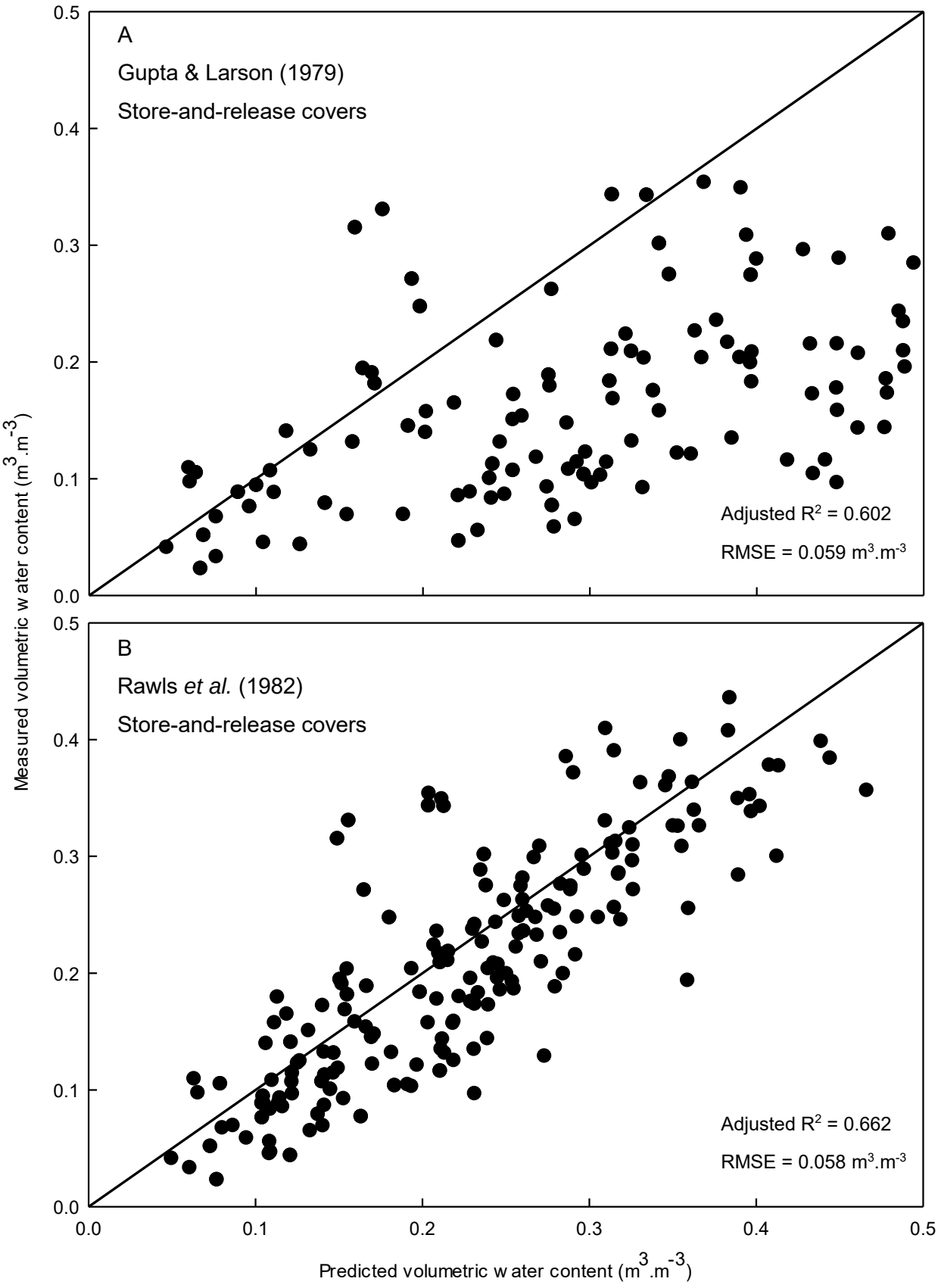

Figure 4.8: Measured versus predicted volumetric water content of Gupta & Larson (1979) model (A) and Rawls *et al*. (1982) model (B) of store-and-release covers data-set.

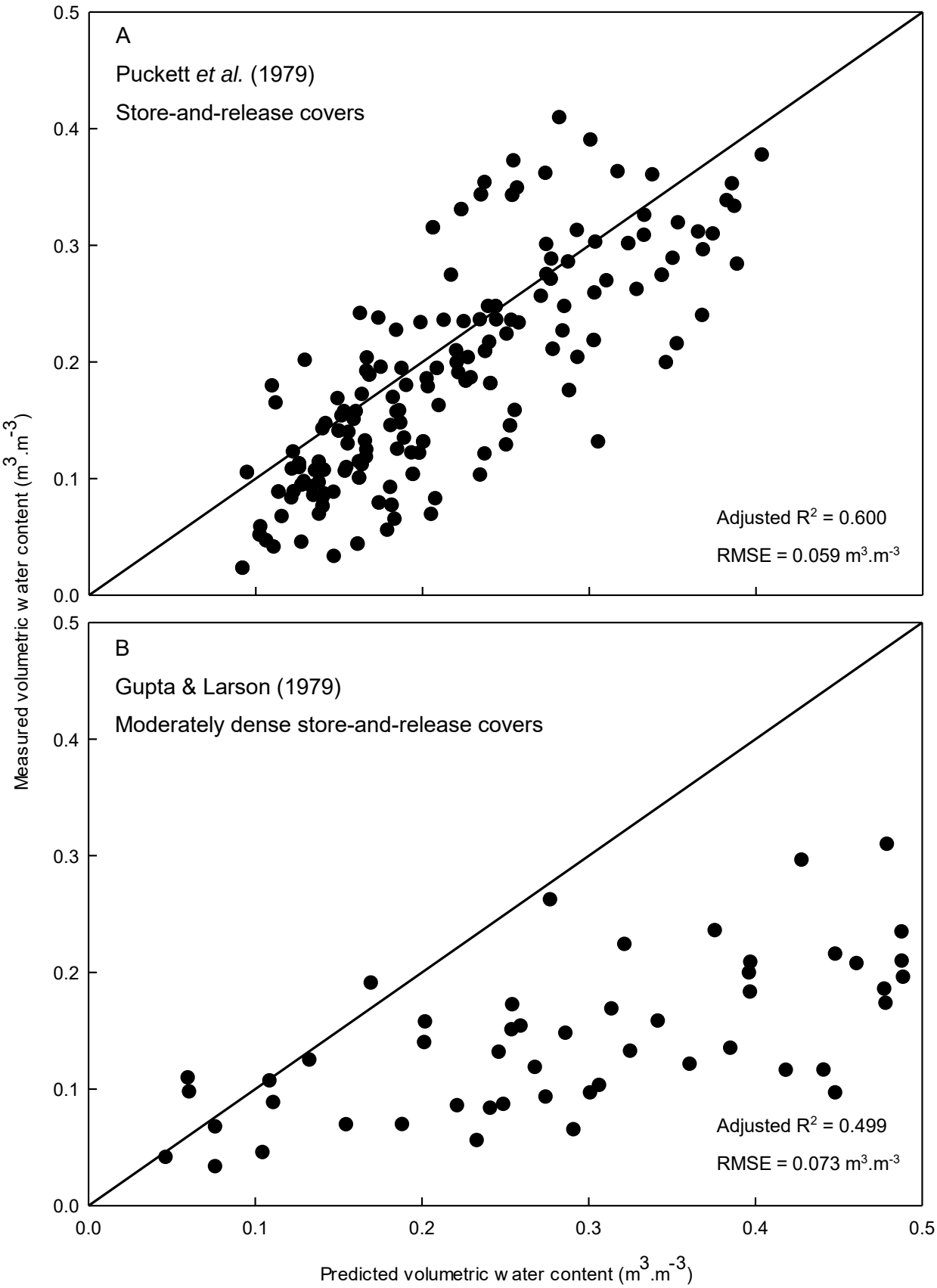

Figure 4.9: Measured versus predicted volumetric water content of Puckett *et al.* (1979) model (A) of store-and-release covers data-set and Gupta & Larson (1979) model (B) of moderate dense store-and-release covers data-set.

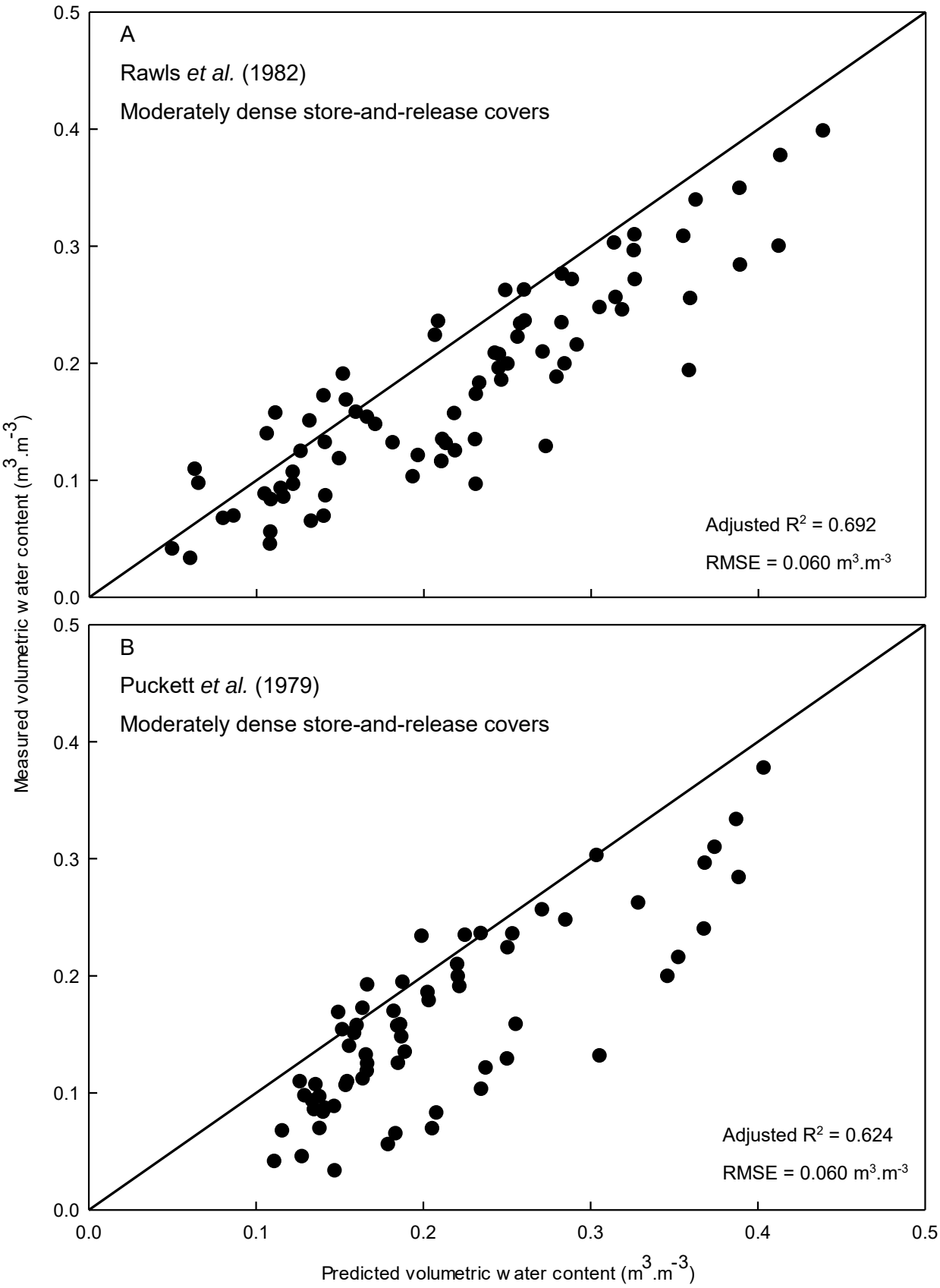

Figure 4.10: Measured versus predicted volumetric water content of Rawls *et al.* (1982) model (A) and Puckett *et al.* (1979) model (B) of moderately dense store-and-release covers data-set.

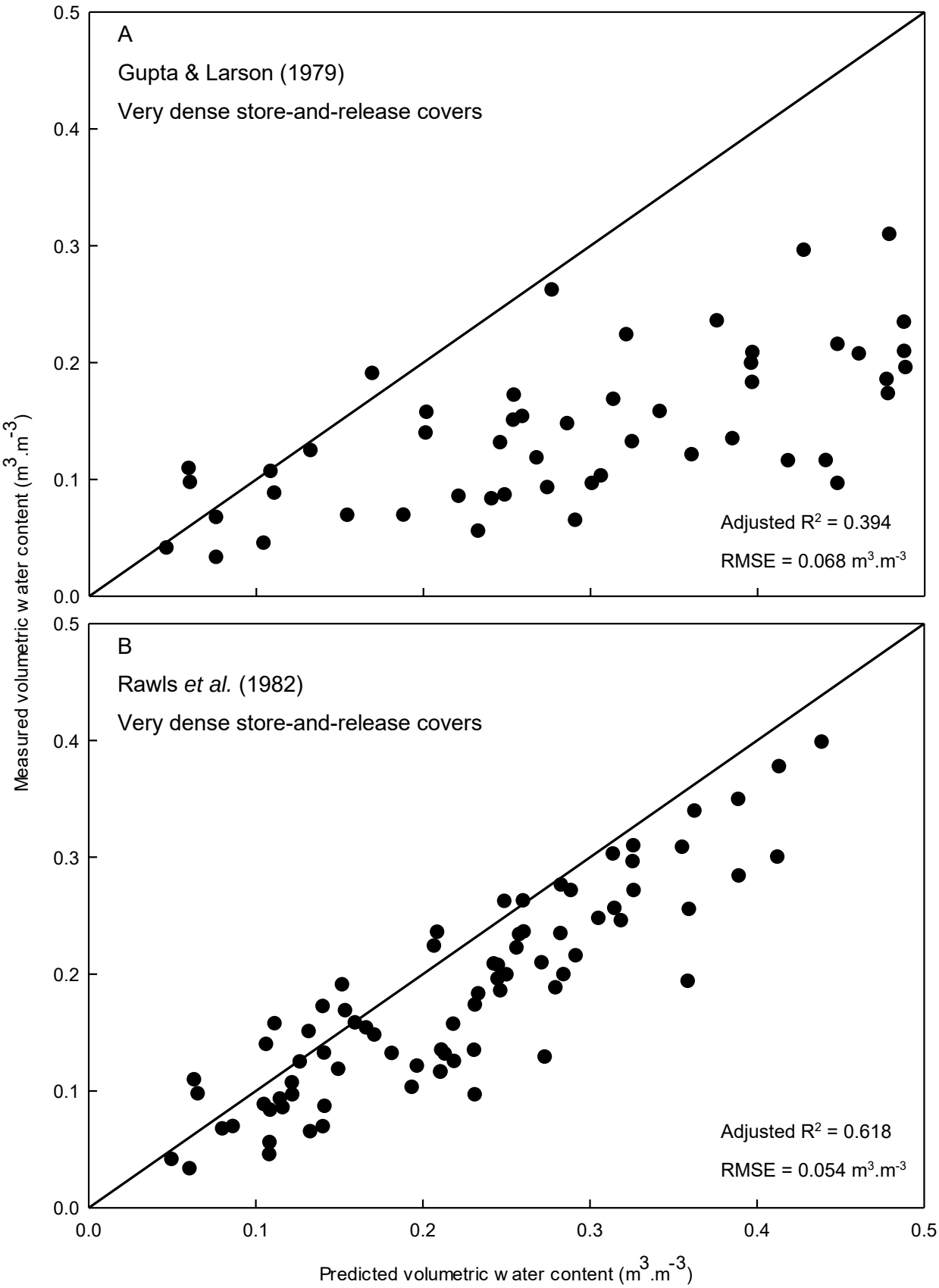

Figure 4.11: Measured versus predicted volumetric water content of Gupta & Larson (1979) model (A) and Rawls *et al.* (1982) model (B) of very dense store-and-release covers data-set.

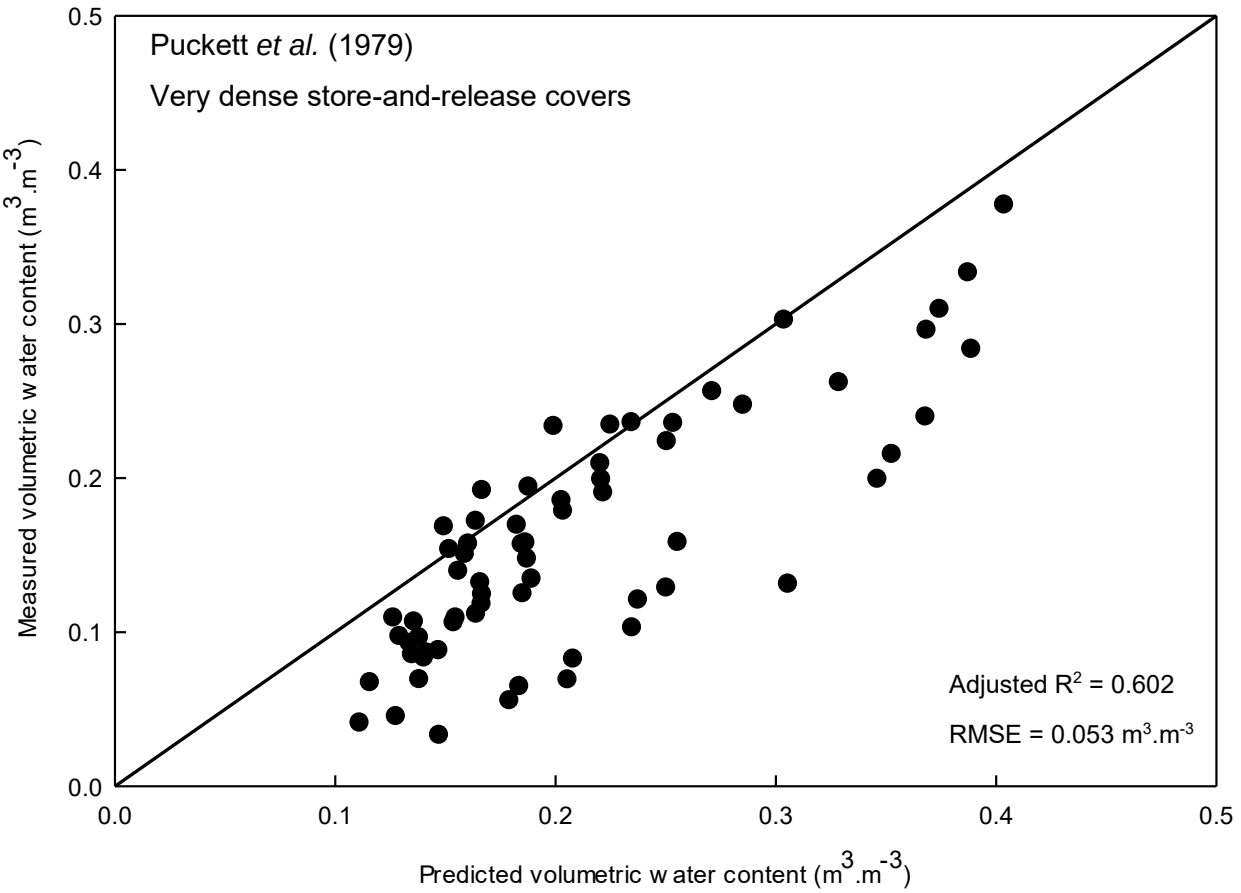

Figure 4.12: Measured versus predicted volumetric water content of Puckett *et al.* (1979) model of very dense store-and-release covers data-set.

There are several authors who found similar results where the developed PTFs performed better compared to the published PTFs. However, some studies indicate a good (Rawls *et al.*, 2001) or intermediate (Givi *et al.*, 2004) performance of the published PTFs, while others reported poor performances (Abdelbaki & Youssef, 2009). Evaluating PTFs outside the area of development can therefore be risky. Tietje & Tapkenhinrichs (1993) further concluded that there are no PFT that could be termed global due to variations in soil-forming factors and pedogenesis.

4.4 Conclusion

Soil texture and bulk density do affect SWRC and WHC. The clayey soils had higher WHC with a more gradual slope in desaturation function and are more suitable as a water retention layer, whilst the sandy soils had lower WHC, but have a steep slope of desaturation functions making them more suitable as growth mediums and water can easily be taken up by the plant roots. Generally, higher bulk density reduced the WHC with a more gradual slope in the desaturation function, and the effect was most noticeable in sandy soils. The lower WHC due to high bulk density of the sandy growth medium may be problematic for plant growth.

All five fractions of sand content as well as bulk density of the SRCs dataset had a negative correlation with volumetric water content at selected matric potentials, whereas the significant correlation of clay content was positive. The correlations changed after the SRCs data-set was split into moderately- and very dense SRCs data sets. The coarse sand content (from -2 to -1500 kPa)

of moderately dense SRCs and fine- (from -25 to -1500 kPa) and very fine sand (from -2 to -10 kPa) content of very dense SRCs had a positive correlation with the volumetric water content at selected matric potentials. The correlation between clay content and volumetric water content at selected matric potentials of both data sets were positive, but not significant, except at the lower matric potential in the very dense SRCs data-set.

The SWRC model for SRCs in Mpumalanga Highveld can predict the volumetric water content accurate from particle-size distribution, SOM and bulk density. This will help to model the water flow of soil covers and to estimate the WHC. The moderately- and very dense SWRC models are not suitable for predicting SWRC due to moderate/poor analysis performances. Moderate/poor performance of moderately- and very dense SWRC models may be caused by the smaller range of soil texture used in the model development and bulk density with a small number of samples. Consultants, geo-engineers or soil scientists may find the SWRC model helpful when estimating the SWRCs of some SRCs with similar mineralogy and genesis without expensive testing.

The evaluation and comparison of the three published PTFs that were considered in this study, enabled the following conclusions. The PTFs of Rawls *et al.* (1982) performed the best among the three PTFs followed by Puckett *et al.* (1979) model and Gupta & Larson (1979). The performance of PTFs changed with the variation of soil textural classes and bulk density after the SRCs data-set was split into moderately- and very dense SRCs data sets. The errors of the published PTFs in predicting the SRCs were higher compared to the developed SWRC model with moderate/poor data uniformity around the 1:1 line. From these tests, it is shown that developing new PTFs for SRCs will probably lead to better accuracy and lower errors.

4.5 References

Abdelbaki, A.M. & Youssef, M.A. 2009. Evaluation of pedotransfer functions for predicting soil water characteristic curve for U.S. soils. In Grand Sierra Resort and Casino Reno, Nevada: American Society of Agricultural and Biological Engineers *2009 ASABE Annual International Meeting*.

Arya, L.M. & Paris, J.F. 1981. A physicoempirical model to predict the soil moisture characteristic from particle-size distribution and bulk density data. *Soil Science Society of America Journal*. 45(6):1023–1030.

Babaeian, E., Homaee, M., Vereecken, H., Montzka, C., Norouzi, A.A. & van Genuchten, M.T. 2015. A comparative study of multiple approaches for predicting the soil water retention curve: Hyperspectral information vs. basic soil properties. *Soil Science Society of America Journal*. 79(4):1043–1058.

Batjes, N.H. 1996. Development of a world data set of soil water retention properties using pedotransfer rules. *Geoderma*. 71(1–2):31–52.

Børgesen, C.D. & Schaap, M.G. 2005. Point and parameter pedotransfer functions for water retention predictions for Danish soils. *Geoderma*. 127(1–2):154–167.

Botula, Y.D., Cornelis, W.M., Baert, G. & Van Ranst, E. 2012. Evaluation of pedotransfer functions for predicting water retention of soils in Lower Congo (D.R. Congo). *Agricultural Water Management*. 111:1–10.

Brooks, R.H. & Corey, A.T. 1966.

Campbell, G.S. 1985. *Soil physics with basic: transport models for soil – plant systems*. Amsterdam, Oxford, New York and Tokyo: Elsevier Science Publisher B.V.

Ceddia, M.B., Vieira, S.R., Villela, A.L.O., Mota, L. dos S., dos Anjos, L.H.C. & de Carvalho, D.F. 2009. Topography and spatial variability of soil physical properties. *Scientia Agricola*. 66(3):338–352.

Cornelis, W.M., Ronsyn, J., Van Meirvenne, M. & Hartmann, R. 2001. Evaluation of pedotransfer functions for predicting the soil moisture retention curve. *Soil Science Society of America Journal*. 65(3):638–648.

Cresswell, H.P., Green, T.W. & McKenzie, N.J. 2008. The adequacy of pressure plate apparatus for determining soil water retention. *Soil Science Society of America Journal*. 72(1):41.

Dane, J.H. & Hopmans, J.W. 2002. Pressure plate extractor. In Madison, W ed. J.H. Dane et al. (eds.). Soil Science Society of America *Methods of soil analysis: Part 4 physical methods*. 688–690.

Das, M. & Verma, O.P. 2011. Derivation and validation of pedotransfer functions for point estimation

of soil moisture in sandy to clayey soil texture. *Journal of Agricultural Physics*. 11(December 2017):21–25.

Deka, R.N., Wairiu, M., Mtakwa, P.W., Mullins, C.E., Veenedal, E.M. & Townend, J. 1995. Use and accuracy of the filter-paper technique for measurement of soil matric potential. *European Journal of Soil Science*. 46(2):233–238.

Dlapa, P., Hriník, D., Hrabovský, A., Šimkovic, I., Žarnovičan, H., Sekucia, F. & Kollár, J. 2020. The impact of land-use on the hierarchical pore size distribution and water retention properties in loamy soils. *Water*. 12(2):339.

Du, C. 2020. Comparison of the performance of 22 models describing soil water retention curves from saturation to oven dryness. *Vadose Zone Journal*. 19(1):1–20.

Filho, T.B.O., Ottoni, M.V., De Oliveira, M.B., De Macedo, J.R. & Reichardt, K. 2014. Revisiting field capacity (FC): Variation of definition of FC and its estimation from pedotransfer functions. *Revista Brasileira de Ciencia do Solo*. 38(6):1750–1764.

Flinchum, B.A., Holbrook, W.S., Grana, D., Parsekian, A.D., Carr, B.J., Hayes, J.L. & Jiao, J. 2018. Estimating the water holding capacity of the critical zone using near-surface geophysics. *Hydrological Processes*. 32(22):3308–3326.

Gamie, R. & De Smedt, F. 2018. Experimental and statistical study of saturated hydraulic conductivity and relations with other soil properties of a desert soil. *European Journal of Soil Science*. 69(2):256–264.

Gee, G.W., Ward, A.L., Zhang, Z.F., Campbell, G.S. & Mathison, J. 2002. The influence of hydraulic nonequilibrium on pressure plate data. *Vadose Zone Journal*. 1(1):172–178.

Ghanbarian-Alavijeh, B. & Millán, H. 2010. Point pedotransfer functions for estimating soil water retention curve. *International Agrophysics*. 24(3):243–251.

Givi, J., Prasher, S.O. & Patel, R.M. 2004. Evaluation of pedotransfer functions in predicting the soil water contents at field capacity and wilting point. *Agricultural Water Management*. 70(2):83–96.

Gupta, S.C. & Larson, W.E. 1979. Estimating soil water retention characteristics from particle size distribution, organic matter percent, and bulk density. *Water Resources Research*. 15(6):1633–1635.

Hahn, G.J. 1977. Fitting regression models with no intercept term. *Journal of Quality Technology*. 9(2):56–61.

Hillel, D. 1980. *Applications of soil physics*. New York: Academic Press.

Hillel, D. 2004. *Introduction to environmental soil physics*. New York: Academic Press.

Hodnett, M.G. & Tomasella, J. 2002. Marked differences between van Genuchten soil water-retention parameters for temperate and tropical soils: A new water-retention pedo-transfer functions developed for tropical soils. *Geoderma*. 108(3–4):155–180.

Kern, J.S. 2000. Geographic patterns of soil water-holding capacity in the contiguous United States. *Soil Science Society of America Journal*. 64(1):382–382.

Khlosi, M. 2015. Predicting water retention properties of dryland soils. University Gent. [Online], Available: https://biblio.ugent.be/publication/5812886/file/5812920.pdf.

Lu, N. 2016. Generalized soil water retention equation for adsorption and capillarity. *Journal of Geotechnical and Geoenvironmental Engineering*. 142(10):04016051.

Madi, R., Huibert De Rooij, G., Mielenz, H. & Mai, J. 2018. Parametric soil water retention models: A critical evaluation of expressions for the full moisture range. *Hydrology and Earth System Sciences*. 22(2):1193–1219.

McQueen, I.S. & Miller, R.F. 1974. Approximating soil moisture characteristics from limited data: Empirical evidence and tentative model. *Water Resources Research*. 10(3):521–527.

Merdun, H. 2006. Pedotransfer functions for point and parametric estimations of soil water retention curve. *Plant, Soil and Environment*. 52(7):321–327.

Minasny, B., McBratney, A.B. & Bristow, K.L. 1999. Comparison of different approaches to the development of pedotransfer functions for water retention curves. *Geoderma*. 93(3–4):225–253.

NCSS 12: Data Analysis & Graphics. 2019. [Online], Available: https://www.ncss.com/software/ncss/.

Nemes, A., Rawls, W.J. & Pachepsky, Y.A. 2006. Use of the nonparametric nearest neighbor approach to estimate soil hydraulic properties. *Soil Science Society of America Journal*. 70(2):327–336.

Nemes, A., Pachepsky, Y.A. & Timlin, D.J. 2011. Toward improving global estimates of field soil water capacity. *Soil Science Society of America Journal*. 75(3):807–812.

Pan, T., Hou, S., Liu, Y. & Tan, Q. 2019. Comparison of three models fitting the soil water retention curves in a degraded alpine meadow region. *Scientific Reports*. 9(1):1–12.

Patil, N.G. & Chaturvedi, A. 2012. Pedotransfer functions based on nearest neighbour and neural networks approach to estimate available water capacity of shrink-swell soils. *Indian Journal of Agricultural Sciences*. 82(1):35–38.

Phuong, N.M., Le Khoa, V. & Cornelis, W. 2014. Predicting soil water retention characteristics for Vietnam Mekong Delta soils. *IAHS-AISH Proceedings and Reports*. 363(October):392–398.

Puckett, W.E., Dane, J.H. & Hajek, B.F. 1985. Physical and mineralogical data to determine soil hydraulic properties. *Soil Science Society of America Journal*. 49(4):831–836.

Rawls, W.J. & Brakensiek, D.L. 1986. *Estimation of soil water retention and hydraulic properties*. H.J. Morel-Seytoux (ed.). Kluwer Academia Publishers.

Rawls, W.J., Brakensiek, D.L. & Saxton, K.E. 1982. Estimation of soil water properties. *Transactions of the ASAE*. 25(5):1316--1320 & 1328.

Rawls, W.J., Gimenez, D. & Grossman, R. 1998. Use of soil texture, bulk density, and slope of the water retention curve to predict saturated hydraulic conductivity. *Transactions of the ASAE*. 41(4):983–988.

Rawls, W.J., Pachepsky, Y. & Shen, M.H. 2001. Testing soil water retention estimation with the MUUF pedotransfer model using data from the southern United States. *Journal of Hydrology*. 251(3–4):177–185.

Reeve, M.J., Smith, P.D. & Thomasson, J. 1973. The effect of density on water retention properties of field soils. *Journal of Soil Science*. 24(3):355–367.

Schaap, M.G. & Bouten, W. 1996. Modeling water retention curves of sandy soils using neural networks. *Water Resources Research*. 32(10):3033–3040.

Shwetha, P. & Varija, K. 2013. Soil water retention prediction from pedotransfer functions for some Indian soils. *Archives of Agronomy and Soil Science*. 59(11):1529–1543.

Skalová, J., Èistý, M. & Bezák, J. 2011. Comparison of three regression models for determining water retention curves. *Journal of Hydrology and Hydromechanics*. 59(4):275–284.

Smith, C.W., Johnston, M.A. & Lorentz, S.A. 2001. The effect of soil compaction on the water retention characteristics of soils in forest plantations. *South African Journal of Plant and Soil*. 18(3):87–97.

Tietje, O. & Tapkenhinrichs, M. 1993. Evaluation of pedo-transfer functions. *Soil Science Society of America Journal*. 57(4):1088–1095.

Tomasella, J., Pachepsky, Y., Crestana, S. & Rawls, W.J. 2003. Comparison of two techniques to develop pedotransfer functions for water retention. *Soil Science Society of America Journal*. 67(4):1085–1092.

U.S. Department of Agriculture Bulletin 462. 1960. *Measuring soil water holding capacity*. Beltsville, Maryland.

Van den Berg, M., Klamt, E., Van Reeuwijk, L.P. & Sombroek, W.G. 1997. Pedotransfer functions for the estimation of moisture retention characteristics of Ferralsols and related soils. *Geoderma*. 78(3–4):161–180.

Van Genuchten, M.T. 1980. A closed-form equation for predicting the hydraulic conductivity of unsaturated soils. *Soil Science Society of America Journal*. 44(5):892–898.

Vermaak, J.J.G., Wates, J.A., Bezuidenhout, N. & Kgwale, D. 2004. *The evaluation of soil covers used in the rehabilitation of coal mines*. Vol. 1002/1/04. Water Research Commission.

Wösten, J.H.M., Lilly, A., Nemes, A. & Le Bas, C. 1999. Development and use of a database of hydraulic properties of European soils. *Geoderma*. 90(3–4):169–185.

Zhang, J.G., Chen, H.S., Su, Y.R., Kong, X.L., Zhang, W., Shi, Y., Liang, H.B. & Shen, G.M. 2011. Spatial variability and patterns of surface soil moisturein a field plot of karst area in southwest China. *Plant, Soil and Environment*. 57(9):409–417.

Chapter 5: Root development and the relationship between peak photosynthetic active leaf area and peak active vegetation biomass

5.1 Introduction

Three parameters of vegetation properties are important for long-term soil cover performance modelling *viz.* root development and photosynthetic active leaf area index (LAI) together with active vegetation biomass. Well-developed root systems with good vegetation cover are important for long-term soil cover performance (Mendez *et al.*, 2008; Norman *et al.*, 2006). Since soil cover properties can vary, the vegetation properties may be influenced by its properties. Bulk density can indirectly influence the root growth and in turn, can decrease plant growth and LAI. Plant biomass is an important factor of functional plant biology and growth analysis (Poorter & Nagel, 2000). Measurements of biomass are the basis for calculation of production and growth rate (Niklas & Enquist, 2002; Tackenberg, 2007; Wilson *et al.*, 1999). One of the acceptable measures to determine biomass, is above-ground biomass which is the measurement of oven-dried samples. In this direct method, leaves or shoots of plants are been harvested and dry weight was measured to determine active vegetation biomass at the end of the experiment. This method, however, can be time-consuming and labour intensive for sampling in large areas or a large number of plants. Photosynthetic active LAI defined as the green part of leaf area (m^2) per ground area (m^{-2}) which determines light interception and most importantly also plant productivity (Koester *et al.*, 2014; Launay & Guérif, 2003). The optimum or peak photosynthetic active LAI depends on species composition, developmental stage, topography, climatic factors, management practices and soil health (Jonckheere *et al.*, 2004). In addition, peak photosynthetic active LAI may vary due to leaf arrangement and the leaf shape can influence the pattern by which light is intercepted which can affect the plant growth (Brougham, 1958). The direct method of LAI measurement is the most accurate, but can be time-consuming. The non-destructive determination of LAI demands contemporary, high-cost equipment such as drones.

Active vegetation biomass and photosynthetic active LAI are dynamic parameters. They change from day to day and are influenced by rainfall and soil water content under semi-arid conditions. Data presented by Mitchell (1953) and Więckowski (1963) indicated that the photosynthetic active LAI to active vegetation biomass relationship may change during plant growth and with environmental conditions. In contrast, Frey & Moss (1976) found no change in LAI of barley during the growth periods. The peak season is the critical state during plant growth. This peak period is important to determine the rate of transpiration and evaporation and in determining biomass. In order to use photosynthetic active LAI as a tool to screen for plants with active vegetation biomass and or as a parameter in soil cover long-term performance modelling, it is important to understand the

relationship between LAI and the accumulation of biomass. According to Poorter *et al.* (2009), growth in leaf mass can result in an increase in biomass and in leaf area or thickness.

The objectives in this Chapter were (1) to determine peak photosynthetic active LAI values for store-and-release covers (SRCs) with good and poor vegetation cover; and (2) to determine the relationship between peak photosynthetic active LAI and peak active vegetation biomass.

5.2 Materials and methods

5.2.1 Vegetation descriptions

The biology of rehabilitated mining areas is dominated by grass species reaching a height of ~1.1 m tall such as *Cymbopogon excavatus* and *Hyparrhenia hirta*. Dominant grass species are *Themeda triandra*, *Sporobolus africanus* and *Setaria sphacelata var. Sphacelata,* whereas shrubs are *Setifera, Asparagus aethiopicus, Helichrysum aureonitens, Oxalis obliquifolia* and *Gnidia krau ssiana*. Some shrubs were identified at Opencast Backfilled Pit 1 & 2. Figure 5.1A provides an overview of the vegetation on the rehabilitated mining areas.

5.2.2 Effective root depth and development

Measurements were taken during the field experiment between the months of August and September 2018. Effective root depth and root development were described for the roots exposed in the profile pits, except D3-1 & 3-2, using the profile wall method of Böhm (1979). The exposed roots were marked with white PVA paint and photographed against a grid pattern (1×1 m) on the profile pit walls. The effect of bulk density on root development and penetration were described by using USDA (1996) general relationship of bulk density to root growth based on soil texture.

5.2.3 Above-ground biomass and leaf area index

The rainfall data was obtained from the weather station at Emalahleni, South Africa (TWC Product and Technology, 2021). To investigate the seasonal change and peak values, above-ground vegetation was collected destructively monthly from September 2018 to August 2019 near the soil/root profile. Each sampling was done on a 1 m^2 quadrant which was marked at each profile pit (one replicate per profile pit), except D3-1 & 3-2. The grasses were cut by hand with pruning shears at ground level, placed in plastic bags and transported to the University of Pretoria, Pretoria, South Africa. Examples of collected grass clippings are shown in Figure 5.1. The green grasses (photosynthetic active) were separated from the dead grasses to measure the photosynthetic active LAI and dead LAI using LI-3100C Area Meter as presented in Figure 5.2. Leave areas were measured in 10 000 cm^2, where the photosynthetic active and total leaf area values were divided with 10 000 cm^2 to determine the LAI of each profile pit which was expressed in $m^2.m^{-2}$. Following this, the green and dead grasses were oven-dried at 60°C and weighed several times until no mass losses occur. Active vegetation and dead dry biomass for each profile pit were calculated as follows:

Active vegetation or dead dry biomass = Dry weight × 1 $g.m^{-2}$ [Eq. 5.1]

where 1 m^2 is the area for each plots.

5.2.4 Data analysis

Total and vegetation active biomass was plotted from 2018–2019 and seasonal changes in total and photosynthetic active LAI were plotted. To explore how the photosynthetic active LAI related to active vegetation biomass, regression analyses were performed. The adjusted coefficient of determination (adjusted R^2) and root mean square error (RMSE) was used to examine how well the regression represented the relationship by using SigmaPlot software (SigmaPlot Team, 2014).

Figure 5.1: Collecting of grass clippings in a 1 m^2 area during the peak season at Discard Dump 2 (A) and vegetation cover after the grass clippings at Discard Dump 2 (B).

Figure 5.2: Relative low photosynthetic active leaf area for grasses as the leaves are narrow (A) and the LI-3100C Area Meter used to determine the leaf area index (B).

5.3 Results and discussion

5.3.1 Effective root depth and development

Bulk density had a significant effect on root development and penetration. The bulk densities where restriction of root development is initiated and root penetration is limited, are summarised in Table 5.1.

Root depth, distribution and development showed a close inverse relationship with extent of compaction/bulk density. The root depth varied according to the vegetation condition (Figure D1–D5

in Appendix D). A root depth of 75% of the cover thickness was specified for vegetation in a fair condition. A deeper root system was associated with good vegetation conditions, and shallower roots with poor vegetation conditions (Pierret *et al.*, 2016). Root development occurred throughout the cover thickness of the moderately dense SRCs (Table 5.1 and Figures D1A & B, D2A, D4A & B, D5B). The root depths of 400–700 mm based on root map diagrams determined by Schoeman *et al.* (2002) for reconstructed soil covers at the Mpumalanga Highveld rehabilitated mines, showed bulk densities lower than 1.750–1.800 g.m^{-3} which did not limit root development. Another study by Versveld *et al.* (1998) indicated that 90% of the root mass occurred in the upper 600 mm of rehabilitated land at coal and gold mines where root development was not impeded. Although the bulk density of P1-3 and 0–500 mm of P2-2 was 1.813 and 1.872 g.m^{-3}, respectively, the root distribution was not affected by bulk density (Table 2.17 in Chapter 2). Taylor & Brar (1991) concluded the soil compaction in some cases does not alter the root development and may have normal above-ground growth if the vegetation receive sufficient water and nutrients.

Root depth and development (~95% root distribution) was limited to the upper 150 mm soil layer at the very dense SRCs, even though the covers were constructed with sufficiently thick growth medium and with suitable growth medium material. Interestingly, the root density in the upper 150 mm soil layer of the very dense SRCs was higher compared to the moderately dense SRCs (Figures D1–D5 in Appendix D). It is important to note that the bulk densities of D2-1 were below 1.800 g.cm^{-3} (Table 2.17 in Chapter 2), however the nutrient availability (Table 2.18 in Chapter 2) and water-holding capacity (Table 4.2 in Chapter 4) were low with gravel content of 10.25% in the 0–450 mm soil cover layer (Table 2.16 in Chapter 2). The bulk density of P2-1 in 100 mm soil layer was 1.740 g.cm^{-3} (Table 2.17 in Chapter 2), but the nutrient availability (Table 2.18 in Chapter 2) was low with electrical conductivity of saturated paste (EC_e) higher than 200 mS.m^{-1} (Table 2.18 in Chapter 2), and the 100–300 mm soil layer's bulk density was 2.286 g.cm^{-3} (Table 2.17 in Chapter 2) which also could prevent further root growth.

Table 5.1: Depth of root development of moderately- and very dense SRCs.

Soil cover condition	Profile pit	Average bulk density (g.cm^{-3})	Root depth (mm)
Moderately dense	D1-1	1.545	900
	D1-2	1.690	600
	D1-3	1.590	550
	P1-3	1.813	350
	P1-4	1.643	400
	P2-2	1.710	700
	P2-3	1.465	500
Very dense	D2-1	1.785	100
	D2-2	1.885	100
	P1-1	2.197	100
	P1-2	1.800	150
	P2-1	1.995	100

These results are an indication of poor cover construction practices resulting in shallow compacted layer limiting root penetration to the surface. Plant water uptake is strongly affected by high bulk densities and the hardsetting behaviour of the cover soil which can limit the root growth from exploiting soil water at a deeper level (Lardner *et al.*, 2011; Twum *et al.*, 2015). Additionally, soils with low nutrient availability, high EC_e and low WHC can limit the root growth. Moreover, grasses growing where root penetration is limited are likely to be at greater risk of drought related mortality (Ashby, 1997; Misra & Gibbon, 1996).

5.3.2 Above-ground biomass and leaf area index

5.3.2.1 *Total above-ground and active vegetation biomass*

The total above-ground biomass and active vegetation biomass together with the rainfall data are shown in Figures 5.3 & 5.4, where the data were split into moderately- and very dense SRCs. The peak active vegetation biomass (Figures 5.3B & 5.4B) occurred in January to March with rainfall of 93.5–181.1 mm during that period. After the peak season when the rainfall started to decrease, the highest total above-ground biomass on moderately dense SRCs was 956.48 on P1-4 followed by P1-3 (794.41 $g.m^{-2}$), D1-2 (769.05 $g.m^{-2}$), D1-3 (669.51 $g.m^{-2}$), D1-1 (645.07 $g.m^{-2}$), where P2-2 (565.1 $g.m^{-2}$) and P2-3 (500.6 $g.m^{-2}$) were the lowest (Figure 5.3A). The vegetation active biomass (Figure 5.3B) during peak season ranged between 186.14–465.80 $g.m^{-2}$. The highest rainfall of 181.1 mm was in January, where P2-3 had the highest vegetation active biomass with 468.8 $g.m^{-2}$ followed by P1-4 of 356.80 $g.m^{-2}$ in February (147.8 mm rainfall). On very dense SRCs, profile pits D2-1 (304.52 $g.m^{-2}$) & 2-2 (356.90 $g.m^{-2}$) had the highest total above-ground biomass during the peak season (Figure 5.4A). The profile pit, P1-1 with a value of 892.63 $g.m^{-2}$, had the highest total above-ground biomass after the peak season followed by P1-2 with 705.43 $g.m^{-2}$ and P2-1 with 535.00 $g.m^{-2}$. All the peak vegetation active biomasses of very dense SRCs occurred during the peak season ranging between 105.10–356.81 $g.m^{-2}$ (Figure 5.4B). The highest vegetation active biomass of 356.81 $g.m^{-2}$ was profile pit of P1-1, whereas the lowest vegetation active biomass was 105.10 $g.m^{-2}$ (D2-1) in March.

Since above-ground biomass is dependent on rainfall (Yang *et al.*, 2009), the vegetation active biomass increased with increasing rainfall (Figures 5.3B & 5.4B). Rad *et al.* (2011) observed similar results, where the above-ground biomass increased with increasing rainfall and, in turn with increased soil water content in dry climatic conditions. After March with decreasing rainfall, the total dead biomass increased with decreasing vegetation active biomass, except D2-1 & 2-2. In February, the dead biomass of D2-1 (203.62 $g.m^{-2}$) & 2-2 (185.98 $g.m^{-2}$) was higher compared to the vegetation active biomass due to high bulk density. High bulk density or hardsetting with low soil nutrient availability had a negative impact on the vegetation growth at discard dumps, D2-1 & D2-2 (P = 0.037), but not at opencast backfilled pits, P1-1 & 1-2 and P2-1 (P = 0.256). However, the vegetation active biomass of P1-3 & 1-4 and P2-2 & 2-3 were higher compared to the P1-1 & 1-2 and P2-1.

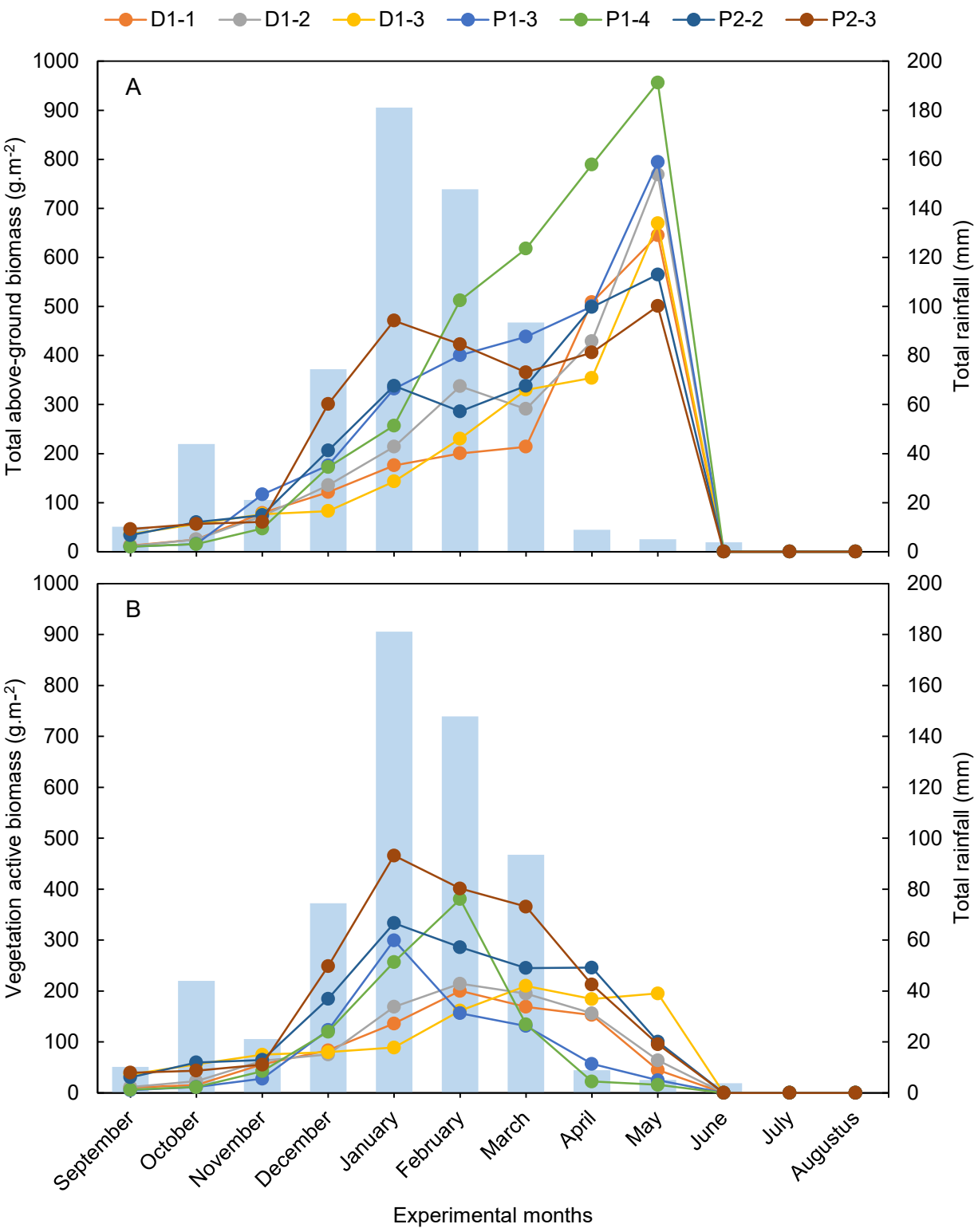

Figure 5.3: Monthly total above-ground biomass (A) and vegetation active biomass (B) with total rainfall of moderately store-and-release covers during 2018–2019.

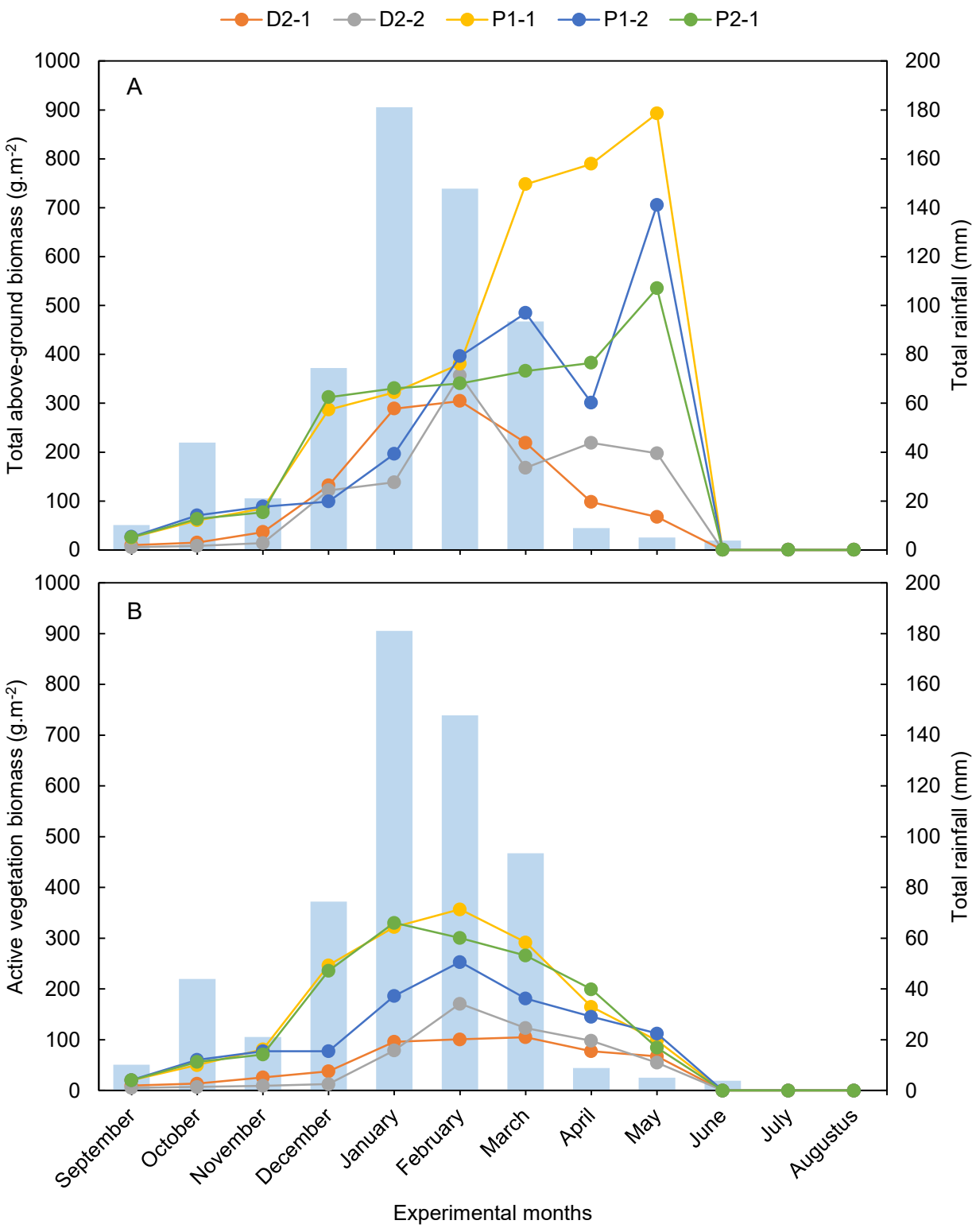

Figure 5.4: Monthly total above-ground biomass (A) and vegetation active biomass (B) with total rainfall of very dense store-and-release covers during 2018–2019.

Due to shorter root lengths and root distribution in the upper 100 mm soil layer with reduced plant water uptake on very dense SRCs, the vegetation active biomass decreased. Similar results were found by Wang *et al.* (2020) that there was little or no vegetation cover in the area with high bulk density (> 1.700 $g.cm^{-3}$) at a rehabilitated mine, Pinglu District, Shuozhou City, Shanxi Province, China. In the study of Stirzaker *et al.* (1996), the roots of barley plants were limited in the upper 80 mm soil layer with a bulk density of 1.780 $g.cm^{-3}$ and a decreased plant growth of about 20%. Examples of the influence of high bulk density on plant growth were also studied by Colombi *et al.* (2017); Masle & Passioura (1987) and Richards & Rowe (1977).

5.3.2.2 *Total and photosynthetic active leaf area index*

The total LAI and photosynthetic active LAI with the rainfall data of moderately- and very dense SRCs are shown in Figures 5.5 & 5.6. The seasonal total LAI varied on an annual basis between dry and wet seasons in the response to the condition of vegetation with moisture availability. The highest total LAIs of moderately SRCs were in May with values of 0.950–2.145 $m^2.m^{-2}$, where D1-3 had the highest total LAI and D1-1 the lowest (Figure 5.5A). In Figure 5.5B, during the peak season, photosynthetic active LAI ranged between 0.800–1.950 $m^2.m^{-2}$ with an average of 1.187 $m^2.m^{-2}$. The profile pit, P2-3, had the highest photosynthetic active LAI followed by P2-2 with the LAI of 1.600 $m^2.m^{-2}$ and the LAI of P1-3 the lowest.

The vegetation covers of moderately dense SRCs were good (Tables 2.3 to 2.5, 2.10, 2.11, 2.13 & 2.14 in Section 2.3.1 of Chapter 2). According to Vermaak *et al.* (2004), the LAI of a good vegetation cover is 3 $m^2.m^{-2}$ at rehabilitated mines in Kwa-Zulu-Natal, which was much higher than the average photosynthetic active LAIs of the current study. Wang *et al.* (2019) further concluded that a good vegetation cover for grassland was LAI > 2 $m^2.m^{-2}$ with vegetation active biomass above 500 $g.m^{-2}$. He & Guo (2006) found that the LAI of grassland was 3 $m^2.m^{-2}$, but the grasses were close to a river with higher soil water content. The study of Banerjee *et al.* (2011) observed that the LAI of grassland is dependent on the topographic factors and thereby, also the level of soil water content in the soils and with the rainfall. Lower rainfall with subsequent lower soil water content in the soil covers may be the other reason for lower LAI. Soil water content plays an important role in the nutrient-uptake rate (Davidson *et al.*, 2000) of plants under semi-arid conditions, which in turn determine the vegetation growth of grasslands. Flanagan *et al.* (2002) further observed a positive linear relationship between LAI and soil water content in a rainy season. Nevertheless, the results of Haupt (2018) supported the result of the current study, where the peak photosynthetic LAI value of grassland was ~1.22 $m^2.m^{-2}$ on a rehabilitated mine in Mpumalanga Highveld, South Africa. Furthermore, the peak photosynthetic LAI for grassland at the Rehabilitation Ranger Uranium mine in northern Australia was 0.80–1.20 $m^2.m^{-2}$ (Hollingsworth, 2010). However, Zhang *et al.* (2009) observed similar results to the grassland's LAIs values of ~1.10 $m^2.m^{-2}$ for a good vegetation cover under a semi-arid climate condition. The current study may imply that lower LAI of grassland with good vegetation cover can be expected when the site is not nearby at a riverbank and have low soil

water content. Additionally, the peak photosynthetic LAI of moderately dense SRCs suggested that the rehabilitated vegetation has reached conditions that are similar to an undisturbed state under semi-arid conditions.

The total LAIs on very dense SRCs were 1.100–1.370 $m^2.m^{-2}$ in May, except D2-1 & 2-2 (Figure 5.6A). The highest total LAI of D2-1 was 0.903 $m^2.m^{-2}$ in January and for D2-2 it was 0.967 $m^2.m^{-2}$ in February. Photosynthetic LAIs in the peak season were 0.401–1.108 $m^2.m^{-2}$ with an average of 0.757 $m^2.m^{-2}$ (Figure 5.6B). The profile pit, P1-1, had the highest photosynthetic LAI followed by P2-1 with a value of 1.021 $m^2.m^{-2}$. The lowest photosynthetic active LAI occurred at D2-1 followed by D2-2 (0.491 $m^2.m^{-2}$). The low photosynthetic active LAIs of very dense SRCs were expected since the vegetation active biomasses were low. Goswami *et al.* (2015) found similar results namely that decreased above-ground biomass that caused a decrease in photosynthetic active LAI. Moreover, the average photosynthetic active LAI of very dense SRCs was ~40% less than the average photosynthetic LAI of moderately dense SRCs. The average photosynthetic active LAI of very dense SRCs with poor vegetation cover (Tables 2.6–2.9 & 2.12 in Section 2.3.1 of Chapter 2) were lower than the 1 $m^2.m^{-2}$ of the LAI value used by Vermaak *et al*. (2004). In addition, He & Guo (2006) supported more or less similar photosynthetic active LAIs for grassland ~0.440–1.000 $m^2.m^{-2}$ of poor vegetation covers. In conclusion, the good or poor vegetation cover of the grassland ecosystem may reflect the difference in richness and abundance of species or patchy growth of species due to poor root growth as explained in Figure 5.7.

5.3.2.3 *Relationship between photosynthetic active leaf area index and peak vegetation active biomass*

The linear and power-law relationship between photosynthetic active LAI and vegetation active biomass of all the profile pits are presented in Figures 5.8A & 5.8B, respectively. The RMSE of linear and power-law relationship was 0.198 $m^2.m^{-2}$ and 0.170 $m^2.m^{-2}$, respectively. Both relationships performed very well, however the power-law relationship performed the best. The strong non-linear relationship between photosynthetic active LAI and vegetation active biomass may suggest that photosynthetic active LAI saturated for higher values of biomass. Whereas, the strong linear relationship between photosynthetic active LAI and vegetation active biomass may suggest no saturation in the measurement of biomass from LAI. The majority of international studies found a better linear relationship rather than a power-law relationship. In the study of Aase (1978), a strong and linear relationship of R^2 = 0.951 was reported. More examples of the linear relationship between photosynthetic active LAI and vegetation active biomass were reported by Addai *et al.* (2015), Aparicio *et al.* (2000), Ashley *et al.* (1965) and Gonzalez-Benecke *et al.* (2018). However, in the Weraduwage *et al.* (2015) study, a non-linear relationship between LAI and biomass was found.

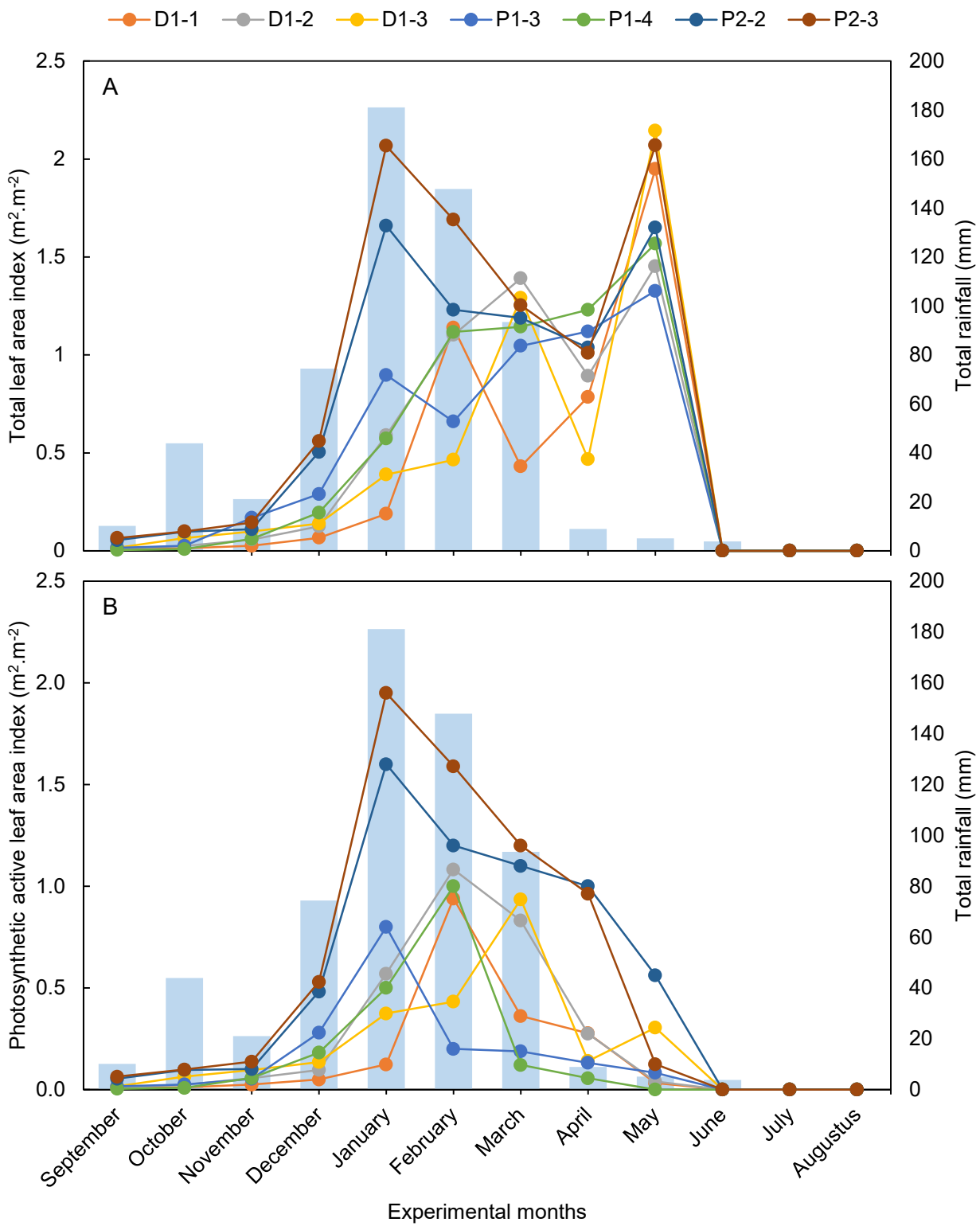

Figure 5.5: Monthly total leaf area index (A) and photosynthetic active leaf area index (B) with total rainfall of moderately store-and-release covers during 2018–2019.

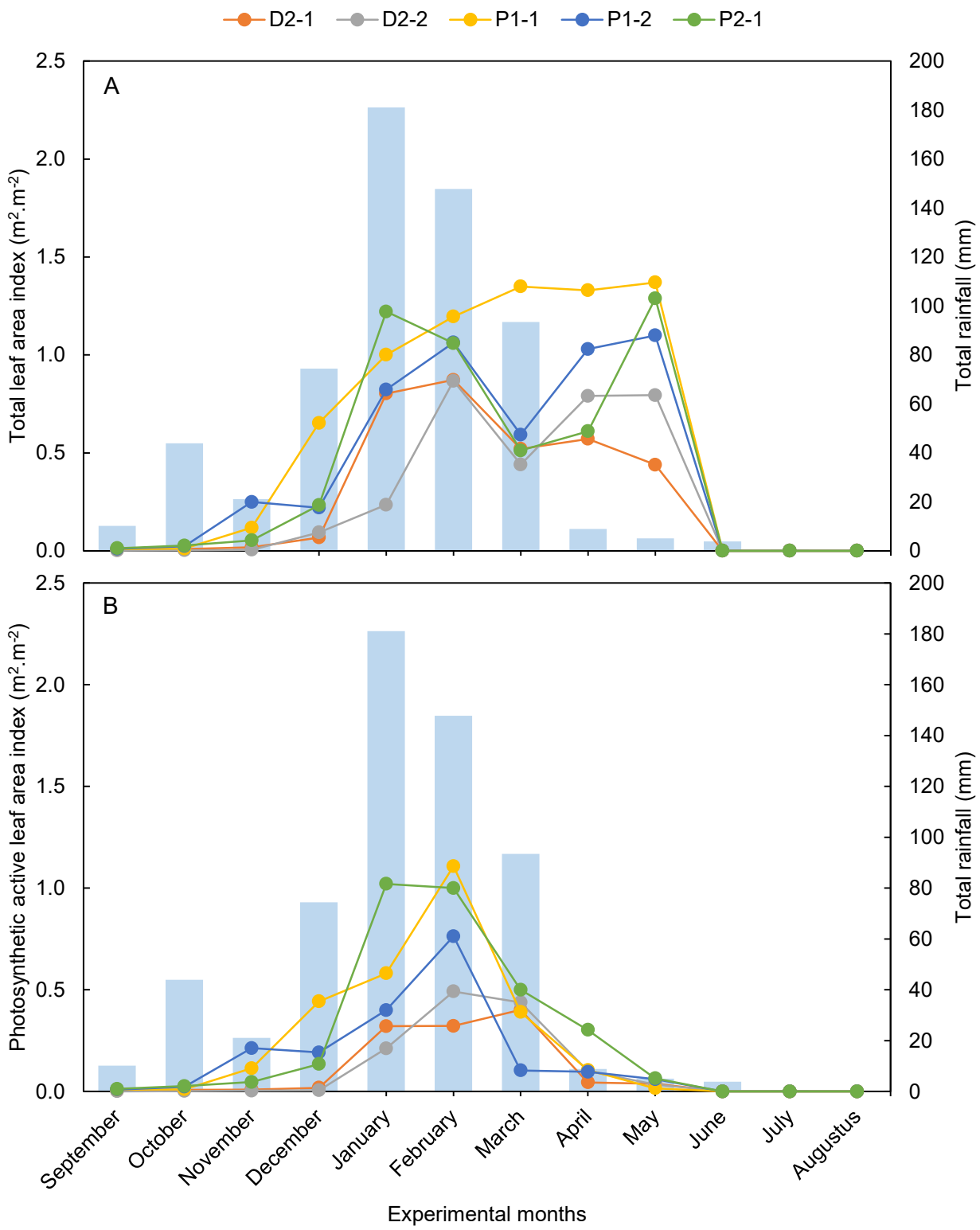

Figure 5.6: Monthly total leaf area index (A) and photosynthetic active leaf area index (B) with total rainfall of very dense store-and-release covers during 2018–2019.

Figure 5.7: The grassland ecosystem at Discard Dump 1 (A) and Discard Dump 2 (B) photographed on February 2018. The richness and abundance of grasses at Discard Dump 1 were higher compared to Discard Dump 2. The grasses at Discard Dump 1 were more green and evenly distributed throughout the dump area due to low bulk density and good root distribution. The grasses at Discard Dump 2 were patchy, smaller and with less greenness due to high bulk density. Moreover, the dead biomass of leaves was higher compared to the vegetation active biomass. High bulk density can decrease the soil nutrient availability, water-holding capacity and infiltration rate. However, one purpose of store-and-release covers is to decrease the water infiltration into the soil, but this is the function of the water retention layer (sublayer). The sandier growth medium is primarily for plant growth. Due to high bulk density which caused poor root distribution in the upper 150 mm soil layer with reduced plant water uptake, led to decreasing growth of grasses. In addition, the surface hardness of Discard Dump 2 was more susceptible to runoff water and erosion which isn't sustainable.

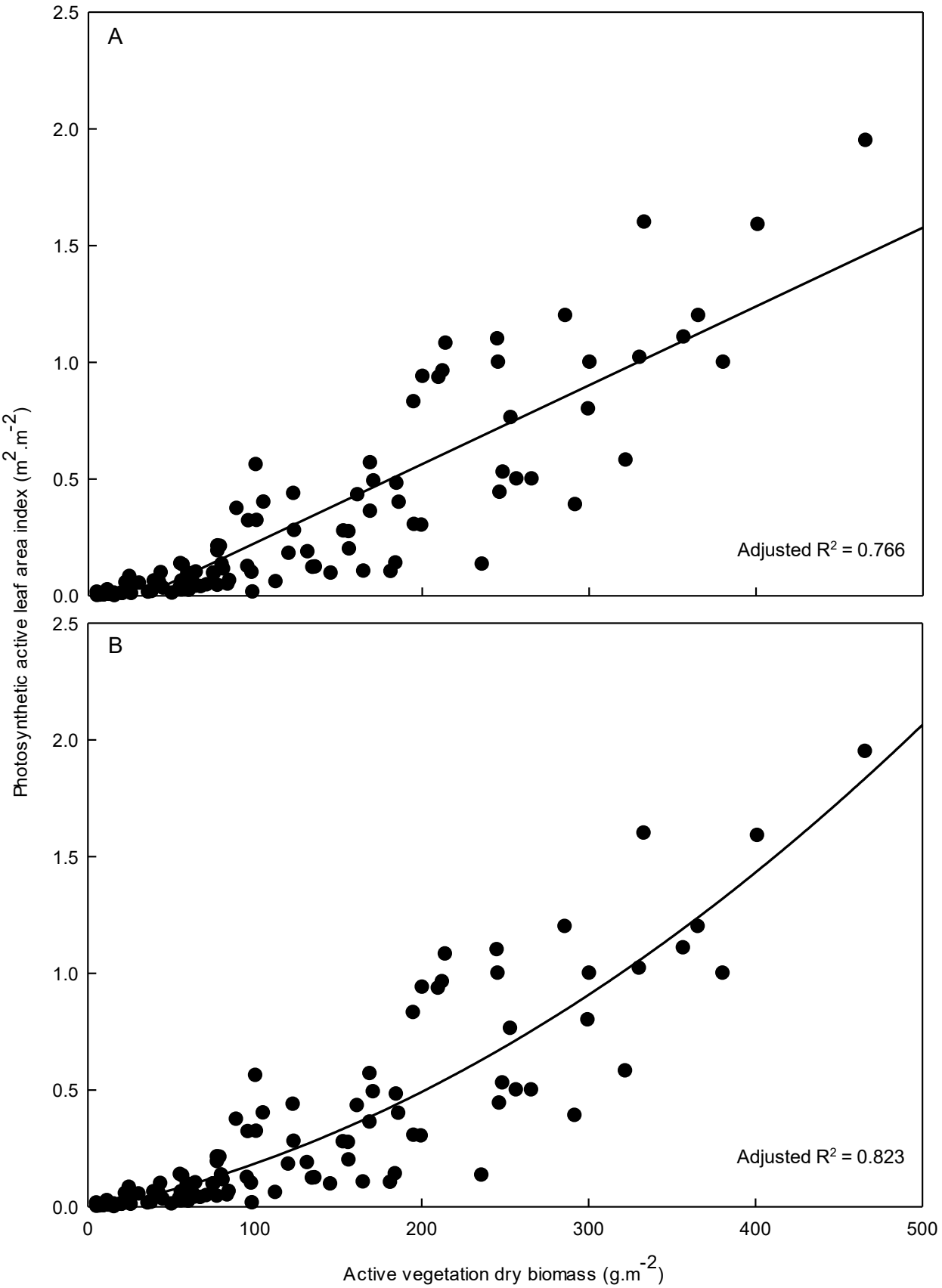

Figure 5.8: The linear (A) and power-law relationship (B) between photosynthetic active leaf area index and active vegetation biomass for all profile pits of store-and-release covers.

Nonetheless, an increase in vegetation active biomass increases LAI or *vice versa*. The results are in conformity with the findings of Ahlrichs & Bauer (1982). In their findings, LAI predicted the photosynthetic capacity of a plant and served as a reference tool for plant growth and development. An increase in LAI, increased light interception and sink strength (Pearce *et al.*, 1965). Therefore, the higher LAI, the higher the photosynthetic activity and assimilate partitioning resulting in better plant growth. Brougham (1956), Rosenthal & Vanderlip (2004) and Tsialtas & Maslaris (2008) made similar observations, supporting the evidence regarding relationship between LAI and plant growth.

5.4 Conclusion

High bulk density had a significant effect on root and plant growth. Higher bulk density impedes root exploration of the soil depth and can lead to differences in plant survival under semi-arid conditions and drought stress. Good vegetation covers reflected good root development, high active vegetation biomass and high photosynthetic active LAI. Poor vegetation cover caused by high bulk density was patchy with poor root development, low active vegetation biomass and low photosynthetic active LAI.

The active vegetation biomass and photosynthetic active LAI changed monthly and were influenced by rainfall and soil water availability. The peak active vegetation biomass and photosynthetic active LAI occurred when the rainfall was in maximum between January to March. After the peak season, dead biomass and LAI increased with decreasing inactive vegetation biomass and photosynthetic active LAI. In the current study, the average photosynthetic active LAI values for good and poor vegetation cover were ~1.2 and 0.8 $m^2.m^{-2}$, respectively. The published LAI value of 3 and 1 $m^2.m^{-2}$ for good and poor vegetation covers, respectively, of SRCs in Mpumalanga Highveld, should be exercised with caution when applied to a long-term soil cover performance model. Reasons for lower LAI may include, amongst others, lower rainfall with lower soil water content and may also be topographic locations and different grass species. Linear and the power-law relationship between photosynthetic active LAI and active vegetation biomass performed well, based on statistical analysis. The power-law relationship performed better than the linear relationship, although both relationships showed increased photosynthetic active LAI as the active vegetation biomass increased.

5.5 References

Aase, J.K. 1978. Relationship between leaf area and dry matter in winter wheat. *Agronomy Journal*. 70(4):563–565.

Addai, I.K. & Alimiyawo, M. 2015. Graphical determination of leaf area index and its relationship with growth and yield parameters of Sorghum (*Sorghum bicolor* L. Moench) as affected by fertilizer application. *Journal of Agronomy*. 14(4):272–278.

Ahlrichs, J.S. & Bauer, M.E. 1982. Relation of agronomic and multispectral reflectance characteristics of spring wheat canopies. *Purdue University, LARS Technical Report*. 121082(May 1975).

Aparicio, N., Villegas, D., Casadesus, J., Araus, J.L. & Royo, C. 2000. Spectral vegetation indices as nondestructive tools for determining durum wheat yield. *Agronomy Journal*. 92(1):83–91.

Ashby, W.C. 1997. Soil ripping and herbicides enhance tree and shrub restoration on stripmines. *Restoration Ecology*. 5(2):169–177.

Ashley, D.A., Doss, B.D. & Bennett, O.L. 1965. Relation of cotton leaf area index to plant growth and fruiting. *Agronomy Journal*. 57(1):61–64.

Banerjee, S., He, Y., Xulin & Si, B.C. 2011. Spatial relationships between leaf area index and topographic factors in a semiarid grassland: Joint multifractal analysis. *Australian Journal of Crop Science*. 5(6):756–763.

Böhm, W. 1979. *Methods of studying root systems*. Berlin: Springer.

Brougham, R. 1956. Effect of intensity of defoliation on regrowth of pasture. *Australian Journal of Agricultural Research*. 7(5):377.

Brougham, R.W. 1958. Interception of light by the foliage of pure and mixed stands of pasture plantsr. *Australian Journal of Agricultural Research*. 9(1):39–52.

Colombi, T., Kirchgessner, N., Walter, A. & Keller, T. 2017. Root tip shape governs root elongation rate under increased soil strength. *Plant Physiology*. 174(4):2289–2301.

Davidson, E.A., Verchot, L. V., Henrique, C., Ackerman, I.L. & Carvalho, J.E.M. 2000. Effects of soil water content on soil respiration in forests and cattle pastures of eastern Amazonia. *Biogeochemistry*. 48:53–69.

Flanagan, L.B., Wever, L.A. & Carlson, P.J. 2002. Seasonal and interannual variation in carbon dioxide exchange and carbon balance in a northern temperate grassland. *Global Change Biology*. 8(7):599–615.

Frey, N.M. & Moss, D.N. 1976. Variation in RuDPCase activity in barley. *Crop Science*. 16(2):209–

213.

Gonzalez-Benecke, C.A., Flamenco, H.N. & Wightman, M.G. 2018. Effect of vegetation management and site conditions on volume, biomass and leaf area allometry of four coniferous species in the Pacific Northwest United States. *Forests*. 9(9).

Goswami, S., Gamon, J., Vargas, S. & Tweedie, C. 2015. Relationships of NDVI, biomass, and leaf area index (LAI) for six key plant species in Barrow, Alaska. *PeerJ PrePrints*. 3(e913v1).

Haupt, S.A. 2018. *Satellite monitoring of post-mining rehabilitation and the quantification of backfill dynamics using differential SAR interferometry.* Degree of Master of Science, Stellenbosch University.

He, Y. & Guo, X. 2006. Leaf area index estimation using remotely sensed data for Grasslands National Park. *Prairie Perspectives*. 105–117. [Online], Available: http://pcag.uwinnipeg.ca/Prairie-Perspectives/PP-Vol09/PP_Vol-09-1.pdf#page=111.

Hollingsworth, I.D. 2010. *Mine landform design using natural analogues*. Doctor degree of Philisophy, The University of Sydney.

Jonckheere, I., Fleck, S., Nackaerts, K., Muys, B., Coppin, P., Weiss, M. & Baret, F. 2004. Review of methods for in situ leaf area index determination Part I. Theories, sensors and hemispherical photography. *Agricultural and Forest Meteorology*. 121(1–2):19–35.

Koester, R.P., Skoneczka, J.A., Cary, T.R., Diers, B.W. & Ainsworth, E.A. 2014. Historical gains in soybean (*Glycine max Merr.*) seed yield are driven by linear increases in light interception, energy conversion, and partitioning efficiencies. *Journal of Experimental Botany*. 65(12):3311–3321.

Lardner, T., Worthington, T., Braimbridge, M., Vlahos, S. & Tibbett, M. 2011. Optimising soil physical properties for rehabilitation of mined land-effects of tine type on soil strength and root proliferation. *Proceedings of the Sixth International Conference on Mine Closure*. 153–162.

Launay, M. & Guérif, M. 2003. Ability for a model to predict crop production variability at the regional scale: An evaluation for sugar beet. *Agronomie*. 23(2):135–146.

Masle, J. & Passioura, J.B. 1987. The effect of soil strength on the growth of young wheat plants. *Australian Journal of Plant Physiology*. 14(6):643–656.

Mendez, M.O. & Maier, R.M. 2008. Phytostabilization of mine tailings in arid and semiarid environments - An emerging remediation technology. *Environmental Health Perspectives*. 116(3):278–283.

Misra, R.K. & Gibbons, A.K. 1996. Growth and morphology of eucalypt seedling-roots, in relation to soil strength arising from compaction. *Plant and Soil*. 182(1):1–11.

Mitchell, K.J. 1953. Influence of light and temperature on the growth of ryegrass (*Lolium spp*.): I. Pattern of vegetative development. *Physiologia Plantarum*. 6(1):21–46.

Niklas, K.J. & Enquist, B.J. 2002. On the vegetative biomass partitioning of seed plant leaves, stems, and roots. *American Naturalist*. 159(5):482–497.

Norman, M.A., Koch, J.M., Grant, C.D., Morald, T.K. & Ward, S.C. 2006. Vegetation succession after bauxite mining in western Australia. *Restoration Ecology*. 14(2):278–288.

Pearce, R.B., Brown, R.H. & Blaser, R.E. 1965. Relationships between leaf area index, light interception and net photosynthesis in orchardgrass. *Crop Science*. 5(6):553–556.

Pierret, A., Maeght, J.L., Clément, C., Montoroi, J.P., Hartmann, C. & Gonkhamdee, S. 2016. Understanding deep roots and their functions in ecosystems: An advocacy for more unconventional research. *Annals of Botany*. 118(4):621–635.

Poorter, H. & Nagel, O. 2000. The role of biomass allocation in the growth response of plants to different levels of light, CO_2, nutrients and water: A quantitative review. *Australian Journal of Plant Physiology*. 27(6):595–607.

Poorter, H., Niinemets, Ü., Poorter, L., Wright, I.J. & Villar, R. 2009. Causes and consequences of variation in leaf mass per area (LMA): A meta-analysis. *New Phytologist*. 182(3):565–588.

Rad, M.H., Assare, M.H., Banakar, M.H. & Soltani, M. 2011. Effects of different soil moisture regimes on leaf area index, specific leaf area and water use efficiency in Eucalyptus (*Eucalyptus camaldulensis* Dehnh) under dry climate conditions. *Asian Journal of Plant Sciences*. 10(5):294–300.

Richards, D. & Rowe, R.N. 1977. Effects of root restriction, root pruning and 6-benzylaminopurine on the growth of peach seedlings. *Annals of Botany*. 41(4):729–740.

Rosenthal, W.D. & Vanderlip, R.L. 2004. Simulation of individual leaf areas in grain sorghum. *Agronomie*. 24(8):493–501.

Schoeman, J.L., van der Walt, M., Monnik, K.A., Thackrah, J., Malherbe, J. & Le Roux, R.E. 2002. Development and application of a land capability classification system for South Africa. Pretoria.

SigmaPlot Team. 2014. [Online], Available: www.systatsoftware.com%0Afrom.

Stirzaker, R.J., Passioura, J.B. & Wilms, Y. 1996. Soil structure and plant growth: Impact of bulk density and biopores. *Plant and Soil*. 185(1):151–162.

Tackenberg, O. 2007. A new method for non-destructive measurement of biomass, growth rates, vertical biomass distribution and dry matter content based on digital image analysis. *Annals of Botany*. 99(4):777–783.

Taylor, H.M. & Brar, G.S. 1991. Effect of soil compaction on root development. *Soil and Tillage Research*. 19(2–3):111–119.

Tsialtas, J.T. & Maslaris, N. 2008. Evaluation of a leaf area prediction model proposed for sunflower. *Photosynthetica*. 46(2):294–297.

TWC Product and Technology. 2021. *South Africa weather history weather underground*.

Twum, E.K.A. & Nii-Annang, S. 2015. Impact of soil compaction on bulk density and root biomass of Quercus petraea L. at reclaimed post-lignite mining site in Lusatia, Germany. *Applied and Environmental Soil Science*. 2015(October 2015):1–5.

U.S. Department of Agriculture. 1996. Soil quality indicators: Bulk Density. *Natural Resources Conservation Service*. 192(April):1836–41.

Vermaak, J.J.G., Wates, J.A., Bezuidenhout, N. & Kgwale, D. 2004. *The evaluation of soil covers used in the rehabilitation of coal mines*. Vol. 1002/1/04. Water Research Commission.

Versveld, D.B., Le Maitre, D.C. & Chapman, R.A. 1998. *Alien invading plants and water resources in South Africa: A preliminary assessment*. Pretoria.

Wang, J., Xiao, X., Bajgain, R., Starks, P., Steiner, J., Doughty, R.B. & Chang, Q. 2019. Estimating leaf area index and aboveground biomass of grazing pastures using Sentinel-1, Sentinel-2 and Landsat images. *ISPRS Journal of Photogrammetry and Remote Sensing*. 154(January):189–201.

Wang, S., Cao, Y., Pietrzykowski, M., Zhou, W., Zhao, Z. & Bai, Z. 2020. Spatial distribution of soil bulk density and its relationship with slope and vegetation allocation model in rehabilitation of dumping site in loess open-pit mine area. *Environmental Monitoring and Assessment*. 192(11).

Weraduwage, S.M., Chen, J., Anozie, F.C., Morales, A., Weise, S.E. & Sharkey, T.D. 2015. The relationship between leaf area growth and biomass accumulation in Arabidopsis thaliana. *Frontiers in Plant Science*. 6(APR):1–21.

Więckowski, S. 1963. The influence of temperature and light intensity on the leaf growth and chlorophyll synthesis. *Acta Societatis Botanicorum Poloniae*. 32(4):719–730.

Wilson, P.J., Thompson, K. & Hodgson, J.G. 1999. Specific leaf area and leaf dry matter content as alternative predictors of plant strategies. *New Phytologist*. 143(1):155–162.

Yang, Y.H., Fang, J.Y., Pan, Y.D. & Ji, C.J. 2009. Aboveground biomass in Tibetan grasslands. *Journal of Arid Environments*. 73(1):91–95.

Zhang, N. & Zhao, Y.S. 2009. Estimating leaf area index by inversion of reflectance model for semiarid natural grasslands. *Science in China, Series D: Earth Sciences*. 52(1):66–84.

Chapter 6: General conclusions and research recommendations

6.1 General conclusions

6.1.1 Soil cover-, hydraulic- and vegetation properties of store-and-release covers

The soil covers of rehabilitated mines on the Mpumalanga Highveld were (> 20 years old) monolithic or dual-layered store-and-release covers (SRCs) with lengthy exposure to prevailing climatic conditions. Since soil properties can affect the long-term performance of SRCs, selecting soil texture type is the crucial step during a SRC design. The growth medium (top layer) of a dual-layered SRC was constructed using apedal-B soil layer and the soil textural classes were sandy loam or sandy clay loam. The water retention layer (sublayer) were constructed from loamy to clayey plinthic soil layers. Monolithic SRCs were constructed using apedal-B soil layers and the soil textural classes were sandy loam and sandy clay loam. All the soil cover layers had low or medium plasticity index and swelling potential, excluding the water retention layer of D2-2, which had a high plasticity index. A high plasticity index together with high swelling potential can be problematic since it can create preferential flows. Good vegetation growth with limiting oxygen- and water ingress is the purpose of SRCs. The soil textures types for growth medium and water retention layers for the SRC in the current study were favourable in terms of hydraulic and vegetation properties.

The following conclusions were reached regarding the moderately dense soil cover conditions. (1) Sandier growth mediums had higher saturated hydraulic conductivity (K_{sat}) values with steeper slopes of the desaturation function due to more macropores. Good vegetation covers and good root growth due to higher soil nutrient availability were observed in the growth medium as well as in monolithic SRCs. The two properties of sandier growth medium indicate soil water can easily be removed *via* evapotranspiration and that good root growth can be supported. (2) The clayey water retention layers had lower K_{sat} values, but higher water-holding capacity (WHC). Together with the low K_{sat} and high WHC, the slower desaturation function in the soil water retention curve (SWRC) of clayey soils can attribute to higher water retention. Higher water retention indicates a high capillary potential which can limit oxygen- and water ingress into coal discard or spoil. Importantly, after >20 years the clayey water retention layers had K_{sat} values similar to that of natural soils, whereas the sandier growth medium had lower K_{sat} values than the threshold due to lower resistance to compaction. However, the lower K_{sat} values of the sandier growth medium did not impede the long-term performance of moderately dense SRCs. Most of the WHC values of moderately dense SRCs were similar to the threshold criteria range of soils, whereas the sandy loam soil cover layers of very dense SRCs were lower than the threshold criteria range. Nevertheless, this is the typical design for SRC and can ensure good long-term performance with a high chance of creating a self-sustainable ecosystem. The SRC design of D1-1 and P2-2 is the perfect example. Although D1-1 had a thin layer between the growth medium and water retention and P2-2 had a low WHC water retention

layer, but had a saprolite cover layer underneath the water retention layer resulting from a deep soil cover depth, these two SRCs performed well.

6.1.2 Soil hydraulic properties

6.1.2.1 *Saturated hydraulic conductivity*

After the SRCs data-set was split into moderately- and very dense SRCs data sets due to changes in porosity and bulk density, the relationship between bulk density and K_{sat} values was positive in moderately dense SRCs. The opposite was found for very dense SRCs, where the relationship was significantly negative. One would expect a negative correlation between bulk density and K_{sat} as was observed in the SRC data-set. The clay content of moderately dense SRCs had a significant negative relationship with K_{sat}, whereas this relationship for very dense SRCs was positive. The relationship between sand content and K_{sat} was negative in the SRCs data-set.

6.1.2.2 *Soil water retention curves*

The relationship between soil texture and volumetric water content at selected matric potentials differed among the SRCs data-set, and moderately- and very dense SRCs data sets. All the sand fractions had a negative relationship with the volumetric water content at selected matric potentials of the SRCs data-set. The two silt fractions, clay content and soil organic matter had a positive relationship with the volumetric water content at selected matric potentials, where the relationship with clay content was strong and significant from -2 to -1500 kPa. Bulk density had a negative relationship with volumetric water content at selected matric potentials with a decreasing trend from -2 to -1500 kPa. In contrast, bulk density had a significant and negative relationship from -2 to -1500 kPa with the volumetric water content in the moderately dense SRCs data-set. In addition, the coarse sand fraction had a positive correlation from -2 to -1500 kPa. The bulk density of the very dense SRCs data-set had a trend similar to SRCs data-set, but the fine sand content had a positive relationship with volumetric water content from -25 to -1500 kPa, and very fine sand content had a positive correlation from -2 to -10 kPa. Additionally, the relationship between coarse silt content and volumetric water content from -30 to -1500 kPa was negative. The correlations of the SRCs data-set showed the expected relationship of particle-size distribution, SOM and bulk density with volumetric water content from -2 to -1500 kPa.

6.1.3 Pedotransfer functions for soil hydraulic properties

Development of pedotransfer functions (PTFs) by using multiple linear regression models for predicting K_{sat} and SWRC highlighted that particle-size distribution, SOM and bulk density are the most important input parameters. Based on changes in bulk density, moderately- and very dense K_{sat} models were developed and the performance of both models were analytically satisfactory, although, the very dense K_{sat} model may have suffered from overfitting because of a small number of samples. Together with the expected relationships between the particle-size distribution, bulk density and volumetric water content at selected matric potentials, the SWRC model of the SRCs

data-set performed the best and was analytically satisfactory. Moreover, a wider soil texture range with bulk density and large number of samples may be the other reason for better model performance. The moderately- and very dense SWRC models performed weaker and may overestimate the predicted volumetric water content at selected matric potentials.

A comparison between the model performance of the published PTFs and developed PTFs in the current study for prediction of the K_{sat} or a fully described SWRC, the latter PTFs performed better due to higher validated adjusted R^2 values with lower RMSE values. To use a published PTF should be exercised with caution since no PTF can be termed global due to variations in soil formation and pedogenesis. Nonetheless, the use of developed PTFs is attractive with lower errors and the flexibility to input parameters. The well-developed PTFs can be used to predict the hydraulic properties for soil covers having soil physical properties similar to the old SRCs at Mpumalanga Highveld. These predicted soil hydraulic properties can be used in a model to predict the long-term performance of SRCs. Furthermore, the well-developed PTFs are easy to use, cost-effective and consultants, geo-engineers or soil scientists may find them useful.

6.1.4 Vegetation properties

The good vegetation covers of SRCs with moderately dense soil conditions showed high vegetation growth with good root development. The vegetation growth changed monthly and was influenced by rainfall, soil water content, soil nutrient availability and bulk density. The peak active vegetation biomass of the grasses of rehabilitated mines at Mpumalanga Highveld was between January to March. During the peak season, the average photosynthetic active leaf area index (LAI) for good and poor vegetation cover were ~1.2 and 0.8 $m^2.m^{-2}$, respectively. Low peak photosynthetic active LAI of the current study may be attributed to lower soil water content with lower rainfall, topographic locations, different grass species, etc. Published LAI values for vegetation covers applying to soil cover modelling for long-term performances should be exercised with caution.

The relationship between the active vegetation biomass and photosynthetic active LAI was provided by power-law, however, the linear relationship also performed well. Nonetheless, as the active vegetation biomass increased, the photosynthetic active LAI increased.

6.1.5 The effect of poorly constructed store-and-release covers on long-term soil cover performance

High bulk density is a problem when soil covers are constructed poorly. Due to improper soil emplacement during soil cover construction or traffic over wet soil or poor traffic during revegetation, the long-term performance of SRCs with very dense soil cover conditions was poor. The very dense SRCs has a higher risk of surface crusting, sheet and rill erosion and vertical cracks which can provide preferential flow, consequently increasing the amount of oxygen- and water ingress into the coal discard and spoil. The high bulk density caused $pH_{(H_2O)}$ values below the critical threshold values, and some electrical conductivity values of the saturated paste extract that were higher than the threshold values. Additionally, the sandy loam and sandy clay loam cover layers of very dense

SRCs had lower K_{sat} values than the threshold and lower WHC compared to the WHC values of the moderately dense SRCs. The high bulk density decreased the field capacity (FC) with increasing permanent wilting point (PWP), albeit the effect is not significant. However, bulk density over 2 g.cm^{-3} significantly decreased FC and PWP, and overall, the WHC. Given that SRCs rely on high WHC especially in the water retention layer, high bulk density was not favourable. High bulk density also has a negative effect on vegetation properties. The very dense SRCs had poor and patchy vegetation covers with poor root distribution which formed a compressed mat in the upper 150 mm soil layers while some roots growing through the cracks. This led to a decrease in active vegetation biomass growth and reduced photosynthetic active leaf area index (LAI) during the peak season. Soil covers with high bulk density can influence plant survival under semi-arid conditions and drought stress. Furthermore, the decreased vegetation growth can cause a decrease in evapotranspiration. Long-term soil cover performance under conditions of high bulk density is not sustainable and poorly constructed soil covers should be avoided at all costs.

6.1.6 Way forward

Based on the project results, the following criteria summary for design, construction and long-term performance of SRC under arid and semi-arid climatic conditions should be considered for possible amendments to the Technical Guideline on SRC development:

(1) *Planning*:

- (i) Objectives of SRCs are (1) to limit the oxygen- and water ingress, (2) isolating coal discard or spoil from the water resources, and (3) establish a self-sustainable ecosystem;

(2) *Design*:

- (i) The soil texture for growth medium should be a sandier medium such as sandy loam or even sandy clay loam while the water retention layer should be more of a clayey medium such as sandy clay loam or clay loam, etc. The soil texture for monolithic SRCs can be sandy loam or sandy clay loam. Low or medium plasticity and swelling potential are preferable;
- (ii) The bulk density should be lower than ~1.800 g.cm^{-3} for the growth medium and ~1.780 g.cm^{-3} for the water retention layer according to the critical threshold values for root development. Lower bulk densities for growth medium and water retention layers will be preferable for SRC since the success of SRCs is determined by the SWRC of soils, rather than very low K_{sat};
- (iii) Low or moderate K_{sat} for growth medium and water retention layer is preferable, however, K_{sat} values according to soil textural classes can be used. Importantly, avoid very high K_{sat} values which can be caused by a high gravel content or too low K_{sat} values caused by high bulk density;

(iv) High WHC, 120.00–207.50 mm.m^{-1}, is desirable for the water retention layer, but should have a steep slope of desaturation function for growth medium;

(v) Pedotransfer functions as MLR models predicting soil hydraulic properties can be used to predict the long-term soil cover performance;

(vi) Photosynthetic active leaf area index values of ~1.2 and 0.8 m^2.m^{-2} for good and poor vegetation covers for SRCs on the Mpumalanga Highveld can be used for to predict the long-term soil cover performance;

(3) *Construction*:

(i) Use the correct machines for soil cover construction as it is discussed in the "Guidelines for the Rehabilitation Mined Land" guideline;

(ii) Avoid traffic on wet soils. Rather work in the winter season when there is no rain than in the summer in Mpumalanga Highveld;

(iii) Use correct implements for tillage during the revegetation as it is discussed in the "Guidelines for the Rehabilitation Mined Land" guideline;

(4) *Post-closure care and maintenance*:

(i) The critical threshold values for bulk density on root development and penetration, soil nutrient availability, K_{sat} and WHC in the current study can be used to evaluate the long-term soil cover performance for soil cover overs 10–20 years old; and

(ii) Occasional monitoring of the SRCs is recommend.

The following PTFs which are moderately- and very dense K_{sat} models can be used to predict the K_{sat} of soil covers having similar soil physical properties to the old SRCs:

Moderately dense K_{sat} = 1.015 - 9.884×10^{-05}*Sand - 0.003*Silt - 0.012*Clay - 0.028*SOM - 0.268*ρ_b [Eq. 6.1]

Very dense K_{sat} = -0.029 + 0.001*Sand + 0.005*Silt + 0.003*Clay + 0.009*SOM - 0.040* ρ_b [Eq. 6.2]

where moderately dense- and very dense K_{sat} is the predicted K_{sat}, sand-, silt-, and clay content and SOM is in %, whereas the bulk density, ρ_b, is in g.cm^{-3}. The following PFTs can be used to predict volumetric water content at selected matric potentials for old SRCs:

θ_p at -2 kPa = 0.435 + 0.015*√Medium sand + 0.029*√Fine sand + 0.049*√Very fine sand + 0.039*√Coarse silt + 0.030*√Fine silt + 0.050*√Clay + 0.670*√SOM - 0.650*√ρ_b [Eq. 6.3]

θ_p at -4 kPa = 0.123 + 0.031*√Medium sand + 0.027*√Fine sand + 0.050*√Very fine sand + 0.053*√Coarse silt + 0.031*√Fine silt + 0.031*√Clay + 0.077*√SOM - 0.539*√ρ_b [Eq. 6.4]

θ_p at -6 kPa = 0.498+ 0.034*√Very fine sand + 0.012*√Coarse silt + 0.020*√Fine silt + 0.046*√Clay + 0.079*√SOM - 0.459*√ρ_b [Eq. 6.5]

θ_p at -8 kPa = 0.281+ 0.033*√Very fine sand + 0.016*√Coarse silt + 0.022*√Fine silt + 0.050*√Clay + 0.094*√SOM - 0.339*√ρ_b [Eq. 6.6]

θ_p at -10 kPa = 0.140+ 0.031*√Very fine sand + 0.019*√Coarse silt + 0.024*√Fine silt + 0.051*√Clay + 0.107*√SOM - 0.260*√ρ_b [Eq. 6.7]

θ_p at -15 kPa = -0.261+ 0.021*√Very fine sand + 0.026*√Coarse silt + 0.021*√Fine silt + 0.054*√Clay + 0.137*√SOM [Eq. 6.8]

θ_p at -20 kPa = -0.286+ 0.019*√Very fine sand + 0.028*√Coarse silt + 0.024*√Fine silt + 0.053*√Clay + 0.145*√SOM [Eq. 6.9]

θ_p at -25 kPa = -0.302+ 0.017*√Very fine sand + 0.030*√Coarse silt + 0.026*√Fine silt + 0.053*√Clay + 0.150*√SOM [Eq. 6.10]

θ_p at -30 kPa = -0.278 + 0.034*√Coarse silt + 0.025*√Fine silt + 0.048*√Clay + 0.168*√SOM [Eq. 6.11]

θ_p at -60 kPa = -0.317 + 0.036*√Coarse silt + 0.028*√Fine silt + 0.046*√Clay + 0.174*√SOM [Eq. 6.12]

θ_p at -100 kPa = -0.332 + 0.036*√Coarse silt + 0.029*√Fine silt + 0.045*√Clay + 0.176*√SOM [Eq. 6.13]

θ_p at -300 kPa = -0.340+ 0.035*√Coarse silt + 0.029*√Fine silt + 0.043*√Clay + 0.172*√SOM [Eq. 6.14]

θ_p at -600 kPa = -0.336+ 0.034*√Coarse silt + 0.029*√Fine silt + 0.042*√Clay + 0.167*√SOM [Eq. 6.15]

θ_p at -1500 kPa = -0.327+ 0.032*√Coarse silt + 0.028*√Fine silt + 0.041*√Clay + 0.161*√SOM [Eq. 6.16]

where θ_p is the predicted volumetric water in $m^3.m^{-3}$ at selected matric potential, medium sand-, fine sand-, very fine sand-, coarse silt-, fine silt-, and clay content and SOM is in %, whereas the unit for bulk density, ρ_b, is in $g.cm^{-3}$.

6.2 Research recommendations

- The following component of the international soil cover guidelines which are lacking in South Africa needs to be developed with the specific objective to limit oxygen- and water ingress and associate acid mine drainage (AMD) generation and seepage:

(1) A technical guideline that integrates the various processes, procedures and tools/models on soil cover design, construction, and care and maintenance to meet the above-mentioned objective;

(2) *Design*:
   (i) Setting soil cover performance criteria for design;
   (ii) Screening level (initial) risk assessment to determine viability of SRCs as alternative cover option to meet required groundwater protection;
   (iii) Procedure to determine soil cover materials for the site;
   (iv) Procedures to characterise the properties of the soil cover materials, including soil hydraulic properties;
   (v) Procedures and tools/models to be used for soil cover water balance modelling based on site-specific climate and properties of soil cover materials on site to predict water ingress and water content required for oxygen ingress modelling;
   (vi) Approach and processes for conceptual- and final cover design;

(3) *Construction*:
   (i) Procedures of soil cover material specification and record keeping;
   (ii) Procedures on quality assurance and quality control program to implemented for soil cover construction;

(4) *Post-closure care and maintenance:*
   (i) Procedures to identify indicators to monitor and evaluate post-closure care and maintenance and long-term soil cover performance; and
   (ii) Monitoring of long-term soil cover performance to evaluate the extent to which the soil cover meets long-term performance criteria.

It is recommended that the Technical Guideline consists of a decision-making tree (Tier 1), protocols and minimum requirement for each element (Tier 2), and supportive information (Tier 3). Soil scientists need to be involved by helping to develop a Technical Guideline since SRCs strive to mimic the natural soil profile which is in the field of Soil Science. Therefore, a working group, consisting of agriculturists, mining environmental managers, resource protection officers, soil scientists and representatives of relevant Government Departments need to work together.

- The acidification potential and pyrite content of coal discard or spoil need to be considered during the making on rehabilitation method, therefore chemical properties of the coal need to be conducted. Along with the chemical properties of coal, the soil fertility needs to be determined. Soil chemical data of the fertilisation programme needs to be available for monitoring the changes in the soil chemical properties over years.
- Initial soil hydraulic properties are needed to evaluate the changes over years. It is recommended that such results should be available for research purposes. The soil water balance in the soil covers also needs to be evaluated to determine the evapotranspiration differences between good and poor constructed soil covers. Since the infiltration tests were done on the soil matrix of poorly

constructed covers, the infiltration tests on vertical and lateral cracks are recommended. However, to develop a K_{sat} model for poorly constructed covers which includes the K_{sat} values of cracks is not ideal since the long-term performance of poorly constructed soil covers may fail the criteria and expectations of rehabilitation success.

Small readily available data sets may probably overestimate the reliability of PTFs. Further improvement of these MLR models should be possible by extending the models to include a wider range in soil physical properties to build a larger data-set. In addition, artificial neural networks can also be an approach to follow and additional validation like bootstrapping or k-fold cross validation are needed. Additionally, several studies have shown that segmental models can perform well. Segmental models can be another approach with appropriate parameters input to develop PTFs for SRCs. Segmental models are easy to use, similar to MLR models.

- The direct method for biomass determination to measure oven-dried biomass or LAI after clippings are time consuming, and destructive. Due to destruction, it is impossible to take several measurements on the same spot or plant at different times. Monitoring of changes in biomass is essential to understand the contribution of grasses. That being said, direct methods are not compatible with the long-term monitoring of spatial and temporal dynamics of biomass and LAI. Hence, non-destructive methods need to be used in the future, for example digital image processing especially the high-end drone models. An improved method to determine LAI, namely Excess Green minus Excess Red can be employing by using digital photography. The Normalised Difference indices (NDI) can also be an approach, however, some studies found that NDI overestimates LAI. There is a new NDI for estimating LAI which is insensitive to pigment contents and relative water contents, but is sensitive to leaf area. Lastly, several indirect measurements need to be tested to determine which method performs best to estimate LAI. Nevertheless, the need for validation of indirect methods remains, therefore the direct methods need to considered as calibration methods.

Appendix A: Category or rating of soil cover layer

Table A.1: Description of categories and ratings of soil cover properties on field sheets.

Description of category or rating of soil cover layer	
ObsNo	(Observation number) Number of profile pit.
Erosion	Any erosion occurrences within a 20000 mm radius of the profile pit evaluated as the following types: - None; - sheet; - rill (<300 mm deep); - gully (300-1000 mm deep); and - donga (> 1000 mm deep).
Terrain unit	The position in the landscape where the sampling point resides divided in: - (1) Crests; - (2) scarps; - (3) midslopes; - (4) footslopes; and - (5) valley bottoms
Surface crust	The occurrence of a crust on the surface varying between 2–5 mm thick consisting of finer material than directly below it and which causes surface sealing and lead to lower infiltration rates and higher runoff. The prominence of the crust within a 5000 mm radius of the sampling point were evaluate in categories of: - None; - Weak; - Moderate, and - Strong
Surface cracks	The occurrence of visible cracks on the surface due to silt and clay particles with shrink and expand properties within a 5000 mm radius around the sampling point categorised as: - None; - Few; - Common; and - Many
Slope percentage	The surface slope within a 20000 mm radius around the sampling point
Vegetation cover	The vegetation cover was broadly assessed in a 10000 mm radius around the sampling point as follows: - Poor – sparse vegetation cover; - Moderate – 30 50% vegetation cover; and - Good - > 50% vegetation cover
Effective soil depth	The depth of the soil profile that appears to be reasonable accessible for roots and water. Compaction and abrupt different textural layers was often identified as properties that limit effective depth.
Effective rooting depth	The maximum depth where roots occurred frequent in soil profile

Table A.2: Description of categories and ratings of soil cover properties on field sheets.

Description of category or rating of soil layer	
Layer	Topsoil layers were labelled “ob” and a sequence number. Subsoil layers were labelled “sub” with a sequence number in order to distinguish between topsoil and subsoil layers. Spoil or discard material was labelled “spoil” or “discard”
Depth	Lower depth of soil layer in mm
Colour	Colour description
Soil homogeneity	The soil homogeneity is an indication to what extent the soil was mixed with different soil layers, subsoil layers such as gleyed layers, plinthic material, clay and weathered rock or coralliferous material. Soil homogeneity was rated as: - Pure; - Slightly mixed; - Moderately mixed; and - Severely mixed.
Soil quality	The soil quality is a rating of the degradation of soil properties due to mixing with other layers, subsoil or spoil material. Any deterioration of the original physical properties which might adversely affect infiltration, internal drainage, water holding capacity and aeration were considered. Soil quality was rated in classes of: - High; - Medium; or - Low.
Soil density	The density noticed in each layer as experienced while augering the pit was rated as: - None; - Slight; - Moderate; - High; - Severe; or - Extreme
Root occurrence	The occurrence of roots within each layer was evaluated in order to determine the depth of root penetration within the soil profile. The amount of roots in each identified layer was rated in classes of: - None; - Few; - Common; and - Many

Appendix B: Saturated hydraulic conductivity training and testing sets

Table B.1: Soil physical property variables of the training data sets used for model validation. Average soil physical properties are gravel, sand, clay, soil organic matter (SOM), bulk density (ρ_b) and average saturated hydraulic conductivity (K_{sat}).

Data-set	Profile name pit	Soil cover layer (mm)	Sand (%)	Silt (%)	Clay (%)	SOM (%)	ρ_b (%)	K_{sat} m.d^{-1}
Moderately dense store-and-release covers	D1-1	0–500	56.24	17.65	23.65	0.87	1.630	0.120
		550–900	49.72	22.04	25.94	0.87	1.460	0.066
	D1-2	0–400	67.98	14.48	17.42	2.87	1.570	0.160
		400–600	48.44	17.57	30.56	1.05	1.810	0.135
	D1-3	Surface	52.09	23.40	23.40	1.58	1.680	0.160
		0–200	64.44	13.59	21.71	0.84	1.570	0.150
		200–550	33.15	24.64	36.94	0.51	1.610	0.077
	P1-3	Surface	71.31	19.55	7.73	1.07	1.813	0.330
	P1-4	Surface	74.90	15.14	7.72	0.89	1.785	0.420
		0–350	65.08	12.88	13.85	1.04	1.643	0.400
	P2-2	Surface	47.28	15.76	10.89	0.33	1.841	0.310
		500–700	27.38	35.87	18.93	0.17	1.548	0.300
	P2-3	0–500	53.16	19.08	23.62	0.01	1.465	0.290
Very dense store-and-release covers	D2-1	0–450	51.50	31.58	6.67	0.61	1.690	0.090
		450–650	64.96	14.23	20.24	0.63	1.770	0.062
		650–850	49.81	20.62	25.02	0.55	1.700	0.092
	D2-2	0–300	65.97	18.58	15.22	0.86	2.030	0.062
	P1-1	200–700	70.03	14.62	9.90	1.95	2.197	0.030
	P1-2	0–400	61.33	20.96	3.59	0.80	1.741	0.040
	P2-1	0–100	51.93	20.45	22.49	0.26	1.703	0.040
		100–300	75.30	7.77	16.31	0.03	2.286	0.003

Table B.2: Soil physical property variables of the testing data sets used for model validation. Average soil physical properties are gravel, sand, clay, soil organic matter (SOM), bulk density (ρ_b) and average saturated hydraulic conductivity (K_{sat}).

Data-set	Profile name pit	Soil cover layer (mm)	Sand (%)	Silt (%)	Clay (%)	SOM (%)	ρ_b (%)	K_{sat} m.d^{-1}
Moderately dense store-and-release covers	D3-1	0–300	81.70	9.17	8.69	0.96	1.841	0.328
		>300	43.09	21.42	28.46	0.80	1.553	0.196
	D3-2	Surface	77.15	9.23	13.42	1.09	1.692	0.275
		0–400	74.61	9.97	15.41	0.24	1.581	0.372
		>400	40.04	23.07	24.60	0.95	1.730	0.141
Very dense store-and-release covers	D2-1	850–1100	32.64	20.87	43.43	0.39	1.700	0.101
	D2-2	300–400	36.20	18.90	41.05	0.10	1.742	0.089
	P1-1	Surface	57.53	22.84	5.31	1.19	1.850	0.032
	P1-2	Surface	51.93	20.45	22.49	0.26	1.700	0.064
	P2-2	0–500	72.00	10.91	16.21	1.85	1.871	0.019

Appendix C: Soil water retention curve training and testing sets and data uniformity graphs

Table C.1: Soil physical properties of the training set used for soil water retention curve model.

Profile name pit	Soil cover layer	Variables												
		Medium gravel	Fine gravel	Very fine gravel	Very coarse sand	Coarse sand	Medium sand	Fine sand	Very fine sand	Coarse silt	Fine silt	Clay	SOM	ρ_b
	(mm)	(%)	(%)	(%)	(%)	(%)	(%)	(%)	(%)	(%)	(%)	(%)	(%)	(g.cm^{-3})
D1-1	0–550	0.00	1.01	1.44	5.56	9.19	14.60	24.54	2.36	15.35	2.30	23.66	0.16	1.631
D1-2	0–400	0.00	0.48	2.96	5.75	9.40	11.76	19.05	2.47	12.43	5.13	30.56	0.09	1.809
D1-3	Surface	0.00	0.27	0.84	4.57	10.18	14.06	21.42	1.86	17.03	6.37	23.40	0.48	1.676
	0–200	0.00	0.00	0.27	6.85	10.76	18.74	26.24	1.85	10.50	3.09	21.71	0.18	1.566
	200–550	0.57	1.22	3.48	4.55	6.89	8.59	11.40	1.71	20.86	3.77	36.94	0.31	1.613
D2-1	0–450	3.34	2.64	4.26	4.47	15.77	6.59	23.03	1.65	29.62	1.96	6.67	0.07	1.686
	850–1100	0.00	0.91	2.23	3.61	7.22	8.51	11.89	1.41	12.44	8.43	43.34	0.39	1.675
D2-2	0–300	0.00	0.00	0.23	5.22	9.78	18.99	30.20	1.79	6.62	11.95	15.22	0.18	2.027
	300-400	2.83	0.00	2.56	4.33	7.30	6.89	12.43	1.88	19.02	5.42	37.34	0.03	1.841
P1-1	Surface	0.00	0.22	14.10	8.68	6.98	13.66	18.09	10.12	19.81	3.03	5.32	0.66	1.848
	200–700	0.00	0.00	5.45	8.89	12.17	19.41	25.75	3.80	11.59	3.03	9.89	0.28	2.197
P1-2	Surface	0.00	1.03	14.05	7.82	8.19	12.31	15.83	11.65	23.07	0.95	5.11	0.87	1.859
	0–400	0.00	0.00	14.12	8.08	6.45	12.75	19.57	14.48	18.96	2.01	3.59	0.36	1.741
P1-3	Surface	0.00	0.00	1.42	12.60	7.25	22.97	18.39	10.09	15.38	4.16	7.73	0.52	1.813
P1-4	Surface	0.00	0.00	2.25	11.51	8.04	28.07	22.33	4.95	7.42	7.72	7.72	0.89	1.785
	0–350	0.00	0.11	7.55	7.92	8.99	19.99	22.12	6.58	11.72	1.19	13.82	0.56	1.643
P2-1	Surface	1.73	0.49	2.90	6.41	9.67	13.15	20.49	2.20	16.04	4.46	22.45	0.13	1.703
P2-2	Surface	0.00	0.00	1.61	8.81	10.25	16.82	25.81	3.59	12.25	1.97	18.89	0.03	1.944
P2-3	0–500	0.00	0.00	0.87	9.11	10.47	19.81	28.87	3.77	7.23	3.68	16.21	0.93	1.872
D3-1	0–300	0.00	0.00	0.74	12.63	4.37	35.59	23.74	2.35	8.15	3.16	9.29	0.28	1.642
D3-2	0–400	0.00	0.00	0.20	9.47	7.59	26.04	32.39	1.65	6.51	2.72	13.42	0.67	1.684
	>400	8.17	0.59	3.53	3.98	8.05	9.96	16.59	1.46	19.27	3.80	24.59	0.38	1.726

Note: SOM = soil organic matter, ρ_b = soil bulk density.

Table C.2: The volumetric water contents of training set for soil water retention curve model.

Profile name pit	Soil cover layer (mm)	Volumetric water content ($m^3.m^{-3}$) at selected matric potential (-kPa)													
		2	4	6	8	10	15	20	25	30	60	100	300	600	1500
D1-1	0–550	0.374	0.368	0.342	0.318	0.301	0.274	0.257	0.245	0.236	0.204	0.184	0.153	0.141	0.131
D1-2	0–400	0.316	0.310	0.297	0.285	0.274	0.256	0.243	0.234	0.227	0.203	0.189	0.164	0.153	0.141
D1-3	Surface	0.365	0.363	0.329	0.302	0.286	0.261	0.248	0.239	0.233	0.217	0.209	0.200	0.197	0.194
	0–200	0.357	0.324	0.289	0.266	0.247	0.215	0.192	0.176	0.163	0.122	0.103	0.087	0.082	0.079
	200–550	0.386	0.384	0.371	0.361	0.353	0.337	0.326	0.318	0.311	0.289	0.274	0.248	0.234	0.218
D2-1	0–450	0.232	0.194	0.162	0.142	0.129	0.108	0.097	0.089	0.083	0.065	0.056	0.043	0.038	0.033
	850–1100	0.402	0.398	0.392	0.385	0.377	0.361	0.349	0.340	0.333	0.310	0.296	0.276	0.269	0.262
D2-2	0–300	0.231	0.222	0.214	0.206	0.199	0.185	0.173	0.164	0.157	0.132	0.118	0.100	0.094	0.088
	300-400	0.300	0.300	0.299	0.293	0.284	0.267	0.255	0.247	0.240	0.216	0.199	0.168	0.151	0.131
P1-1	Surface	0.266	0.246	0.230	0.219	0.210	0.194	0.183	0.175	0.170	0.151	0.140	0.123	0.116	0.109
	200–700	0.167	0.157	0.148	0.141	0.135	0.124	0.116	0.110	0.106	0.093	0.086	0.075	0.071	0.067
P1-2	Surface	0.293	0.271	0.255	0.243	0.235	0.219	0.209	0.201	0.194	0.172	0.157	0.130	0.115	0.097
	0–400	0.289	0.256	0.227	0.204	0.186	0.154	0.135	0.122	0.112	0.083	0.069	0.052	0.046	0.041
P1-3	Surface	0.312	0.299	0.277	0.256	0.238	0.202	0.178	0.160	0.147	0.108	0.089	0.065	0.057	0.052
P1-4	Surface	0.311	0.281	0.263	0.251	0.242	0.226	0.215	0.208	0.201	0.179	0.165	0.137	0.122	0.105
	0–350	0.334	0.310	0.283	0.257	0.236	0.197	0.173	0.157	0.145	0.114	0.100	0.084	0.080	0.076
P2-1	Surface	0.328	0.308	0.287	0.266	0.247	0.212	0.188	0.171	0.158	0.121	0.103	0.081	0.074	0.069
P2-2	Surface	0.249	0.232	0.215	0.200	0.186	0.161	0.144	0.131	0.122	0.092	0.077	0.057	0.049	0.044
P2-3	0–500	0.277	0.263	0.251	0.242	0.234	0.218	0.207	0.199	0.192	0.168	0.154	0.129	0.118	0.107
D3-1	0–300	0.249	0.249	0.217	0.181	0.157	0.123	0.104	0.092	0.083	0.059	0.047	0.032	0.027	0.023
D3-2	0–400	0.267	0.253	0.231	0.210	0.195	0.172	0.158	0.149	0.143	0.123	0.113	0.098	0.093	0.088
	>400	0.344	0.343	0.339	0.333	0.326	0.304	0.285	0.270	0.259	0.227	0.211	0.192	0.186	0.181

Table C.3: Soil physical properties of the training sets used for moderately- and very dense soil water retention curve models validations.

Data-set	Profile name pit	Soil cover layer (mm)	Variables												
			Medium gravel (%)	Fine gravel (%)	Very fine gravel (%)	Very coarse sand (%)	Coarse sand (%)	Medium sand (%)	Fine sand (%)	Very fine sand (%)	Coarse silt (%)	Fine silt (%)	Clay (%)	SOM (%)	ρ_b (g.cm^{-3})
Moderately dense store-and-release covers	D1-1	0–500	0.00	0.56	1.73	5.42	10.48	13.02	18.76	2.04	13.11	8.94	25.94	0.01	1.551
		550–900	0.00	1.01	1.44	5.56	9.19	14.60	24.54	2.36	15.35	2.30	23.65	0.16	1.631
	D1-2	0–400	0.00	0.00	0.12	7.40	8.85	21.12	28.66	1.95	10.16	4.32	17.42	0.51	1.566
		400–600	0.00	0.48	2.96	5.75	9.40	11.78	19.05	2.47	12.43	5.13	30.56	0.09	1.809
	D1-3	Surface	0.00	0.27	0.84	4.57	10.18	14.06	21.42	1.86	17.03	6.37	23.40	0.48	1.676
		0–200	0.00	0.00	0.27	6.85	10.76	18.74	26.23	1.85	10.50	3.09	21.71	0.18	1.566
		200–550	0.57	1.22	3.48	4.55	6.89	8.59	11.40	1.71	20.86	3.77	36.94	0.31	1.613
	P1-3	Surface	0.00	0.00	1.42	12.60	7.25	22.97	18.39	10.09	15.38	4.16	7.73	0.52	1.813
	P1-4	Surface	0.00	0.00	2.25	11.51	8.04	28.07	22.33	4.95	7.42	7.72	7.72	0.89	1.785
		0–350	0.00	0.11	7.55	7.92	9.00	19.99	22.12	6.58	11.72	1.20	13.82	0.56	1.643
	P2-2	Surface	0.00	0.00	1.61	8.81	10.25	16.82	25.81	3.59	12.25	1.97	18.89	0.03	1.944
		500–700	9.94	1.10	2.60	1.94	9.99	3.46	10.81	1.00	21.21	11.52	26.44	0.43	1.637
	P2-3	0–500	0.00	0.18	3.95	6.37	11.28	12.59	19.03	3.90	16.23	2.84	23.63	0.31	1.465
Very dense store-and-release covers	D2-2	0–450	3.35	2.64	4.26	4.47	15.77	6.59	23.03	1.65	29.62	1.95	6.67	0.07	1.686
		450–650	0.00	0.00	0.61	6.20	10.58	19.34	26.83	1.69	10.37	4.56	19.82	0.09	1.861
		650–850	0.00	0.80	3.75	3.38	7.72	10.50	26.43	1.78	19.24	1.38	25.02	0.04	1.704
	D2-2	0–300	0.00	0.00	0.23	5.21	9.78	18.99	30.20	1.79	6.62	11.95	15.22	0.18	2.027
	P1-1	200–700	0.00	0.00	5.45	8.89	12.17	19.41	25.75	3.80	11.60	3.02	9.90	0.29	2.197
	P1-2	Surface	0.00	1.03	14.05	7.82	8.18	12.31	15.83	11.65	23.07	0.95	5.11	0.87	1.859
		0–400	0.00	0.00	14.11	8.08	6.45	12.75	19.57	14.48	18.96	2.00	3.59	0.36	1.741
	P2-1	100-300	0.00	0.00	0.62	8.88	15.67	20.18	27.87	2.99	6.42	0.99	16.37	0.03	2.286

Note: SOM = soil organic matter, ρ_b = soil bulk density.

Table C.4: The volumetric water contents of training sets for moderately- and very dense soil water retention curve models.

Data-set	Profile name pit	Soil cover layer (mm)	Volumetric water content ($m^3.m^{-3}$) at selected matric potential (-kPa)													
			2	4	6	8	10	15	20	25	30	60	100	300	600	1500
Moderately dense store-and-release covers	D1-1	0–500	0.412	0.407	0.402	0.396	0.390	0.379	0.371	0.366	0.362	0.349	0.343	0.335	0.332	0.331
		550–900	0.374	0.368	0.342	0.318	0.301	0.274	0.257	0.245	0.236	0.204	0.184	0.153	0.141	0.131
	D1-2	0–400	0.403	0.400	0.388	0.374	0.363	0.343	0.330	0.320	0.313	0.288	0.275	0.258	0.252	0.247
		400–600	0.316	0.310	0.297	0.285	0.274	0.256	0.243	0.234	0.227	0.203	0.189	0.164	0.153	0.141
	D1-3	Surface	0.365	0.363	0.329	0.302	0.286	0.261	0.248	0.239	0.233	0.217	0.209	0.200	0.197	0.194
		0–200	0.357	0.324	0.289	0.266	0.247	0.215	0.192	0.176	0.163	0.122	0.103	0.087	0.082	0.079
		200–550	0.386	0.384	0.371	0.361	0.353	0.337	0.326	0.318	0.311	0.289	0.274	0.248	0.234	0.218
	P1-3	Surface	0.312	0.299	0.277	0.256	0.238	0.202	0.178	0.160	0.147	0.108	0.089	0.065	0.057	0.052
	P1-4	Surface	0.311	0.281	0.263	0.251	0.242	0.226	0.215	0.208	0.201	0.179	0.165	0.137	0.122	0.105
		0–350	0.334	0.310	0.283	0.257	0.236	0.197	0.173	0.157	0.145	0.114	0.100	0.084	0.080	0.076
	P2-2	Surface	0.249	0.232	0.215	0.200	0.186	0.161	0.144	0.131	0.122	0.092	0.077	0.057	0.049	0.044
		500–700	0.371	0.356	0.348	0.342	0.338	0.331	0.326	0.322	0.319	0.309	0.301	0.288	0.280	0.271
	P2-3	0–500	0.445	0.436	0.425	0.417	0.409	0.395	0.385	0.378	0.372	0.354	0.343	0.327	0.321	0.315
Very dense store-and-release covers	D2-2	0–450	0.232	0.194	0.162	0.142	0.129	0.108	0.097	0.089	0.083	0.065	0.056	0.043	0.038	0.033
		450–650	0.276	0.276	0.272	0.253	0.236	0.210	0.196	0.186	0.179	0.158	0.148	0.134	0.129	0.125
		650–850	0.347	0.339	0.326	0.314	0.303	0.284	0.271	0.263	0.256	0.236	0.224	0.206	0.198	0.191
	D2-2	0–300	0.231	0.222	0.214	0.206	0.199	0.185	0.173	0.164	0.157	0.132	0.118	0.100	0.094	0.088
	P1-1	200–700	0.167	0.157	0.148	0.141	0.135	0.124	0.116	0.110	0.106	0.093	0.086	0.075	0.071	0.067
	P1-2	Surface	0.293	0.271	0.255	0.243	0.235	0.219	0.209	0.201	0.194	0.172	0.157	0.130	0.115	0.097
		0–400	0.289	0.256	0.227	0.204	0.186	0.154	0.135	0.122	0.112	0.083	0.069	0.052	0.046	0.041
	P2-1	100-300	0.133	0.132	0.129	0.127	0.125	0.120	0.116	0.112	0.109	0.096	0.087	0.067	0.057	0.045

Table C.5: Soil physical properties of the testing sets used for soil water retention curve model, and moderately- and very dense soil water retention curve models validations.

Data-set	Profile name pit	Soil cover layer (mm)	Variables												
			Medium gravel (%)	Fine gravel (%)	Very fine gravel (%)	Very coarse sand (%)	Coarse sand (%)	Medium sand (%)	Fine sand (%)	Very fine sand (%)	Coarse silt (%)	Fine silt (%)	Clay (%)	SOM (%)	ρ_b (g.cm^{-3})
Store-and-release covers	D1-1	0–500	0.00	0.56	1.73	5.42	10.48	13.02	18.76	2.04	13.11	8.94	8.94	0.01	1.551
	D1-2	400–600	0.00	0.00	1.56	2.16	5.89	12.87	20.16	8.75	14.61	4.51	4.51	0.05	1.782
	D2-1	450–650	0.00	0.00	0.61	6.20	10.58	19.34	26.83	1.69	10.37	4.56	4.56	0.09	1.861
	D2-1	650–850	0.00	0.80	3.75	3.38	7.72	10.50	26.43	1.78	19.24	1.38	1.38	0.04	1.704
	P2-1	100–300	0.00	0.00	0.80	2.79	8.97	19.56	29.73	10.91	9.51	1.78	1.78	0.03	2.309
	P2-2	500–700	9.94	1.10	2.60	1.94	9.99	3.46	10.81	1.00	21.21	11.52	11.52	0.43	1.637
	P2-3	0–500	0.00	0.18	3.95	6.37	11.28	12.59	19.03	3.90	16.23	2.84	2.84	0.31	1.465
	D3-1	>300	3.78	1.14	3.40	4.08	7.62	10.33	18.09	1.43	16.79	4.76	4.76	0.04	1.613
	D3-2	0-400	0.00	0.00	0.00	8.63	7.49	23.69	33.42	1.38	8.07	1.90	1.90	0.09	1.592
Moderately dense store-and-release covers	D3-1	0–300	0.00	0.00	0.73	12.63	4.37	35.59	23.74	2.35	8.15	3.16	9.28	0.28	1.642
		>300	1.14	1.14	3.40	4.08	7.62	10.33	18.09	1.43	16.79	4.76	28.57	0.04	1.613
	D3-2	Surface	0.00	0.00	0.20	9.47	7.60	26.04	32.38	1.65	6.51	2.72	13.42	0.67	1.684
		0–400	0.00	0.00	0.00	8.63	7.49	23.69	33.42	1.38	8.07	1.90	15.41	0.09	1.592
		>400	0.59	0.59	3.53	3.97	8.04	9.96	16.60	1.46	19.27	3.80	24.60	0.38	1.726
Very dense store-and-release covers	D2-1	850–1100	0.00	0.91	2.23	3.61	7.22	8.51	11.90	1.41	12.44	8.43	43.34	0.40	1.675
	D2-2	300–400	2.83	0.00	2.56	4.33	7.30	6.89	12.43	1.88	19.02	5.41	37.34	0.04	1.841
	P1-1	Surface	0.00	0.22	14.10	8.68	6.97	13.66	18.10	10.11	19.81	3.03	5.32	0.66	1.848
	P1-2	Surface	1.73	0.49	2.90	6.41	9.67	13.15	20.49	2.20	16.04	4.46	22.45	0.13	1.703
	P2-2	0–500	0.00	0.00	0.87	9.11	10.47	19.81	28.86	3.77	7.23	3.68	16.21	0.92	1.872

Note: SOM = soil organic matter, ρ_b = soil bulk density.

Table C.6: The volumetric water contents of testing sets for soil water retention model, and moderately- and very dense soil water retention curve models to determine how uniformly the data points were scattered.

Data-set	Profile name pit	Soil cover layer (mm)	Volumetric water content ($m^3.m^{-3}$) at selected matric potential (-kPa)													
			2	4	6	8	10	15	20	25	30	60	100	300	600	1500
Store-and-release covers	D1-1	0–500	0.374	0.368	0.342	0.318	0.301	0.274	0.257	0.245	0.236	0.204	0.184	0.153	0.141	0.131
	D1-2	400–600	0.403	0.400	0.388	0.374	0.363	0.343	0.330	0.320	0.313	0.288	0.275	0.258	0.252	0.247
	D2-1	450–650	0.276	0.276	0.272	0.253	0.236	0.210	0.196	0.186	0.179	0.158	0.148	0.134	0.129	0.125
	D2-1	650–850	0.347	0.339	0.326	0.314	0.303	0.284	0.271	0.263	0.256	0.236	0.224	0.206	0.198	0.191
	P2-1	100–300	0.133	0.131	0.129	0.127	0.125	0.120	0.116	0.112	0.109	0.096	0.087	0.067	0.057	0.045
	P2-2	500-–700	0.371	0.356	0.348	0.342	0.338	0.331	0.326	0.322	0.319	0.309	0.301	0.288	0.280	0.271
	P2-3	0–500	0.445	0.435	0.425	0.416	0.409	0.395	0.385	0.377	0.372	0.353	0.343	0.335	0.332	0.330
	D3-1	>300	0.380	0.378	0.374	0.368	0.360	0.338	0.313	0.290	0.270	0.204	0.175	0.151	0.147	0.145
	D3-2	0–400	0.278	0.255	0.220	0.196	0.180	0.156	0.143	0.135	0.130	0.114	0.107	0.099	0.096	0.094
Moderately dense store-and-release covers	D3-1	0–300	0.249	0.249	0.217	0.181	0.157	0.123	0.104	0.092	0.083	0.058	0.046	0.031	0.026	0.023
		>300	0.380	0.378	0.374	0.368	0.360	0.338	0.313	0.290	0.270	0.204	0.175	0.151	0.147	0.145
	D3-2	Surface	0.267	0.253	0.231	0.210	0.195	0.172	0.158	0.149	0.143	0.123	0.113	0.098	0.093	0.088
		0–400	0.278	0.255	0.220	0.196	0.180	0.156	0.143	0.135	0.130	0.114	0.107	0.099	0.096	0.094
		>400	0.344	0.343	0.339	0.333	0.326	0.304	0.285	0.270	0.259	0.227	0.211	0.192	0.186	0.181
Very dense store-and-release covers	D2-1	850–1100	0.402	0.398	0.392	0.385	0.377	0.361	0.349	0.340	0.333	0.310	0.296	0.276	0.269	0.262
	D2-2	300–400	0.300	0.300	0.299	0.293	0.284	0.267	0.255	0.247	0.240	0.216	0.199	0.168	0.151	0.131
	P1-1	Surface	0.266	0.246	0.230	0.219	0.210	0.194	0.183	0.175	0.170	0.151	0.140	0.123	0.116	0.109
	P2-2	Surface	0.328	0.308	0.287	0.266	0.247	0.212	0.188	0.171	0.158	0.121	0.103	0.081	0.074	0.069
	P2-3	0–500	0.277	0.263	0.251	0.242	0.234	0.218	0.207	0.199	0.192	0.168	0.154	0.129	0.118	0.107

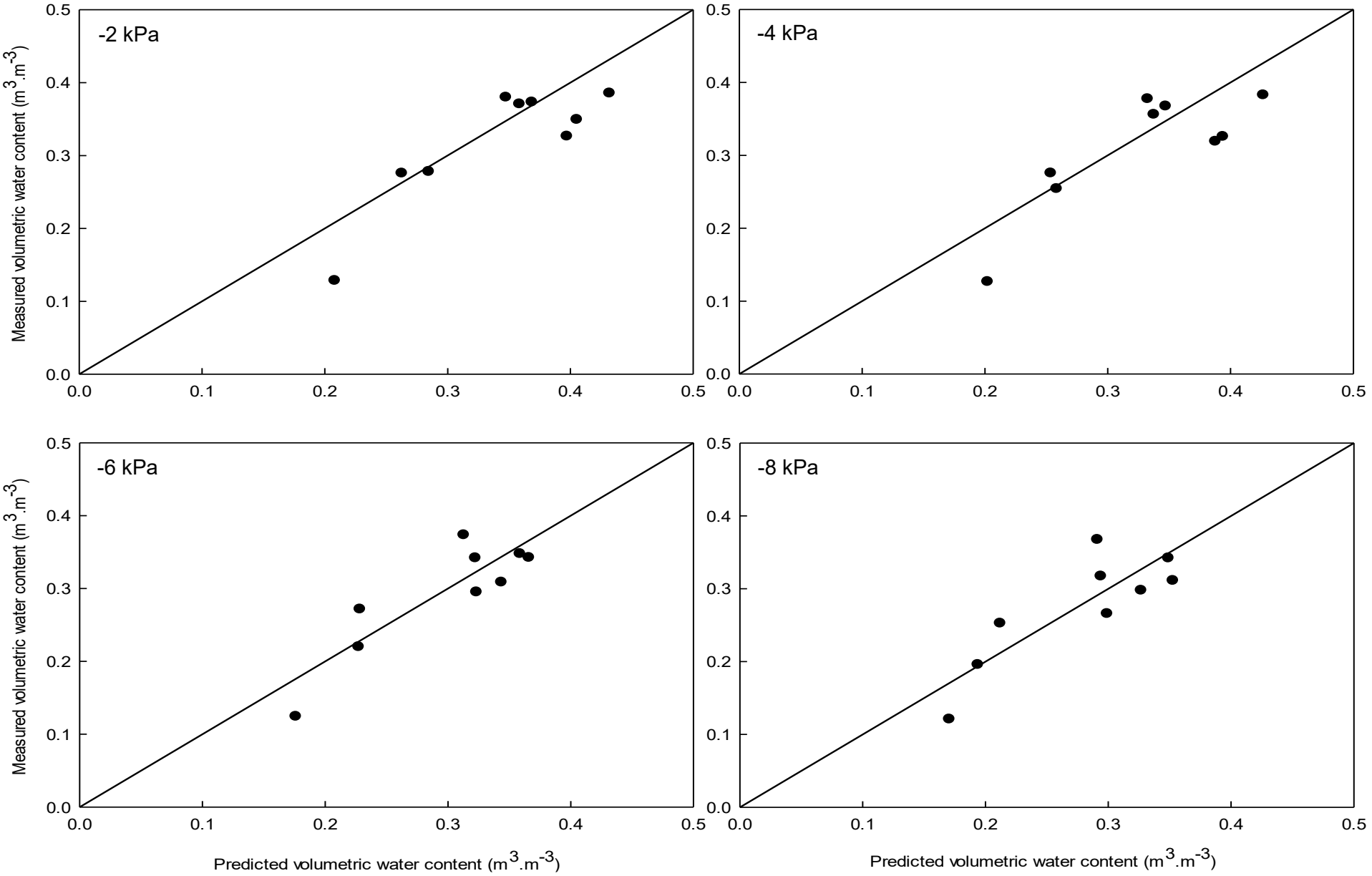

Figure C.1: Measured versus predicted volumetric water content of soil water retention curve model validations at -2 to -8 kPa.

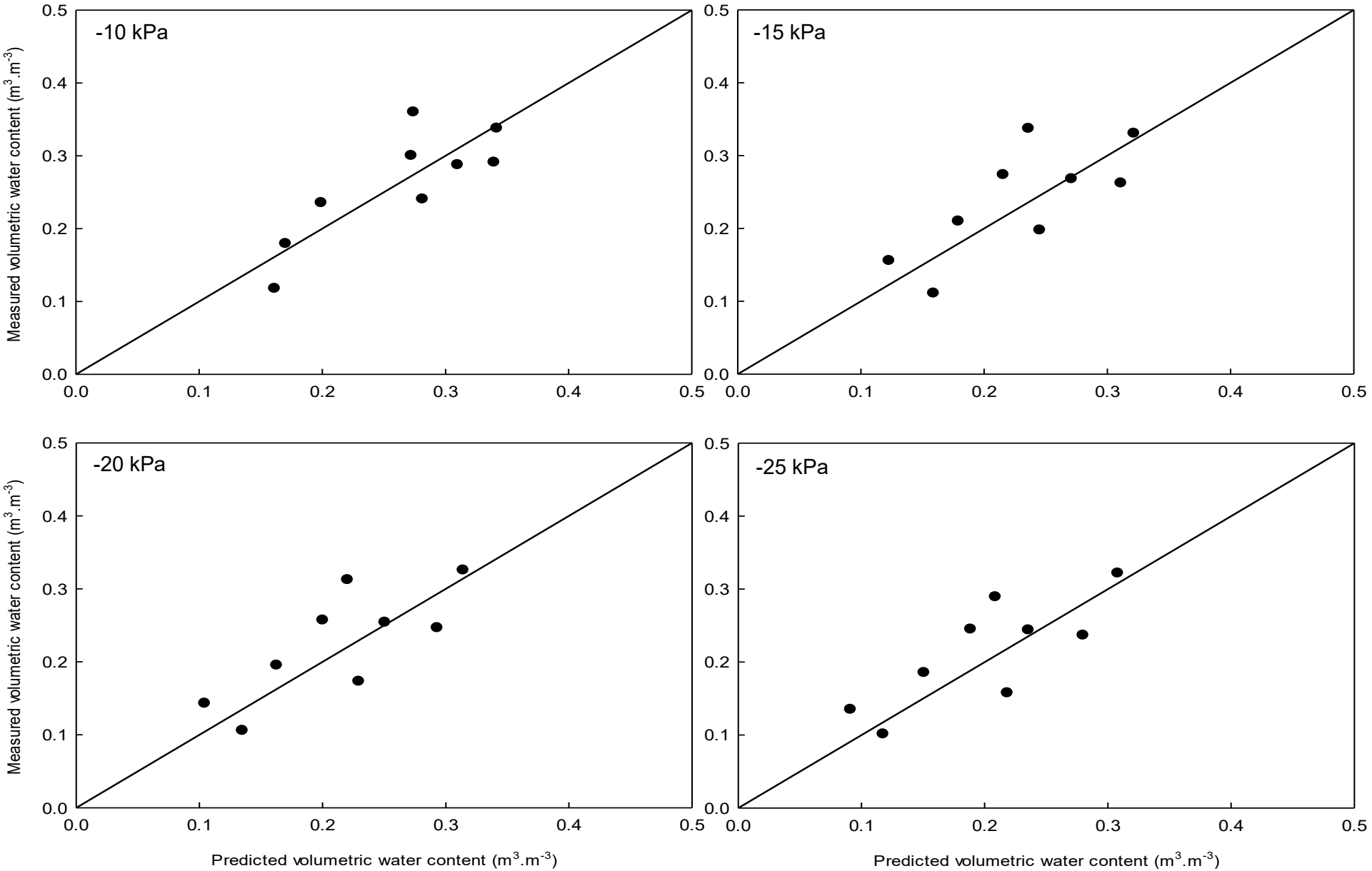

Figure C.2: Measured versus predicted volumetric water content of soil water retention curve model validations at -10 to -25 kPa.

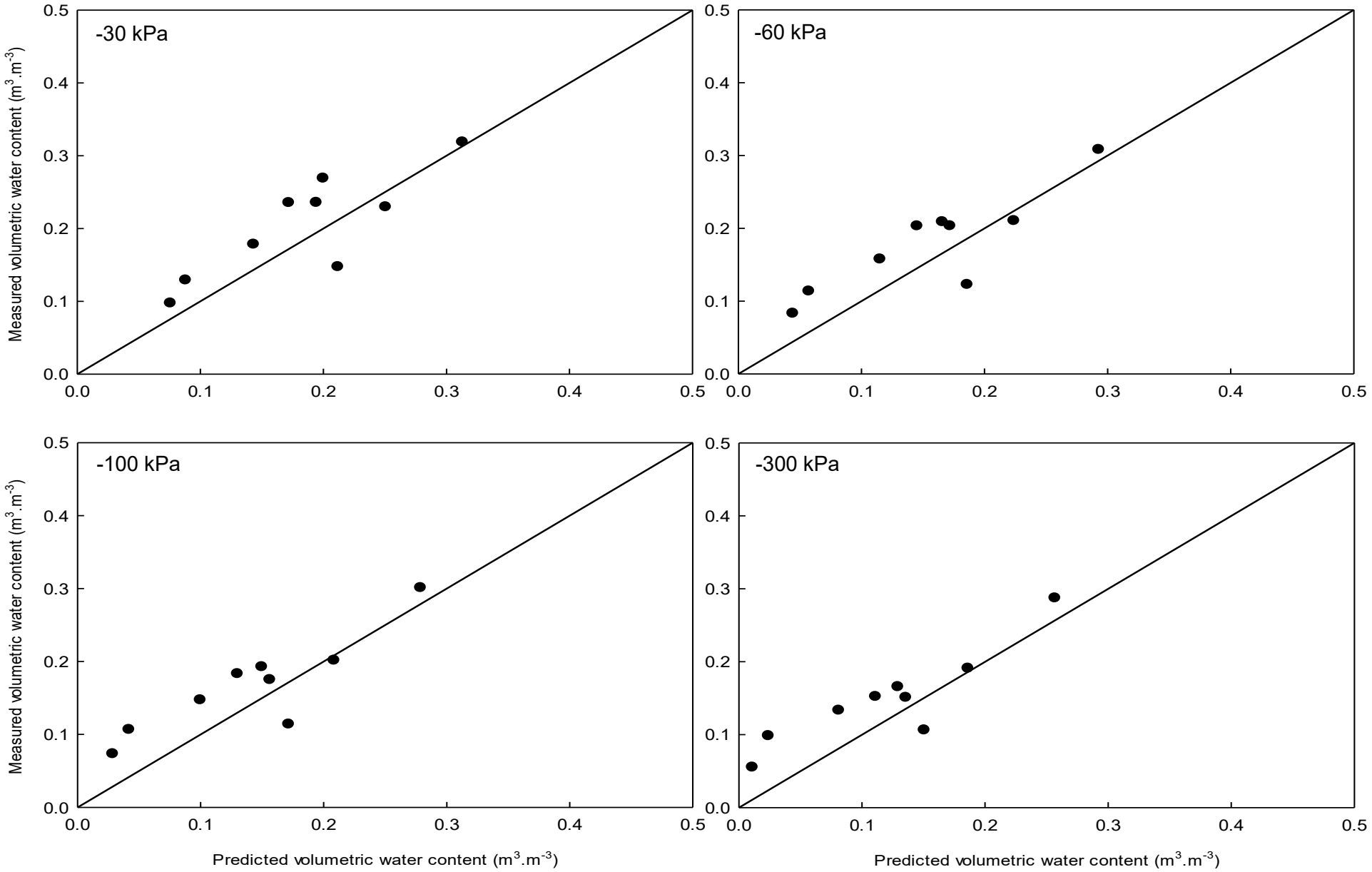

Figure C.3: Measured versus predicted volumetric water content of soil water retention curve model validations at -30 to -300 kPa.

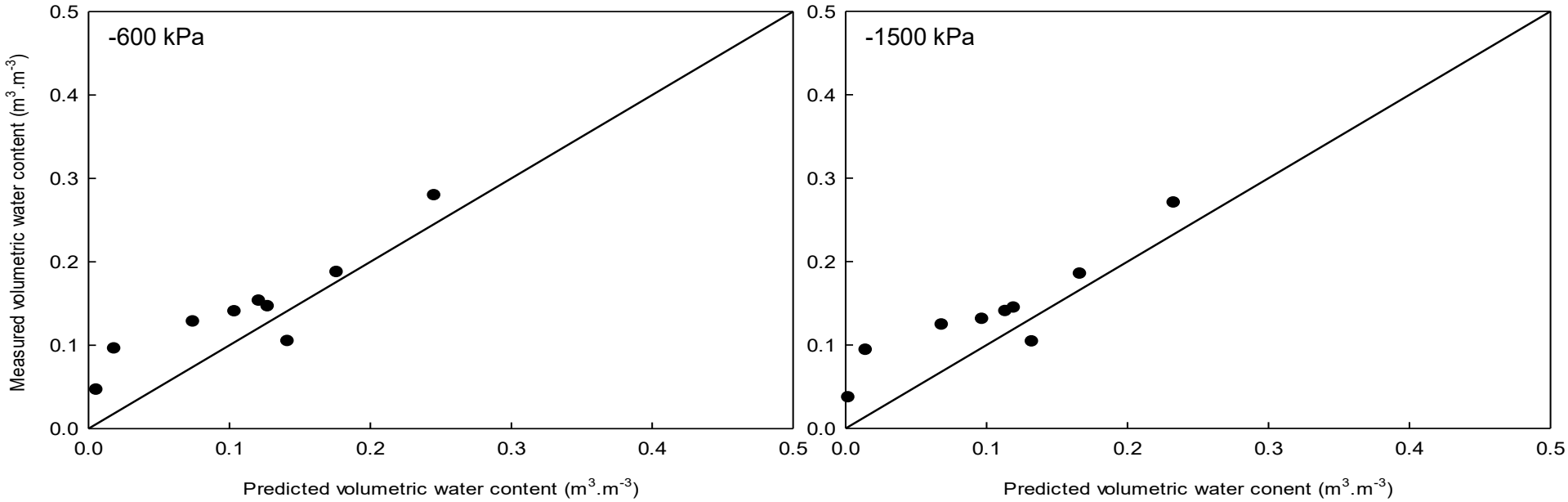

Figure C.4: Measured versus predicted volumetric water content of soil water retention curve model validations at -600 & -1500 kPa.

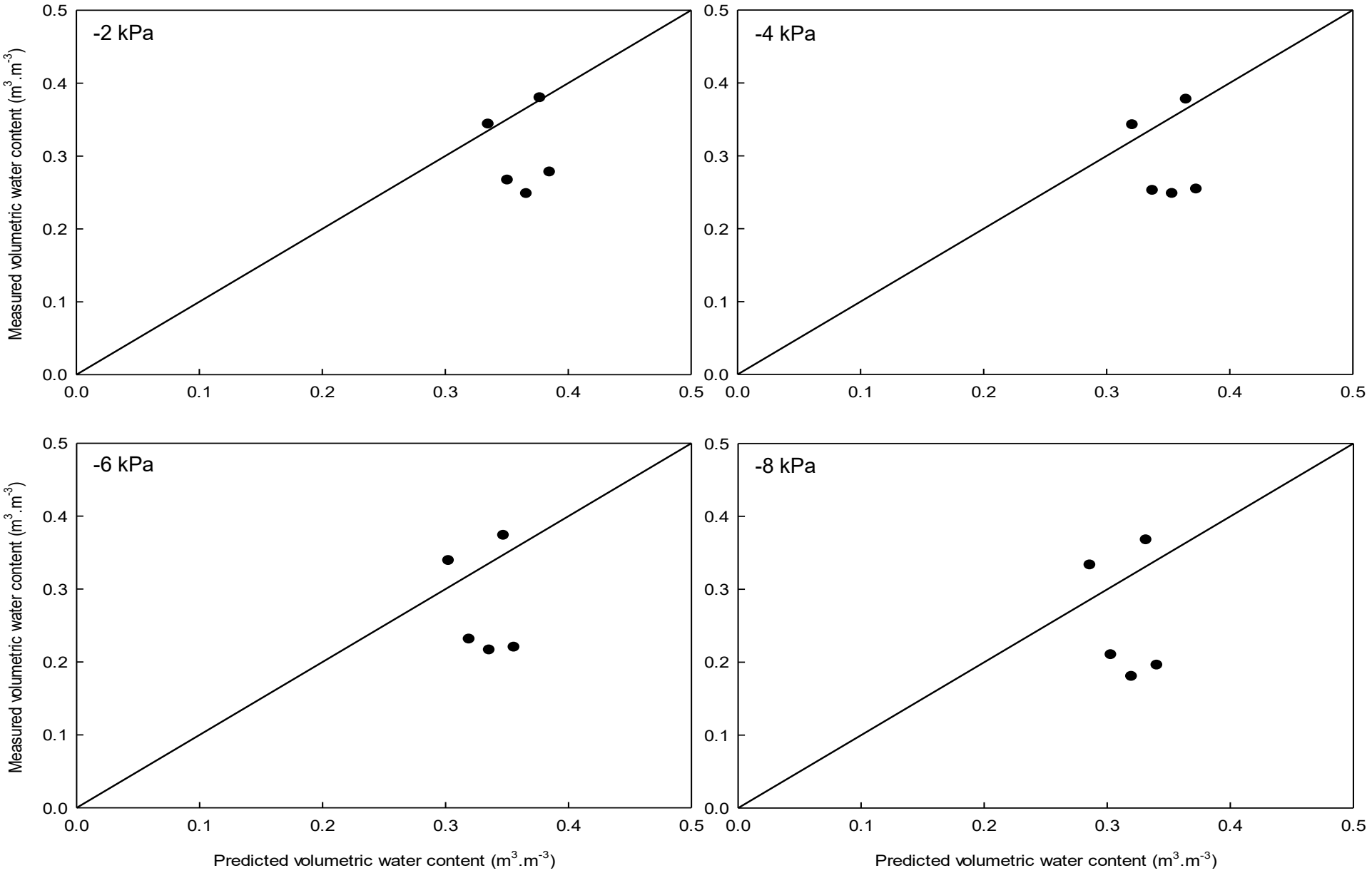

Figure C.5: Measured versus predicted volumetric water content of moderately dense soil water retention curve model validations at -2 to -8 kPa.

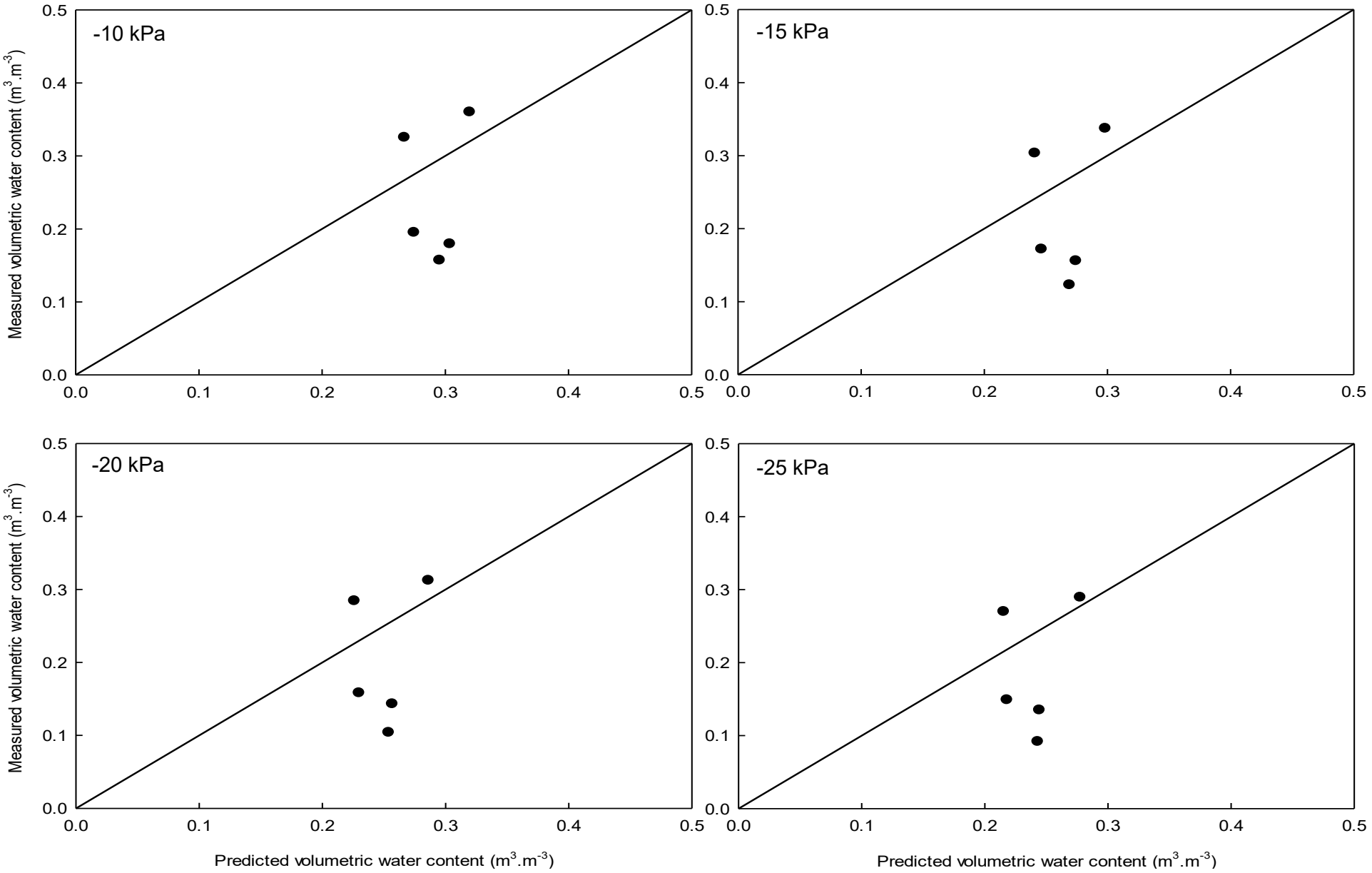

Figure C.6: Measured versus predicted volumetric water content of moderately dense soil water retention curve model validations at -10 to -25 kPa.

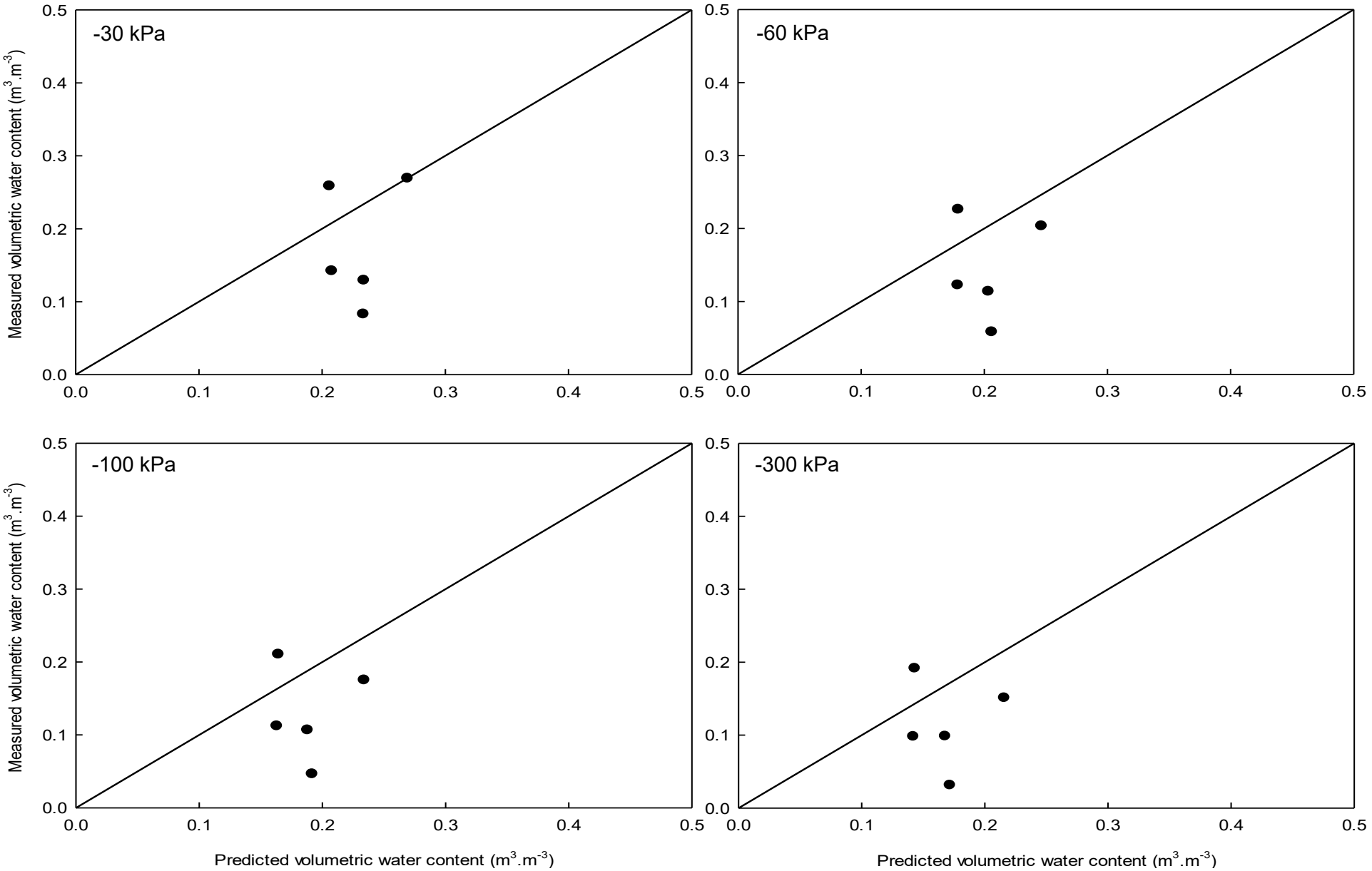

Figure C.7: Measured versus predicted volumetric water content of moderately dense soil water retention curve model validations at -30 to -300 kPa.

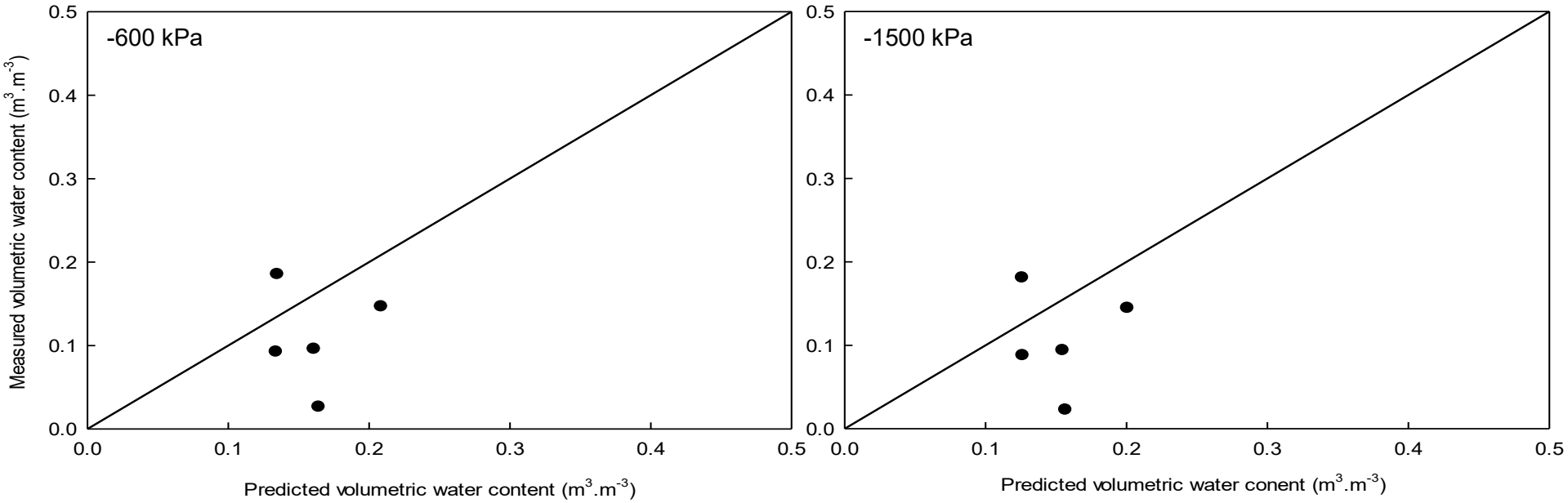

Figure C.8: Measured versus predicted volumetric water content of moderately dense soil water retention curve model validations at -600 & -1500 kPa.

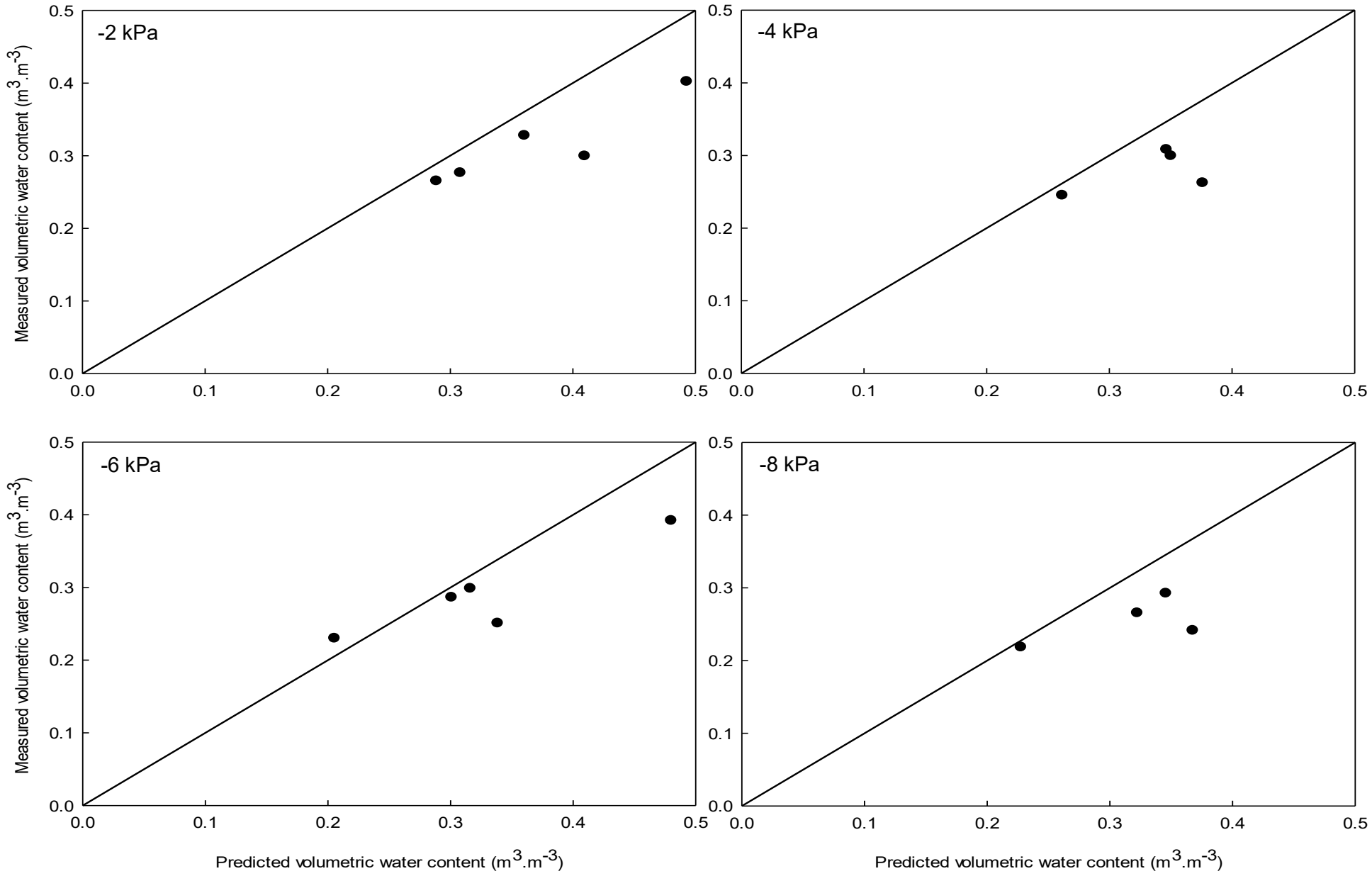

Figure C.9: Measured versus predicted volumetric water content of very dense soil water retention curve model validations at -2 to -8 kPa.

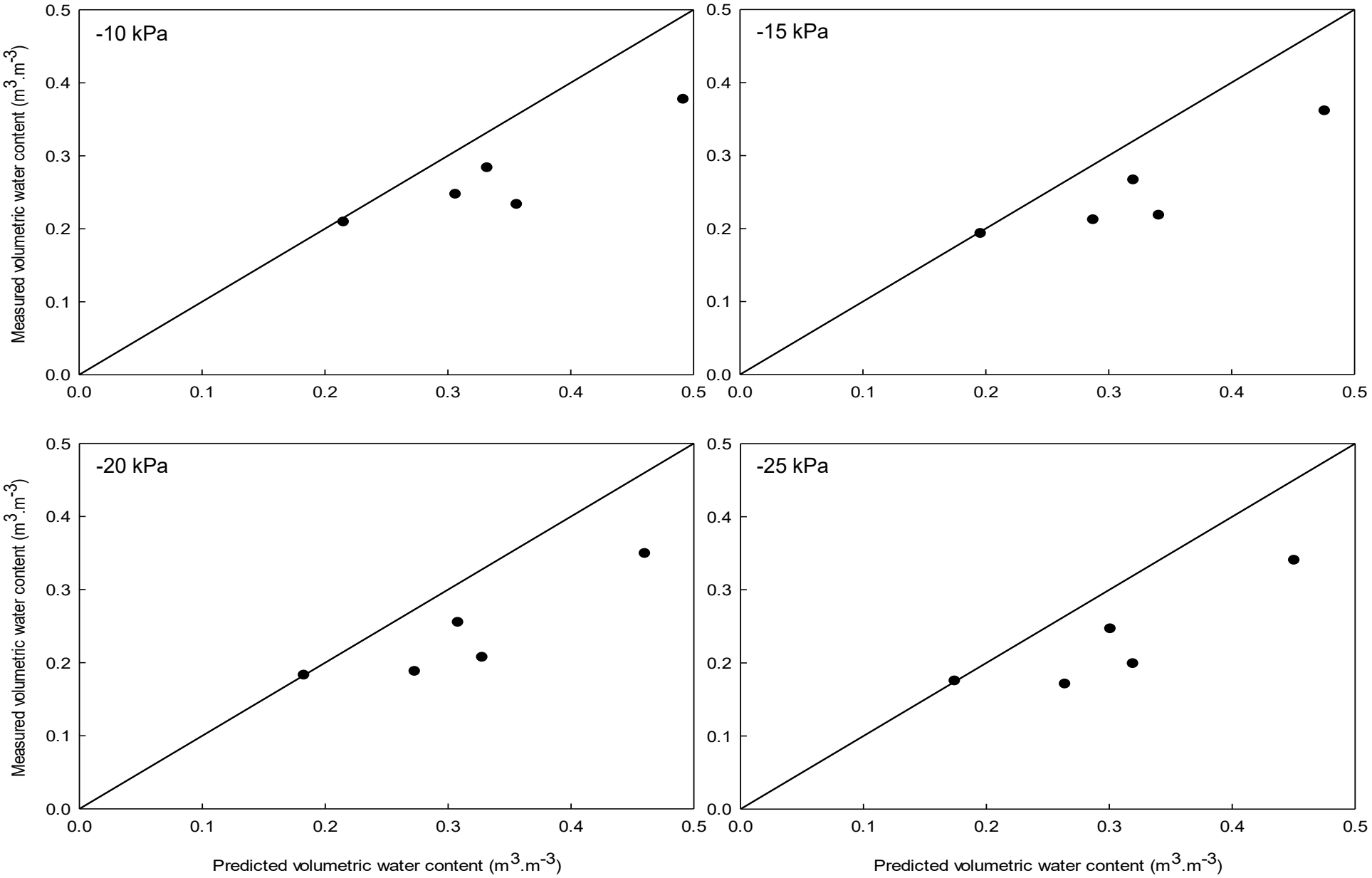

Figure C.10: Measured versus predicted volumetric water content of very dense soil water retention curve model validations at -10 to -25 kPa.

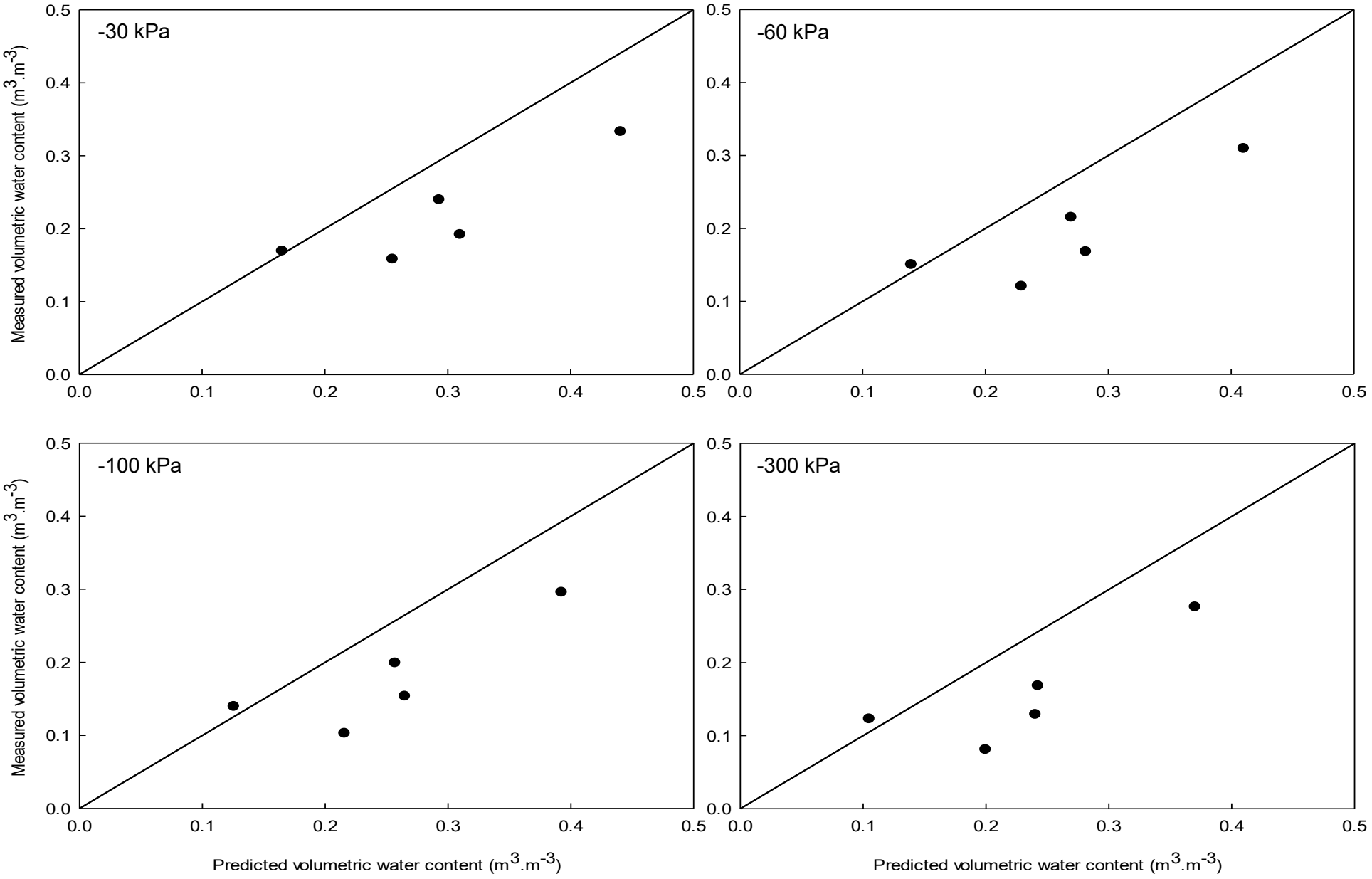

Figure C.11: Measured versus predicted volumetric water content of moderately dense soil water retention curve model validations at -30 to -300 kPa.

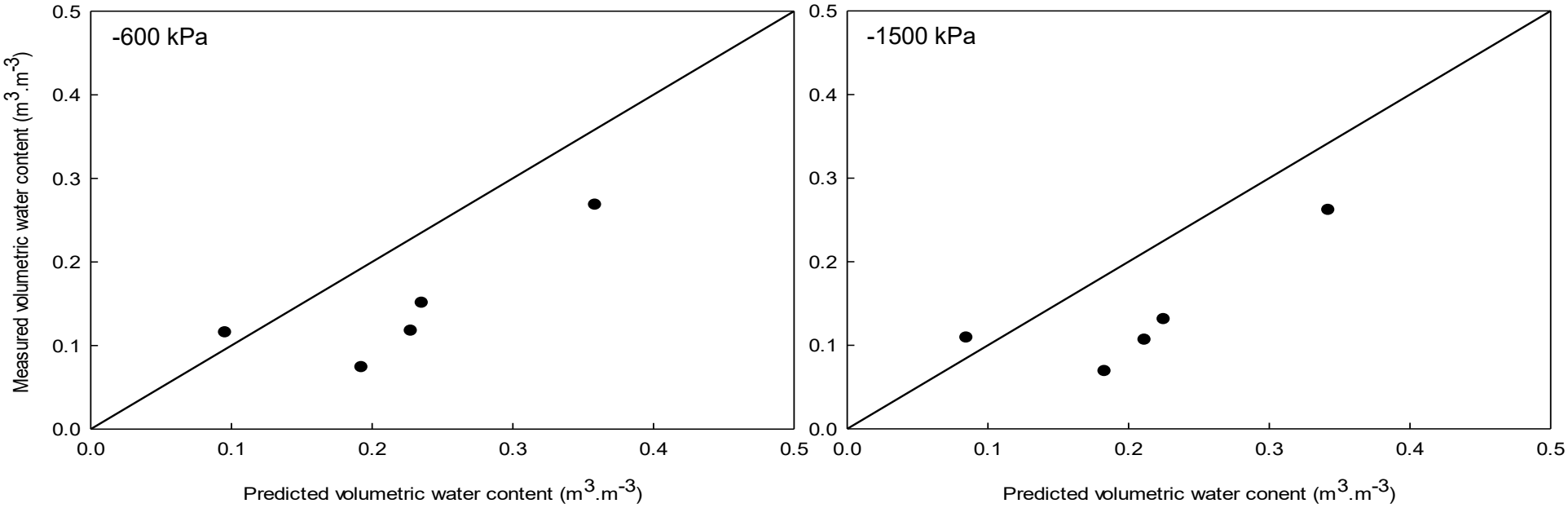

Figure C.12: Measured versus predicted volumetric water content of very dense soil water retention curve model validations at -600 & -1500 kPa.

Appendix D: Root distribution of store-and-release covers

Figure D.1: Root distribution of profile pit D1-1 (A) and D1-2 (B).

Figure D.2: Root distribution of profile pit D1-3 (A) and D2-2 (B).

Figure D.3: Root distribution of profile pit P1-1 (A) and P1-2 (B).

Figure D.4: Root distribution of profile pit P1-3 (A) and P1-4 (B).

Figure D.5: Root distribution of profile pit P2-1 (A) and P2-2 (B).